NOVEL INSIGHTS INTO THE RESPONSES OF THE PLANT MICROBIOME TO ABIOTIC FACTORS

EDITED BY: Collin M. Timm, Tomislav Cernava, Feth el Zahar Haichar and Jia Liu

PUBLISHED IN: Frontiers in Plant Science and Frontiers in Microbiology

frontiers Research Topics

ISSN 1664-8714
ISBN 978-2-88971-092-8
DOI 10.3389/978-2-88971-092-8

About Frontiers

Frontiers is more than just an open-access publisher of scholarly articles: it is a pioneering approach to the world of academia, radically improving the way scholarly research is managed. The grand vision of Frontiers is a world where all people have an equal opportunity to seek, share and generate knowledge. Frontiers provides immediate and permanent online open access to all its publications, but this alone is not enough to realize our grand goals.

Frontiers Journal Series

The Frontiers Journal Series is a multi-tier and interdisciplinary set of open-access, online journals, promising a paradigm shift from the current review, selection and dissemination processes in academic publishing. All Frontiers journals are driven by researchers for researchers; therefore, they constitute a service to the scholarly community. At the same time, the Frontiers Journal Series operates on a revolutionary invention, the tiered publishing system, initially addressing specific communities of scholars, and gradually climbing up to broader public understanding, thus serving the interests of the lay society, too.

Dedication to Quality

Each Frontiers article is a landmark of the highest quality, thanks to genuinely collaborative interactions between authors and review editors, who include some of the world's best academicians. Research must be certified by peers before entering a stream of knowledge that may eventually reach the public - and shape society; therefore, Frontiers only applies the most rigorous and unbiased reviews.
Frontiers revolutionizes research publishing by freely delivering the most outstanding research, evaluated with no bias from both the academic and social point of view. By applying the most advanced information technologies, Frontiers is catapulting scholarly publishing into a new generation.

What are Frontiers Research Topics?

Frontiers Research Topics are very popular trademarks of the Frontiers Journals Series: they are collections of at least ten articles, all centered on a particular subject. With their unique mix of varied contributions from Original Research to Review Articles, Frontiers Research Topics unify the most influential researchers, the latest key findings and historical advances in a hot research area! Find out more on how to host your own Frontiers Research Topic or contribute to one as an author by contacting the Frontiers Editorial Office: frontiersin.org/about/contact

NOVEL INSIGHTS INTO THE RESPONSES OF THE PLANT MICROBIOME TO ABIOTIC FACTORS

Topic Editors:
Collin M. Timm, Johns Hopkins University, United States
Tomislav Cernava, Graz University of Technology, Austria
Feth el Zahar Haichar, Adaptation et Pathogenie (MAP) Villeurbanne, France
Jia Liu, Chongqing University of Arts and Sciences, China

Citation: Timm, C. M., Cernava, T., Haichar, F. Z., Liu, J., eds. (2021). Novel Insights Into the Responses of the Plant Microbiome to Abiotic Factors.
Lausanne: Frontiers Media SA. doi: 10.3389/978-2-88971-092-8

Table of Contents

frontiers in Plant Science

EDITORIAL
published: 28 May 2021
doi: 10.3389/fpls.2021.607874

Editorial: Novel Insights Into the Response of the Plant Microbiome to Abiotic Factors

Feth el Zahar Haichar[1]*, *Tomislav Cernava*[2], *Jia Liu*[3] and *Collin M. Timm*[4]

[1] INSA-Lyon, Université Claude Bernard Lyon1, CNRS, UMR5240, Microbiologie, Adaptation, Pathogénie, Univ Lyon, Villeurbanne, France, [2] Institute of Environmental Biotechnology, Graz University of Technology, Graz, Austria, [3] Chongqing Key Laboratory of Economic Plant Biotechnology, College of Landscape Architecture and Life Science/Institute of Special Plants, Chongqing University of Arts and Sciences, Yongchuan, China, [4] Johns Hopkins University Applied Physics Laboratory, Laurel, MD, United States

Keywords: plant microbiome, plant-microbe interactions, abiotic stress, nutrient limitation, agricultural practices

Editorial on the Research Topic

Novel Insights Into the Response of the Plant Microbiome to Abiotic Factors

The plant-associated microbiota was previously shown to play a crucial role in plant health and growth through its ability to protect plants against pathogens, increasing plant nutrient uptake, modulating plant hormone signaling, and improving abiotic stress tolerance (Berg et al., 2014; Haichar et al., 2014). Recently, it was shown that certain members of the microbiota can even holistically shape disease resistance of their host plant (Matsumoto et al., 2021). Under adverse growth conditions, the diversity and function of microorganisms within the plant's native microbiota can be affected directly by environmental stresses or indirectly *via* specific plant responses (Naylor et al., 2017; Santos-Medellín et al., 2017; Timm et al., 2018). In addition to climatic factors, agricultural management and especially agrochemical inputs were identified as major drivers of microbiome shifts (Wang and Cernava, 2020). Commonly applied agricultural practices can affect up to 50% of naturally occurring microorganisms in crop plants (Chen et al., 2020). A better understanding of microbiome responses to environmental changes and host adaption will contribute to the development of new management strategies that will improve plant stress tolerance and increase plant productivity *via* targeted microbiota modulation (**Figure 1**). Advances in the development of new high-throughput sequencing technologies and other methods for assessing complex microbiomes will help to achieve this challenge (Berg et al., 2020). The current *Frontiers in Plant Science* Research Topic of nine articles sheds light on how the plant microbiome responds to changes in the environment, such as drought, salt stress, climate change, environmental pollution, and agricultural plant treatments. Furthermore, the included articles contribute to the understanding of processes involved in plant holobiont assembly and provide additional clues how the environmental and human activities play a role in them.

One strategy to meet global food demands is to further boost crop yields. Crops are largely impacted by a variety of biotic and abiotic stresses, such as increasing pathogen pressure and drought. In one of the articles, the plant microbiome response to drought conditions was studied by Simmons et al.. The authors demonstrated through 16S rRNA gene fragment sequencing that the degree of drought correlates with enrichment of *Actinobacteria* in four species of millet and that this enrichment occurs along the length of the root. The authors also provided evidence that the enrichment only occurs in roots that are directly exposed to drought, therefore it is not likely evoked due signaling within the root system

OPEN ACCESS

Edited and reviewed by:
Thomas Roitsch,
University of Copenhagen, Denmark

***Correspondence:**
Feth el Zahar Haichar
zahar.haichar@univ-lyon1.fr

Specialty section:
This article was submitted to Plant Abiotic Stress, a section of the journal Frontiers in Plant Science

Received: *18 September 2020*
Accepted: *03 May 2021*
Published: *28 May 2021*

Citation:
Haichar FZ, Cernava T, Liu J and Timm CM (2021) Editorial: Novel Insights Into the Response of the Plant Microbiome to Abiotic Factors. Front. Plant Sci. 12:607874. doi: 10.3389/fpls.2021.607874

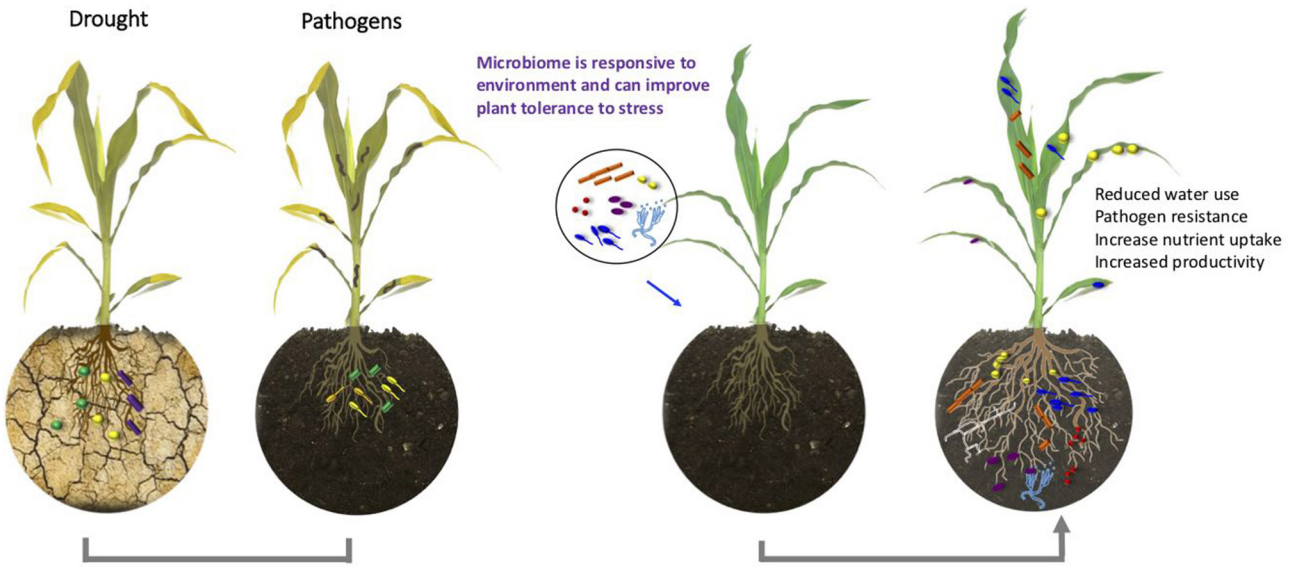

FIGURE 1 | Plants can recruit and maintain microbial communities that can affect their health, fitness, and productivity when exposed to external stressors such as drought and pathogens. Inoculation of plants with microorganisms or modulation of the microbiome via various amendments can increase drought tolerance, improve nutrient uptake, and disease resistance. These practices provide valuable management strategies for sustainable agriculture.

Crop fitness also depends on the seed microbiota, which can be altered during storage in response to fumigation. Solanki et al. characterized the composition of the fungal and bacterial communities in stored wheat grains and determined the impact of phosphine fumigation on the wheat grain microbiome during storage. They found that phosphine fumigation had a significant impact on the diversity and abundance of various components of the wheat grain microbiome. Indeed, highly abundant bacteria, such as *Streptomyces, Prevotella*, *Bilophila,* as well as unidentified groups of *Parabacteroides* disappeared after phosphine treatment. This change corresponded with a significant increase in *Bacillus* representatives. Distinct species of this genus are known to be able to use phosphine and hence to take advantage of this ability to enhance their survival and proliferation. The same result was observed for fungi with, for example, a greater number of *Fusarium* species were detected after changes in microbial community composition following phosphine fumigation and correlated with the presence of *Fusarium* toxins. More research will be needed in the future to understand pesticide-evoked microbial community changes in order to develop strategies to overcome mycotoxin contaminations and other adverse effects.

To prevent food loss different post-harvest treatments are nowadays applied such as hot water treatment (HWT). Wassermann et al. have investigated the microbiome responses to HWT in apples, a sustainable method to reduce pathogen-induced postharvest fruit decay. They demonstrated by combining metabarcoding analysis and real time qPCR that only minor shifts were caused by HWT within the fungal microbiome while the bacterial community was insignificantly affected. These results suggested that HWT treatment was highly effective in reducing rot symptoms on apples while preserving the natural microbiota. Pathogen infection on the other hand, was shown to significantly affect the bacterial community. A total of 18 bacterial and 4 fungal taxa were shared between HWT-subjected and untreated, healthy apples, while being absent in diseased apples. These taxa may participate in reducing post-harvest decay and present promising candidates for biological control. Interestingly, the authors evidenced that by combining a biological control consortium (previously isolated from apples) and HWT, the total infection rates can be reduced up to 42%. In summary, this study provides various evidences that a combination of methods is most promising, in terms of sustainable approaches, to reduce post-harvest decay of apples.

Commonly applied management practices for fruit processing (organic and conventional) are connected to defined abiotic treatments pre- and post-harvest and thus are likely to impact fruit-associated bacteria. The study by Wassermann et al. conducted a study designed to identify (i) differences in microbial community composition in defined tissues of apples fruits and (ii) the impact of management practices on apple-associated bacteria. This study is of particular interest, because apples are the most consumed fruits worldwide and fruit-associated microbiota might transiently colonize our gut; thus influence our own microbiota. Using 16S rRNA gene amplicon analyses with qPCR experiments, and complementary fluorescence *in situ*

hybridization combined with confocal laser scanning microscopy (FISH-CLSM) to visualize the presence of bacteria, the authors identified tissue-specific (stem, peel, fruit pulp, seeds, and calyx) and management-specific microbiome structures. Each of the analyzed apple tissues was found to be colonized by distinct bacterial communities. Fruit pulp and peel were characterized by a high diversity and low bacterial abundance. In contrast, seeds were less diverse than other tissues, but harbored the highest bacterial abundance. Complementary visualizations by FISH-CLSM indicated the highest bacterial abundance on stem, stem end, and calyx end samples, whereas peel and fruit pulp were less colonized. The management practice was found to significantly influence the microbiome of all tissues within apples. The microbiome composition was distinct between organic and conventional tissue analogs with a strong reduction in bacterial diversity and evenness in conventionally managed apples. The abundance was not affected by the management practices, suggesting that a similar quantity of bacteria occupy tissues of organically and conventionally produced apples. Notably, the authors identified signature taxa in conventional apples, among which were OTUs assigned to *Escherichia-Shigella* known to potentially affect human health. The authors hypothesize that the highly diverse microbiome of organically managed apples might limit the effects of human pathogens, through competition.

Köberl et al. used a large-scale approach to study the response of the soil microbiome in vineyards and orchards to different agricultural practices. The impact of soil parameters as well as usage of herbicides were also investigated. Comparative analyses based on microbial profiling of prokaryotic 16S rRNA gene fragments and the fungal ITS region revealed specific adaptions of the microbial community composition to agricultural treatments, especially at higher taxonomic levels. *Proteobacteria, Acidobacteria,* and *Verrucomicrobia* were the most dominant bacterial phyla in Styrian vineyards, orchards and other agriculturally used soils. They are known to harbor plant-associated microorganisms, thus their adaption to agricultural management practices likely also has consequences for their plant hosts. Within the fungal communities, *Ascomycota* represented the most dominant fungal phylum followed by *Zygomycota,* and *Basidiomycota.* Vineyards revealed a significantly higher fungal diversity in combination with a distinct fungal community composition when compared with orchards and other agricultural soils, whereas the prokaryotic diversity was unaffected by soil usage. Soil pH was identified as the most important driver of the microbial community structure among edaphic modulators in both vineyards and orchards soils. In general, the authors showed that responses to distinct soil parameters differ in orchards and vineyards as well as that bacterial and fungal community showed different responses to the same abiotic parameters. In comparison to orchards, the microbiome of vineyards soils maintained higher stability in term of taxonomy and inferred functionality when herbicides were applied. In contrast to vineyards, where the application of herbicides was associated with a general reduction in microbial soil diversity, orchards soils were characterized by drastic shifts in terms of community composition at taxonomic and predicted functional level. This study provides deepening insights on how soil management practices affect the microbiome in agricultural soils and thus an important basis for soil microbiome management in the future.

One of the major abiotic stresses which has a severe negative impact on agricultural productivity globally is salt stress. Tisarum et al. investigated the putative role of Arbuscular Mycorrhizal Fungi (AMF) in salt stress regulation of upland pigmented rice cv. Leum Pua (LP) and compared it with a salt tolerant cultivar (cv. Pokkali; PK). LP plantlets subjected to 0 or 150 mM NaCl were inoculated with *Glomus etunicatum* (GE), *Glomus geosporum* (GG), and *Glomus mosseae* (GM) strains and compared to the salt tolerant cultivar. Among the tested AMF, GE inoculation was found to induce soluble sugar (fructose) and free proline production in host rice plants that act as osmolytes to reduce salt toxicity and hence physiological processes of LP were maintained at stable levels compared to LP without AMF inoculation. Changes in morphological and phenotypic characteristics in cvs. PK and LP under control conditions and salt stress were also observed. Interestingly, in the pericarp of rice grains inoculated with AMF and subsequently exposed to salt stress, anthocyanin accumulation was clearly observed after GE inoculation. This study underscores the important role of AMF inoculation in reducing salt toxicity rice crops and provides new perspectives to employ AMF for salt stress alleviation.

Most studies on the response of microbiome to abiotic factors were conducted below-ground in the past. Less is known about endophytic communities associated with the phyllosphere, the above-ground plant tissues. Firrincieli et al. analyzed phyllosphere endophytic bacterial communities colonizing wild *Populus trichocarpa* (black cottonwood) plants growing in native, nutrient-limited environments including hot-dry (xeric) riparian zones (Yakima River, WA), riparian zones with mid hot-dry (Tieton and Teanaway Rivers, WA), and moist (mesic) climates (Snoqualmie, Skykomish and Skagit Rivers, WA). The sampling sites had experienced different historical drought regimes as a consequence of differences in temperature, vapor pressure deficit, and precipitation. Only *Enterobacteriaceae* and *Pseudomonadaceae* occurred in a high relative abundance in the core microbiome of the poplar trees. Several plant-associated representatives of these bacterial families are known to be able to secrete specific secondary metabolites or to produce enzymes that enhance drought tolerance. In addition, the authors found that the number of observed bacterial species and the overall diversity tended to be lower in the phyllosphere of plants inhabiting the hot-dry environment. They conclude that the major driver of variation was the sampling site while climate and weather data had only a limited effect.

Little is also known about the role of air-carried microbes in the context of plant microbiome assembly. Abdelfattah et al. investigated the role of the atmosphere as a source for the recruitment and dissemination of the plant microbiota. The authors hypothesized that the atmospheric microbiome influences the composition of the fungal communities associated with the aboveground organs (flowers, fruit, and leaves) of table grapes. Surprisingly, the authors found that the atmosphere surrounding the grape phyllosphere had a significantly higher level of fungal diversity than the grape phyllosphere itself. They

also found that 92% of the atmospheric fungal community originated from the local plants (grapevines). In contrast, only 4–35% of the plant-associated fungi originated from the atmosphere, providing evidence that the plants were the major source of their own microbiota. These results demonstrated that the atmosphere serves as a complementary source of recruitment for fungal communities inhabiting leaves, flowers, and fruits.

The effect of soil-applied biochars derived from different sources, on soil physicochemical properties, plant performance, and rhizosphere microbiota in durum wheat was analyzed by Latini et al. Two durum wheat varieties exhibiting different behavior and traits and two biochars (from wood chips and wheat straw pellets) were grown in a greenhouse using a low-nutrient gleyic fluvisol containing a very small amount of Pb and Zn with the aim of assessing the effect of biochar type and/or durum genotype on the diversity and composition of the microbiome associated with rhizosphere soil, soil properties, and plant growth. The authors found that the soil, plants, and rhizosphere microbial communities are affected by biochar addition. This might be linkable to general properties of biochar amendments, they enhance soil carbon content, pH and cation exchange capacity. Interestingly, biochar from a straw-based feedstock was more suitable then woody biochar for improving crop yields as its porous arrangement, distribution, and size, creates a large surface area that improves the soil and plant connection, resulting in enhanced plant growth. Biochar also had a positive effect on the soil, which possessed both zinc and lead contamination. The use of a biochar amendment resulted in a decrease in the Zn available to plants, justifying its use for the remediation of soils with low levels of heavy metal contamination. By implementing high-throughput 16S rRNA gene fragment amplicon sequencing, the authors observed that biochar treatments but not the wheat genotype had a significant influence on microbial α-diversity in the rhizosphere and that nutrient-rich biochar did not negatively impact the rhizosphere bacterial species richness, but rather stabilized it. In the future, more comparative studies will be needed to compare different biochar-cultivar interactions to determine combinations that consistently enhance yield.

In summary, the contributions of this Research Topic have allowed to decipher several detrimental effects of prevalent abiotic stress factors on the plant microbiome, including management practices used to increase production and preserve products. Across these studies, the authors investigated a variety of adverse growth conditions or human inputs that have potential to affect microbiome. Of these 9 studies, natural abiotic stresses including drought and high temperature showed reduced microbial diversity in the rhizosphere or phyllosphere communities. Management practices including pesticide application and addition of untreated woody biochar led to reduced grain and soil diversity, while activated biochar retained soil microbial diversity and hot water treatment of fruits results in increased microbial diversity. More broadly, these studies showed that non-organic agricultural soils have the lowest microbial diversity compared to vineyards or orchards, and that organic production of fruits can increase diversity in the fruit tissues, potentially affecting fruit quality and longevity. They may even have implications for human health that remain to be investigated further. The overall results also suggest that maintenance of a diverse microbial community is important when considering agricultural production, as various environmental and human induced factors can lead to reduction of soil microbial diversity. Reductions in soil microbial diversity may ultimately feedback on plant health, instigating a negative feedback loop on productivity from these systems. More research to understand implications of natural and human factors on soil microbial diversity is needed and will inform long term sustainability and soil health. There still important knowledge gaps that remain to be closed in the future. Many of them are related to common agricultural practices like the application of agrochemicals; they are widespread, yet we are only beginning to understand how they interfere with plant and soil microbiomes (Wang and Cernava, 2020). The findings in this Research Topic and upcoming topics will serve as a basis to improve agricultural management practices in the future.

AUTHOR CONTRIBUTIONS

FH prepared the first draft of this editorial. All authors contributed to the article and approved the submitted version.

FUNDING

The research of FH was supported by the French National Research Agency (ANR-18-CE32-0005, DIORE).

ACKNOWLEDGMENTS

The authors gratefully thank Hamid Baya for the design of the figure.

REFERENCES

Berg, G., Grube, M., Schloter, M., and Smalla, K. (2014). Unraveling the plant microbiome: looking back and future perspectives. *Front. Microbiol.* 5:148. doi: 10.3389/fmicb.2014.00148

Berg, G., Rybakova, D., Fischer, D., Cernava, T., Vergès, M. C. C., Charles, T., et al. (2020). Microbiome definition re-visited: old concepts and new challenges. *Microbiome* 8, 1–22. doi: 10.1186/s40168-020-00905-x

Chen, X., Krug, L., Yang, M., Berg, G., and Cernava, T. (2020). Conventional seed coating reduces prevalence of proteobacterial endophytes in Nicotiana tabacum. *Indust. Crops Products* 155:112784. doi: 10.1016/j.indcrop.2020.112784

Haichar, F. Z., Santaella, C., Heulin, T., and Achouak, W. (2014). Root exudates mediated interactions belowground. *Soil Biol. Biochem.*, 77, 69–80. doi: 10.1016/j.soilbio.2014.06.017

Matsumoto, H., Fan, X., Wang, Y., Kusstatscher, P., Duan, J., Wu, S., et al. (2021). Bacterial seed endophyte shapes disease resistance in rice. *Nat. Plants* 7, 60–72. doi: 10.1038/s41477-020-00826-5

Naylor, D., DeGraaf, S., Purdom, E., and Coleman-Derr, D. (2017). Drought and host selection influence bacterial community dynamics in the grass root microbiome. *ISME J.* 11, 2691–2704. doi: 10.1038/ismej.2017.118

Santos-Medellín, C., Edwards, J., Liechty, Z., Nguyen, B., and Sundaresan, V. (2017). Drought stress results in a compartment-specific restructuring of the rice root-associated microbiomes. *MBio* 8, e00764–e00717. doi: 10.1128/mBio.00764-17

Timm, C. M., Carter, K. R., Carrell, A. A., Jun, S.-R., Jawdy, S. S., Vélez, J. M., et al. (2018). Abiotic stresses shift belowground *Populus*-associated bacteria toward a core stress microbiome. *mSystems* 3, e00070–e00017. doi: 10.1128/mSystems.00070-17

Wang, M., and Cernava, T. (2020). Overhauling the assessment of agrochemical-driven interferences with microbial communities for improved global ecosystem integrity. *Environ. Sci. Ecotechnol.* 4:100061. doi: 10.1016/j.ese.2020.100061

Conflict of Interest: The authors declare that the research was conducted in the absence of any commercial or financial relationships that could be construed as a potential conflict of interest.

frontiers in Microbiology

ORIGINAL RESEARCH
published: 17 May 2019
doi: 10.3389/fmicb.2019.01098

Shifts in the Composition of the Microbiota of Stored Wheat Grains in Response to Fumigation

Manoj Kumar Solanki[1†], Ahmed Abdelfattah[2,3†], Malka Britzi[4], Varda Zakin[1], Michael Wisniewski[5], Samir Droby[1] and Edward Sionov[1*]*

[1] Institute of Postharvest and Food Sciences, Agricultural Research Organization – The Volcani Center, Rishon LeZion, Israel, [2] Dipartimento di Agraria, Università Mediterranea di Reggio Calabria, Calabria, Italy, [3] Department of Ecology, Environment and Plant Sciences, Stockholm University, Stockholm, Sweden, [4] National Residue Control Laboratory, Kimron Veterinary Institute, Beit Dagan, Israel, [5] United States Department of Agriculture, Agricultural Research Service, Kearneysville, WV, United States

OPEN ACCESS

Edited by:
Jia Liu,
Chongqing University of Arts and Sciences, China

Reviewed by:
Simona Marianna Sanzani, University of Bari Aldo Moro, Italy
Xuehong Wu, China Agricultural University, China

***Correspondence:**
Samir Droby
samird@volcani.agri.gov.il
Edward Sionov
edwardsio@volcani.agri.gov.il

[†] These authors have contributed equally to this work

Specialty section:
This article was submitted to Microbial Symbioses, a section of the journal Frontiers in Microbiology

Received: *12 March 2019*
Accepted: *30 April 2019*
Published: *17 May 2019*

Citation:
Solanki MK, Abdelfattah A, Britzi M, Zakin V, Wisniewski M, Droby S and Sionov E (2019) Shifts in the Composition of the Microbiota of Stored Wheat Grains in Response to Fumigation. Front. Microbiol. 10:1098. doi: 10.3389/fmicb.2019.01098

While the wheat-associated microbiome is of major agricultural importance, little is known about the alterations in wheat grain microbial community composition during storage. Characterization of the bacterial and fungal communities in stored wheat grains revealed the impact of phosphine fumigation, one of the most effective methods to eliminate insects in stored commodities, on the composition of the wheat grain microbiome. High-throughput amplicon sequencing of the bacterial 16S rRNA gene and fungal internal transcribed spacer (ITS) region was used to analyze the wheat grain microbiome at different times over as 6 months period of storage. Higher bacterial diversity was found across the samples during the first (immediately after harvest) and second (3 months later) time points, with a predominance of *Proteobacteria*, *Firmicutes*, *Actinobacteria*, *Bacteroidetes* and *Planctomycetes*. A two-fold decrease in the number of bacterial operational taxonomic units (OTUs) was observed in wheat grains at the last time point (6 months later), following phosphine treatment. In contrast to the effect of phosphine on bacteria, it did not affect fungal diversity in stored grains. The majority of fungal sequences were assigned to *Ascomycota*, followed by *Basidiomycota*, *Glomeromycota*, and unidentified fungi, which were evenly distributed throughout the storage period. Alpha and beta diversity analyses were confirmed by examination of the cultured microbial taxa obtained from the stored wheat grains. Mycotoxin analysis of wheat grains collected after phosphine fumigation revealed the presence of *Fusarium* toxins, primarily deoxynivalenol (DON). Several mycotoxigenic *Fusarium* spp. were also detected in the same samples. Results of the present study indicate that microbiome of stored, whole wheat grains was strongly affected by phosphine fumigation, which changed the structure of the microbial community leading to shifts in species composition toward mycotoxigenic strains. A better understanding of the complex interactions within the microbial communities of stored grains will assist in the development of novel biocontrol strategies to overcome mycotoxin contamination.

Keywords: stored wheat grain, microbiome analysis, phosphine fumigation, mycotoxigenic fungi, mycotoxins

INTRODUCTION

Wheat is one of the most important cultivated cereals produced and consumed globally. It provides, on average, about 20% of the daily caloric requirement and about 21% of the daily protein intake in the human diet (Shiferaw et al., 2013). The availability of high-quality wheat grains is essential for maintaining the stability of the world's food supply and for global food security. Wheat grains are colonized by complex microbial communities that play different roles in grain quality and susceptibility to disease (Links et al., 2014). Some of the bacteria and fungi that are associated with seeds can be harmful to human health and cause plant diseases, while others can have beneficial effects on the host and actually improve nutrient uptake and increase tolerance to biotic and abiotic stresses through multiple mechanisms (Brader et al., 2017). For example, specific species of *Fusarium*, *Aspergillus*, *Penicillium*, and *Alternaria* can cause spoilage in stored wheat grains and produce mycotoxins that severely decrease crop value and are harmful to animal and human health (Placinta et al., 1999; Magan et al., 2010). Conversely, the plant protective ability of some bacterial epiphytes and endophytes against fungal pathogens has been reported in several crops (Links et al., 2014; Mousa et al., 2016; Gdanetz and Trail, 2017). A better knowledge of the composition and dynamics of wheat-grain-associated microbiota is needed to identify novel beneficial microorganisms that may improve crop health and suppress the growth of potential pathogens in a sustainable manner. Several studies on the composition of the rhizosphere microbiome of wheat and other parts of the wheat plant have been conducted (Ofek et al., 2014; Hartmann et al., 2015; Gdanetz and Trail, 2017; Mahoney et al., 2017). Few studies, however, have characterized the microbiota of wheat grains and the seeds of other crop species (Links et al., 2014; Yuan et al., 2018).

In addition to fungal pathogens that cause seed deterioration during storage, insects can infest and spoil grain that is handled or stored improperly. Thus, a fumigation treatment is often required to prevent insect infestations in stored grains. Phosphine gas is by far the most common fumigation agent used worldwide for the treatment of stored grain against insects, and has recently increased in usage following the prohibition of methyl bromide, an alternative fumigant. Although phosphine is very toxic to insects, it does not leave toxic residues after treatment or impact seed viability (Bell, 2000). While this fumigant is known to have broad biological activity (Berners-Price and Sadler, 1988; Nath et al., 2011), its effect on the microbial community of stored wheat grains is largely unknown. Few studies have been reported on the effect of phosphine on the growth of molds in stored wheat and corn grains (Hocking and Banks, 1991; Castro et al., 2000). These studies reported that phosphine only causes a slight decrease in the population of *Aspergillus flavus* in stored maize and *Eurotium chevalieri*, *A. flavus,* or *Aspergillus parasiticus* in stored wheat grains.

The objective of the present study was to characterize the composition of the fungal and bacterial communities in stored wheat grains, which produced annually for human and animal consumption, and to determine the impact of phosphine fumigation on the wheat grain microbiome during storage. Amplicon-based high-throughput sequencing (HTS) and chemical analysis of mycotoxins were used to characterize the wheat grain microbiome at different time points over a storage period of 6 months. Significant changes in the composition of the microbial community were identified when phosphine treatment was applied to stored wheat grains. *Fusarium*-related toxins were also detected in stored wheat grains as a result of shifts in the microbial population profiles which took place following fumigation with phosphine.

MATERIALS AND METHODS

Wheat Grain Samples

Wheat grain (*Triticum aestivum*) samples were collected from seven wheat grain storage facilities located in northern and southern districts of Israel. Samples were designated as T1 when obtained immediately after harvest during the first week of storage (June 2016), T2 after storage for 3 months, and T3 after storage for 6 months. Four months after harvest (before collecting T3 samples) the stored grains in all locations were exposed to phosphine (3 g/m^3) for a period of 10 days to control insect pests. In each storage facility, three samples (1 kg of grain each), destined for human consumption, were collected at each time point (3 samples × 7 storage sites = a total of 21 samples at each time point) in equal proportions from the front face and the center, at points located 1 m in horizontal depth within the grain mass, and from areas close to the walls. Grain temperature and moisture content were in the ranges of 27–33°C and 10.5–12.9%, respectively, throughout the study. The collected samples were kept in sterile plastic bags during transport to the laboratory and on the same day a 100 g aliquot was taken from each sample, thoroughly mixed, frozen in liquid nitrogen, freeze dried and milled into a fine powder with a grain grinder. The grain grinder was cleaned and disinfected with 70% ethanol solution between sample grinding. Powders were stored at 4°C until further pending analysis (2–4 weeks).

DNA Extraction, Amplification and Sequencing

DNA extraction from wheat grain samples was performed as previously described (Sadhasivam et al., 2017). Total DNA was extracted from 300 mg of wheat powder using a lysis buffer containing hexadecyltrimethylammonium bromide (CTAB). Ten milliliters of DNA extraction buffer (l.0 M Tris–HCl, pH 7.5; 1% (*w*/*v*) CTAB; 5 M NaCl; 0.5 M EDTA; 1% (*v*/*v*) 2-mercaptoethanol; and proteinase K at 0.3 mg/ml) were added to the powder, mixed gently, and the mixture was incubated at 65°C for 30 min. The extracts were cooled prior to the addition of an equal volume of chloroform, gently mixed and centrifuged at 6000 rpm for 10 min. The aqueous supernatant was recovered and an equal volume of 2-propanol was added. The DNA was precipitated by centrifugation at 4800 × *g* for 5 min and resuspended in TE buffer solution (Tris-EDTA, pH 8.0) containing RNase A at 10 μg/ml. DNA was further purified by phenol-chloroform extraction. Finally, the DNA was precipitated with 100% ethanol containing 3 M sodium acetate,

rinsed in 70% (*v*/*v*) ethanol and resuspended in TE buffer. The purity of the extracted DNA was assayed with a NanoDrop One spectrophotometer (Thermo Fisher Scientific, Wilmington, DE, United States), and the total DNA concentration in each sample was adjusted to 50 ng/μl. The universal primers 515F/926R and 5F/86R were used to amplify the 16S and ITS2 rRNA gene regions of bacteria and fungi, respectively (**Supplementary Table S1**). The primers were modified to include Illumina adapters[1] for subsequent multiplexing. PCR amplification of each sample was performed in triplicate. The PCR mixture (25 μl) contained 12.5 μl 2× DreamTaq green PCR master-mix (Thermo Fisher Scientific, Lithuania), 1 μl of each primer (5 μM), and 1 μl of DNA template. Nuclease-free water (Thermo Fisher Scientific, Lithuania) replaced template DNA in negative controls. All amplicons and amplification mixtures including negative controls were sequenced using Illumina MiSeq V3 (2 × 300 bp) chemistry.

Data Analysis

Illumina adaptors were clipped and low-quality reads removed by Trimmomatic 0.36 (Bolger et al., 2014) using a sliding window trimming, cutting once the average quality within the window of 4 bases falls below a quality threshold of 15. Paired-end reads were merged utilizing PEAR (Zhang et al., 2014) for 16S rRNA gene, and PANDAseq (Masella et al., 2012) for ITS rRNA gene region sequences with default parameters. Chimeric sequences were identified and removed using USEARCH (Edgar, 2010; McDonald et al., 2012) for 16S rRNA gene, and VSEARCH 1.4.0 (Rognes et al., 2016) for ITS rRNA gene region sequences. UCLUST algorithm (Edgar, 2010), as implemented in QIIME 1.9.1 (Caporaso et al., 2010) was used to cluster sequences queried against the Greengenes 13_8_97 database for 16S rRNA gene (DeSantis et al., 2006), and for ITS UNITE dynamic database released on 01.12.2017 (Abarenkov et al., 2010) at a similarity threshold of 97%, respectively. Sequences that failed to cluster against the database were *de novo* clustered using the same algorithm. After removing singletons, the most abundant sequences in each OTU were selected as representative sequences and used for the taxonomic assignment using the BLAST algorithm (Altschul et al., 1990; McDonald et al., 2012) as implemented in QIIME 1.9.1. The OTU table was normalized by rarefaction to an even sequencing depth in order to remove sample heterogeneity. The rarefied OTU table was used to calculate alpha diversity indices including Observed Species (Sobs), and Shannon metrics. Alpha diversities were compared based on a two-sample *t*-test using non-parametric (Monte Carlo) methods and 999 Monte Carlo permutations. Results were visualized in boxplots figures.

Metagenome Seq's Cumulative Sum Scaling (CSS) (Paulson et al., 2013) was used as a normalization method for other downstream analyses. The CSS normalized OTUs table was analyzed using Bray Curtis metrics (Bray and Curtis, 1957) and utilized to evaluate β-diversity and construct PCoA plots using Emperor (Lozupone and Knight, 2005). Similarity in community composition was tested via ANOSIM in QIIME 1.9.1 using 999 permutations. Differential OTU abundance of the most abundant taxa (≥0.1%) between sample groups were determined using a *t*-test and the Kruskal-Wallis test (Kruskal and Wallis, 1952). In all tests, significance was determined using 999 Monte Carlo permutations, and the false discovery rate (FDR) was used to adjust the calculated *P*-values and when the FDR $P < 0.05$ it was considered significant.

Microbial Isolation and Identification

Grains samples (10 g each) were shaken on an orbital shaker at 150 rpm in 90 ml sterile saline (0.9% NaCl) solution at room temperature for 1 h, then 100 μL of serial 1/10 dilutions were plated on Luria-Bertani (LB) agar plates for isolation of bacteria and Potato Dextrose Agar (PDA) plates supplemented with chloramphenicol (20 μg/ml) for isolation of filamentous fungi and yeasts. LB agar plates were incubated at 37°C for 24–48 h, whereas PDA plates were incubated at 28°C for 48–72 h. Bacterial colonies were randomly selected from the plates and streaked on fresh culture media to obtain pure cultures. Filamentous fungi and yeasts were transferred singly to PDA plates and subcultured twice to obtain a pure culture.

DNA was extracted from each bacterial strain using a lysozyme lysis method described by De et al. (2010). Fungal DNA extraction was performed on lyophilized mycelium/yeasts cells using CTAB-based method as previously described (Sadhasivam et al., 2017). DNA quality and yield were determined using a NanoDrop One spectrophotometer. The 16S rRNA gene in bacteria and ITS rRNA gene region in fungi were amplified with universal primers 27F/1492R and ITS1/ITS4, respectively (**Supplementary Table S1**). PCR products were purified and sequenced through standard Sanger sequencing; sequences were identified via BLAST matches to the NCBI database[2] and deposited as accession number MK229027–MK229144 (Bacterial 16S rRNA gene) and MK226203–MK226306 (Fungal ITS rRNA gene region).

Quantitative Real-Time PCR

qPCR was performed to quantify the presence of mycotoxigenic fungi, such as *Fusarium, Aspergillus*, and *Alternaria* spp., in the stored grains at different time points. A broad-spectrum primer pair ITSPF/ITSPR was used to target the fungal ITS region and single genus-specific TaqMan probes were tested for their ability to detect fungal DNA (**Supplementary Table S2**). The probes were labeled on the 5′ end with the fluorescent reporters FAM, HEX and TEX, and on the 3′ end with TAMRA, BHQ1, and BHQ2. The qPCR reactions were carried out using qPCRBIO Probe Mix (PCR Biosystems, London, United Kingdom), 10 μM of each primer, 10 μM of each probe, and 5 ng of genomic DNA template. Amplification reactions were performed in a total reaction volume of 10 μl and were run on the Eco Real-Time PCR System (Illumina) with the following program: 2 min at 50°C [Uracil-DNA glycosylases (UDG) activation], 2 min at 95°C (denaturation and Taq polymerase activation), an amplification program of 45 cycles at 95°C for 15 s, 55°C for 15 s, and 60°C for 15 s. Real-time qPCR reactions were performed in triplicate

[1] www.illumina.com

[2] https://blast.ncbi.nlm.nih.gov/Blast.cgi

for each biological replicate and each sampling date contained three biological replicates. The cycle threshold value (Ct), which refers to the cycle number where the sample's fluorescence significantly increases above the background level, was calculated automatically by the Eco software. The detection limit of the probes was assessed under optimized PCR conditions with the DNA extracted from pure cultures of *Fusarium proliferatum* (NRRL 31866), *A. flavus* (NRRL 3518), and *Alternaria infectoria* (F11, isolated from stored wheat grains). Serial dilutions were made of DNA from the three fungal species. The real-time PCR data indicated that the Ct values correlated well with known DNA quantities from 8 pg to 5 ng, with R^2 values of 0.98 (slope -1.70) for *Fusarium*, 0.99 (slope -1.48) for *Aspergillus*, and 0.99 (slope -1.72) for *Alternaria* (**Supplementary Figure S1**).

To test the efficacy of the method, sterilized wheat grain samples (10 g) were inoculated with each of *A. flavus*, *F. proliferatum,* and *A. infectoria* cultures at final concentration of 10^4 spores/g and incubated for 3 days. Non-inoculated sterilized grain samples used as control. DNA extracts isolated from the samples were analyzed using the qPCR assay. The obtained Ct values (23–30) revealed high reproducibility and demonstrated the ability to quantify fungal DNA in artificially contaminated wheat grains. qPCR analysis indicated the average values of DNA content for *F. proliferatum*, *A. flavus,* and *A. infectoria* spp. in seeds at concentrations of 268, 44 and 30 ng/mg, respectively.

Mycotoxin Analysis

Detection, identification, and quantification of mycotoxins in wheat grain samples were performed using high-performance liquid chromatography coupled with tandem mass-spectrometry (LC/MS/MS) as described previously (Sadhasivam et al., 2017). Briefly, individual stock standard solutions (1 mg/ml) of aflatoxin B_1, B_2, G_1, G_2 (AFB_1, AFB_2, AFG_1, AFG_2), ochratoxin A (OTA), zearalenone (ZEN), deoxynivalenol (DON), fumonisin B_1, B_2 (FB_1, FB_2) and T-2 toxin (T-2) (Fermentek, Israel) were prepared in methanol. Multi-toxin working standard solutions with a series of toxin concentrations were prepared by dilution of the stock solutions of the analytes in methanol. For sample preparation, 5 g of the ground seeds were mixed with 20 ml of 25:75 (v/v) water/methanol and placed in an orbital shaker at 200 rpm for 30 min at room temperature. After centrifugation at 8500 × *g* for 15 min, 5 ml of the supernatant were transferred to a 15-ml glass tube and evaporated under a stream of nitrogen at 50°C. The dry residue was reconstituted with 0.25 ml of a 95:5 (v/v) water/methanol mixture and centrifuged for 10 min at 17,000 × *g*, at 4°C; the supernatant was used directly for the analysis. Three non-contaminated wheat grain samples were spiked with multi-mycotoxin standard solutions at three concentration levels for construction of calibration curves, which were used for mycotoxin quantification. The spiking experiments were performed in triplicate at three different time points. Chromatographic separation was carried out using Nexera X2 UHPLC (Shimadzu, Tokyo, Japan) equipped with 100 × 2.1 mm, 2.6 μm Kinetex C_{18} column, (Phenomenex, Torrance, CA, United States). The mobile phase consisted of 2.5 mM ammonium acetate acidified with 0.1% acetic acid (A), and methanol (B). The LC system was coupled with API 6500 hybrid triple quadrupole/linear ion trap mass spectrometer (Sciex, Concord, ON, Canada), equipped with a turbo-ion electrospray (ESI) ion source. Validation parameters, such as precision, accuracy, limit of detection (LOD), limit of quantification (LOQ), and specificity, were determined (**Supplementary Table S3**).

RESULTS

Amplicon Sequencing

After paired-end alignments, quality filtering, and deletion of chimeric, singletons, and plant sequences, 22,338 16S rRNA gene sequences were assigned to 806 bacterial OTUs and 5,383,776 ITS sequences were assigned to 6,064 fungal OTUs. The number of 16S sequences varied between 186 and 5019 (Std. dev. 702) and ITS sequences varied between 23,948 and 359,517 (Std. dev. 42565) reads per sample. The number of OTUs, after rarefaction collapsing biological replicates, varied between 66 and 187 OTUs in the 16S rRNA gene dataset and between 350 and 515 OTUs in the ITS rRNA gene region dataset per category of samples (**Supplementary Table S4**).

Wheat Grain Microbial Communities

Bacterial OTUs were mainly assigned to *Proteobacteria* (41.1%), *Firmicutes* (35.4%), *Actinobacteria* (11.9%), *Bacteroidetes* (6.9%), and *Acidobacteria* (1.9%) (**Figure 1A**). *Proteobacteria* was dominated by the presence of *Gammaproteobacteria* (21.7%), *Alphaproteobacteria* (8.2%), *Betaproteobacteria* (7.7%), and *Deltaproteobacteria* (3.3%).

Fungal members of the *Ascomycota* were the dominant fungal phylum across all samples, accounting for 88.5% of the total number of detected sequences (**Figure 1B**). This was followed by *Basidiomycota* (9.8%), *Glomeromycota* (1.4%), and unidentified fungi (0.2%). *Chytridiomycota*, *Entorrhizomycota*, *Mortierellomycota*, *Mucoromycota*, and *Olpidiomycota* were detected at a very low frequency (<0.1%). Ascomycota were largely identified as members of the classes *Dothideomycetes* (87.0%), and *Sordariomycetes* (1.1%). Whereas *Basidiomycota* were represented by *Tremellomycetes* (4.4%), *Microbotryomycetes* (2.8%), and *Pucciniomycetes* (1.5%), *Glomeromycota* was almost exclusively dominated by *Glomeromycetes* (1.4%).

Compositional Differences in the Microbial Community After Different Lengths of Storage

Alpha diversity comparisons based on Shannon index, indicated that bacterial diversity varied significantly ($P < 0.003$) between T1 and T3, and T2 and T3 in both cases (**Table 1** and **Figure 2A**). In contrast, Shannon index indicated no significant difference ($P \geq 0.1$) in fungal community composition between the sampled time-points (**Table 1** and **Figure 2B**). On the other hand, based on the Bray Curtis dissimilarity metric, the three time points (T1, T2, and T3) varied significantly ($P < 0.01$) in their bacterial and fungal community composition and structure (**Table 1**). The differences between the time points were also evident in the Principal Coordinate Analysis

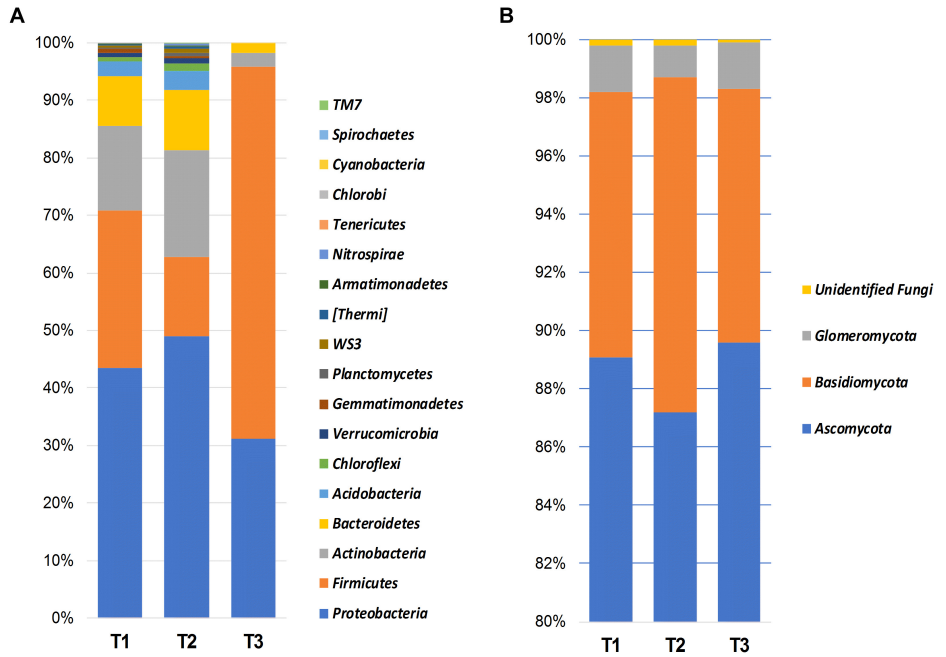

FIGURE 1 | Bar charts showing the relative abundance of most dominant bacterial **(A)** and fungal **(B)** phyla detected using high-throughput sequencing technology across the samples collected at three storage time-points (T1, T2, T3).

TABLE 1 | *P*-values of the comparisons between the samples collected at three storage time-points (T1, T2, T3)[a].

Microbial community	Comparison	Alpha diversity (Shannon index)[b]	Alpha diversity (Observed OTUs)[b]	Beta diversity (Bray Curtis)[c]
Bacteria	T1 vs. T2	0.228	0.174	0.010
	T2 vs. T3	0.003	0.003	0.001
	T1 vs. T3	0.003	0.003	0.001
Fungi	T1 vs. T2	0.222	0.003	0.001
	T2 vs. T3	0.1	0.429	0.003
	T1 vs. T3	0.624	0.003	0.001

[a]P-values were determined using alpha diversity (observed OTUs and Shannon index) and beta diversity based on Bray Curtis metric. [b]Index and statistical analysis conducted on a rarefied OTU table at an even sequencing depth. [c]Index and statistical analysis conducted on a normalized OTU table using a CSS method.

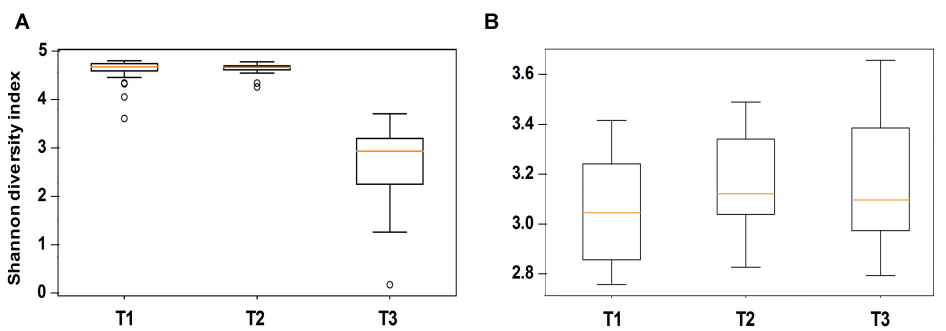

FIGURE 2 | Alpha diversity analysis (based on Shannon diversity index) of the bacterial **(A)** and fungal **(B)** communities in stored wheat grain samples. Analyzed samples were collected immediately after harvest during the first week of storage (T1), after 3 months of storage (T2), and after 6 months of storage (T3). The centered square represents the mean, orange line inside the box represents the median, and circles indicate outliers.

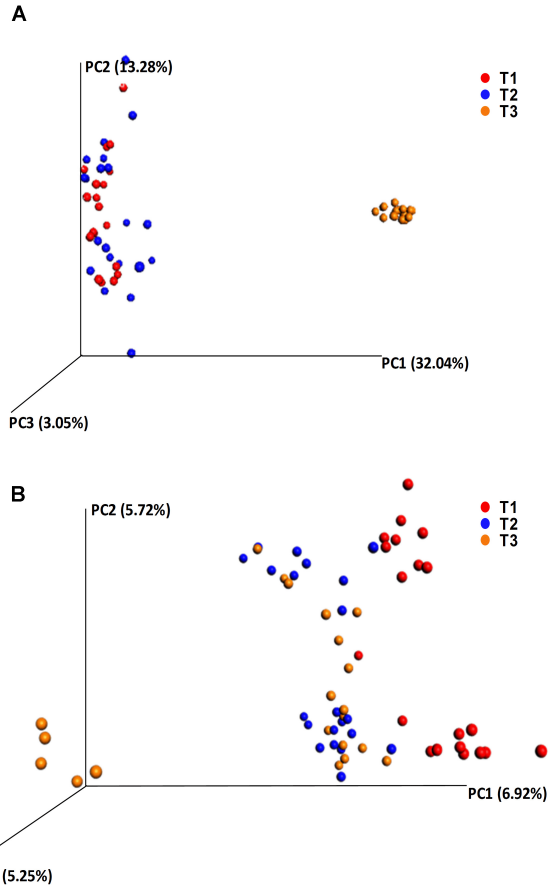

FIGURE 3 | Principle coordinate analysis (PCoA) based on the beta diversity Bray Curtis dissimilarity metrics, showing the distance in the bacterial **(A)** and fungal **(B)** communities between the samples collected at T1 (red dots), T2 (blue dots), and T3 (orange dots).

(PCoA) of the bacterial community, where samples from T3 were positioned far from T1 and T2 samples which formed a separate cluster (**Figure 3A**). PCoA analysis of the fungal community, however, did not provide any clear clustering based on sampling time (**Figure 3B**).

The relative abundance of fungal and bacterial genera detected in wheat grain samples across three sampling time points is shown in **Figure 4**. Bacterial communities of stored grains mainly consisted of genera of *Bacillus* (22.5%), followed by *Erwinia* (9.9%), *Pseudomonas* (5.9%), unidentified genera that belong to the family *Oxalobacteraceae* (4.3%), *Enterobacteriaceae* (3.7%), *Streptomyces* (3.3%), *Curtobacterium* (2.2%), and *Paenibacillus* (1.6%) (**Figure 4A**). Interestingly, *Bacillus* and *Erwinia* were the most abundant bacterial genera found at the last sampling time point (T3), which represented more than 70% of the total bacteria detected after phosphine fumigation (**Figure 4A**). In addition to the variations in community structure, the relative abundance of several other bacterial taxa, varied significantly between the different time points. Bacterial phylotypes that belongs to *Sphingomonas*, *Frigoribacterium*, *Ruminococcus*, *Hymenobacter*, *Acinetobacter*, *Chryseobacterium*, *Methylobacterium*, *Saccharibacillus*, *Staphylococcus*, *Agrobacterium*, *Pedobacter*, and *Comamonadaceae* were only present at the third sampling time point. In contrast, bacterial taxa such as *Ellin6067*, *Bdellovibrio*, *Prevotella*, *Bilophila*, *Parabacteroides*, and an unidentified group of *Leuconostocaceae* were present at almost equal relative abundance in T1 and T2 and then disappeared entirely in T3 (**Supplementary Figure S2**). Unlike bacteria, the most abundant fungal genera, such as *Alternaria* (59.2%), *Stemphylium* (10%), unidentified *Pleosporales* (8.6%), *Cladosporium* (3.4%), *Mycosphaerella* (3%), *Sporobolomyces* (2.7%), *Filobasidium* (2.6%), and *Puccinia* (1.5%), which accounted for more than 90% of the total fungal community, were equally present in all three of the sampled points (**Figure 4B**). Only three fungal genera, *Cortinarius*, *Dioszegia*, and *Monographella*, significantly changed in abundance over the three time points (**Supplementary Figure S3**).

Isolation and Identification of Bacteria and Fungi From Wheat Grains

Bacterial and fungal isolates were cultured from wheat grains sampled at the three storage time points to assess the impact of phosphine fumigation on microbial diversity and to evaluate potential interactions between the members of the shared microbiome. Forty bacterial and 44 fungal (24 yeasts and 20 filamentous fungi) isolates were cultured from seeds at the first time point (**Figure 5**). *Bacillus* spp. were predominant among cultured bacterial community (55%) followed by *Pseudomonas* spp. (12.5%) and *Pantoea* spp. (10%) (**Figure 5A**). *Cryptococcus* and *Rhodotorula* species predominated among the isolated yeasts cultures (39%) based on morphological features (colony color, texture, microscopic observation) and sequencing analysis. The same criteria indicated that 13 out of 44 cultured filamentous fungal isolates were *Alternaria* spp. (30%), followed by *Aspergillus* spp. (7%) (**Figure 5B**).

A more diverse bacterial community was identified in the bacterial isolates cultured at the second time point (60 isolates), where *Bacillus* spp. were most common (58%) (**Figure 5A**). The 38 fungal isolates cultured from wheat grains at the second time point were identified as *Alternaria* spp. (21%), *Fusarium* spp., *Massarina* spp., *Penicillium* spp., and *Phoma* spp. (5% for each genus). *Cryptococcus* and *Rhodotorula* spp. were still the most abundant (36%) yeast taxa (**Figure 5B**). A dramatic decrease was observed in the number of bacterial strains isolated from wheat grains sampled at the third time point (18 isolates). *Bacillus* and *Pseudomonas* spp. were the predominant isolates cultured from T3 samples (28% for each genus) (**Figure 5A**). The number of yeast isolates cultured from T3 samples was also significantly reduced compared to T1 and T2 (**Figure 5B**). Fungal abundance and diversity in T3 samples did not change, however, relative to T1 and T2. Fifteen filamentous fungal isolates, out of a total 22 fungal microorganisms, were cultured from stored seeds collected at the T3 time point. Mycotoxigenic fungi, such as *Alternaria* (27%) and *Fusarium* (18%) species, were predominant. The changes in microbial community composition identified in the culturing assay were

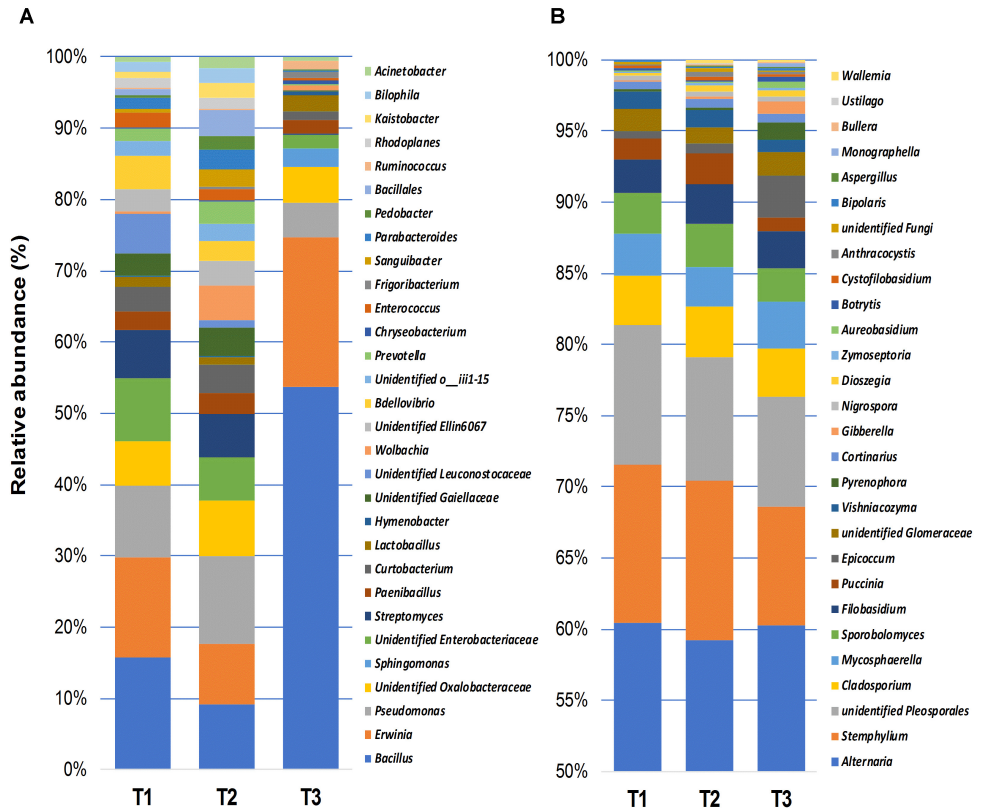

FIGURE 4 | Relative abundance of bacterial (≥0.5%) **(A)**, and fungal (≥0.1%) **(B)** genera detected using high-throughput sequencing technology across the samples collected at three storage time-points (T1, T2, T3).

in good agreement with results obtained in the alpha- and beta-diversity analyses (**Figures 2**, **3**).

Analysis of Mycotoxigenic Fungi in Stored Grains by Real-Time PCR

Since cultured fungal diversity was not influenced by phosphine fumigation and was generally consistent across the three sampled time points, real-time PCR method was utilized to quantify fungal DNA in stored grain samples. The broad-spectrum primers and specific fluorescent probes were used to amplify the targeted genomic DNA and to detect and quantify the major mycotoxigenic fungal genera, *Aspergillus*, *Fusarium,* and *Alternaria*.

The wheat grain samples collected throughout the entire study did not exhibit any evidence of spoilage. Nevertheless, the qPCR analysis indicated the presence of all three pathogenic genera in majority of the samples, which corroborates the results obtained in the culture assay of wheat grains. *Fusarium* DNA was detected in 11, 12, and 15 out of 21 wheat grain samples at T1, T2, and T3 time points, respectively, with an increased DNA content at T3 (**Figure 6A**). The obtained Ct values ranging between 27.62 and 32.78 indicated the presence of relatively low concentrations of *Fusarium* DNA in the samples (0.5 – 8 ng/mg; **Figure 6A**), suggesting that qPCR is more sensitive in detecting mycotoxigenic fungi compared to culture-based approaches. *Aspergillus* DNA was detected in only 10 and 3 out of 21 wheat grain samples collected at the T1 and T3 time points, respectively, with no detection in the T2 samples (**Figure 6B**). In contrast, 9 to 11 wheat grain samples in all three time points were found to be positive for *Alternaria* spp. by qPCR, and with a relatively higher fungal DNA content relative to the other tested mycotoxigenic species (**Figure 6C**).

Mycotoxin Detection in Stored Wheat Grains

The LC/MS/MS multi-toxin method was optimized for the simultaneous detection and quantification of 10 mycotoxins in wheat grain samples to investigate potential changes in mycotoxin levels in grains over the storage period of 6 months, including after phosphine fumigation for insect control. Results indicated that 17 wheat samples were positive for mycotoxin contamination and were above their limit of detection (LOD) but under the maximum EU regulatory limits (**Table 2**). AFB_2 was detected at 0.4 ppb in three wheat samples collected at T1 and the co-occurrence of AFG_2 was only observed in one of the samples. Two grain samples from T3 were also found to be contaminated with AFB_2 (**Table 2**). These findings are consistent with data obtained in the culturing assay and by qPCR, where *Aspergillus* spp. were also detected in T1 and T3 samples. The LC/MS/MS analysis also indicated the presence of fumonisins at values below

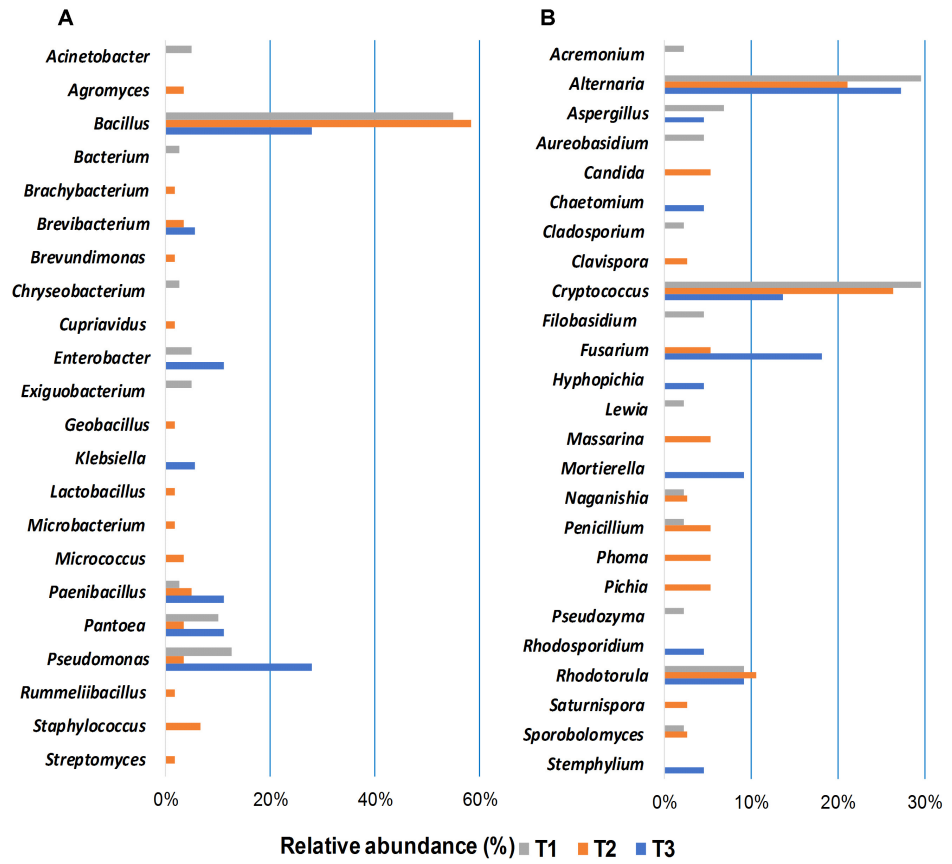

FIGURE 5 | Relative abundance of bacterial **(A)**, and fungal **(B)** genera isolated by plating from grain samples collected at three storage time-points (T1, T2, T3). The isolates were identified by sequencing the 16S rRNA gene in bacteria and ITS region in fungi; the sequences were determined via BLAST matches to the NCBI database.

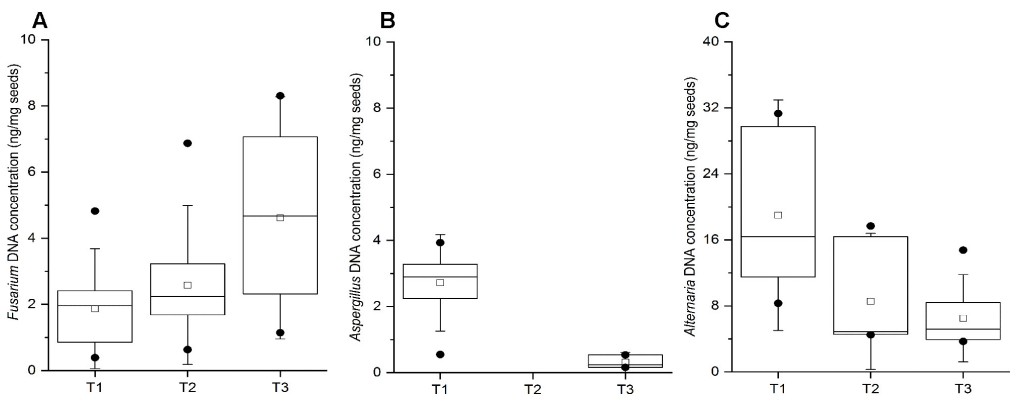

FIGURE 6 | Quantification by qPCR of *Fusarium* spp. **(A)** *Aspergillus* spp. **(B)**, and *Alternaria* spp. **(C)** in stored wheat grain at three storage time-points (T1, T2, T3). qPCR results are from at least two biological replicates (DNA extractions) and three technical replicates per sample. The lower and upper edges of each box correspond to the 25th and 75th percentiles. The black line inside the box represents the median, and centered square represents the mean. The whiskers represent 1.5× interquartile range. Dots indicate outliers.

the regulatory guidelines in the samples analyzed at all three time points. Notably, a strong link was observed between increased abundance of *Fusarium* spp. in T3 wheat grain samples, and the presence of DON toxin only in T3 samples (**Table 2**). These results indicate that phosphine fumigation significantly altered the structure of microbial community of stored wheat grains and induced shift in the abundance of mycotoxin-producing *Fusarium* taxa.

TABLE 2 | Mycotoxin contamination in stored wheat grain samples (ng/g)[a,b].

Sampling time-points	Sample #	AFB_1	AFB_2	AFG_1	AFG_2	FB_1	FB_2	DON	OTA	T-2	ZEN
T1	1	–	–	–	–	2.3 ± 0.48	–	–	–	–	–
	8	–	–	–	–	1.7 ± 0.23	–	–	–	–	–
	9	–	0.4 ± 0.01	–	–	–	–	–	–	–	–
	11	–	–	–	–	–	9.4 ± 1.75	–	–	–	–
	14	–	–	–	–	1.9 ± 0.09	–	–	–	–	–
	16	–	0.4 ± 0.012	–	–	2.0 ± 0.14	–	–	–	–	–
	17	–	0.4 ± 0.002	–	1.9 ± 0.01	3.4 ± 0.12	–	–	–	–	–
T2	22	–	–	–	–	2.4 ± 0.02	–	–	–	–	–
	24	–	–	–	–	–	9.5 ± 0.78	–	–	–	–
	25	–	–	–	–	–	–	–	–	–	–
	30	–	–	–	–	2.5 ± 0.02	–	–	–	–	–
T3	45	–	0.4 ± 0.017	–	–	2 ± 0.01	–	–	–	–	–
	46	–	–	–	–	–	–	38.8 ± 1.90	–	–	–
	47	–	0.4 ± 0.022	–	–	–	–	–	–	–	–
	48	–	–	–	–	–	–	21.2 ± 1.10	–	–	–
	51	–	–	–	–	1.4 ± 0.08	–	–	–	–	–
	58	–	–	–	–	–	–	144.1 ± 9.1	–	–	–
	60	–	–	–	–	–	–	7.7 ± 0.69	–	0.2 ± 0.001	–

[a] *The table represents the positive samples data only.* [b] *Average values of mycotoxin concentration ± standard error (the measurements were repeated 3 times). "–" not detected.*

DISCUSSION

An objective of the present study was to characterize the composition of microbial communities associated with stored wheat grains and to identify any changes in the diversity and composition of the wheat microbiome during storage and in response to phosphine fumigation to control insect pests. Characterizing the microbiota of wheat grains after harvest is an essential step to understanding the interactions that potentially occur between different members of the community in relation to the colonization of the grains with common mycotoxigenic fungi (*Aspergillus*, *Fusarium*, *Penicillium,* and *Alternaria* species). Results of the HTS analysis indicated that fumigation of the grains with phosphine had a significant effect on the diversity and abundance of various components of the wheat-grain microbiome. It is known that many other factors could affect the stored seed microbial community such as temperature, humidity, water activity, grain moisture (Schmidt et al., 2018). Nevertheless, in the current study, the impact of such environmental factors was minor due to the optimal and stable weather conditions during a 6-months storage period. In general, the composition of the bacterial and fungal microbiota of wheat grains found in the current study is in agreement with previous studies (Karlsson et al., 2014, 2017; Comby et al., 2016; Díaz Herrera et al., 2016; Gdanetz and Trail, 2017). Genera, including *Bacillus, Erwinia, Pseudomonas,* and *Paenibacillus* were dominant bacterial taxa identified, while *Alternaria*, *Stemphylium*, *Cladosporium*, *Sporobolomyces*, *Mycosphaerella*, and *Filobasidium* were the most prevalent fungi and represent the most common members of the wheat grain mycobiome. The majority of the detected bacteria taxa, with the exception of *Erwinia*, are known to have a beneficial impact on plants. For instance, *Bacillus* species are known to have a growth promotive effect on wheat plants and are generally isolated from both grains and the rhizosphere (Tao et al., 2014; Pan et al., 2015; Cherif-Silini et al., 2016). *Paenibacillus* is recognized as a predominantly endophytic bacterium in wheat plants and seeds, also with growth promotive effects (Díaz Herrera et al., 2016; Hao and Chen, 2017). Similarly, *Pseudomonas* contains several species that promote plant growth by suppressing pathogenic microorganisms, and synthesizing growth-stimulating plant hormones (Preston, 2004). Notably, however, other species of *Pseudomonas* may be phytopathogenic. In the present study, the results obtained with the culturing assay of stored wheat grains microbes were in agreement with the results obtained by HTS sequencing data. *Bacillus*, *Pseudomonas,* and *Pantoea* were found to be most abundant genera obtained in the cultured bacterial taxa isolated from stored wheat grains throughout the study, and the same was true in the HTS analysis.

The data indicated that phosphine fumigation significantly affected the microbial community associated with wheat grains. Phosphine or hydrogen phosphide (PH_3) is a low molecular weight compound that diffuses rapidly and penetrates deeply into materials, such as the bulk storage of grain (Bond, 1989). It is the dominant fumigant used to control insect pests in stored grain and many other stored commodities. Since phosphine is toxic to aerobically respiring organisms, it also has effects on the survival and growth of some aerobic bacteria and fungi (Hocking and Banks, 1991; Castro et al., 2000). In the present study, bacterial population exhibited a drastic reduction in their level of diversity and the number of observed species after fumigation. Highly abundant bacteria, including *Streptomyces*, *Ellin606*, *Bdellovibrio*, *Prevotella*, *Bilophila*, and unidentified groups of *Parabacteroides*, and *Leuconostocaceae* that collectively

accounted for approximately 45% of the total bacterial OTUs in the first two time points (T1 and T2), disappeared entirely in T3 after the phosphine treatment. This change corresponded with a significant increase in *Bacillus* from an average of 2.2% in T1 and T2 to more than 50% in T3 (**Supplementary Figure S2**). A similar trend was reported by Yuan et al. (2018), who reported that the abundance of *Bacillus* spp. in wheat grains increased from 2 to 36% after 9 months of storage and up to 48% after 12 months of storage at different position within a storage silo. Interestingly, in that study, the authors indicated that stored wheat grain was treated with ozone to kill insects.

Small quantities of stable but harmless breakdown products of phosphine, which become incorporated into normal cellular metabolism as phosphates and phosphites, may remain in fumigated materials (Nath et al., 2011). *Bacillus* and *Pseudomonas* spp. are capable of utilizing phosphite and belong to the group of phosphate solubilizing bacteria, which play an important role in plant growth promotion (Foster et al., 1978; Metcalf and Wolfe, 1998; Igual et al., 2001; Park et al., 2009; Kang et al., 2014). *Bacillus* and *Pseudomonas* may take advantage of these unique abilities after phosphine fumigation to enhance their survival and proliferation. The exclusive increase in the abundance of *Sphingomonas* species, which are aerobic bacteria utilized for environmental remediation due to their ability to degrade aromatic compounds (Story et al., 2004), after phosphine fumigation, may indicate their involvement in the degradation of this toxic substance. Since one of the main modes of action of phosphine is the inhibition of *cytochrome c oxidase* (Price, 1980), apparently some oxidase-negative bacteria (*i.e.,* those that do not rely on cytochrome c oxidase in respiration), such as *Acinetobacter, Lactobacillus, Ruminococcus, Methylobacterium, Saccharibacillus,* and *Frigoribacterium* species, may survive and proliferate following phosphine treatment.

Results indicated that neither the diversity nor abundance of fungi were affected by phosphine fumigation. Only a few studies have described the influence of phosphine on the survival and growth of molds in stored grains. Phosphine was reported to have little effect on populations of fungi that were unable to grow in stored grains under conditions of limiting water activity (a_w 0.8–0.86) (Raghunathan et al., 1969; Sinha et al., 1967; Hocking and Banks, 1991). Natarajan and Bagyaraj (1984) noted some reduction in fungal growth on legumes when exposed to very high phosphine levels (100 g/m^3), particularly at limiting a_w conditions (0.8). It seems that the effect of phosphine on fungal growth, however, may vary between fungal species and the type of stored grain or seed. Phosphine was shown to inhibit the growth of *A. flavus* and/or *A. parasiticus* and aflatoxin production on peanuts in both laboratory and warehouse experiments (Castro et al., 1992, 1995, 1996). A reduction of *A. flavus* growth and aflatoxin production was also observed in response to phosphine treatment of maize kernels stored at different moisture levels (Castro et al., 2000). In the same study, however, the authors stated that *Penicillium* species and *F. verticillioides*, which are commonly found in freshly harvested grains, were tolerant to phosphine (Castro et al., 2000). Those findings are consistent with the results obtained in the current study of wheat-grain-associated microflora, in which a greater number of *Fusarium* species, such as *F. culmorum* and *F. proliferatum*, were detected at the last sampling time point (T3), probably due to the changes that occurred in microbial community composition following phosphine fumigation. Notably, the presence of mycotoxigenic *Fusarium* isolates in the stored wheat grains after fumigation was strongly associated with the occurrence of DON in T3 samples, suggesting that phosphine induced a shift in the microbial composition toward more toxigenic strains. Shifts in *Fusarium* species composition on cereal grain due to changes in climate and cultivation practices have been previously reported (Garrett et al., 2011). Magan et al. (2011) investigated the effect of climate change on mycotoxin-producing fungi and indicated that shifts toward *Fusarium* pathogens and DON contamination in cereals may occur due to changes in management practices. For example, the effect of fungicides on *Fusarium* infections could be different depending on the antifungal compound, the time of treatment, and the composition of the microbial flora in cereals (Pirgozliev et al., 2003). Henriksen and Elen (2005) reported that different fungicides (such as propiconazole and cyprodinil) significantly increased the infection level of DON-producing *F. avenaceum*, *F. tricinctum,* and *F. culmorum* in grains.

CONCLUSION

In summary, our study demonstrated that phosphine fumigation had a significant impact on microbial community composition in stored wheat grain. The shifts in bacterial and yeast populations, coincident with the fumigant application may have also led to changes in the functional diversity of those communities. Fumigation did not change filamentous fungal abundance in stored grains at T3; however, phosphine treatment apparently altered the community composition of molds, relative to T1 and T2. Previous studies have extensively investigated the effect of different fumigants on soil bacterial communities (Engelen et al., 1998; Ibekwe et al., 2001; van Agtmaal et al., 2015; Zhang et al., 2017). To our knowledge, however, there are no published studies describing the impact of pesticide treatment on the microbiome of stored wheat grains using combined HTS analysis and culture assays. The development of next generation sequencing (NGS) technologies have provided a deeper understanding of the microbiome on plant material, as well human and animal subjects, and a host of different physical environments. Since many of the microorganisms identified by NGS technology are not culturable, it would be very difficult to detect alterations in microbial community diversity and abundance after phosphine treatment using only classical culturing and molecular identification approaches. Findings in the current study are consistent with previous studies, where NGS technology was able to identify changes in the microbiome that were not detectable using classical methodologies (Sylla et al., 2013; Schmidt et al., 2014). A better understanding of the interactions that occur among the different members of the microbial community of stored wheat grains at specific time points (e.g., before and/or after fumigant application) can assist in the prediction of fungal disease incidence and mycotoxin production, as well as in the development of novel approaches

for controlling mycotoxin contamination in grains and managing crop diseases in general.

DATA AVAILABILITY

The raw sequence files supporting the findings of this article are available in the NCBI Sequence Read Archive (SRA) under the BioProject ID PRJNA503713.

AUTHOR CONTRIBUTIONS

MKS, AA, SD, and ES conceived and designed the experiments, analyzed the data, and wrote the manuscript. MKS, AA, MB, VZ, and MW performed the experiments. MW provided critical comments on the study and edited the manuscript. All authors read and approved the final manuscript.

FUNDING

This study was supported by a grant (No. 20–06–0055) from the Chief Scientist of the Israeli Ministry of Agriculture and Rural Development.

ACKNOWLEDGMENTS

We thank Dr. Moshe Kostyukovsky for his assistance during the wheat grains samples collection from storage facilities.

SUPPLEMENTARY MATERIAL

The Supplementary Material for this article can be found online at: https://www.frontiersin.org/articles/10.3389/fmicb.2019.01098/full#supplementary-material

REFERENCES

Abarenkov, K., Henrik Nilsson, R., Larsson, K.-H., Alexander, I. J., Eberhardt, U., Erland, S., et al. (2010). The UNITE database for molecular identification of fungi - recent updates and future perspectives. *New Phytol.* 186, 281–285. doi: 10.1111/j.1469-8137.2009.03160.x

Altschul, S. F., Gish, W., Miller, W., Myers, E. W., and Lipman, D. J. (1990). Basic local alignment search tool. *J. Mol. Biol.* 215, 403–410. doi: 10.1016/S0022-2836(05)80360-2

Bell, C. (2000). Fumigation in the 21st century. *Crop Prot.* 19, 563–569. doi: 10.1016/S0261-2194(00)00073-9

Berners-Price, S. J., and Sadler, P. J. (1988). Phosphines and metal phosphine complexes: relationship of chemistry to anticancer and other biological activity. *Bioinorg. Chem.* 70, 27–102. doi: 10.1007/3-540-50130-4_2

Bolger, A. M., Lohse, M., and Usadel, B. (2014). Trimmomatic: a flexible trimmer for Illumina sequence data. *Bioinformatics* 30, 2114–2120. doi: 10.1093/bioinformatics/btu170

Bond, E. J. (1989). *Manual of Fumigation for Insect Control*. FAO Plant Protection Paper no. 54. Rome: Food and Agriculture Organization of the United Nations, 432.

Brader, G., Compant, S., Vescio, K., Mitter, B., Trognitz, F., Ma, L.-J., et al. (2017). Ecology and genomic insights into plant-pathogenic and plant-nonpathogenic endophytes. *Annu. Rev. Phytopathol.* 55, 61–83. doi: 10.1146/annurev-phyto-080516-0-35641

Bray, J. R., and Curtis, J. T. (1957). An ordination of the upland forest communities of southern Wisconsin. *Ecol. Monogr.* 27, 325–349. doi: 10.2307/1942268

Caporaso, J. G., Kuczynski, J., Stombaugh, J., Bittinger, K., Bushman, F. D., Costello, E. K., et al. (2010). QIIME allows analysis of high-throughput community sequencing data. *Nat. Methods* 7, 335–336. doi: 10.1038/nmeth.f.303

Castro, M. F. P. M., De Pacheco, I. A., and Taniwaki, M. H. (1992). Effects of phosphine on aflatoxin production in peanuts stored with a high content. *Methyl Bromide Technical Options Workshop*, Washington.

Castro, M. F. P. P. M., de Pacheco, I. A., Soares, L. M. V., Furlani, R. P. Z., Paula, D. C., de, et al. (1996). Warehouse control of *Aspergillus flavus* Link and A. Parasiticus speare on peanuts (*Arachis hypogaea*) by phosphine fumigation and its effect on aflatoxin production. *J. Food Prot.* 59, 407–411. doi: 10.4315/0362-028X-59.4.407

Castro, P. P. M. F. M., Pacheco, I. A., Soares, L. M. V., and Furlani, R. P. (1995). Phosphine fumigation of stored peanuts for *Aspergillus flavus* Link/*Aspergillus parasiticus* speare and aflatoxins control. *Rev. Microbiol.* 26, 296–301.

Castro, M. F. P. M., De Leitao, M. F. F., Do Vale, J. O., Bragnolo, N., Anichiareo, E. S., and Mills, K. A. (2000). "Effects of phosphine in the development of *Aspergillus flavus* aflatoxin production in maize grains stored at different moisture contents," in *Proceedings of the International Working Conference on Controlled Atmosphere and Fumigation in Stored Products*, Vol. 29, eds E. J. Donahaye, S. Navarro, and J. G. Leesch (Fresno, CA: Executive Printing Services), 179–191.

Cherif-Silini, H., Silini, A., Yahiaoui, B., Ouzari, I., and Boudabous, A. (2016). Phylogenetic and plant-growth-promoting characteristics of *Bacillus* isolated from the wheat rhizosphere. *Ann. Microbiol.* 66, 1087–1097. doi: 10.1007/s13213-016-1194-6

Comby, M., Lacoste, S., Baillieul, F., Profizi, C., and Dupont, J. (2016). Spatial and temporal variation of cultivable communities of co-occurring endophytes and pathogens in wheat. *Front. Microbiol.* 7:403. doi: 10.3389/fmicb.2016.00403

De, S., Kaur, G., Roy, A., Dogra, G., Kaushik, R., Yadav, P., et al. (2010). A simple method for the efficient isolation of genomic DNA from *Lactobacilli* isolated from traditional indian fermented milk (dahi). *Indian J. Microbiol.* 50, 412–418. doi: 10.1007/s12088-011-0079-4

DeSantis, T. Z., Hugenholtz, P., Larsen, N., Rojas, M., Brodie, E. L., Keller, K., et al. (2006). Greengenes, a chimera-checked 16S rRNA gene database and workbench compatible with ARB. *Appl. Environ. Microbiol.* 72, 5069–5072. doi: 10.1128/AEM.03006-05

Díaz Herrera, S., Grossi, C., Zawoznik, M., and Groppa, M. D. (2016). Wheat seeds harbour bacterial endophytes with potential as plant growth promoters and biocontrol agents of *Fusarium graminearum*. *Microbiol. Res.* 186, 37–43. doi: 10.1016/J.MICRES.2016.03.002

Edgar, R. C. (2010). Search and clustering orders of magnitude faster than BLAST. *Bioinformatics* 26, 2460–2461. doi: 10.1093/bioinformatics/btq461

Engelen, B., Meinken, K., von Wintzingerode, F., Heuer, H., Malkomes, H. P., and Backhaus, H. (1998). Monitoring impact of a pesticide treatment on bacterial soil communities by metabolic and genetic fingerprinting in addition to conventional testing procedures. *Appl. Environ. Microbiol.* 64, 2814–2821.

Foster, T. L., Winans, L., Helms, S. J., and Helms, S. J. (1978). Anaerobic utilization of phosphite and hypophosphite by bacillus sp. *Appl. Environ. Microbiol.* 35, 937–944.

Garrett, K. A., Forbes, G. A., Savary, S., Skelsey, P., Sparks, A. H., Valdivia, C., et al. (2011). Complexity in climate-change impacts: an analytical framework for effects mediated by plant disease. *Plant Pathol.* 60, 15–30. doi: 10.1111/j.1365-3059.2010.02409.x

Gdanetz, K., and Trail, F. (2017). The wheat microbiome under four management strategies, and potential for endophytes in disease protection. *Phytobiomes* 1, 158–168. doi: 10.1094/PBIOMES-05-17-0023-R

Hao, T., and Chen, S. (2017). Colonization of wheat, maize and cucumber by *Paenibacillus polymyxa* WLY78. *PLoS One* 12:e0169980. doi: 10.1371/journal.pone.0169980

Hartmann, M., Frey, B., Mayer, J., Mäder, P., and Widmer, F. (2015). Distinct soil microbial diversity under long-term organic and conventional farming. *ISME J.* 9, 1177–1194. doi: 10.1038/ismej.2014.210

Henriksen, B., and Elen, O. (2005). Natural *Fusarium* grain infection level in wheat, barley and oat after early application of fungicides and herbicides. *J. Phytopathol.* 153, 214–220. doi: 10.1111/j.1439-0434.2005.00955.x

Hocking, A. D., and Banks, H. J. (1991). Effects of phosphine fumigation on survival and growth of storage fungi in wheat. *J. Stored Prod. Res.* 27, 115–120. doi: 10.1016/0022-474X(91)90021-4

Ibekwe, A. M., Papiernik, S. K., Gan, J., Yates, S. R., Yang, C. H., and Crowley, D. E. (2001). Impact of fumigants on soil microbial communities. *Appl. Environ. Microbiol.* 67, 3245–3257. doi: 10.1128/AEM.67.7.3245-3257.2001

Igual, J., Valverde, A., Cervantes, E., and Velazquez, E. (2001). Phosphate-solubilizing bacteria as inoculants 979 for agriculture: use updated molecular techniques in their study. *Agronomie* 21, 561–568. doi: 10.1051/agro:2001145

Kang, S.-M., Radhakrishnan, R., You, Y.-H., Joo, G.-J., Lee, I.-J., Lee, K.-E., et al. (2014). Phosphate solubilizing *Bacillus megaterium* mj1212 regulates endogenous plant carbohydrates and amino acids contents to promote mustard plant growth. *Indian J. Microbiol.* 54, 427–433. doi: 10.1007/s12088-014-0476-6

Karlsson, I., Friberg, H., Kolseth, A.-K., Steinberg, C., and Persson, P. (2017). Organic farming increases richness of fungal taxa in the wheat phyllosphere. *Mol. Ecol.* 26, 3424–3436. doi: 10.1111/mec.14132

Karlsson, I., Friberg, H., Steinberg, C., and Persson, P. (2014). Fungicide effects on fungal community composition in the wheat phyllosphere. *PLoS One* 9:e111786. doi: 10.1371/journal.pone.0111786

Kruskal, W. H., and Wallis, W. A. (1952). Use of ranks in one-criterion variance analysis. *J. Am. Stat. Assoc.* 47, 583–621. doi: 10.1080/01621459.1952.10483441

Links, M. G., Demeke, T., Gräfenhan, T., Hill, J. E., Hemmingsen, S. M., and Dumonceaux, T. J. (2014). Simultaneous profiling of seed-associated bacteria and fungi reveals antagonistic interactions between microorganisms within a shared epiphytic microbiome on *Triticum* and *Brassica* seeds. *New Phytol.* 202, 542–553. doi: 10.1111/nph.12693

Lozupone, C., and Knight, R. (2005). UniFrac: a new phylogenetic method for comparing microbial communities. *Appl. Environ. Microbiol.* 71, 8228–8235. doi: 10.1128/AEM.71.12.8228-8235.2005

Magan, N., Aldred, D., Hope, R., and Mitchell, D. (2010). Grain and Grapes: effects on growth, deoxynivalenol and ochratoxin production by *Fusarium culmorum* and *Aspergillus carbonarius*. *Toxins* 2, 353–366. doi: 10.3390/toxins2030353

Magan, N., Medina, A., and Aldred, D. (2011). Possible climate-change effects on mycotoxin contamination of food crops pre- and postharvest. *Plant Pathol.* 60, 150–163. doi: 10.1111/j.1365-3059.2010.02412.x

Mahoney, A. K., Yin, C., and Hulbert, S. H. (2017). Community structure, species variation, and potential functions of rhizosphere-associated bacteria of different winter wheat (*Triticum aestivum*) cultivars. *Front. Plant Sci.* 8:132. doi: 10.3389/fpls.2017.00132

Masella, A. P., Bartram, A. K., Truszkowski, J. M., Brown, D. G., and Neufeld, J. D. (2012). PANDAseq: paired-end assembler for Illumina sequences. *BMC Bioinformatics* 13:31. doi: 10.1186/1471-2105-13-31

McDonald, D., Price, M. N., Goodrich, J., Nawrocki, E. P., DeSantis, T. Z., Probst, A., et al. (2012). An improved greengenes taxonomy with explicit ranks for ecological and evolutionary analyses of bacteria and archaea. *ISME J.* 6, 610–618. doi: 10.1038/ismej.2011.139

Metcalf, W. W., and Wolfe, R. S. (1998). Molecular genetic analysis of phosphite and hypophosphite oxidation by *Pseudomonas* stutzeri WM88. *J. Bacteriol.* 180, 5547–5558.

Mousa, W. K., Shearer, C., Limay-Rios, V., Ettinger, C. L., Eisen, J. A., and Raizada, M. N. (2016). Root-hair endophyte stacking in finger millet creates a physicochemical barrier to trap the fungal pathogen *Fusarium graminearum*. *Nat. Microbiol.* 1:16167. doi: 10.1038/nmicrobiol.2016.167

Natarajan, T., and Bagyaraj, D. J. (1984). Fumigation effect on micro flora and viability of black gram and field bean seeds. *Pesticides* 18, 40–42.

Nath, N. S., Bhattacharya, I., Tuck, A. G., Schlipalius, D. I., and Ebert, P. R. (2011). Mechanisms of phosphine toxicity. *J. Toxicol.* 2011:494168. doi: 10.1155/2011/494168

Ofek, M., Voronov-Goldman, M., Hadar, Y., and Minz, D. (2014). Host signature effect on plant root-associated microbiomes revealed through analyses of resident vs. Active communities. *Environ. Microbiol.* 16, 2157–2167. doi: 10.1111/1462-2920.12228

Pan, D., Mionetto, A., Tiscornia, S., and Bettucci, L. (2015). Endophytic bacteria from wheat grain as biocontrol agents of *Fusarium graminearum* and deoxynivalenol production in wheat. *Mycotoxin Res.* 31, 137–143. doi: 10.1007/s12550-015-0224-8

Park, K.-H., Lee, C.-Y., and Son, H.-J. (2009). Mechanism of insoluble phosphate solubilization by *Pseudomonas fluorescens* RAF15 isolated from ginseng rhizosphere and its plant growth-promoting activities. *Lett. Appl. Microbiol.* 49, 222–228. doi: 10.1111/j.1472-765X.2009.02642.x

Paulson, J. N., Stine, O. C., Bravo, H. C., and Pop, M. (2013). Differential abundance analysis for microbial marker-gene surveys. *Nat. Methods* 10, 1200–1202. doi: 10.1038/nmeth.2658

Pirgozliev, S. R., Edwards, S. G., Hare, M. C., and Jenkinson, P. (2003). Strategies for the control of Fusarium head blight in cereals. *Eur. J. Plant Pathol.* 109, 731–742. doi: 10.1023/A:1026034509247

Placinta, C. M., D'Mello, C. P. F., and MacDonald, A. M. C. (1999). A review of worldwide contamination of cereal grains and animal feed with *Fusarium* mycotoxins. *Anim. Feed Sci. Technol.* 78, 21–37. doi: 10.1016/s0377-8401(98)00278-8

Preston, G. M. (2004). Plant perceptions of plant growth-promoting *Pseudomonas*. *Philos. Trans. R. Soc. Lond. B. Biol. Sci.* 359, 907–918. doi: 10.1098/rstb.2003.1384

Price, N. R. (1980). Some aspects of the inhibition of cytochrome c oxidase by phosphine in susceptible and resistant strains of *Rhyzopertha dominicia*. *Insect Biochem.* 10, 147–150. doi: 10.1016/0020-1790(80)90065-7

Raghunathan, A. N., Muthu, M., and Majumder, S. K. (1969). Control of internal fungi of sorghum by fumigation. *J. Stored Prod. Res.* 5, 389–392. doi: 10.1016/0022-474X(69)90012-5

Rognes, T., Flouri, T., Nichols, B., Quince, C., and Mahé, F. (2016). VSEARCH: a versatile open source tool for metagenomics. *PeerJ* 4:e2584. doi: 10.7717/peerj.2584

Sadhasivam, S., Britzi, M., Zakin, V., Kostyukovsky, M., Trostanetsky, A., Quinn, E., et al. (2017). Rapid detection and identification of mycotoxigenic fungi and mycotoxins in stored wheat grain. *Toxins* 9:302. doi: 10.3390/toxins9100302

Schmidt, M., Zannini, E., and Arendt, E. (2018). Recent advances in physical post-harvest treatments for shelf-life extension of cereal crops. *Foods* 7:45. doi: 10.3390/foods7040045

Schmidt, R., Köberl, M., Mostafa, A., Ramadan, E. M., Monschein, M., Jensen, K. B., et al. (2014). Effects of bacterial inoculants on the indigenous microbiome and secondary metabolites of chamomile plants. *Front. Microbiol.* 5:64. doi: 10.3389/fmicb.2014.00064

Shiferaw, B., Smale, M., Braun, H.-J., Duveiller, E., Reynolds, M., and Muricho, G. (2013). Crops that feed the world 10. Past successes and future challenges to the role played by wheat in global food security. *Food Secur.* 5, 291–317. doi: 10.1007/s12571-013-0263-y

Sinha, R. N., Berck, B., and Wallace, H. A. H. (1967). Effect of phosphine on mites, insects, and microorganisms. *J. Econ. Entomol.* 60, 125–132. doi: 10.1093/jee/60.1.125

Story, S. P., Kline, E. L., Hughes, T. A., Riley, M. B., and Hayasaka, S. S. (2004). Degradation of aromatic hydrocarbons by *Sphingomonas paucimobilis* Strain EPA505. *Arch. Environ. Contam. Toxicol.* 47, 168–176. doi: 10.1007/s00244-004-3069-2

Sylla, J., Alsanius, B. W., Krüger, E., Reineke, A., Strohmeier, S., and Wohanka, W. (2013). Leaf microbiota of strawberries as affected by biological control agents. *Phytopathology* 103, 1001–1011. doi: 10.1094/PHYTO-01-13-0014-R

Tao, A., Pang, F., Huang, S., Yu, G., Li, B., and Wang, T. (2014). Characterisation of endophytic *Bacillus thuringiensis* strains isolated from wheat plants as biocontrol agents against wheat flag smut. *Biocontrol Sci. Technol.* 24, 901–924. doi: 10.1080/09583157.2014.904502

van Agtmaal, M., van Os, G. J., Hol, W. H. G., Hundscheid, M. P. J., Runia, W. T., Hordijk, C. A., et al. (2015). Legacy effects of anaerobic soil disinfestation on soil bacterial community composition and production of pathogen-suppressing volatiles. *Front. Microbiol.* 6:701. doi: 10.3389/fmicb.2015.00701

Yuan, Q.-S., Yang, P., Wu, A.-B., Zuo, D.-Y., He, W.-J., Guo, M.-W., et al. (2018). Variation in the microbiome, trichothecenes, and aflatoxins in stored wheat grains in Wuhan, China. *Toxins* 10:171. doi: 10.3390/toxins10050171

Zhang, J., Kobert, K., Flouri, T., and Stamatakis, A. (2014). PEAR: a fast and accurate illumina paired-end reAd mergeR. *Bioinformatics* 30, 614–620. doi: 10.1093/bioinformatics/btt593

Zhang, S., Liu, X., Jiang, Q., Shen, G., and Ding, W. (2017). Legacy effects of continuous chloropicrin-fumigation for 3-years on soil microbial community composition and metabolic activity. *AMB Express* 7:178. doi: 10.1186/s13568-017-0475-1

Conflict of Interest Statement: The authors declare that the research was conducted in the absence of any commercial or financial relationships that could be construed as a potential conflict of interest.

frontiers in Microbiology

ORIGINAL RESEARCH
published: 24 July 2019
doi: 10.3389/fmicb.2019.01629

An Apple a Day: Which Bacteria Do We Eat With Organic and Conventional Apples?

*Birgit Wassermann, Henry Müller and Gabriele Berg**

Institute of Environmental Biotechnology, Graz University of Technology, Graz, Austria

Apples are among the most consumed fruits world-wide. They represent a source of direct human exposure to bacterial communities, which is less studied. We analyzed the apple microbiome to detect differences between tissues and the impact of organic and conventional management by a combined approach of 16S rRNA gene amplicon analysis and qPCR, and visualization using fluorescence *in situ* hybridization and confocal laser scanning microscopy (FISH-CLSM). Each apple fruit harbors different tissues (stem, peel, fruit pulp, seeds, and calyx), which were colonized by distinct bacterial communities. Interestingly, fruit pulp and seeds were bacterial hot spots, while the peel was less colonized. In all, approximately 10^8 16S rRNA bacterial gene copy numbers were determined in each g apple. Abundances were not influenced by the management practice but we found a strong reduction in bacterial diversity and evenness in conventionally managed apples. In addition, despite the similar structure in general dominated by *Proteobacteria* (80%), *Bacteroidetes* (9%), *Actinobacteria* (5%), and *Firmicutes* (3%), significant shifts of almost 40% of bacterial genera and orders were monitored. Among them, especially bacterial signatures known for health-affecting potential were found to be enhanced in conventionally managed apples. Our results suggest that we consume about 100 million bacterial cells with one apple. Although this amount was the same, the bacterial composition was significantly different in conventionally and organically produced apples.

Keywords: *Malus domestica*, management practice, plant protection, microbiota, carposphere, edible microbiome, one health concept

OPEN ACCESS

Edited by:
Jia Liu,
Chongqing University of Arts and Sciences, China

Reviewed by:
Samir Droby,
Volcani Center, Israel
Xuehong Wu,
China Agricultural University (CAU), China

***Correspondence:**
Gabriele Berg
gabriele.berg@tugraz.at

Specialty section:
This article was submitted to Microbial Symbioses, a section of the journal Frontiers in Microbiology

Received: *29 May 2019*
Accepted: *02 July 2019*
Published: *24 July 2019*

Citation:
Wassermann B, Müller H and Berg G (2019) An Apple a Day: Which Bacteria Do We Eat With Organic and Conventional Apples? Front. Microbiol. 10:1629. doi: 10.3389/fmicb.2019.01629

INTRODUCTION

The host-associated microbiota is involved in health issues of the host; this was shown for humans and plants as well (Derrien and van Hylckama Vlieg, 2015; Berg et al., 2017). Despite being specifically composed and partly deeply embedded within the host, microbial communities are essentially open and interconnected ecosystems (Berg, 2015). However, this connection and the exchange between microbiomes are less understood, despite their importance to health reflected now also in the one health concept (Flandroy et al., 2018). The plant-gut microbiome axis could be of special importance for human health, and raw-eaten plants

seem an important source for microbes (Leff and Fierer, 2013; Berg et al., 2014; Wassermann et al., 2017). Recently it was shown that plant-associated microbiota including bacteria, fungi and viruses transiently colonized the gut (David et al., 2014); thus, forming our transient microbiome (Derrien and van Hylckama Vlieg, 2015). However, the microbial diversity associated with vegetables, fruits and herbs is less studied, especially in this context. In contrast, research and rules in this area focus on food-borne pathogens and food safety; food-borne diseases are recognized as a global burden (World Health Organization [WHO], 2015). First microbiome studies suggest that improved understanding of how certain ecologies provide supportive resources for human pathogens on plants, and how components of certain agro-ecologies may play a role in the introduction of human pathogens to plants (Ottesen et al., 2019). However, more knowledge on fresh produce-associated microbiota and a holistic view on the system is crucial for food safety inquiries (Blau et al., 2018).

The plant microbiota play an essential role in plant development and health and exert influence on resilience toward biotic as well as abiotic factors (Berg et al., 2016). In general, the plant microbiota is driven by the plant genotype, differs strongly between below and above ground parts and is affected by soil quality and biotic and abiotic conditions (Berg and Smalla, 2009; Vorholt, 2012; Philippot et al., 2013). While a core plant microbiome is vertically transmitted by seeds, the surrounding environment is another source of the plant microbiota (Berg and Raaijmakers, 2018). Many driving and assembly factors of the plant microbiome are already identified; in agricultural ecosystems management practices have a crucial influence on microbiota composition, diversity and functionality, subsequently affecting health and performance of the host plant (Philippot et al., 2013). Our understanding of the plant microbiome was improved by studies on the model plant *Arabidopsis thaliana* and important crops such as rice and maize (Bulgarelli et al., 2012; Lundberg et al., 2012; Peiffer et al., 2013) but the specific fruit and vegetable microbiome is understudied (Leff and Fierer, 2013). Tomato is a model vegetable for microbiome studies (Bergna et al., 2018; Kwak et al., 2018; Ottesen et al., 2019); in parallel, apples are models for fruit microbiomes.

Apples are among the most consumed fruits world-wide; their production is increasing constantly, and comprise about 83 million t (FAO, 2019). Apples represent the most important dietary source for various flavonoids in our diets, and a beneficial impact on human health due to apple procyanidins and pectin has been frequently described (Shoji and Miura, 2014; Sanz et al., 2015; Shtriker et al., 2018). Studies suggest that apple supplementation can induce substantial changes in microbiota composition and metabolic activity *in vitro*, which could be associated with potential benefits to human health (Koutsos et al., 2017; Garcia-Mazcorro et al., 2019). However, less is known about the apple microbiome; previous work has focused largely on plant pathogens and here, mainly the phyllosphere was studied (Burr et al., 1996; Pusey et al., 2009; Stockwell et al., 2010; Yashiro et al., 2011; He et al., 2012; Liu et al., 2018). Interestingly, apple flowers are colonized by thousands of bacterial taxa, and followed successional groups with coherent dynamics whose abundances peaked at different times before and after bud opening (Shade et al., 2013). The fungal community associated with the apple endosphere is pedigree-specific (Liu et al., 2018), and significantly dependent on different tissues (stem end, calyx end, peel, and wounded flesh) within the apple carposphere (Abdelfattah et al., 2016). However, basic insights into the bacterial communities of apple fruits are still missing.

The objective of this study are basic insights into the apple fruit microbiome. In detail, we aim to identify (i) differences between tissues of apple fruits and (ii) the impact of organic and conventional management practices – which represent diverse defined abiotic treatments pre- and post-harvest – on abundance and composition of apple fruit-associated bacteria. We hypothesize (i) that each apple provides different niches for bacterial communities and (ii) that the management practice has substantial impact on the apple microbiome, which is crucial for plant (post-harvest) and human health issues. With our experimental design we targeted to decipher to which microbiota the consumer is usually directly exposed, and used an integrated design of methods combining 16S rRNA amplicon libraries and qPCR and FISH-CLSM.

MATERIALS AND METHODS

Sampling and Experimental Design

In order to investigate and compare the microbiome of organically and conventionally managed apples (*Malus pumila* Mill.) the cultivar "Arlet" was selected. Both the organically and the conventionally produced apples were cultivated in Styria (Austria) under AMAG.A.P. Certification (AMA-Gütesiegel-Produktion), which represent the Austrian law for the international guidelines for agricultural management program GLOBALG.A.P. Matured, fully developed apples were sampled at harvest time in September 2017 in Styria (Austria). Organically managed apples originated from an organic orchard, which follows the international "demeter" guidelines for organic farming[1], using sterile gloves and instruments. Conventional apples originated from a conventional orchard in Styria. In contrast to the organically produced apples, they underwent the following post-harvest treatments: directly after harvest, apples were short-term stored under controlled atmosphere (1–2°C, 1.5–2% CO_2), washed and wrapped in polythene sheets for sale. Both apple management groups ("organic" and "conventional") were transported to laboratory immediately and processed under sterile conditions. All apples were visually examined for consistency in shape, size, color, flawlessness, firmness, and freshness prior to processing. Four apples, weighing 190 $\pm$ 5 g, were selected from each of the two management groups and each apple was divided into six tissues with the following weights: stem: 0.2 g, stem end: 2 g, peel: 9 g, fruit pulp: 12 g, seeds: 0.2 g, and calyx end: 3 g. Thus, each tissue was represented by four replicates, where each replicate consists of the respective tissue of one apple. Here it has to be mentioned that seeds of

[1]https://www.demeter.at/richtlinien/

conventionally managed apples contained on average only half as many seeds as organically managed ones.

Microbial DNA Extraction and Amplicon Library Construction

In order to extract microorganism, stem end, peel, fruit pulp and calyx end samples were homogenized in a Stomacher laboratory blender (BagMixer, Interscience, Saint-Nom-la-Bretèche, France) with 4 ml sterile NaCl (0.85%) solution for 3 min. Seeds and stems were physically disrupted in a sterilized mortar. For the upcoming cultivation-independent analyses, 2 ml of apple suspensions were centrifuged for 20 min at 16,000 *g* and pellets were used to extract bacterial genomic DNA using FastDNA SPIN Kit for Soil (MP Biomedicals, Solon, OH, United States) and a FastPrep Instrument (MP Biomedicals, Illkirch, France) for 30 s at 5.0 m/s. For culture-independent Illumina MiSeq v2 (250 bp paired end) amplicon sequencing, the primers 515f – 806r (Caporaso et al., 2010) were used to amplify the 16S rRNA gene using three technical replicates per sample. Peptide nucleic acid (PNA) clamps were added to PCR mix to block amplification of host plastid and mitochondrial 16S DNA (Lundberg et al., 2013). PCR for 16S rRNA gene amplification was performed in a total volume of 30 µl [5× Taq&Go (MP Biomedicals, Illkirch, France), 1.5 µM PNA mix, 0.25 mM of each primer, PCR-grade water and 1 µl template DNA] under the following cycling conditions: 95°C for 5 min, 30 cycles of 96°C for 1 min, 78°C for 5 s, 54°C for 1 min, 74°C for 60 s and a final elongation at 74°C for 10 min. Technical replicates were pooled and purified by Wizard SV Gel and PCR Clean-Up System (Promega, Madison, WI, United States). For amplicon sequencing, DNA concentrations were measured with Nanodrop 2000 (Thermo Fisher Scientific, Wilmington, DE, United States) and samples were combined in equimolar concentration.

Illumina MiSeq Data Analysis and Statistics

Raw sequence data preparation and data analysis was performed using QIIME 1.9.1 (Caporaso et al., 2010). After paired reads were joined and quality filtered (phred q20), chimeric sequences were identified using usearch7 (Edgar, 2010) and removed. Representative sequences were aligned, open reference database SILVA (ver128_97_01.12.17) was used to pick operational taxonomic units (OTUs) and *de novo* clustering of OTUs was performed using usearch. After taxonomy assignment, sequences assigned to host mitochondria and chloroplasts were discarded. OTU tables were rarefied to 1,525 sequences per sample, according to the sample with lowest amount of sequences. Rarefied OTU tables served as input matrix for upcoming alpha and beta diversity analyses and according statistics were calculated in QIIME. Beta diversity, based on unweighted UniFraq distance matrix, was visualized by Principle Coordinates Analysis (PCoA) and statistical significance was calculated by Analysis of Similarity (ANOSIM). Box-and-Whiskers-Plots, based on Shannon diversity indices, were constructed to visualize microbiota diversity of apple samples using IBM SPSS program (version 25.0, IBM Corporation, Armonk, NY, United States) and statistics were calculated using non-parametric Kruskal–Wallis test and False Discovery Rate (FDR) multiple test correction. For taxonomy charts and in order to trace differentially abundant taxa between organically and conventionally managed apples, OTUs with less than 0.01% abundance were excluded from the dataset. Significant differences ($\alpha < 0.05$) in taxa abundance on genus and order level were calculated in QIIME, using non-parametric Kruskal–Wallis/FDR test. Taxonomy charts were constructed by merging the core microbiota (taxa occurring in 75% of all replicates) of each tissue of the corresponding management group and the taxonomic network was constructed using Cytoscape version 3.5.1 (Shannon et al., 2003).

Quantitative PCR (qPCR)

For determining bacterial abundance, qPCRs were conducted with the bacterial directed primer pair 515f – 927r (10 µm each; Köberl et al., 2011). The qPCR reaction mix contained 5 µl KAPA SYBR Green, 0.15 µl PNA mix, 0.5 µl of each primer, 2.85 µl PCR-grade water, and 1 µl template DNA (fruit pulp and seed samples were diluted 1:10 in PCR grade water). Quantification of fluorescence was detected in a Rotor-Gene 6000 real-time rotary analyzer (Corbett Research, Sydney, Australia) with the following cycling conditions: 95°C for 5 min, 40 cycles of 95°C for 20 s, 54°C for 30 s, 72°C for 30 s and a final melt curve of 72 to 96°C. Three individual qPCR runs with R^2-values of standard curves of 0.12 were conducted separately and each replicate was measured in triplicate. Intermittently occurring gene copy numbers that were detected in negative control reactions were subtracted from the respective sample. Significant differences ($p < 0.05$) of bacterial gene copy numbers per gram of tissue between management groups and apple tissues were calculated using IBM SPSS program by applying non-parametric Kruskal–Wallis test including FDR multiple test correction.

Fluorescent *in situ* Hybridization (FISH) and Confocal Laser Scanning Microscopy (CLSM)

Native colonization patterns of bacteria associated with the apple tissues were visualized by FISH-CLSM, using a Leica TCS SPE confocal laser scanning microscope (Leica Microsystems, Mannheim, Germany) with oil immersion objective lenses Leica ACS APO 40.0× oil CS and Leica ACS APO 63× oil CS. Apple samples were fixed with 4% paraformaldehyde/phosphate-buffered saline over-night at 4°C prior to FISH application, according to the protocol of Cardinale et al. (2008). Cy3-labeled EUB338MIX (Daims et al., 1999; Amann et al., 2001) was used to stain overall bacterial colonization and for specific visualization of *Firmicutes* and *Gammaproteobacteria*, Cy5-labeled LGC-mix (Meier et al., 1999) and ALEXA-labeled GAM42a (Manz et al., 1992), respectively, were applied. For contrasting host cell walls, FISH samples were treated with Calcoflour White. By maximum projections of optical z-stack slices, micrographs of the bacterial colonization were generated.

RESULTS

Quantitative Records of Bacterial 16S rRNA Gene Abundance in Apple Tissues

Gene copy numbers of bacterial 16S rRNA per gram tissue of organic and conventional apples were measured by qPCR inquiry (**Figure 1**). Bacterial abundances were observed to be mostly consistent between the management analogs of each tissue; no significant differences ($p < 0.05$) were observed according to non-parametric Kruskal–Wallis/FDR. In contrast, bacterial abundance was strongly tissue-specific. Overall, stem (mean value 1.54×10^8 16S rRNA gene copy numbers per gram) and seeds (mean value 1.26×10^8) showed highest bacterial abundance, followed by calyx end, stem end and fruit pulp; peel microbiota (mean value 4.49×10^4) were lowest abundant. **Table 1**, therefore, shows only the significant difference in 16S rRNA gene abundance per gram between the tissues within the two management groups. Combining all tissue samples of the corresponding management group resulted in the mean values 4.85×10^7 and 4.67×10^7 per gram organic and conventional apple, respectively. The difference was not significant. In order to give a notion on the amount of bacteria ingested during the consumption of a whole apple, we excluded stem samples and multiplied the values of 16S rRNA gene copy numbers per g tissue with the mean weight of the respective tissue within one "Arlet" apple: stem end: 6 g, peel: 35 g, fruit pulp: 145 g, seeds: 0.3 g, calyx end: 5 g. Calculated values were then added up; accordingly, consumption of one organic and one conventional "Arlet" apple includes ingestion of 1.39×10^8 and 4.19×10^7 16S rRNA gene copy numbers, respectively. If you eat only peel and fruit pulp, 3.87×10^7 and 3.39×10^6 16S rRNA gene copies are ingested with one organic and one conventional apple, respectively. The differences were not statistically significant. "Arlet" apples represent a relatively small apple variety; considering the standard size of an apple with 240 g, consuming the whole apple includes a mean uptake of 1.14×10^8 16S rRNA gene copy numbers.

Quantitative Records of Diversity Estimates of Apple Microbiota

Shannon diversity estimates revealed organically managed apples to harbor a significantly more diverse microbiota than conventionally managed ones (**Figure 2** and **Table 2**). The difference was even more significant when the two management analogs of each tissue were compared; Shannon diversity index was significantly higher for the microbiota of all organic tissues, compared to conventional ones, with the sole exception of calyx end microbiota. **Table 2** shows furthermore the comparison of the tissues within one management group. For organic apples, fruit pulp showed highest microbial diversity, followed by peel and stem, stem end, seed and calyx end, in ascending order. Diversity of the fruit pulp microbiota was significantly higher than stem, seeds and calyx end microbiota. Regarding conventional tissues, Shannon diversity index was highest for peel microbiota, followed by stem, stem end, fruit pulp, calyx end, and seed microbiota. Here, peel microbiota was significantly more diverse than seed, calyx end, and fruit pulp microbiota.

Highest beta diversity measures were observed when the replicates were grouped by the tissue of the respective management group (ANOSIM values: $R = 0.8$, $p = 0.001$; **Figure 3A**). Grouping samples by organic and conventional management revealed the ANOSIM values $R = 0.26$, $p = 0.001$

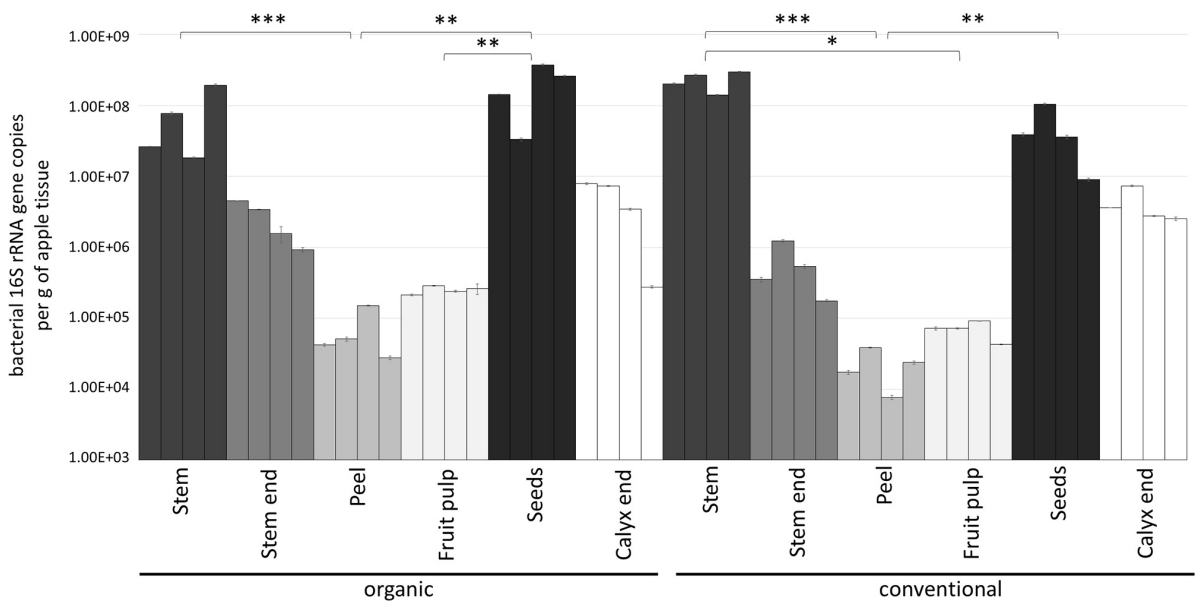

FIGURE 1 | Bacterial abundance in carposphere tissues of organically and conventionally managed apples. Microbial community abundance within each tissue was measured in four replicates by qPCR using PNAs to block mitochondrial and plastid 16S DNA. Asterisks indicate significant differences in 16S rRNA gene abundance (calculated per g of apple tissue) between the tissues within a management group.

TABLE 1 | Significant differences in 16S rRNA gene abundance per gram of tissue between organically and conventionally managed apple tissues.

	Group1*	Group2*	Group1 mean	Group2 mean	*p*-Value
Organic tissues	Stem O	Peel O	7.91E+07 ± 6.99E+07	6.81E+04 ± 4.89E+04	0.001
	Peel O	Seeds O	6.81E+04 ± 4.89E+04	2.04E+08 ± 1.28E+08	0.002
	Fruit pulp O	Seeds O	2.51E+05 ± 2.80E+04	6.81E+04 ± 1.28E+08	0.004
Conventional tissues	Seeds C	Peel C	4.71E+07 ± 3.50E+07	2.18E+04 ± 1.12E+04	0.002
	Stem C	Peel C	2.28E+08 ± 6.16E+07	2.18E+04 ± 1.12E+04	0.001
	Stem C	Fruit pulp C	2.28E+08 ± 6.16E+07	6.96E+04 ± 1.76E+04	0.02

**O and C denote for organically and conventionally managed apples, respectively. Only significant differences in microbial abundance between apple tissues are listed.*

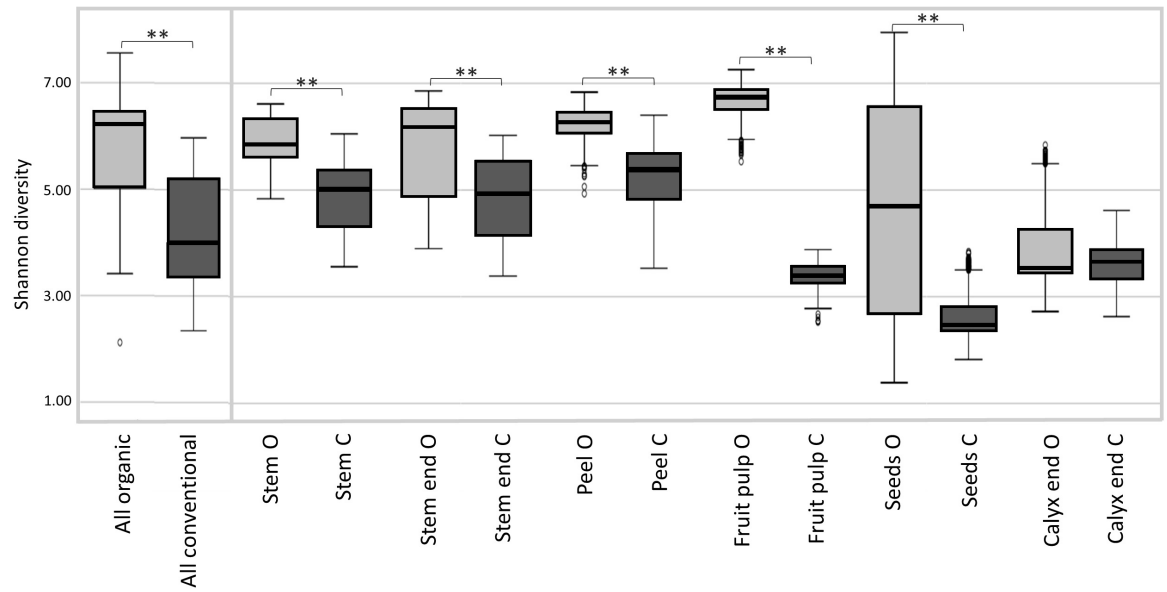

FIGURE 2 | Microbial diversity estimates of organically and conventionally managed apples and apple tissues. Suffixes O and C of carposphere tissue in the bottom legend, denote for organic and conventional management, respectively. Significant differences in Shannon diversity estimates of the apple management analogs are indicated by brackets and asterisks.

(**Figure 3B**). Hence, we had a closer look on the management effect on each tissue separately, resulting in the ANOSIM values $R > 0.8$, $p < 0.05$ for all tissues, except seeds (ANOSIM values for seeds: $R = 0.4$, $p = 0.05$). The management practice therefore seems to have a profound impact on the microbiota composition of all tissues while the management effect on seed microbiota was lower. This observation was confirmed when seed samples were excluded from the dataset; ANOSIM values increased to $R = 0.45$ and $p = 0.001$ (**Figure 3C**).

The General Structure of the Bacterial Apple Microbiota

After removing chimeric, mitochondrial and chloroplast sequences, the overall bacterial community of all apple samples, assessed by 16S rRNA gene amplicon sequencing, contained 6,711,159 sequences that were assigned to 92,365 operational taxonomic units (OTUs). The taxonomic assignment of OTUs revealed 44 different phyla, 325 orders and 1,755 genera. Among bacterial phyla, *Proteobacteria* highly dominated with 80%, followed by *Bacteroidetes* (9%), *Actinobacteria* (5%), and *Firmicutes* (3%). *Burkholderiales* were highly abundant concerning bacterial orders (31% abundance), followed by *Sphingomonadales* (14%), *Rhizobiales* (12%), *Pseudomonadales* (11%), *Enterobacteriales* (7%) and *Cytophagales* (5%); *Micrococcales*, *Sphingobacteriales*, *Bacillales*, *Rhodospirillales*, and *Flavobacteriales*, in ascending order, represented between 5 and 1% of total OTUs. OTUs assigned to the genus *Ralstonia* were most frequent with 13%, while *Sphingomonas* (12%), *Pseudomonas* (11%), *Massilia* (7%), *Methylobacterium* (7%), *Burkholderia* (5%), *Pantoea* (5%), and *Hymenobacter* (5%) were furthermore high abundant.

The Specific Structure of the Microbiota in Tissues of Organic and Conventional Apples

A clustering network based on the core taxa of the tissues of each apple management group was constructed to visualize the taxa present in all apples as well as the taxa that are specific for

TABLE 2 | Alpha diversity measures of differentially managed apples and apple tissues based on Shannon diversity estimates.

	Group1*	Group2*	Group1 mean	Group2 mean	*p*-Value**
Whole apple	All organic	All conventional	5.60±1.36	4.17±1.11	0.003
Organic vs. conventional tissues	Stem end O	Stem end C	5.87±0.81	4.94±0.71	0.001
	Stem O	Stem C	5.92±0.41	4.98±0.64	0.001
	Peel O	Peel C	6.22±0.32	5.32±0.57	0.001
	Fruit pulp O	Fruit pulp C	6.67±0.35	3.39±0.25	0.001
	Seeds O	Seeds C	4.97±2.13	2.68±0.50	0.001
	Calyx end O	Calyx end C	3.96±0.87	3.70±0.47	0.782
Organic tissues	Peel O	Stem end O	6.22±0.32	5.87±0.81	1
	Peel O	Stem O	6.22±0.32	5.92±0.41	1
	Peel O	Seeds O	6.22±0.32	4.97±2.13	0.157
	Peel O	Calyx end O	6.22±0.32	3.96±0.87	0.002
	Peel O	Fruit pulp O	6.22±0.32	6.67±0.35	0.157
	Stem end O	Stem O	5.87±0.81	5.92±0.41	0.157
	Stem end O	Seeds O	5.87±0.81	4.97±2.13	0.002
	Stem end O	Calyx end O	5.87±0.81	3.96±0.87	0.001
	Stem end O	Fruit pulp O	5.87±0.81	6.67±0.35	1
	Stem O	Seeds O	5.92±0.41	4.97±2.13	1
	Stem O	Calyx end O	5.92±0.41	3.96±0.87	0.175
	Stem O	Fruit pulp O	5.92±0.41	6.67±0.35	0.002
	Seeds O	Calyx end O	4.97±2.13	3.96±0.87	1
	Seeds O	Fruit pulp O	4.97±2.13	6.67±0.35	0.001
	Calyx end O	Fruit pulp O	3.96±0.87	6.67±0.35	0.001
Conventional tissues	Peel C	Stem end C	5.32±0.57	4.94±0.71	1
	Peel C	Stem C	5.32±0.57	4.98±0.64	0.157
	Peel C	Seeds C	5.32±0.57	2.68±0.50	0.001
	Peel C	Calyx end C	5.32±0.57	3.70±0.47	0.001
	Peel C	Fruit pulp C	5.32±0.57	3.39±0.25	0.001
	Stem end C	Stem C	4.94±0.71	4.98±0.64	1
	Stem end C	Seeds C	4.94±0.71	2.68±0.50	0.001
	Stem end C	Calyx end C	4.94±0.71	3.70±0.47	0.003
	Stem end C	Fruit pulp C	4.94±0.71	3.39±0.25	0.116
	Stem C	Seeds C	4.98±0.64	2.68±0.50	0.002
	Stem C	Calyx end C	4.98±0.64	3.70±0.47	0.209
	Stem C	Fruit pulp C	4.98±0.64	3.39±0.25	1
	Seeds C	Calyx end C	2.68±0.50	3.70±0.47	1
	Seeds C	Fruit pulp C	2.68±0.50	3.39±0.25	0.209
	Calyx end C	Fruit pulp C	3.70±0.47	3.39±0.25	1

*O and C denote for organically and conventionally managed apples, respectively. **Statistics were calculated based on Kruskal–Wallis/FDR test.

each management group (**Figure 4**). Only taxa occurring with at least 0.01% abundance in the whole dataset were included in the network analysis. All apples were found to share a high abundant core microbiota; 73 out of 141 genera were shared. Among them, highly abundant *Proteobacteria* were most dominant and abundant with 45 genera. In total 16 genera were found only in organically managed apples, and 50 genera, predominated by *Proteobacteria* (33 genera) were specific for conventional apples. Overall, the specific microbiota for each management group were less abundant than the shared microbiota.

In order to visualize the differences between the community compositions of the management analog of each tissue on a taxonomic level, **Figure 5** was prepared. Pie charts include only taxa that are abundant with at least 0.1% in the whole dataset. Here, differences between organically and conventionally managed apples are obvious for all tissues. Contradictory to beta diversity analysis (described above and **Figure 3**), seeds appear to feature very different microbiota, especially due to the dominance of *Ralstonia* in conventional seeds. The inconsistency of the results can be explained by the fact that beta diversity measures were calculated on the entire OTU table and **Figure 5** was constructed on the high abundant (>0.1%) core taxa of each tissue.

Indicator Species for Organically and Conventionally Managed Apples

Differences in abundance of specific bacterial taxa associated with either organically or conventionally managed apples, were assessed by applying non-parametric Kruskal–Wallis/FDR

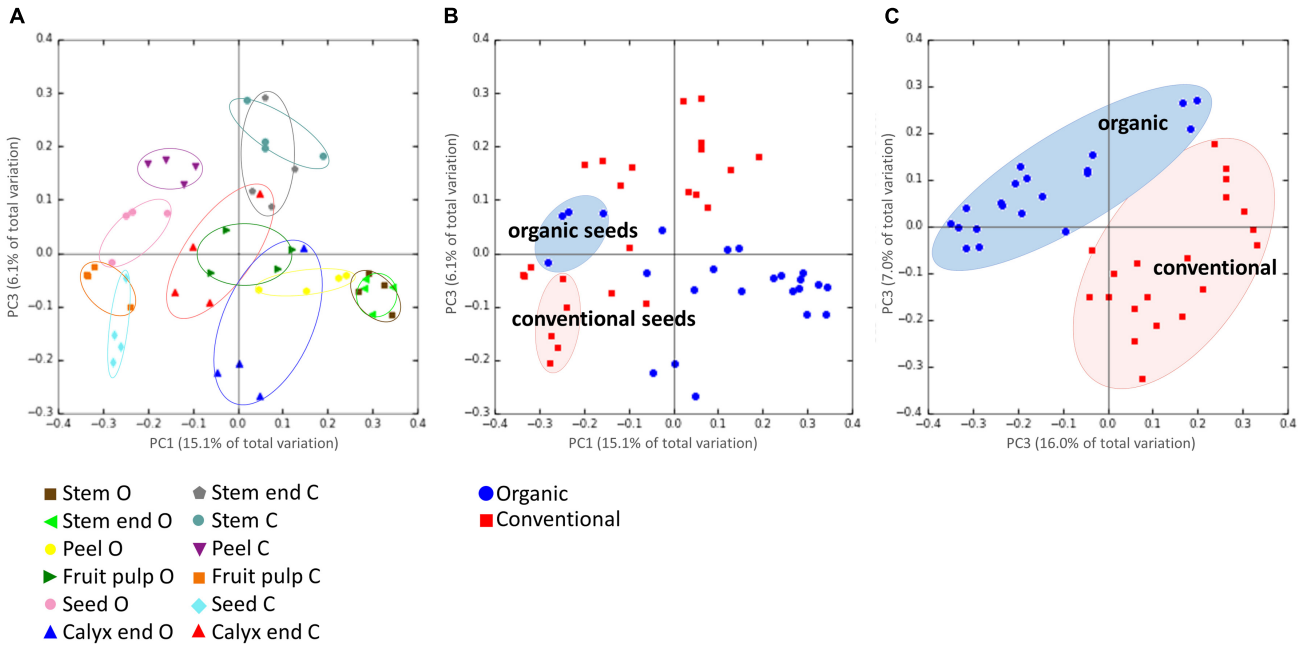

FIGURE 3 | Beta-diversity analysis on microbiota composition dependencies. Panel **(A)** shows the microbiota composition grouped by the tissue of the respective management group, where O and C in the bottom legend denote for organically and conventionally managed apples, respectively. Panel **(B)** visualizes composition of all tissue replicates, colored by organic (blue circles) and conventional (red squares); seeds of organically and conventionally managed apples are highlighted. In Panel **(C)**, same dataset is shown but seed samples of both management groups were excluded. PCoA plots are based on unweighted UniFraq distance matrix.

test. Priorly, OTU table was filtered by excluding OTUs with less than 0.01% abundance, resulting in a total of 172 taxa on genus level. Calculations assigned 67 taxa a significantly higher abundance in either organically or conventionally managed apples (**Supplementary Table 1**); accordingly, 39% of the taxa were significantly different abundant. Noteworthy among them are *Methylobacterium*, *Hymenobacter*, *Spirosoma*, and *Zymomonas* which were high abundant in organically managed apples, and *Burkholderia*, *Pantoea*, *Erwinia*, and *Acinetobacter*, especially high abundant in conventional apples. Significantly different abundance between microbiota of organically and conventionally managed apples was furthermore calculated on higher taxonomic level. The 172 genera were condensed to 66 different bacterial orders; among them, 25 orders were significantly different abundant, accounting to 37.8% (**Supplementary Table 1**). Among those, *Cytophagales* were high abundant in organic apples while the orders *Burkholderiales*, *Pseudomonadales*, *Enterobacteriales*, and *Flavobacteriales* prevailed in conventional apples.

Indicator Species for Health With Focus on *Enterobacteriales*

The microbiota of conventional and organic apples were screened for their potential to feature health-relevant properties for humans. For that purpose, we constructed an OTU table containing only *Enterobacteriales*, as especially this order is described to contain taxa responsible for food-borne outbreaks. In our dataset the order *Enterobacteriales* was found to be significantly more abundant in conventionally managed apples (described above and **Supplementary Table 1**). **Figure 6** shows the relative abundance of taxa to total *Enterobacteriales* in the tissues of organically and conventionally managed apples. *Pantoea* was most abundant among all samples, representing between 60 and 99% of *Enterobacteriales* microbiota; however, *Pantoea* was significantly more abundant in conventionally managed apples (**Supplementary Table 1**). *Pectobacterium*, *Tatumella*, and *Enterobacter* were furthermore abundant in almost all tissues, independent of their management practice. Abundance of a not further assigned *Enterobacteriaceae* taxon (*Enterobacteriaceae* sp. in **Figure 6**), *Erwinia* and *Escherichia-Shigella* were significantly more abundant in conventional apples.

Native Colonization Patterns of Microbiota in Apple Tissues

By using CLSM in combination with FISH we were able to visualize bacteria native to all carposphere tissues *in situ* (**Figure 7**). Visualization of stem, stem end, peel, and calyx end microbiota turned out to be successful; *Gammaproteobacteria* (fluorescing pink) and *Firmicutes* (yellow) were distinguishable from remaining bacteria (red). In fruit pulp and seed samples, few bacteria were detected as well, however, due to high autofluorescence of host tissues, imaging was more challenging compared to remaining tissues. During microscopic observations, no differences were observed between organic and

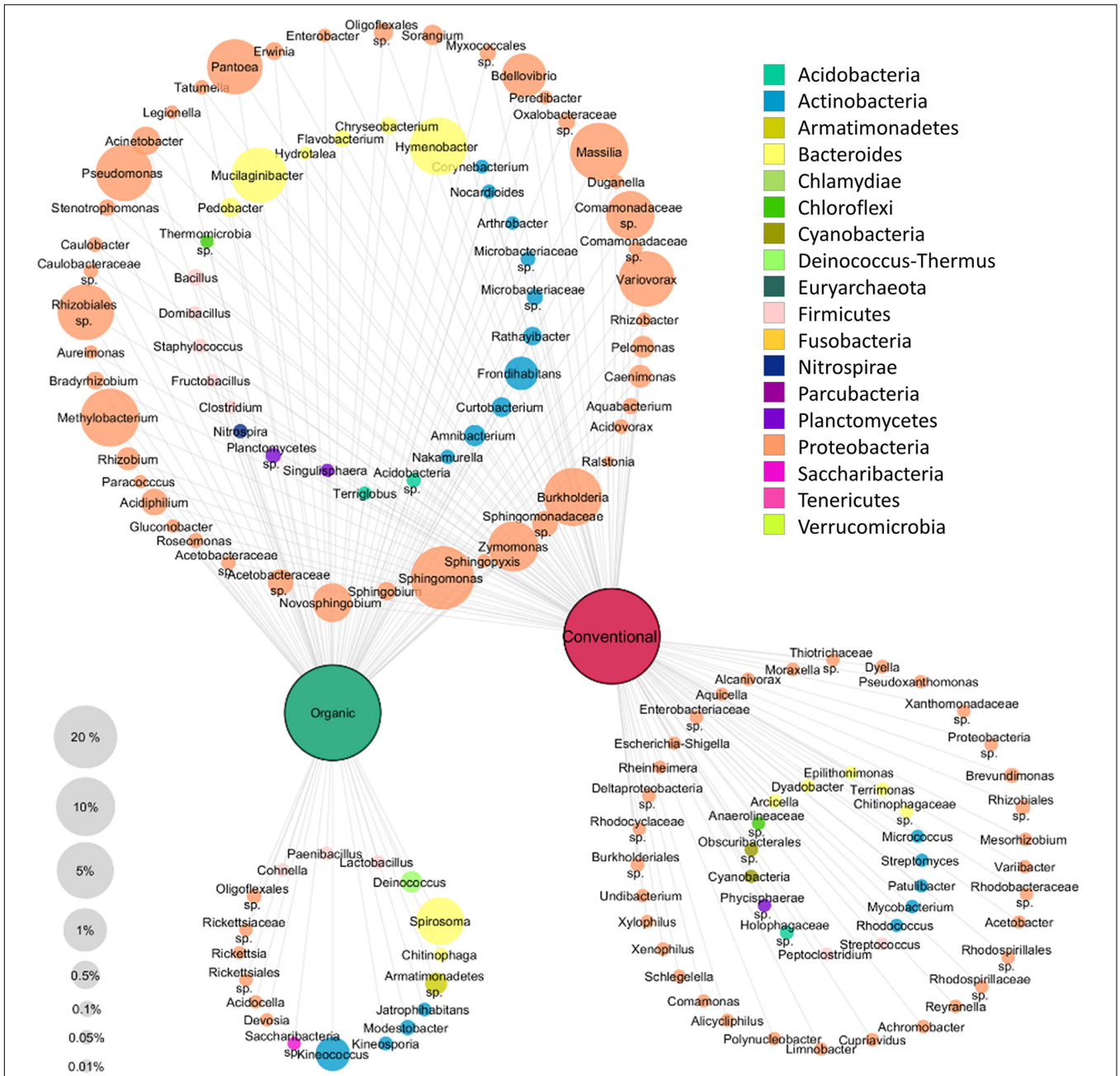

FIGURE 4 | Core and specific microbiota for organic and conventional apples. Core microbiota (taxa occurring in 75% of all replicates) of each management group (conventional and organic) were combined for network analysis. To be included, taxa had to exhibit at least 0.01% abundance in the whole dataset. Node size correspond to relative abundance in the dataset as denoted in the legend on the bottom left, node labels display taxonomic identification of OTUs on genus level wherever possible and node color indicates appropriate phylum, as described in the legend on the top right.

conventional apples, therefore **Figure 7** illustrates only tissues of organic apples.

DISCUSSION

In the present study we identified tissue-specific and management-specific microbial communities for apple fruits. This specificity was apparent for all tissues regarding both microbiota composition and diversity, but not abundance. The observed differences between organic and conventional apples could certainly be attributable to a variety of factors within farming and storage conditions.

Deciphering the bacterial microbiota of Austrian "Arlet" apples resulted in a drastic diversification between the six tissues within the apple carposphere for bacterial abundance,

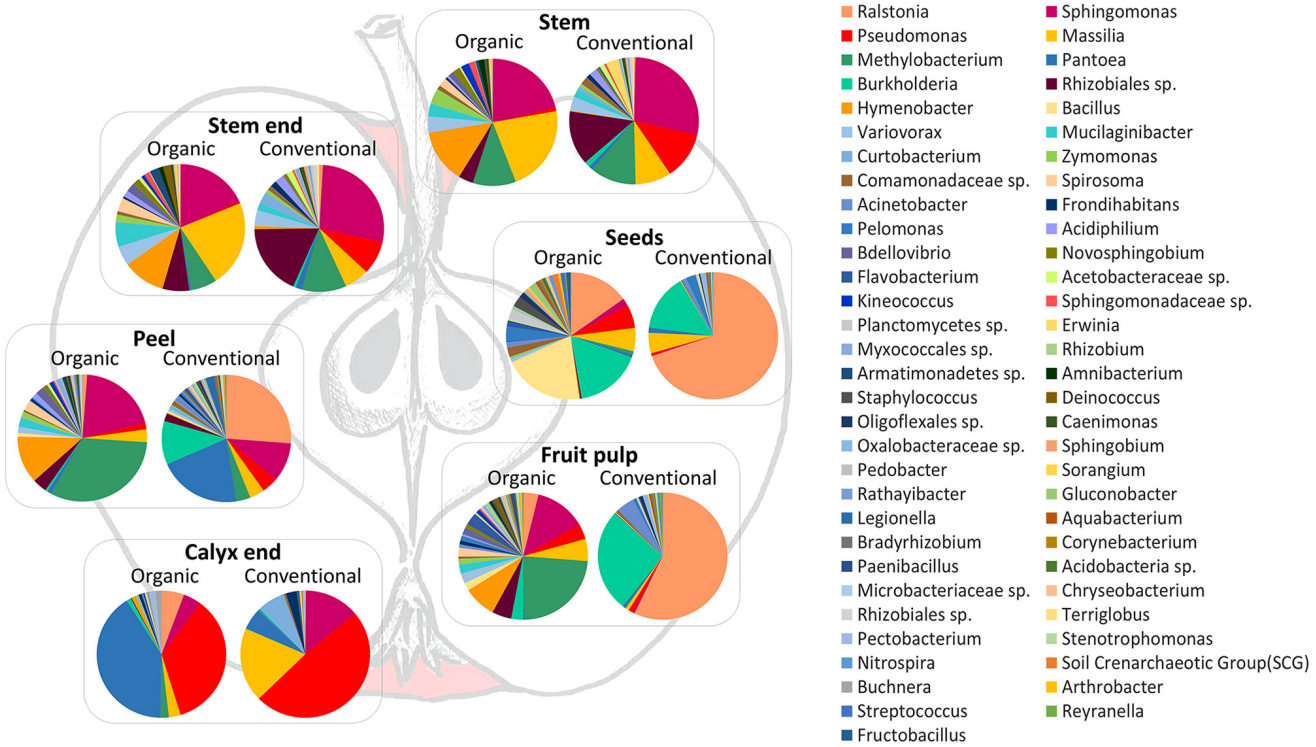

FIGURE 5 | Taxonomic composition of organic and conventional apple tissue microbiota. Pie charts visualize taxa occurring in the core microbiomes of each tissue, with at least 0.1% abundance in the whole dataset, and visualize differences between conventional and organic apples.

diversity and composition. Interestingly, alpha diversity estimates and calculations of bacterial abundance (according to qPCR) were pretty much inconsistent. Whereas fruit pulp and peel featured highest values for diversity, microbiota abundance was lowest in those tissues. Seeds, on the other hand, were less divers than other tissues, but showed highest abundance. Those results were partially confirmed by FISH-CLSM; high microbial abundance was visualized on stem, stem end and calyx end samples, whereas peel and fruit pulp turned out to be less colonized. However, for seeds it was not possible to visualize the high bacterial abundances indicated by qPCR which was due to exceptionally high autofluorescence in seed tissues. Differences between the tissue-associated microbiota were expected beforehand, as varying metabolic and nutrient conditions in the specific parts are certain. The sole responsibility of all the different parts of a fruit is to protect the seeds and enable their dispersal for a successful reproduction of the plant. Apple seed microbiota showed interesting features: among all tissues, seeds, together with stem, were found to significantly prevail in bacterial quantity, hosting an average of 126 billion bacterial gene copy numbers per gram seeds. Seed microbiota composition was most similar to fruit pulp microbiota which underline the vertical microbiome transmission in plants (Hardoim et al., 2012).

The management practice was found to significantly drive the microbiota of all tissues within the apple. Diversity was significantly higher in all organically grown tissues (except for calyx end) and the microbiota composition was distinct between organic and conventional tissue analogs. Compared to the other tissues, seed microbiota was lowest affected by the management practice, while the exclusion of low abundant taxa from the dataset resulted in dramatic dissimilarities between organic and conventional seeds. Organic seeds showed a much more even composition than conventional seeds which were highly dominated by *Ralstonia*. Altogether, organic apple microbiota was significantly more divers and differentially composed; the remarkable amount of 39% of genera and 38% of bacterial orders was significantly different abundant. Referring to a previous work on the apple flower microbiome, *Deinococcus-Thermus* and *Saccharibacteria* (formally known as TM7) dominated the community (Shade et al., 2013). In the present study, both taxa were present in almost all replicates of organic apples (0.6 and 0.08%, respectively), in contrast to conventional ones (0.01% *Deinococcus-Thermus* and 0.007% *Saccharibacteria*). This promotes exceptional specificity and functionality of the microbiota for successive development stages from the flower to the mellow fruit and potentially suggests organic management to rather allow the formation of a stable and beneficial community. Conventional apple microbiota was furthermore found to be less even constructed and highly dominated by *Burkholderiales*, accounting to almost 43% abundance. The order *Enterobacteriales* was one of the signature taxa of conventional apples as well; among them, we would like to highlight the almost ubiquitous occurrence

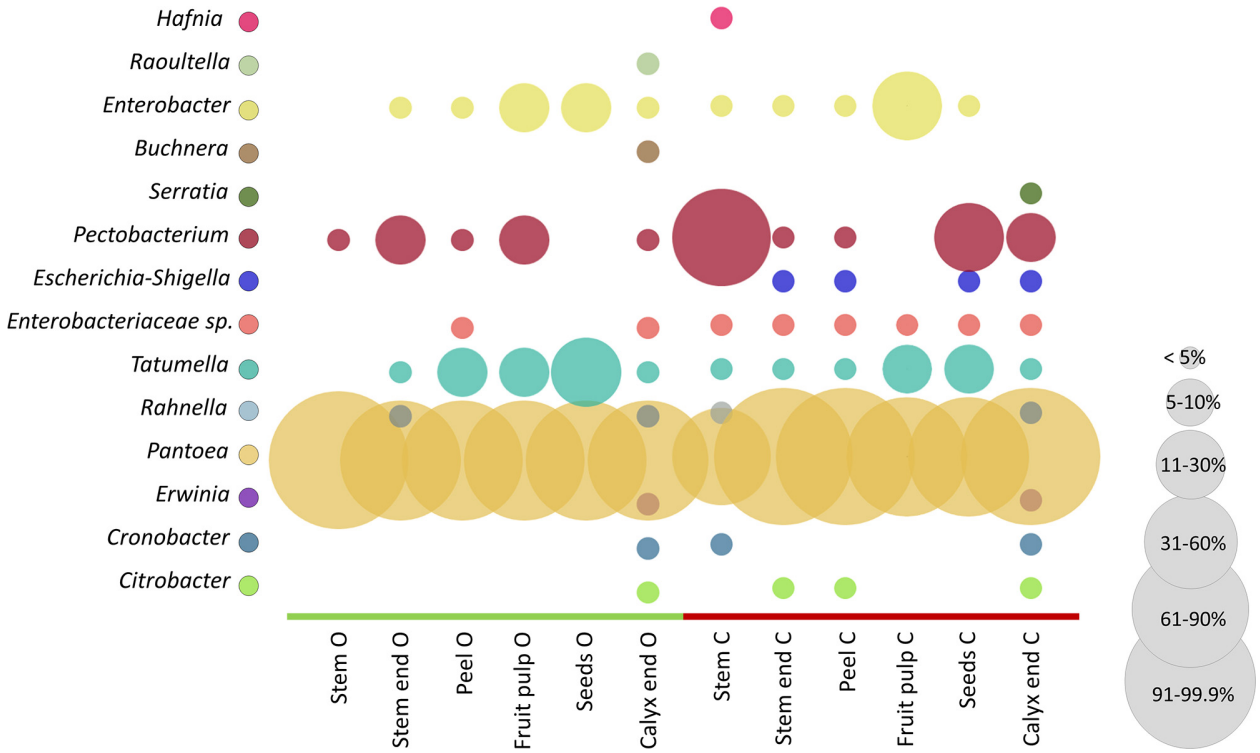

FIGURE 6 | Comparison of conventional and organic apple tissues regarding *Enterobacteriales* abundance. Color code for bubbles is depicted in the legend on the left and bubble size indicates relative abundance of taxa within total *Enterobacteriales* microbiota, as explained in the legend on the right. The abbreviations O and C denote for organically and conventionally managed apple tissues, respectively.

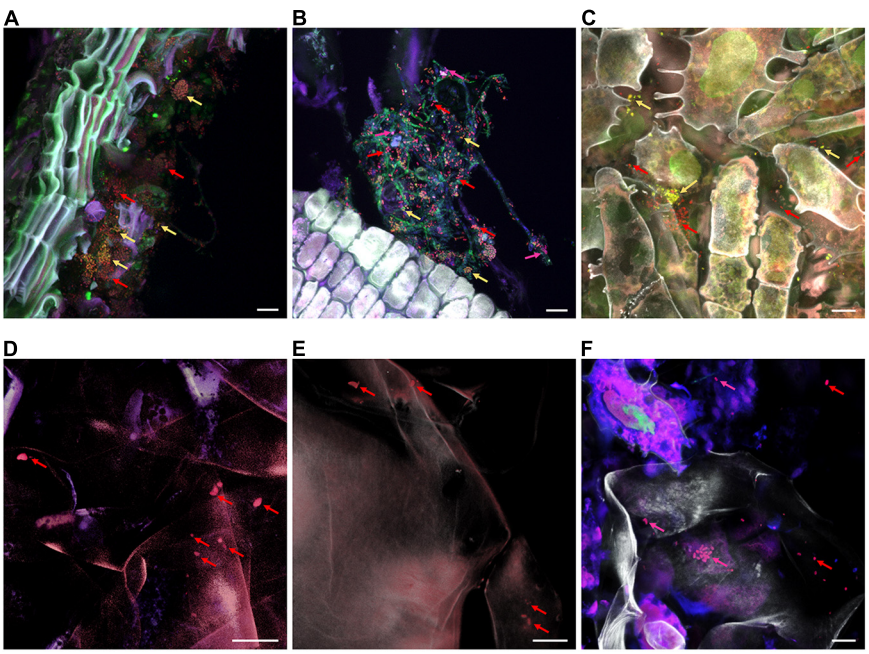

FIGURE 7 | FISH-CLSM micrographs showing bacterial colonization of organic apple tissues. Panels **(A–F)** visualize stem, stem end, peel, fruit pulp, seeds and calyx end samples, respectively. Bacteria were stained with FISH probes specific for *Gammaproteobacteria* (fluorescing pink and indicated by pink arrows), *Firmicutes* (yellow) and remaining bacteria of other classes (red); host structures are fluorescing white. Bar on the bottom right of each panel denotes for 10 μm.

of OTUs assigned to *Escherichia-Shigella* in the tissues of conventional apples (although low abundant) and their absence in organically managed apples. Higher abundances of *Enterobacteriales* in conventional fresh produces compared to organic equivalents have already been reported by Leff and Fierer (2013). Controversially, *Lactobacillus*, which is frequently used within probiotics (Derrien and van Hylckama Vlieg, 2015), was one of the core taxa of organic apples. The highly diverse microbiome of organically managed apples might probably limit or hamper the abundance of human pathogens, simply by outcompeting them; negative correlations between human pathogen abundance and the natural microbiome of fresh produce has already been described (Cooley et al., 2006). The described microbial patterns in organic apples resemble the impact of apple polyphenols on human health, which have not only been shown to alleviate allergic symptoms (Zuercher et al., 2010), but also to promote growth of *Lactobacillus* and *Bifidobacterium* in the human gut and to reduce abundance of food-borne pathogens (Taguri et al., 2004; Bialonska et al., 2010). Considering that specific microbial signatures have potential to reduce food allergies (Kalliomäki et al., 2010), the native microbiome of organic and unprocessed apples could be an advantageous tool to manage and prevent allergic diseases. *Methylobacterium*, identified to enhance the biosynthesis of strawberry flavor compounds (Verginer et al., 2010), was significantly higher abundant in organic apples; here especially on peel and fruit pulp samples. In contrast, *Ralstonia* and *Erwinia*, frequently described for adverse impact on plant health (Denny, 2007; Pirhonen et al., 2018), prevailed in conventional apples. Our results are in significant accordance to a recent study on the apple fruit-associated fungal community (Abdelfattah et al., 2016), where the authors observed specificity of the fungal microbiota to different tissues and management practices. Concordantly, the management practice is suggested to be accountable for the different bacterial and fungal community composition. The lowest effect was observed on seed microbiota, which is mainly cultivar-driven (Berg and Raaijmakers, 2018).

Calculations of 16S rRNA gene abundance resulted in significant differences between tissues but not for the management. This suggests bacteria to occupy the tissues of organically and conventionally produced apples in a similar quantity, while the management practice drives composition and diversity. For the quantitative analyses we used PNAs to block amplification of 16S rRNA of host origin; nevertheless, there is still a possibility that non-bacterial 16S rRNA genes are amplified. Furthermore, qPCR results do not exclusively represent the viable bacterial community. However, comparing gene abundances between tissues and management groups is possible and reliable in this regard.

CONCLUSION

Investigating the apple fruit microbiota resulted in profound differences between the tissues, applicable for microbiota diversity, composition and abundance. A significant management effect on the microbiota was furthermore apparent for all tissues, even for seeds. Organic and conventional apples are occupied by a similar quantity of microbiota; consuming the whole apple includes an approximate uptake of 100 million bacterial gene copy numbers. However, freshly harvested, organically managed apples harbor a significantly more diverse, more even and distinct microbiota, compared to conventional ones; the abundance of almost 40% of bacterial genera and orders differed significantly between organically and conventionally managed apples. Moreover, organic apples conceivably feature favorable health effects for the consumer, the host plant and the environment in contrast to conventional apples, which were found to harbor potential food-borne pathogens.

DATA AVAILABILITY

The raw sequence files supporting the findings of this manuscript are available from the European Nucleotide Archive (ENA) at the study Accession Number: PRJEB32455.

AUTHOR CONTRIBUTIONS

BW performed the experiments, analyzed the data, and wrote the manuscript. HM analyzed the data. GB designed the study, discussed the results, and wrote the manuscript. All authors read and approved the final version of the manuscript.

FUNDING

This study was funded by the Sparkling Science Research Program (Grant No. SPA 06051) of the Austrian Federal Ministry of Education, Science and Research (BMBWF).

ACKNOWLEDGMENTS

We gratefully acknowledge funding by the Sparkling Science Research Program of the Austrian Federal Ministry of Education, Science and Research (BMBWF). Collaboration with the students Josefine Mayer and Fiona Petio (both "Akademisches Gymnasium Graz"), Clara Duft and Paula Fürschuss (both "Modellschule Graz"), and Anna Steingruber and Viktoria Lamot (both "Sacré Coeur Graz"), who participated in laboratory experiments, was inspiring and a valuable experience. We thank their teachers Elisabeth Glavic, Gerhard Kapper, Iris Lichtenwagner, and Astrid Süssenbacher-Skofitsch (all Graz) for their committed cooperation. We appreciate the work of Tobija Glawogger (Graz) who guided the students, contacted PCRs, and

created CLSM images. We also thank Daria Rybakova (Graz) for her inputs to the project. Last but not the least, we are very thankful to Birgit Birnstingl (Hitzendorf), who provided organic apple samples and shared her knowledge on apple management practices.

SUPPLEMENTARY MATERIAL

The Supplementary Material for this article can be found online at: https://www.frontiersin.org/articles/10.3389/fmicb.2019.01629/full#supplementary-material

REFERENCES

Abdelfattah, A., Wisniewski, M., Droby, S., and Schena, L. (2016). Spatial and compositional variation in the fungal communities of organic and conventionally grown apple fruit at the consumer point-of-purchase. *Horticult. Res.* 3:16047. doi: 10.1038/hortres.2016.47

Amann, R. I., Binder, B. J., Olson, R. J., Chisholm, S. W., Devereux, R., and Stahl, D. A. (2001). Combination of 16S RRNA-targeted oligonucleotide probes with flow cytometry for analyzing mixed microbial populations. *Appl. Environ. Microbiology* 67, 142–147. doi: 10.1128/AEM.67.1.142

Berg, G. (2015). Beyond borders: investigating microbiome interactivity and diversity for advanced biocontrol technologies. *Microbial. Biotechnol.* 8, 5–7. doi: 10.1111/1751-7915.12235

Berg, G., Erlacher, A., Smalla, K., and Krause, R. (2014). Vegetable microbiomes: is there a connection among opportunistic infections, human health and our 'gut feeling'? *Microbial. Biotechnol.* 7, 487–495. doi: 10.1111/1751-7915.12159

Berg, G., Köberl, M., Rybakova, D., Müller, H., Grosch, R., and Smalla, K. M. (2017). Plant microbial diversity is suggested as the key to future biocontrol and health trends. *FEMS Microbiol. Ecol.* 93:fix050

Berg, G., and Raaijmakers, J. M. (2018). Saving seed microbiomes. *ISME J.* 12, 1167–1170. doi: 10.1038/s41396-017-0028-2

Berg, G., Rybakova, D., Grube, M., and Köberl, M. (2016). The plant microbiome explored: implications for experimental botany. *J. Exp. Bot.* 67, 995–1002. doi: 10.1093/jxb/erv466

Berg, G., and Smalla, K. (2009). Plant species and soil type cooperatively shape the structure and function of microbial communities in the rhizosphere. *FEMS Microbiol. Ecol.* 68, 1–13. doi: 10.1111/j.1574-6941.2009.00654.x

Bergna, A., Cernava, T., Rändler, M., Grosch, R., Zachow, C., and Berg, G. (2018). Tomato seeds preferably transmit plant beneficial endophytes. *Phytobio. J.* 2, 183–193. doi: 10.1094/pbiomes-06-18-0029-r

Bialonska, D., Ramnani, P., Kasimsetty, S. G., Muntha, K. R., Gibson, G. R., and Ferreira, D. (2010). The influence of pomegranate by-product and punicalagins on selected groups of human intestinal microbiota. *Int. J. Food Microbiol.* 140, 175–182. doi: 10.1016/j.ijfoodmicro.2010.03.038

Blau, K., Bettermann, A., Jechalke, S., Fornefeld, E., Vanrobaeys, Y., Stalder, T., et al. (2018). The transferable resistome of produce. edited by Mark J. Bailey. *MBio* 9, 1–15. doi: 10.1128/mBio.01300-18

Bulgarelli, D., Rott, M., Schlaeppi, K., Ver Loren van Themaat, E., Ahmadinejad, N., Assenza, F., et al. (2012). Revealing structure and assembly cues for arabidopsis root-inhabiting bacterial microbiota. *Nature* 488, 91–95. doi: 10.1038/nature11336

Burr, T. J., Matteson, M. C., Smith, C. A., Corral-Garcia, M. R., and Huang, T. C. (1996). Effectiveness of bacteria and yeasts from apple orchards as biological control agents of apple scab. *Biol. Control* 6, 151–157. doi: 10.1006/bcon.1996.0019

Caporaso, J. G., Kuczynski, J., Stombaugh, J., Bittinger, K., Bushman, F. D., Costello, E. K., et al. (2010). QIIME allows analysis of high-throughput community sequencing data. *Nat. Methods* 7, 335–336. doi: 10.1038/nmeth.f.303

Cardinale, M., Viera, J., de Castro Müller, H., Berg, G., and Grube, M. (2008). In situ analysis of the bacterial community associated with the reindeer lichen cladonia arbuscula reveals predominance of alpha *proteobacteria*. *FEMS Microbiol. Ecol.* 66, 63–71. doi: 10.1111/j.1574-6941.2008.00546.x

Cooley, M. B., Chao, D., and Mandrell, R. E. (2006). *Escherichia Coli* O157:H7 survival and growth on lettuce is altered by the presence of epiphytic bacteria. *J. Food Prot.* 69, 2329–2335. doi: 10.4315/0362-028X-69.10.2329

Daims, H., Brühl, A., Amann, R., Schleifer, K. H., and Wagner, M. (1999). The domain-specific probe EUB338 is insufficient for the detection of all bacteria: development and evaluation of a more comprehensive probe set. *Syst. Appl. Microbiol.* 22, 434–444. doi: 10.1016/s0723-2020(99)80053-8

David, L. A., Maurice, C. F., Carmody, R. N., Gootenberg, D. B., Button, J. E., Wolfe, B. E., et al. (2014). Diet rapidly and reproducibly alters the human gut microbiome. *Nature* 505, 559–563. doi: 10.1038/nature12820

Denny, T. (2007). "Plant pathogenic ralstonia species," in *Plant-Associated Bacteria*. S. S. Gnanamanickam (Dordrecht: Springer)

Derrien, M., and van Hylckama Vlieg, J. E. T. (2015). Fate, activity, and impact of ingested bacteria within the human gut microbiota. *Trends Microbiol.* 23, 354–366. doi: 10.1016/j.tim.2015.03.002

Edgar, R. C. (2010). Search and clustering orders of magnitude faster than BLAST. *Bioinformatics* 26, 2460–2461. doi: 10.1093/bioinformatics/btq461

FAO (2019). *Agricultural Crop Production Statistics The Food and Agriculture Organization of the United Nations. 2019*. Rome: FAO

Flandroy, L., Poutahidi, T., Berg, G., Clarke, G., Dao, M. C., Decaestecker, E., et al. (2018). The impact of human activities and lifestyles on the interlinked microbiota and health of humans and of ecosystems. *Sci. Total Environ.* 627, 1018–1038. doi: 10.1016/j.scitotenv.2018.01.288

Garcia-Mazcorro, J. F., Pedreschi, R., Yuan, J., Kawas, J. R., Chew, B., Dowd, S. E., et al. (2019). Apple consumption is associated with a distinctive microbiota, proteomics and metabolomics profile in the gut of dawley sprague rats fed a high-fat diet. *PLoS One* 14:e0212586. doi: 10.1371/journal.pone.0212586

Hardoim, P. R., Hardoim, C. C., van Overbeek, L. S., and van Elsas, J. D. (2012). Dynamics of seed-borne rice endophytes on early plant growth stages. *PLoS One* 7:e30438. doi: 10.1371/journal.pone.0030438

He, Y. H., Isono, S., Shibuya, M., Tsuji, M., Purushothama, C. R., Tanaka, K., et al. (2012). Oligo-DNA custom macroarray for monitoring major pathogenic and non-pathogenic fungi and bacteria in the phyllosphere of apple trees. *PLoS One* 7:e34249 doi: 10.1371/journal.pone.0034249

Kalliomäki, M., Antoine, J. M., Herz, U., Rijkers, G. T., Wells, J. M., and Mercenier, A. (2010). Guidance for substantiating the evidence for beneficial effects of probiotics: prevention and management of allergic diseases by probiotics. *J. Nutr.* 140, 713S–721S. doi: 10.3945/jn.109.113761

Köberl, M., Müller, H., Ramadan, E. M., and Berg, G. (2011). desert farming benefits from microbial potential in arid soils and promotes diversity and plant health. edited by jack anthony gilbert. *PLoS One* 6:e24452. doi: 10.1371/journal.pone.0024452

Koutsos, A., Lima, M., Conterno, L., Gasperotti, M., Bianchi, M., Fava, F., et al. (2017). Effects of commercial apple varieties on human gut microbiota composition and metabolic output using an in vitro colonic model. *Nutrients* 9:533. doi: 10.3390/nu9060533

Kwak, M.-J., Kong, H. G., Choi, K., Kwon, S.-K., Song, J. Y., Lee, J., et al. (2018). Rhizosphere microbiome structure alters to enable wilt resistance in tomato. *Nat. Biotechnol.* 36, 1100–1109. doi: 10.1038/nbt.4232

Leff, J. W., and Fierer, N. (2013). Bacterial communities associated with the surfaces of fresh fruits and vegetables. *PLoS One* 8:e59310. doi: 10.1371/journal.pone.0059310

Liu, J., Abdelfattah, A., Norelli, J., Burchard, E., Schena, L., Droby, S., et al. (2018). Apple endophytic microbiota of different rootstock/scion combinations suggests a genotype-specific influence. *Microbiome* 6:18. doi: 10.1186/s40168-018-0403-x

Lundberg, D. S., Lebeis, S. L., Paredes, H. S., Yourstone, S., Gehring, J., Malfatti, S., et al. (2012). Defining the core *Arabidopsis Thaliana* root microbiome. *Nature* 488, 86–90. doi: 10.1038/nature11237

Lundberg, D. S., Yourstone, S., Mieczkowski, P., Jones, C. D., and Dangl, J. L. (2013). Practical innovations for high-throughput amplicon sequencing. *Nat. Methods* 10, 999–1002. doi: 10.1038/nmeth.2634

Manz, W., Amann, R., Ludwig, W., Wagner, M., and Schleifer, K.-H. (1992). Phylogenetic oligodeoxynucleotide probes for the major subclasses of *Proteobacteria*: problems and solutions. *Syst. Appl. Microbiol.* 15, 593–600. doi: 10.1016/s0723-2020(11)80121-9

Meier, H., Amann, R., Ludwig, W., and Schleifer, K. H. (1999). Specific oligonucleotide probes for in situ detection of a major group of gram-positive bacteria with low DNA G+C content. *Syst. Appl. Microbiol.* 22, 186–196. doi: 10.1016/s0723-2020(99)80065-4

Ottesen, A., Ramachandran, P., Reed, E., Gu, G., Gorham, S., Ducharme, D., et al. (2019). Metagenome tracking biogeographic agroecology: phytobiota of tomatoes from virginia, maryland, north carolina and california. *Food Microbiol.* 79, 132–136. doi: 10.1016/j.fm.2018.12.001

Peiffer, J. A., Spor, A., Koren, O., Jin, Z., Tringe, S. G., Dangl, J. L., et al. (2013). Diversity and heritability of the maize rhizosphere microbiome under field conditions. *Proc. Natl. Acad. Sci. U.S.A.* 110, 6548–6553. doi: 10.1073/pnas.1302837110

Philippot, L., Raaijmakers, J. M., Lemanceau, P., and van der Putten, W. H. (2013). Going back to the roots: the microbial ecology of the rhizosphere. *Nat. Rev. Microbiol.* 11, 789–799. doi: 10.1038/nrmicro3109

Pirhonen, M., Flego, D., Heikinheimo, R., and Palva, E. T. (2018). A small diffusible signal molecule is responsible for the global control of virulence and exoenzyme production in the plant pathogen erwinia carotovora. *EMBO J.* 12, 2467–2476. doi: 10.1002/j.1460-2075.1993.tb05901.x

Pusey, P. L., Stockwell, V. O., and Mazzola, M. (2009). Epiphytic bacteria and yeasts on apple blossoms and their potential as antagonists of erwinia amylovora. *Phytopathology* 99, 571–581. doi: 10.1094/PHYTO-99-5-0571

Sanz, Y., Olivares, M., Moya-Pérez, A., and Agostoni, C. (2015). Understanding the role of gut microbiome in metabolic disease risk. *Pediatr. Res.* 77, 236–244. doi: 10.1038/pr.2014.170

Shade, A., McManus, P. S., and Handelsman, J. (2013). Unexpected diversity during community succession in the apple flower microbiome. edited by Jizhong Zhou. *MBio* 4, 3–15. doi: 10.1128/mBio.00602-12

Shannon, P., Markiel, A., Ozier, O., Baliga, N. S., Wang, J. T., Ramage, D., et al. (2003). Cytoscape: a software environment for integratedmodels of biomolecular interaction networks. *Genome Res.* 13, 2498–2504. doi: 10.1101/gr.1239303

Shoji, T., and Miura, T. (2014). Apple polyphenols in cancer prevention. *Poly. Hum. Health Dis.* 2, 1373–1383. doi: 10.1016/B978-0-12-398456-2.00104-3

Shtriker, M. G., Hahn, M., Taieb, E., Nyska, A., Moallem, U., Tirosh, O., et al. (2018). Fenugreek galactomannan and citrus pectin improve several parameters associated with glucose metabolism and modulate gut microbiota in mice. *Nutrition* 46, 134.e–142.e. doi: 10.1016/j.nut.2017.07.012

Stockwell, V. O., Johnson, K. B., Sugar, D., and Loper, J. E. (2010). Control of fire blight by *Pseudomonas* Fluorescens A506 and pantoea vagans C9-1 applied as single strains and mixed inocula. *Phytopathology* 100, 1330–1339. doi: 10.1094/PHYTO-03-10-0097

Taguri, T., Tanaka, T., and Kouno, I. (2004). Antimicrobial activity of 10 different plant polyphenols against bacteria causing food-borne disease. *Biol. Pharm. Bull.* 27, 1965–1969. doi: 10.1248/bpb.27.1965

Verginer, M., Siegmund, B., Cardinale, M., Müller, H., Choi, Y., Míguez, C. B., et al. (2010). Monitoring the plant epiphyte methylobacterium extorquens DSM 21961 by real-Time PCR and its influence on the strawberry flavor. *FEMS Microbiol. Ecol.* 74, 136–145. doi: 10.1111/j.1574-6941.2010.00942.x

Vorholt, J. A. (2012). Microbial life in the phyllosphere. *Nat. Rev. Microbiol.* 10, 828–840. doi: 10.1038/nrmicro2910

Wassermann, B., Rybakova, D., Müller, C., and Berg, G. (2017). Harnessing the microbiomes of brassica vegetables for health issues. *Sci. Rep.* 7:17649. doi: 10.1038/s41598-017-17949-z

World Health Organization [WHO] (2015). World Health Statistics 2015 indicator compendium. *Ind. Code Book* 92:1564441.

Yashiro, E., Spear, R. N., and McManus, P. S. (2011). Culture-dependent and culture-independent assessment of bacteria in the apple phyllosphere. *J. Appl. Microbiol.* 110, 1284–1296. doi: 10.1111/j.1365-2672.2011.04975.x

Zuercher, A. W., Holvoet, S., Weiss, M., and Mercenier, A. (2010). Polyphenol-enriched apple extract attenuates food allergy in mice. *Clin. Exp. Aller.* 40, 942–950. doi: 10.1111/j.1365-2222.2010.03460.x

Conflict of Interest Statement: The authors declare that the research was conducted in the absence of any commercial or financial relationships that could be construed as a potential conflict of interest.

frontiers in Plant Science

ORIGINAL RESEARCH
published: 25 July 2019
doi: 10.3389/fpls.2019.00922

Revealing Cues for Fungal Interplay in the Plant–Air Interface in Vineyards

Ahmed Abdelfattah[1,2], Simona M. Sanzani[3†], Michael Wisniewski[4], Gabriele Berg[5], Santa O. Cacciola[6] and Leonardo Schena[1]**

[1] Dipartimento di Agraria, Università Mediterranea di Reggio Calabria, Reggio Calabria, Italy, [2] Department of Ecology, Environment and Plant Sciences, Stockholm University, Stockholm, Sweden, [3] Dipartimento di Scienze del Suolo, della Pianta e degli Alimenti, Università degli Studi di Bari Aldo Moro, Bari, Italy, [4] U.S. Department of Agriculture–Agricultural Research Service (USDA-ARS), Kearneysville, WV, United States, [5] Institute of Environmental Biotechnology, Graz University of Technology, Graz, Austria, [6] Dipartimento di Agricoltura, Alimentazione e Ambiente, Università degli Studi di Catania, Catania, Italy

OPEN ACCESS

Edited by:
Jia Liu,
Chongqing University of Arts and Sciences, China

Reviewed by:
Walter Chitarra,
Council for Agricultural and Economics Research, Italy
Yan Li,
China Agricultural University (CAU), China

***Correspondence:**
Ahmed Abdelfattah
ahmed.abdelfattah@su.se
Leonardo Schena
lschena@unirc.it

†Present address:
Simona M. Sanzani,
Mediterranean Agronomic Institute of Bari (CIHEAM – IAMB), Valenzano, Italy

Specialty section:
This article was submitted to Plant Abiotic Stress, a section of the journal Frontiers in Plant Science

Received: *07 April 2019*
Accepted: *01 July 2019*
Published: *25 July 2019*

Citation:
Abdelfattah A, Sanzani SM, Wisniewski M, Berg G, Cacciola SO and Schena L (2019) Revealing Cues for Fungal Interplay in the Plant–Air Interface in Vineyards. Front. Plant Sci. 10:922. doi: 10.3389/fpls.2019.00922

Plant-associated microorganisms play a crucial role in plant health and productivity. Belowground microbial diversity is widely reported as a major factor in determining the composition of the plant microbiome. In contrast, much less is known about the role of the atmosphere in relation to the plant microbiome. The current study examined the hypothesis that the atmospheric microbiome influences the composition of fungal communities of the aboveground organs (flowers, fruit, and leaves) of table grape and *vice versa*. The atmosphere surrounding grape plantings exhibited a significantly higher level of fungal diversity relative to the nearby plant organs and shared a higher number of phylotypes (5,536 OTUs, 40.3%) with the plant than between organs of the same plant. Using a Bayesian source tracking approach, plant organs were determined to be the major source of the atmospheric fungal community (92%). In contrast, airborne microbiota had only a minor contribution to the grape microbiome, representing the source of 15, 4, and 35% of the fungal communities of leaves, flowers, and fruits, respectively. Moreover, data indicate that plant organs and the surrounding atmosphere shared a fraction of each other's fungal communities, and this shared pool of fungal taxa serves as a two-way reservoir of microorganisms. Microbial association analysis highlighted more positive than negative interactions between fungal phylotypes. Positive interactions were more common within the same environment, while negative interactions appeared to occur more frequently between different environments, i.e., atmosphere, leaf, flower, and fruit. The current study revealed the interplay between the fungal communities of the grape phyllosphere with the surrounding air. Plants were identified as a major source of recruitment for the atmospheric microbiome, while the surrounding atmosphere contributed only a small fraction of the plant fungal community. The results of the study suggested that the plant–air interface modulates the plant recruitment of atmospheric fungi, taking a step forward in understanding the plant holobiont assembly and how the atmosphere surrounding plants plays a role in this process. The impact of plants on the atmospheric microbiota has several biological and epidemiological implications for plants and humans.

Keywords: grapes, microbiota, fungal community, aerobiology, spore trap, ITS amplicon libraries, holobiont, metagenomics

INTRODUCTION

Microorganisms play a major role in shaping ecosystems, contributing to nutrient cycling, primary production, litter decomposition, and multitrophic interactions (Mahnert et al., 2015; Abdelfattah et al., 2018). In recent years, the importance of the functional role that plant-associated microorganisms play in plant health, productivity, and environmental resilience has been increasingly recognized (Berendsen et al., 2012; Berg et al., 2014a). The beneficial effects of the microbiota on plant health include increased tolerance to biotic and abiotic stresses (Eleonora et al., 2015; Unyarat et al., 2016), growth promotion, and increased nutrient intake (van der Heijden et al., 2015). In recognition of these effects, the hologenome theory suggests that the holobiont (host plus symbionts) with its hologenome (host genome plus microbiome) act as a single evolutionary unit (Zilber-Rosenberg and Rosenberg, 2008). In this regard, the source, dissemination, spatial distribution, and conservation of the plant microbiome are critical to understanding the plant holobiont. Although soil is often reported to be a major source of plant microbiota (Bulgarelli et al., 2013; Edwards et al., 2015; Belda et al., 2017; Hassani et al., 2018), the role of the atmosphere as a source for the recruitment and dissemination of the plant microbiota is poorly understood.

The atmosphere (air) has long been considered a poor ecosystem for the growth and multiplication of microbes, but recent studies, especially of indoor, artificial environments, have demonstrated the presence of a substantial number of microorganisms in air samples (Elbert et al., 2007; Fröhlich-Nowoisky et al., 2009; Mahnert et al., 2015). These atmospheric microorganisms have been implicated in metabolizing atmospheric organic matter, influencing the earth's biogeochemical cycles, affecting atmospheric chemistry, precipitation cycles, and even climate change (Delort et al., 2010; Rosenfeld et al., 2014; Behzad et al., 2015). Among airborne microorganisms, fungi have a particular importance when it comes to plants, since major plant pathogens are dispersed by air currents.

The microbiome of grapevine (*Vitis vinifera* L., 1753) has been extensively studied. It comprises approximately 10^3 and 10^5 colony-forming units (cfu) of fungi and bacteria per gram of fresh tissue, respectively (Verginer et al., 2010; Pinto et al., 2014; Marasco et al., 2018). The importance of microorganisms associated with grape plants in vineyards has been progressively recognized due to their impact on plant health and productivity (Grube et al., 2011; Schmid et al., 2011; Berg et al., 2014a). The composition of the grape microbiome was also found to distinguish different viticultural regions and contribute to determining wine properties (Bokulich et al., 2016). While soil is often reported to be a major source of grapevine microbiota (Belda et al., 2017; Hassani et al., 2018), the impact of the surrounding atmosphere as a source of recruitment is completely unknown. The hypothesis examined in the present study is that the atmospheric microbiome influences the composition of the fungal communities associated with the aboveground organs (flowers, fruit, and leaves) of table grapes and *vice versa*. Therefore, the fungal microbiota associated with plant organs (flowers, leaves, and fruits) and the surrounding air were investigated in order to evaluate their reciprocal role in the modulation of fungal communities.

MATERIALS AND METHODS

Vineyards

Table grape vineyards, variety "Italia" grafted on Kober 5BB (Berlandieri × Riparia), with plantation of the same age (10 years old) were used in the present study. Both vineyards were located in Castellaneta, Province of Taranto, Italy (40°34′35.1″N 16°56′27.4″E and 40°33′35.0″N 16°55′47.3″E, respectively). The vineyards were approximately 2 km distant from each other and situated at the same altitude (approximately 70 m a.s.l). The grapevines were trained with the "tendone" system, which favors horizontal growth of the canopy at around 2 m from the ground.

Sample Collection

Samples were collected from vineyards, located in Castellaneta, Province of Taranto, Italy (40°34′35.1″N 16°56′27.4″E and 40°33′35.0″N 16°55′47.3″E), in three uniform plots consisting of 10 plants. Plots were approximately 150 m apart. To collect airborne fungal spores, specific traps containing a thin layer (1 ml) of liquid Vaseline containing phenol were prepared with standard Petri dishes (100 mm × 15 mm) without lid. Traps were hung using iron wires, and suspended 20 cm below the main vegetation layer, which was approximately 150 cm above the soil surface. Each sampling plot consisted of 10 spore traps (one per plant), making a total of 30 traps per vineyard. Spore traps were left for 1 week at the beginning of each month, starting from flowering (first half of June), and continued monthly until harvest (first half of October), resulting in five sampling time points and an overall total of 300 spore traps. Flowers, fruit, and leaves were sampled from the same plots, simultaneously to traps. Ten leaves and fruit bunches were collected from each pot (one per plant). These samples were pooled to have three biological replicates per each sampling time and vineyard ($n = 90$).

DNA Extraction

All collected samples were transported to the lab in cool containers (5°C). Leaves and bunches where frozen, lyophilized (Labconco® FreeZone 2.5), and grounded in liquid nitrogen with sterile mortars and pestles. Total DNA was extracted from 80 mg of homogenate tissues using DNeasy Plant Mini Kit (Qiagen®). Concentration and quality of extracted DNA were assessed using Nanodrop spectrophotometer (Thermo Fisher Scientific, Inc., United States). All samples were diluted to have a uniform DNA concentration of 10 ng μl^{-1}.

To extract DNA from spore traps, 1.5 ml of a preheated (65°C) buffer, containing 2% cetyltrimethylammonium bromide (CTAB), 1.4 M NaCl, 20 mM EDTA, pH 8, 100 mM Tris–HCl, pH 8, and 1% PVP, was added to each plate and the surface was scrubbed with a sterile L-shaped plastic rod in order to detach fungal spores. The resulting suspension obtained from each plate was used for total DNA using the protocol described by Schena and Cooke (2006). Extracts were purified

with the Agencourt AMPure XP system (Beckman Coulter, Inc.) to eliminate any phenol or traces of Vaseline. Purified DNA extracts from plates of each plot (10 subsamples) were pooled together to have three biological replicates per each sampling time and vineyard. Pooled samples were analyzed using a Nanodrop spectrophotometer (Thermo Fisher Scientific, Inc., Waltham, MA, United States) and DNA concentration was adjusted to a uniform concentration of 10 ng/μl.

Amplicon Generation and Sequencing

The universal primers ITS3_KYO2 and ITS4 were used to amplify the ITS2 region of the ribosomal DNA (Toju et al., 2012). Both primers were modified to include Illumina adaptors[1] for subsequent multiplexing. PCR reactions were conducted in a total volume of 25 μl containing 12.5 μl of KAPA HiFi HotStart ReadyMix (Kapa Biosystems, Wilmington, MA, United States), 1.5 μl of each primer (10 μM), and 2.5 μl of DNA template. Reactions were incubated in a T100 thermal cycler (Bio-Rad, Hercules, CA, United States) for 3 min at 98°C, followed by 30 cycles of 30 s at 95°C, 30 s at 50°C, and 30 s at 72°C. All reaction cycles ended with a final extension time of 1 min at 72°C. A negative control in which nuclease-free water (QIAGEN, Valencia, CA, United States) replaced template DNA was included at all of the assessment times. All amplicons, including amplification mixtures from negative controls were sequenced using Illumina MiSeq V3 (2 × 300 bp) chemistry according to the manufacturer's instructions.

Data Analysis

Illumina adaptors were clipped and low-quality reads were removed by Trimmomatic 0.36 (Bolger et al., 2014) using a sliding window trimming, cutting once the average quality within the window of four bases falls below a quality threshold of 15. Paired-end reads were then merged utilizing PANDAseq with default parameters and read overlap of 20 bp (Masella et al., 2012). Chimeric sequences were identified and removed using VSEARCH 1.4.0 (Rognes et al., 2016). UCLUST algorithm (Edgar, 2010), as implemented in QIIME 1.9.1 (Caporaso et al., 2010), was used to cluster sequences queried against the UNITE dynamic database released on 01.12.2017 (Abarenkov et al., 2010) at a similarity threshold of 97%. Sequences that failed to cluster against the database were *de novo* clustered using the same algorithm. After removing singletons, the most abundant sequences in each Operational Taxonomic Unit (OTU) were selected as representative sequences and used for the taxonomic assignment using the BLAST algorithm (Altschul et al., 1990) as implemented in QIIME 1.9.1.

Diversity Metrics and Statistics

Rarefaction to an even sequencing depth of 1,000 reads per sample was used to normalize the OTU table. The rarefied OTU table was used to calculate alpha diversity indices including Observed Species (*Sobs*) and Shannon metrics. Non-parametric two-sample *t* test was used to compare alpha diversities. MetagenomeSeq's cumulative sum scaling (CSS) (Paulson et al., 2013) was used as a normalization method for other downstream analyses. The CSS normalized OTUs table was analyzed using Bray–Curtis metrics (Bray and Curtis, 1957) and utilized to evaluate beta diversity and construct PCoA plots using Emperor (Lozupone and Knight, 2005). Similarity in community composition was tested *via* ANOSIM in QIIME 1.9.1 using 999 permutations. The most prevalent taxa (≥0.1%) were selected in order to evaluate the significance of differences in the relative abundance of the detected taxa using Kruskal–Wallis method (Kruskal and Wallis, 1952). Significance in all of the analyses was determined using 999 Monte Carlo permutations, and Benjamini–Hochberg (FDR) corrections were used to adjust the calculated *p* values. Cytoscape 3.3.0 was used to analyze the CSS normalized OTU table and construct network figures to visually display unique and shared OTUs between samples.

Source Tracking

To estimate the source of the fungal community present in air as well as leaf, fruit, and flower (designated here environments), we used SourceTracker2[2]. This tool was designed to estimate proportion/fraction of community that originates from a set of source environments by using a Bayesian approach and Gibb's sampling method (Knights et al., 2011). Here, we tested each environment for being a source or a sink. For this purpose, we conducted multiple runs by setting one environment as sink while setting the others as sources and repeated this process for all environments. To estimate the fraction of communities that is shared between source and sink, the following assumptions were made: if x is the fraction of environment A that originate from environment B, and y is the fraction of environment B that originate from environment A, then z (fraction of fraction), calculated as ($x * y$) represents the fraction of communities that return from A to B and/or B to A. Furthermore, the sum of z obtained from all sources in a given environment represents the total fraction of a community that return to the same environment. Hence, the sum of z can be considered as an index of conservation; higher values indicate a stable community and lower values indicate variable communities.

Interaction Network

Inferred fungal associations (co-occurrence and mutual exclusion) within grape and air samples were computed using the CoNet (v1.1.1. beta) plugin within Cytoscape (v3.6.1). Rare taxa were discarded from the analysis by considering only OTUs present in at least 20 samples. The associations/interaction between fungal phylotypes were calculated using a combination of five methods, i.e., Spearman, Pearson coefficients, Bray–Curtis and Kullback–Leibler dissimilarity metrics, and Mutual Information (Kullback and Leibler, 1951; Bray and Curtis, 1957). *p* values for each metric were calculated by 100 permutation using edgeScores routine and shuffle rows as resampling strategy. This was followed by bootstrapping step using 100 iterations, where unstable edges were removed. All the calculated method-specific *p* values of an edge were merged into one *p* value using Brown's method (Brown, 1975), and Benjamini–Hochberg multiple

[1] www.illumina.com

[2] https://github.com/biota/sourcetracker2

testing correction was used false-discovery rate correction (Benjamini and Hochberg, 1995). The created network was clustered using simple division based on connectivity, based on Connected Components algorithm as implemented in clusterMaker2 (Morris et al., 2011).

RESULTS

OTUs Distribution and Shared Communities

After quality evaluation and deletion of chimeric reads, singletons, and plant sequences, a total of 5,566,210 fungal sequences were obtained from the 90 analyzed samples (air, leaves, and flowers/fruits) collected monthly (from June to October) from table grape vineyards. The sequences were assigned to 13,773 OTUs using a 97% similarity threshold (**Supplementary Table S1**). The number of OTUs varied significantly between air samples and grape organs. The highest number of OTUs was present in air samples (11,700 OTUs) followed by leaves (4,926 OTUs), fruit (4,011 OTUs), and flowers (1,373 OTUs). The number of unique OTUs followed the same order, accounting for 6,164, 622, and 74 OTUs, respectively. The largest fraction of shared OTUs (5,536 OTUs, 40.3%) was between air samples and the various grape organs. Overall, atmospheric samples shared 3,461, 2,844, and 957 OTUs with leaves, fruits, and flowers, respectively, of which 2,184, 1,669, and 342 OTUs were exclusively shared between air and each of these organs, respectively (**Figure 1**). Notably, 385 OTUs (2.8%) were common to all samples and only 43 OTUs (0.3%) were shared between grape organs (leaves, fruit, and flowers).

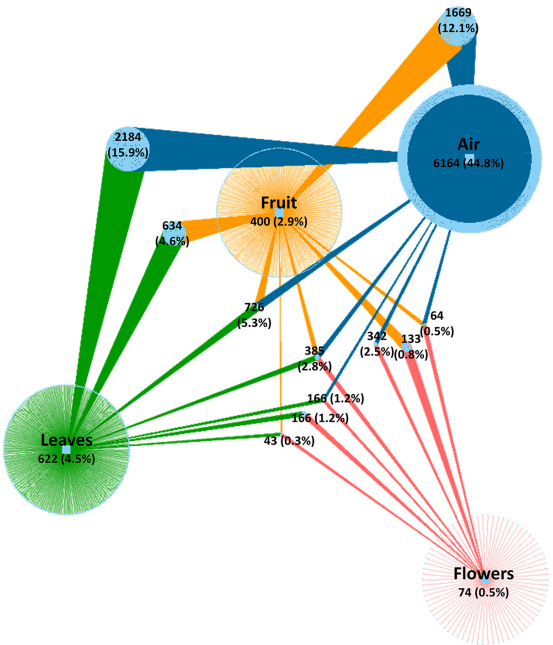

FIGURE 1 | Network of shared and unique fungal OTUs among investigated samples. Colored edges (links) represent OTUs associated to sample types (air, fruit, leaves, and flowers). Light blue circle nodes connecting two or more samples represent shared OTUs. Numerical values indicate the number of OTUs and their percentage relative to the total number of OTUs.

Source and Dissemination of the Fungal Communities

SourceTracker2 software was used to determine the source of the fungal community (Knights et al., 2011). Results indicated that fungi associated with grape organs (leaf, flower, and fruit) mainly originated from the plant itself (**Table 1** and **Figures 2A,B**). The leaf community originated from flower (52%), fruit (32%), and atmospheric (15%) communities. Fungi associated with flowers were primarily recruited from leaves (81%), fruit (12%), and air (4%). Furthermore, the fruit community originated from leaves (47%), flowers (17%), and air (35%). In contrast, most of the atmospheric community (92%) originated from plant tissues, i.e., fruit (54%), leaves (30%), and flowers (8%), while the remaining 8% was from an unknown source.

To test whether the communities associated with each environment could return to the same environment, the plant contribution to the atmospheric community was multiplied by the corresponding contribution of the atmospheric microbiota to that plant fungal community. Based on these calculations, the fungal taxa that may have originated from fruit, leaves, and flowers and returned to the same organs through the air was estimated to be 19, 4.5, and 0.3%, respectively (**Figure 2B**). Similarly, 14.8 and 2.0% of the leaf and flower fungal taxa were estimated to contribute to the fruit fungal community and may have originated from the fruit itself. Lastly, 42% of leaf fungal taxa contributed to the flower fungal community and may have originated from the flowers themselves. These estimates were considered as factions of communities that return to the same organ and that were common to both sinks and sources. Therefore, the sum of these fractions represents the overall fraction of a community associated with an environment (plant organ or air) that may have returned to the same environment from different sources. The sum of fractions indicated that 23.7, 35.7, 61.3, and 44.3% of air, fruit, leaf, and flower communities, respectively, returned to the same organs and were interchangeable with all of the other environments.

TABLE 1 | Estimated source of fungal communities associated to air, fruit, leaves, and flowers (read data according to the first column).

	Air	Fruit	Leaf	Flower	Unknown
Air	–	54%	30%	8%	8%
Fruit	35%	–	47%	17%	1%
Leaves	15%	32%	–	52%	2%
Flowers	4%	12%	81%	–	4%

Fungal Interaction Within and Between Plant Organ and Atmospheric Communities

The co-occurrence and mutual exclusion of specific fungal OTUs were analyzed taking their origin into

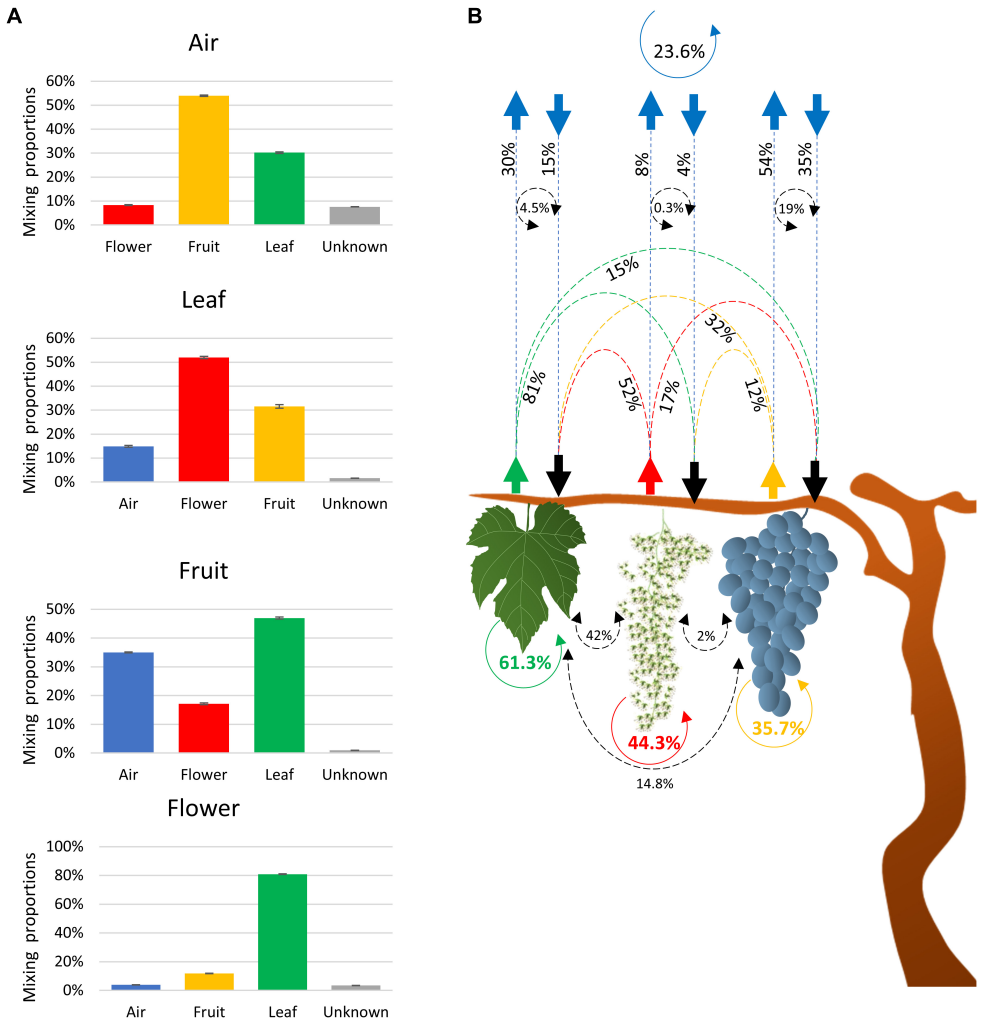

FIGURE 2 | Charts showing fractions of the estimated sources of fungal communities in each sink environment (air, leaves, and flowers/fruit) **(A)** and schematic description of the estimated source of the fungal communities associated with air and plant organs **(B)**. The scheme shows the estimated movement of communities originated from leaves (green dashed arrows), flower (red dashed arrows), fruit (orange dashed arrows), and air (blue arrows). Dashed black circle arrows indicate the percentages of community commonly exchanged between two environments. Solid colored circle arrows showed the percentages of community that retune to the same environment from all the other sources **(B)**.

consideration, i.e., flowers, fruit, leaves, and/or air. The resulting network, after statistical calculations and removal of unstable edges/links, was characterized by 161 nodes (OTUs) linked with 300 edges, and a clustering coefficient of 0.253 (**Figure 3**). Overall, the interactions between fungal phylotypes were characterized by a higher number of co-occurrences (237) compared to mutual exclusions (62). Highly connected OTUs included taxa of the genus *Cladosporium*, *Alternaria*, *Stemphylium*, *Mycosphaerella*, and an unidentified genus in the order *Pleosporales* (**Figure 3**). The latter unidentified genus had the highest number of interactions (20) and also the highest number of mutual exclusion relationships (17).

Twelve clusters with an average size of 13.417 were identified using a simple division based on connectivity (**Figure 3**). A single cluster contained the most interacting OTUs while the other clusters contained 2, 3, or 4 OTUs. Within the main cluster, four sub-clusters appeared to be influenced by the average relative abundance distribution of the interacting OTUs in the investigated samples. These sub-clusters consisted of OTUs mainly associated with plant tissue (sub-cluster A), air samples (sub-cluster B), or evenly distributed among the investigated samples (sub-clusters C and D). Sub-cluster D was similar to sub-cluster A but contained OTUs with the highest abundances. Interactions mainly involved taxa in the phylum *Ascomycota* followed by *Basidiomycota*, unidentified fungi, *Mucoromycota*, and *Glomeromycota*. *Basidiomycota* seemed especially abundant in sub-cluster C. Taxa that were more prevalent in one organ tended to be highly interactive, creating subgroups with fewer connections to other subgroups. This was particularly evident in the air and flowers communities. Furthermore, the majority, if not all, of the negative interactions

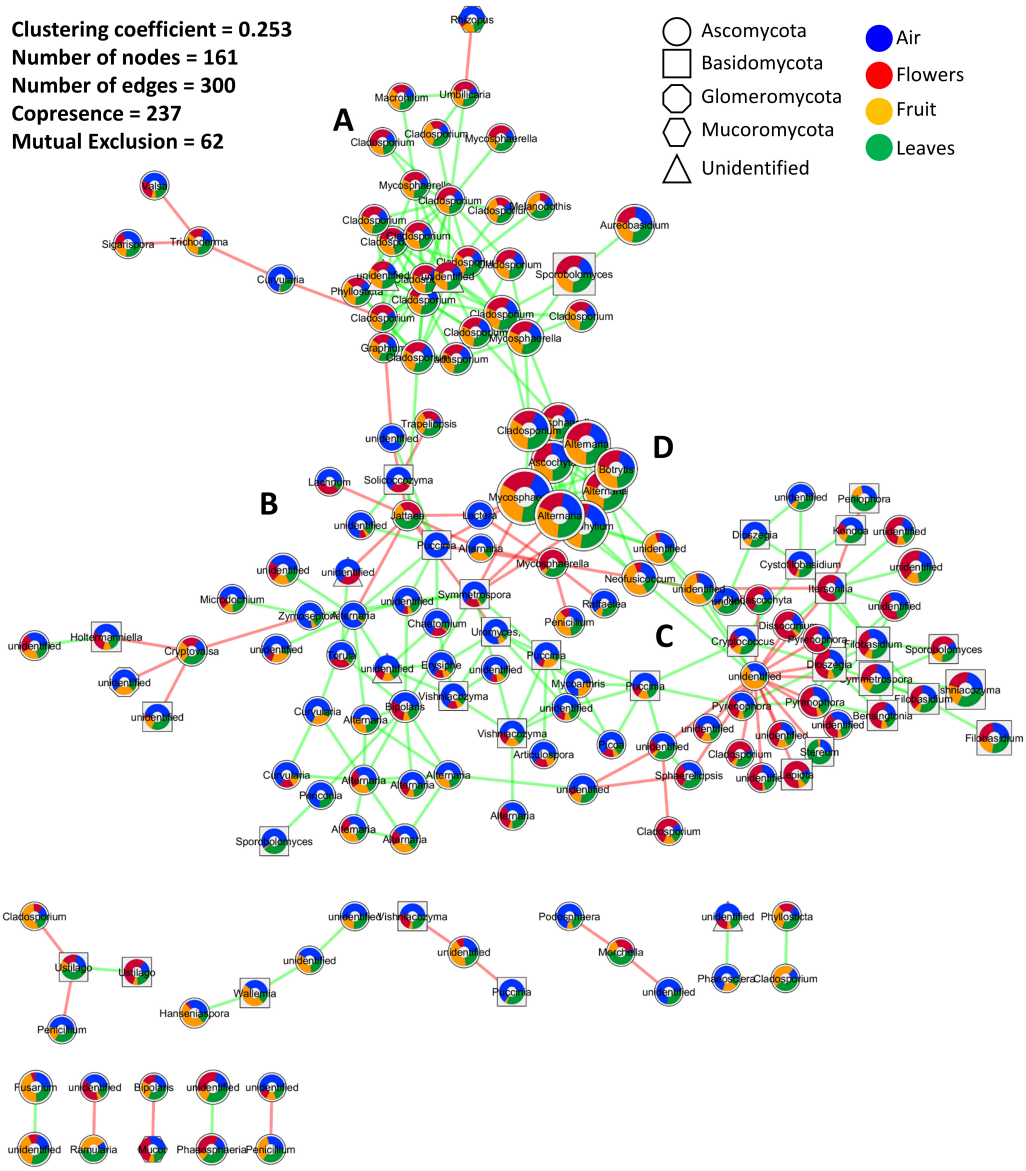

FIGURE 3 | Microbial association network showing interactions (co-occurrence and mutual exclusion) represented by green and red links, respectively. The size of the nods indicates the average relative abundance of OTUs across all investigated samples, while colored pie charts embedded inside the nodes show the relative distribution of each OTU in different samples (air, flowers, fruit, and leaves). Node shapes are used to differentiate fungal phyla. **(A–D)** are used to indicate the four sub-clusters that appeared to be influenced by the average relative abundance distribution of the interacting OTUs in the investigated samples. Interactions were calculated by CoNet, clustered using Connected Components algorithm as implemented in clusterMaker2, and visualized in Cytoscape 3.6.

occurred between taxa from two different subgroups while within-subgroup interactions were more highly characterized by positive interactions.

Community Composition

The identified OTUs were assigned to 14 fungal phyla, 51 classes, and 1,032 genera. Overall, *Ascomycota* (80.60%), *Basidiomycota* (16.40%), an unidentified phylum (1.60%), *Glomeromycota* (0.5%), and *Mucoromycota* (0.3%) accounted for 99.3% of the total detected taxa (**Supplementary Figure S1**). At the genus level, *Alternaria*, *Cladosporium*, *Mycosphaerella*, unidentified *Pleosporales*, unidentified *Ascomycota*, *Stemphylium*, *Aspergillus*, *Penicillium*, *Sporobolomyces*, *Vishniacozyma*, and *Ascochyta* represented over 50% of the total detected fungal genera (**Supplementary Figure S2**). Beta diversity (Bray–Curtis dissimilarity metric) analyses indicated that air, leaf, and flowers/fruit samples across all sampling times were characterized by significantly different fungal communities (**Table 2**). In contrast, alpha diversity, evaluated using the Shannon index, varied significantly between atmospheric samples and plant organs but not between samples collected from different plant organs (**Table 2**). These results were consistent in both vineyards.

TABLE 2 | Comparisons between grape organs (flowers, fruits, and leaves) and air samples regardless of the sampling time using alpha (Shannon index) and beta diversity (Bray–Curtis metric).

	Flower		Fruit		Leaves	
	Shannon	**ANOSIM**	**Shannon**	**ANOSIM**	**Shannon**	**ANOSIM**
Fruit	0.511	0.008 (0.333)				
Leaves	0.743	0.415 (0.017)	0.571	0.002 (0.184)		
Air	0.004	0.001 (0.653)	0.003	0.001 (0.688)	0.006	0.001 (0.560)

p-values are the results of Student t-test method for alpha diversity and ANOSIM test for beta diversity with R values between parentheses.

The majority of fungal genera characterized by a ≥1% relative abundance was detected in all of the investigated sample types. The fungal community composition and relative abundance of different genera, however, varied significantly between the investigated sample types (**Figure 4**). Some taxa distinguished atmospheric samples from plant organs, having either a significantly lower (*Cladosporium* and *Mycosphaerella*) or higher (unidentified *Ascomycota*) relative abundance. In contrast, genera such as *Alternaria*, unidentified *Pleosporales*, *Neofusicoccum*, and *Fusarium* were more abundant in fruits than in the other sample types, while *Sporobolomyces*, *Pyrenophora*, and *Dioszegia* dominated in flowers. A complete list of the fungal genera that significantly differed in their relative abundance between the investigated sample types is presented in **Supplementary Table S2**.

DISCUSSION

The present study demonstrated that the atmosphere surrounding the grape phyllosphere has a significantly higher level of fungal diversity than the grape phyllosphere composed of flowers, leaves, and fruits. The high level of fungal diversity was unexpected considering the low availability of nutrients, which is regarded as a key factor in determining microbial diversity in any specific environment (Waldrop et al., 2006; Cline et al., 2018). The data suggest that other factors, such as air currents and the attributes of the local physical environment have more influence on determining atmospheric fungal diversity than nutrient availability.

Several studies have shown that airborne microorganisms are influenced by and may originate from nearby sources such as soil, water, and vegetation (Cho et al., 2006; Behzad et al., 2015). In agreement with these studies, our data indicated that air samples shared a high number of phylotypes (5536 OTUs, 40.3%) with plant organs, and actually a fraction higher than those shared between organs within the same plant.

The Bayesian approach used to estimate the source of the fungal communities also confirmed that a large portion (92%) of the atmospheric fungal community originated from the local plants (grapevines). The same analysis indicated that a smaller percentage (4 to 35%) of the plant-associated fungi originated from the atmosphere, whereas the plant was the major source of its own microbiota. These results, in addition to confirming the

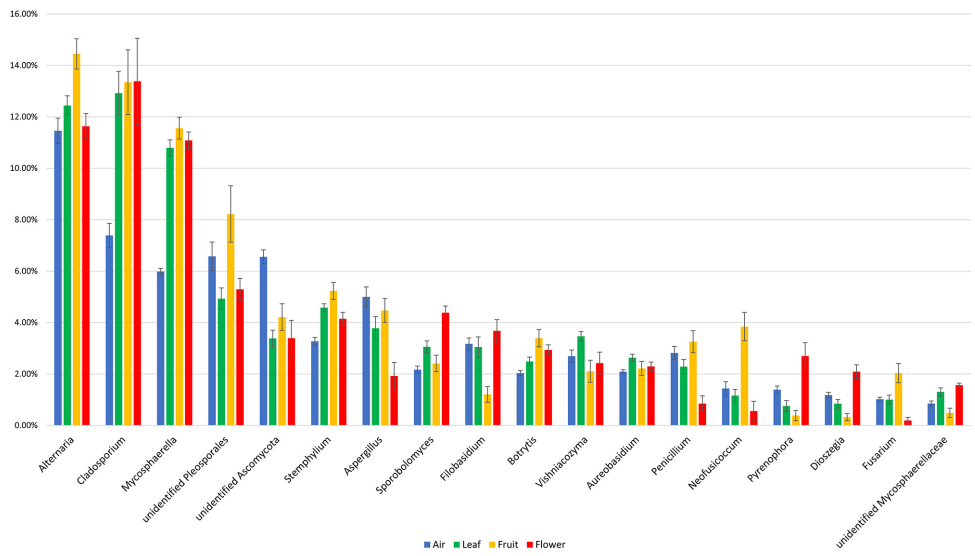

FIGURE 4 | Fungal taxa with significant temporal variations and a relative abundance of at least taxa 1% in different investigated samples (air, fruit, flowers, and leaves). The statistical comparison was done using a non-parametric Kruskal–Wallis test, and the *p* values were calculated through 1000 permutation and corrected using FDR method (**Supplementary Table S2**).

role of vegetation in determining the atmospheric microbiome, have important implications on the role of the atmosphere in modulating and mediating the movement of taxa within the plant microbiome. It appears that the plant recruits phyllosphere microorganisms from the atmosphere, which is analogous to the process that occurs between the soil and rhizosphere. Thus, the study demonstrated that the atmosphere serves as a source of recruitment for the fungal communities inhabiting leaves, flowers, and fruits. However, since the atmospheric microbiota surrounding vegetation is highly conditioned by the plants, data also indicate that a fraction of the plant microbiota acquired from the air is originally derived from the same plant. This result raises an important question about the mechanisms of movement/dissemination of microorganisms in the plant canopy ecosystem. Although the internal movement of microbial taxa from one organ to another through the plant is a plausible avenue, the current study makes it difficult to exclude a scenario in which external microbial exchange between plant organs can occur through the atmosphere. Additionally, if a plant genotype selects, and at least partially determines, the microbial species present in its phyllosphere (Berg et al., 2014b), the impressive concentration and diversity of plant-related fungal taxa in the air surrounding a plant surface (plant–air interface) could limit the exchange of microorganisms (between air and plant) to those that already make part of the plant microbiota. Moreover, since the fungal taxa shared between the atmosphere and the plant differed according to the organ, organ-specific selection may also occur. These results, in addition to the fact that we used passive spore traps that were placed for only 1 week, reduces the likelihood that the plant fungal community originated from the atmosphere are merely a random deposition. If random deposition had occurred, similar or even higher levels of fungal diversity would be expected in plant organs than in spore traps and the same shared communities would have been observed between the atmospheric samples and the various plant organs.

The study also demonstrated that a portion of the plant community returns to the plant by recruitment from the atmosphere. This portion of microorganisms can play an important role in the conservation of the plant microbiome. The obtained data support this premise in that all of the tested environments (plant organs and air samples) contained a shared community that served as a two-way source/reservoir of microorganisms. For example, the data analysis indicated that 23.7, 35.7, 61.3, and 44.4% of air, fruit, leaf, and flower communities return to these organs by recruitment from the other investigated environments. These shared factions represent a common reservoir/storage of microorganisms that could aid in maintaining and preserving the identity of the microbial signature associated with each organ. In this regard, leaves appear to be the most influential environment, sharing and receiving 61.3% of their communities with/from other environments. In contrast, air samples appeared to be the least influential environment, sharing only 23% of its fungal taxa with the various plant organs. These results, even though surprising, are supported by the well-documented stability of a plant's microbiome within a species (Laforest-Lapointe et al., 2016, 2017; Liu et al., 2018). The plant–air interface not only plays a role as a reservoir of the taxa making up the plant microbiome, mediating the movement of these microorganisms, but also shelters the plant from invasive species. Some of the observed mutual exclusions between OTUs prevalent on the plant and OTUs prevalent in air samples suggest competition at the niche level, mainly between the plant and atmosphere. These findings also support the idea that microorganisms emitted by the plant into the atmosphere could serve as a shield, protecting the plant itself and the plant's indigenous microorganisms from alien/invasive species of microorganisms. It is important to note that a considerable number of taxa detected in both air and plant samples were phytopathogens, including *Botrytis*, *Erysiphe*, *Eutypa*, *Phomopsis*, *Fomitiporia*, *Phaeomoniella*, *Phaeoacremonium*, *Botryosphaeria*, and *Neofusicoccum*, *Aspergillus*, *Didymella*, *Mucor*, and *Rhizopus*. Therefore, understanding the microbial movement between plant organs and the atmosphere, as well as the interactions between microorganisms, presents a new paradigm for the development of disease management strategies.

DATA AVAILABILITY

The datasets generated during the current study were deposited and are available at the National Center for Biotechnology Information (NCBI), Sequence Read Archive (SRA), under the accession number PRJNA494163 (www.ncbi.nlm.nih.gov/sra/PRJNA494163). Other data generated or analyzed during this study are included in this published article and its additional files.

AUTHOR CONTRIBUTIONS

AA and LS conceived and designed the experiments and analyzed the data. AA performed the experiments. LS coordinated the overall study and edited the manuscript. All authors interpreted the results, wrote the manuscript, and read and approved the manuscript.

SUPPLEMENTARY MATERIAL

The Supplementary Material for this article can be found online at: https://www.frontiersin.org/articles/10.3389/fpls.2019.00922/full#supplementary-material

FIGURE S1 | Krona chart showing the relative abundance of the detected phyla, classes, and order across all the investigated samples.

FIGURE S2 | Krona chart showing the relative abundance of the detected families, and genera across all the investigated samples.

TABLE S1 | Summary of the investigated samples in the current study (air, leaf, flower, and fruit) from different sampling points (June, July, August, September, and October) from table grape vineyards. The table shows the total number of reads and OTUs observed in each sample as well as alpha diversity (Shannon index).

TABLE S2 | List of fungal genera that significantly changed between the investigated environments according Kruskal–Wallis test.

REFERENCES

Abarenkov, K., Henrik Nilsson, R., Larsson, K. H., Alexander, I. J., Eberhardt, U., Erland, S., et al. (2010). The UNITE database for molecular identification of fungi—Recent updates and future perspectives. *New Phytol.* 186, 281–285. doi: 10.1111/j.1469-8137.2009.03160.x

Abdelfattah, A., Malacrinò, A., Wisniewski, M., Cacciola, S. O., and Schena, L. (2018). Metabarcoding: a powerful tool to investigate microbial communities and shape future plant protection strategies. *Biol. Control.* 120, 1–10. doi: 10.1016/j.biocontrol.2017.07.009

Altschul, S. F., Gish, W., Miller, W., Myers, E. W., and Lipman, D. J. (1990). Basic local alignment search tool. *J. Mol. Biol.* 215, 403–410. doi: 10.1016/S0022-2836(05)80360-2

Behzad, H., Gojobori, T., and Mineta, K. (2015). Challenges and opportunities of airborne metagenomics. *Genome Biol. Evol.* 7, 1216–1226. doi: 10.1093/gbe/evv064

Belda, I., Zarraonaindia, I., Perisin, M., Palacios, A., and Acedo, A. (2017). From vineyard soil to wine fermentation: microbiome approximations to explain the "terroir" concept. *Front. Microbiol.* 8:821. doi: 10.3389/fmicb.2017.00821

Benjamini, Y., and Hochberg, Y. (1995). Controlling the false discovery rate: a practical and powerful approach to multiple testing. *J. R. Stat. Soc. Series B Methodol.* 57, 289–300. doi: 10.1111/j.2517-6161.1995.tb02031.x

Berendsen, R. L., Pieterse, C. M. J., and Bakker, P. A. H. M. (2012). The rhizosphere microbiome and plant health. *Trends Plant Sci.* 17, 478–486. doi: 10.1016/j.tplants.2012.04.001

Berg, G., Grube, M., Schloter, M., and Smalla, K. (2014a). The plant microbiome and its importance for plant and human health. *Front. Microbiol.* 5:491. doi: 10.3389/fmicb.2014.00491

Berg, G., Grube, M., Schloter, M., and Smalla, K. (2014b). Unraveling the plant microbiome: looking back and future perspectives. *Front. Microbiol.* 5:148. doi: 10.3389/fmicb.2014.00148

Bokulich, N. A., Collins, T. S., Masarweh, C., Allen, G., Heymann, H., Ebeler, S. E., et al. (2016). Associations among wine grape microbiome, metabolome, and fermentation behavior suggest microbial contribution to regional wine characteristics. *mBio* 7:e00631-16. doi: 10.1128/mBio.00631-16

Bolger, A. M., Lohse, M., and Usadel, B. (2014). Trimmomatic: a flexible trimmer for illumina sequence data. *Bioinformatics* 30, 2114–2120. doi: 10.1093/bioinformatics/btu170

Bray, J. R., and Curtis, J. T. (1957). An ordination of the upland forest communities of southern Wisconsin. *Ecol. Monogr.* 27, 325–349. doi: 10.2307/1942268

Brown, M. B. (1975). 400: A method for combining non-independent, one-sided tests of significance. *Biometrics* 31, 987–992. doi: 10.2307/2529826

Bulgarelli, D., Schlaeppi, K., Spaepen, S., Themaat, E. V. L. V., and Schulze-Lefert, P. (2013). Structure and functions of the bacterial microbiota of plants. *Ann. Rev. Plant Biol.* 64, 807–838. doi: 10.1146/annurev-arplant-050312-120106

Caporaso, J. G., Kuczynski, J., Stombaugh, J., Bittinger, K., Bushman, F. D., Costello, E. K., et al. (2010). QIIME allows analysis of high-throughput community sequencing data. *Nat. Methods* 7, 335–336.

Cho, J. H., Hee Min, K., and Paik, N. W. (2006). Temporal variation of airborne fungi concentrations and related factors in subway stations in Seoul, Korea. *Int. J. Hyg. Environ. Health* 209, 249–255. doi: 10.1016/j.ijheh.2005.10.001

Cline, L., Hobbie, S. E., Madritch, M. D., Buyarski, C. R., Tilman, D., and Cavender-Bares, J. M. (2018). Resource availability underlies the plant–fungal diversity relationship in a grassland ecosystem. *Ecology* 99, 204–216. doi: 10.1002/ecy.2075

Delort, A.-M., Vaïtilingom, M., Amato, P., Sancelme, M., Parazols, M., Mailhot, G., et al. (2010). A short overview of the microbial population in clouds: potential roles in atmospheric chemistry and nucleation processes. *Atmos. Res.* 98, 249–260. doi: 10.1016/j.atmosres.2010.07.004

Edgar, R. C. (2010). Search and clustering orders of magnitude faster than BLAST. *Bioinformatics* 26, 2460–2461. doi: 10.1093/bioinformatics/btq461

Edwards, J., Johnson, C., Santos-Medellín, C., Lurie, E., Podishetty, N. K., Bhatnagar, S., et al. (2015). Structure, variation, and assembly of the root-associated microbiomes of rice. *Proc. Nat. Acad. Sci. U.S.A.* 112, E911–E920. doi: 10.1073/pnas.1414592112

Elbert, W., Taylor, P. E., Andreae, M. O., and Pöschl, U. (2007). Contribution of fungi to primary biogenic aerosols in the atmosphere: wet and dry discharged spores, carbohydrates, and inorganic ions. *Atmos. Chem. Phys.* 7, 4569–4588. doi: 10.5194/acp-7-4569-2007

Eleonora, R., Ramona, M., Gianpiero, V., Besma, E., Francesca, M., Laura, D. M., et al. (2015). Improved plant resistance to drought is promoted by the root-associated microbiome as a water stress-dependent trait. *Environ. Microbiol.* 17, 316–331. doi: 10.1111/1462-2920.12439

Fröhlich-Nowoisky, J., Pickersgill, D. A., Després, V. R., and Pöschl, U. (2009). High diversity of fungi in air particulate matter. *Proc. Nat. Acad. Sci.* 106, 12814–12819. doi: 10.1073/pnas.0811003106

Grube, M., Schmid, F., and Berg, G. (2011). Black fungi and associated bacterial communities in the phyllosphere of grapevine. *Fungal Biol.* 115, 978–986. doi: 10.1016/j.funbio.2011.04.004

Hassani, M. A., Durán, P., and Hacquard, S. (2018). Microbial interactions within the plant holobiont. *Microbiome* 6:58. doi: 10.1186/s40168-018-0445-0

Knights, D., Kuczynski, J., Charlson, E. S., Zaneveld, J., Mozer, M. C., Collman, R. G., et al. (2011). Bayesian community-wide culture-independent microbial source tracking. *Nat. Methods* 8, 761–763. doi: 10.1038/nmeth.1650

Kruskal, W. H., and Wallis, W. A. (1952). Use of ranks in one-criterion variance analysis. *J. Am. Stat. Assoc.* 47, 583–621. doi: 10.1080/01621459.1952.10483441

Kullback, S., and Leibler, R. A. (1951). On information and sufficiency. *Ann. Math. Statist.* 22, 79–86. doi: 10.1214/aoms/1177729694

Laforest-Lapointe, I., Messier, C., and Kembel, S. W. (2016). Host species identity, site and time drive temperate tree phyllosphere bacterial community structure. *Microbiome* 4:27. doi: 10.1186/s40168-016-0174-1

Laforest-Lapointe, I., Paquette, A., Messier, C., and Kembel, S. W. (2017). Leaf bacterial diversity mediates plant diversity and ecosystem function relationships. *Nature* 546, 145–147. doi: 10.1038/nature22399

Liu, J., Abdelfattah, A., Norelli, J., Burchard, E., Schena, L., Droby, S., et al. (2018). Apple endophytic microbiota of different rootstock/scion combinations suggests a genotype-specific influence. *Microbiome* 6:18. doi: 10.1186/s40168-018-0403-x

Lozupone, C., and Knight, R. (2005). UniFrac: a new phylogenetic method for comparing microbial communities. *Appl. Environ. Microbiol.* 71, 8228–8235. doi: 10.1128/AEM.71.12.8228-8235.2005

Mahnert, A., Moissl-Eichinger, C., and Berg, G. (2015). Microbiome interplay: plants alter microbial abundance and diversity within the built environment. *Front. Microbiol* 6:887. doi: 10.3389/fmicb.2015.00887

Marasco, R., Rolli, E., Fusi, M., Michoud, G., and Daffonchio, D. (2018). Grapevine rootstocks shape underground bacterial microbiome and networking but not potential functionality. *Microbiome* 6:3. doi: 10.1186/s40168-017-0391-2

Masella, A. P., Bartram, A. K., Truszkowski, J. M., Brown, D. G., and Neufeld, J. D. (2012). PANDAseq: paired-end assembler for illumina sequences. *BMC Bioinform.* 13:31. doi: 10.1186/1471-2105-13-31

Morris, J. H., Apeltsin, L., Newman, A. M., Baumbach, J., Wittkop, T., Su, G., et al. (2011). clusterMaker: a multi-algorithm clustering plugin for cytoscape. *BMC Bioinform.* 12:436. doi: 10.1186/1471-2105-12-436

Paulson, J. N., Stine, O. C., Bravo, H. C., and Pop, M. (2013). Differential abundance analysis for microbial marker-gene surveys. *Nat. Methods* 10, 1200–1202. doi: 10.1038/nmeth.2658

Pinto, C., Pinho, D., Sousa, S., Pinheiro, M., Egas, C., and Gomes, C. (2014). Unravelling the diversity of grapevine microbiome. *PLoS One* 9:e85622. doi: 10.1371/journal.pone.0085622

Rognes, T., Flouri, T., Nichols, B., Quince, C., and Mahé, F. (2016). VSEARCH: a versatile open source tool for metagenomics. *PeerJ* 4:e2584. doi: 10.7287/peerj.preprints.2409v1

Rosenfeld, D., Sherwood, S., Wood, R., and Donner, L. (2014). Climate effects of aerosol–cloud interactions. *Science* 343, 379–380. doi: 10.1126/science.1247490

Schena, L., and Cooke, D. E. (2006). Assessing the potential of regions of the nuclear and mitochondrial genome to develop a "molecular tool box" for the detection and characterization of Phytophthora species. *J. Microbiol. Methods* 67, 70–85. doi: 10.1016/j.mimet.2006.03.003

Schmid, F., Moser, G., Müller, H., and Berg, G. (2011). Functional and structural microbial diversity in organic and conventional viticulture: organic farming benefits natural biocontrol agents. *Appl. Environ. Microbiol.* 77, 2188–2191. doi: 10.1128/aem.02187-10

Toju, H., Tanabe, A. S., Yamamoto, S., and Sato, H. (2012). High-coverage ITS primers for the DNA-based identification of ascomycetes and basidiomycetes

in environmental samples. *PLoS One* 7:e40863. doi: 10.1371/journal.pone.0040863

Unyarat, R., Laurent, F., Artit, V., Antoine, B., Jean-Pierre, M., and Floriane, L. H. (2016). The microbiome of the leaf surface of arabidopsis protects against a fungal pathogen. *New Phytol.* 210, 1033–1043. doi: 10.1111/nph.13808

van der Heijden, M. G. A., Bruin, S. D., Luckerhoff, L., van Logtestijn, R. S. P., and Schlaeppi, K. (2015). A widespread plant-fungal-bacterial symbiosis promotes plant biodiversity, plant nutrition and seedling recruitment. *Isme J.* 10, 389–399. doi: 10.1038/ismej.2015.120

Verginer, M., Leitner, E., and Berg, G. (2010). Production of volatile metabolites by grape-associated microorganisms. *J. Agric. Food Chem.* 58, 8344–8350. doi: 10.1021/jf100393w

Waldrop, M. P., Zak, D. R., Blackwood, C. B., Curtis, C. D., and Tilman, D. (2006). Resource availability controls fungal diversity across a plant diversity gradient. *Ecol. Lett.* 9, 1127–1135. doi: 10.1111/j.1461-0248.2006.00965.x

Zilber-Rosenberg, I., and Rosenberg, E. (2008). Role of microorganisms in the evolution of animals and plants: the hologenome theory of evolution. *FEMS Microbiol. Rev.* 32, 723–735. doi: 10.1111/j.1574-6976.2008.00123.x

Conflict of Interest Statement: The authors declare that the research was conducted in the absence of any commercial or financial relationships that could be construed as a potential conflict of interest.

frontiers in Microbiology

ORIGINAL RESEARCH
published: 06 November 2019
doi: 10.3389/fmicb.2019.02502

Microbiome Response to Hot Water Treatment and Potential Synergy With Biological Control on Stored Apples

*Birgit Wassermann†, Peter Kusstatscher† and Gabriele Berg**

Graz University of Technology, Institute of Environmental Biotechnology, Graz, Austria

Postharvest food decay is one major issue for today's food loss along the supply chain. Hot water treatment (HWT), a sustainable method to reduce pathogen-induced postharvest fruit decay, has been proven to be effective on a variety of crops. However, the microbiome response to HWT is still unknown, and the role of postharvest microbiota for fruit quality is largely unexplored. To study both, we applied a combined approach of metabarcoding analysis and real time qPCR for microbiome tracking. Overall, HWT was highly effective in reducing rot symptoms on apples under commercial conditions, and induced only slight changes to the fungal microbiota, and insignificantly affected the bacterial community. Pathogen infection, however, significantly decreased the bacterial and fungal diversity, and especially rare taxa were almost eradicated in diseased apples. Here, about 90% of the total fungal community was composed by co-occurring storage pathogens *Neofabraea alba* and *Penicillium expansum.* Additionally, the prokaryote to eukaryote ratio, almost balanced in apples before storage, was shifted to 0.6% bacteria and 99.4% fungi in diseased apples, albeit the total bacterial abundance was stable across all samples. Healthy stored apples shared 18 bacterial and 4 fungal taxa that were not found in diseased apples; therefore, defining a health-related postharvest microbiome. In addition, applying a combined approach of HWT and a biological control consortium consisting of *Pantoea vagans* 14E4, *Bacillus amyloliquefaciens* 14C9 and *Pseudomonas paralactis* 6F3, were proven to be efficient in reducing both postharvest pathogens. Our results provide first insights into the microbiome response to HWT, and suggest a combined treatment with biological control agents.

Keywords: *Malus domestica*, microbiota, postharvest losses, biological control consortium, *Neofabraea sp.*, bull's eye rot, *Penicillium expansum*, blue mold

OPEN ACCESS

Edited by:
Feth-el-Zahar Haichar, Microbial Ecology, France

Reviewed by:
Samir Droby, ARO, The Volcani Center, Israel
Daniel Muller, Université Claude Bernard Lyon 1, France

****Correspondence:***
Gabriele Berg
gabriele.berg@tugraz.at

†These authors have contributed equally to this work

Specialty section:
This article was submitted to Microbial Symbioses, a section of the journal Frontiers in Microbiology

Received: *07 August 2019*
Accepted: *17 October 2019*
Published: *06 November 2019*

Citation:
Wassermann B, Kusstatscher P and Berg G (2019) Microbiome Response to Hot Water Treatment and Potential Synergy With Biological Control on Stored Apples. Front. Microbiol. 10:2502. doi: 10.3389/fmicb.2019.02502

INTRODUCTION

Food loss is one of the major problems of modern society; about one-third of all produced food is either lost or wasted globally (FAO, 2015a). Especially, the postharvest period plays a crucial role and has a lot of potential for improvements (Kader, 2003; Aulakh and Regmi, 2013). A high proportion of postharvest food loss is induced by postharvest pathogens

colonizing and damaging the fruits (Johnston et al., 2002; Morales et al., 2010). Until now, mainly chemical and physical treatments are used to suppress pathogens; microbiome research is expected to bring notable understanding and improvements into future biological applications and treatments (Janisiewicz and Korsten, 2002; Droby and Wisniewski, 2018).

Plants closely interact with their colonizing microorganisms, which are crucial for plant health and growth (Berg, 2009; Berendsen et al., 2012; Vandenkoornhuyse et al., 2015). Microorganisms not only protect the plant before harvest, even after harvest, the shielding effect is prolonged (Droby et al., 2016). Studying plant-microbe interactions, beneficial bacteria and their functions were shown to be substantial for advanced biotechnological agriculture applications (Berg et al., 2017). Even though the development of biocontrol application for postharvest use can be challenging, numerous biocontrol products were developed over the last decades as an alternative to classical synthetic pesticides not only for on-field, but also for postharvest applications (Droby et al., 2016). Additionally, health considerations and potential prohibition of currently used pesticides as well as trends toward a fully biological production increased the demand for highly efficient biological alternatives over the last years (Droby et al., 2009). To increase the efficiency of biological control product also, a combined approach of classical and biological methods was suggested (Porat et al., 2002; Spadaro and Gullino, 2005).

Apple, with worldwide over 83 million tons harvested each year with China, the US, and Poland being the top producers, is one of the major fruit crops worldwide (FAOSTAT, 2017). Apples are stored for several months (up to 12 months) under controlled air conditions (Thompson et al., 2018). Prolonged storage of apples has been investigated around the globe and several technologies have been developed to mitigate pathological and physiological disorders during storage (Janisiewicz and Korsten, 2002; Konopacka and Plocharski, 2004; Thompson et al., 2018). Postharvest fungal infections, however, still cause major shortfalls during storage and along the supply chain (FAO, 2015b). *Penicillium expansum* Link, causing blue mold and the three *Neofabraea* species *N. alba* Jacks, *N. malicorticis* (Jacks) Nannfeld and *N. perennans* Kienholz, being the causal agents of bull's eye rot, also referred to as gloeosporium rot (Snowdon, 1990) or bitter rot (Corke, 1956) are two of the main postharvest pathogens of apple. Apart from chemical treatments to control postharvest pathogens, hot water treatment (HWT) for 3 min at 50–53°C, a relatively simple method that is used since the 20th century, was shown to be rather effective in reducing pathogen-induced postharvest losses (Fallik et al., 2001; Maxin et al., 2012b, 2014); both bull's eye rot and blue mold haven been proven to be successfully controlled by HWT (Trierweiler et al., 2003; Maxin et al., 2005). Additionally to the direct killing of fungal spores, the efficiency of HWT is also based on a physiological plant response by inducing transcription and translation of heat shock proteins, where a subset of which comprise pathogenesis-related proteins (Lurie, 1998; Fallik et al., 2001; Pavoncello et al., 2001; Maxin et al., 2012a). However, HWT can cause heat damage to the fruit surface and therefore, additional biocontrol approaches could further improve fruit storability (Spadaro et al., 2004; Schloffer and Linhard, 2016). Recently, combined approaches of HWT with bioactive molecules and biocontrol agents were proven to be efficient in controlling postharvest diseases in apples and other fruits (Conway et al., 2004; Spadaro et al., 2004). Even though these developments were promising, there are still missing links between postharvest diseases on apples and their colonizing microbiota following postharvest treatments including the impact of HWTs on the latter.

The present study provides the first investigation of the apple microbiome changes induced by the currently in-use HWT at an industrial scale. Stored apples that were not subjected to HWT and remaining unaffected by fungal infection and rot development, were investigated, giving some potential insights to postharvest pathogen resistance. Additionally, the indigenous apple microbiota were harnessed for the development of biocontrol agents to combat postharvest pathogens *P. expansum* and *N. malicorticis*. Their additive protective pathogen control effect as well as their applicability in the HWT process was evaluated, providing the first evaluation of a combined process with biological control consortia developed from apple epiphytes. This way, an integrative strategy combining the knowledge of the inherent apple microbiome and its postharvest changes with the development of a novel postharvest treatment was applied.

MATERIALS AND METHODS

Experimental Design and Sample Processing

Organically produced apple fruits (*Malus domestica*) of the cultivar "Topaz" were obtained from the organic storage company Rosenbaum Franz GmbH & Co KG (Pöllau, Austria). Apple samples were taken directly after harvest and after a 6-months storage period. Freshly harvested apples were immediately taken to the laboratory and processed under sterile conditions (in the following named "before storage"). For analyzing impact of HWT on the apple microbiota, 100 apples were stored untreated and 100 apples were subjected to HWT by immersing apples in a 53°C water bath for 3 min. The two groups were stored separately but under the same controlled conditions in the company's storage chamber for 6 months. Directly after opening storage chambers, fungal infection rate by any fungal pathogen on apples was evaluated. HWT was found to be highly efficient as no disease patterns were observed. Among the 100 apples that were untreated 10% were infected, exhibiting rot diameters of 2.5–4 cm in diameter. A subset of each group, consisting of 10 randomly selected apples, was subjected to amplicon analyses; untreated apples were defined into "untreated healthy" and "untreated diseased." The apples were transported to the laboratory and processed under sterile conditions. One whole apple for each category and sample ("before storage," "HWT," "untreated healthy," and "untreated diseased") was cut into smaller pieces and homogenized in a Stomacher laboratory blender (BagMixer, Interscience, St. Nom, France) with 40 ml sterile NaCl (0.85%) solution for 3 min. A total of 4 ml of

the solution was centrifuged at 16,000 *g* for 20 min and the pellet stored at −70°C for further DNA extraction. This way 10 biological replicates for each category were produced.

Microbial DNA Extraction and Metabarcoding Library Construction

The resulting pellets from the previous step were subjected to total microbial DNA extraction using the FastDNA SPIN Kit for Soil (MP Biomedicals, Solon, USA) and a FastPrep Instrument (MP Biomedicals, Illkirch, France) for 30 s at 5.0 m/s. Amplicons were prepared in three technical replicates using the primer pair 515f-926r, specific for bacteria and ITS1f-ITS2r specific for fungi. Sequences of primers are listed in **Supplementary Table S1**. Peptide nucleic acid (PNA) clamps were added to the PCR mix to block amplification of host plastid and mitochondrial 16S DNA (Lundberg et al., 2013). Amplification of the 16S rRNA gene was performed in a total volume of 20 µl [5 × Taq&Go (MP Biomedicals, Illkirch, France), 1.5 µM PNA mix, 10 µM of each primer, PCR-grade water and 1 µl template DNA] under the following cycling conditions: 95°C for 5 min, 35 cycles of 78°C for 5 s, 55°C for 45 s, 72°C for 90 s, and a final elongation at 72°C for 5 min. PCR for amplifying the fungal ITS region was conducted in 20 µl (5 × Taq&Go, 10 µM of each primer, 25 µM $MgCl_2$, PCR-grade water and 2 µl template DNA) using the cycling conditions: 94°C for 5 min, 30 cycles of 94°C for 30 s, 58°C for 35 s, 72°C for 40 s and a final elongation at 72°C for 10 min. A nested PCR step was performed to add barcoded primers (10 µM) in a total volume of 30 µl for both 16S rRNA gene and ITS region: 95°C for 5 min, 15 cycles of 95°C for 30 s, 53°C for 30 s, 72°C for 30 s, and a final elongation at 72°C for 5 min. Three technical replicates, conducted for each sample, were combined and purified by Wizard SV Gel and PCR Clean-Up System (Promega, Madison, WI, USA). DNA concentrations were measured with Nanodrop 2000 (Thermo Scientific, Wilmington, DE, USA) and samples were combined in equimolar concentration. The amplicons were sequenced on a Illumina MiSeq v2 (2 × 250 bp) machine.

Illumina MiSeq Data Evaluation of 16S rRNA Gene and Its Region and Statistics

After joining forward and reversed paired end reads in QIIME 1.9.1, sequencing data was imported into QIIME 22019.1 and demultiplexed following the QIIME 2 tutorials. The DADA2 algorithm was applied for quality filtering, discarding chimeric sequences and to obtain a feature table [containing sequence variants (SVs)] and representative sequences. Feature classification was performed using a Naïve-Bayes feature classifier trained on the Silva132 release (16S rRNA gene) (Quast et al., 2013) or the UNITE v7.2 release (ITS) (Kõljalg et al., 2013). Sequences of features of interest were further identified on species level using NCBI blast alignment tool. Mitochondria and chloroplast reads were discarded from 16S data. Alpha and Beta diversity was investigated running the core diversity script in QIIME 2 rarefying feature tables to the lowest value of reads present in one sample. Core microbiomes (features present in 50% of the samples) were defined for each sample group and core tables were rejoined to obtain barplots and evaluate taxonomic differences. A taxonomy network was constructed on core genera using Cytoscape version 3.5. (Shannon et al., 2003).

Statistical analysis of metabarcoding data was performed using scripts in QIIME 1.9 as well as QIIME2 2019.1. Alpha diversity was tested using the Kruskal-Wallis test and Beta diversity using Analysis of Similarity (ANOSIM) test. Significant differences (alpha $\leq$ 0.05) in taxa abundance on genus level were calculated using non-parametric Kruskal-Wallis test and False Discovery Rate (FDR) multiple test correction.

Quantitative Real-Time PCR

A quantitative real-time PCR (qPCR) was conducted to quantify overall bacterial 16S rRNA and fungal ITS gene copy numbers, as well as postharvest pathogens *P. expansum* and *Neofabraea* spp. For specific quantification of bull's eye rot-causing *Neofabraea* strains, a primer pair (NeoF, NeoR) was selected that specifically targets the highly conserved β-tubulin gene which was found to amplify the three major pathogens associated with bull's eye rot (*N. alba, N. malicorticis, N. perennans*), but no other related fungi (Cao et al., 2013). The primer pair (Pexp_patF_F, Pexp_patF_R) for *P. expansum* targeted the *patF* gene (involved in the patulin biosynthesis) and was previously tested for its specificity (Tannous et al., 2015). Primer pairs were used each in 5 pmol/µl concentration and are listed in **Supplementary Table S1**. All reaction mixes contained 5 µl KAPA CYBR Green, 0.5 µl of each primer, 1 µl template DNA (diluted 1:10 in PCR-grade water), adjusted with PCR-grade water to a final volume of 10 µl. Reaction mix for bacterial amplification was supplemented with 0.15 µl PNA mix to block amplification of host-derived 16S rRNA gene copies. Fluorescence intensities were detected using a Rotor-Gene 6000 real-time rotary analyzer (Corbett Research, Sydney, Australia) with the following cycling conditions: Bacteria: 95°C for 5 min, 45 cycles of 95°C for 20 s, 54°C for 30 s, 72°C for 30 s and a final melt curve of 72 to 95°C. Fungi: 95°C for 5 min, 45 cycles of 95°C for 30 s, 58°C for 35 s, 72°C for 40 s and a final melt curve of 72–95°C. *P. expansum*: 95°C for 5 min, 45 cycles of 95°C for 20 s, 65°C for 15 s, 72°C for 15 s and a final melt curve of 72–95°C. *Neofabraea* sp.: 95°C for 5 min, 45 cycles of 95°C for 20 s, 57°C for 15 s, 72°C for 40 s followed by melt curve of 72–95°C. Amplification efficiency of the target was analyzed with the melting curve (**Supplementary Figure S1**). Three individual qPCR runs were conducted for each replicate. Intermittently occurring gene copy numbers that were found in negative controls were subtracted from the respective sample. Significant differences ($p \leq 0.05$) of bacterial and fungal gene copy numbers per apple between the different apple groups were calculated using a pairwise Wilcoxon test (Bonferroni correction) and visualized using ggplot2 in R version 3.5.1.

Small-Scale Storage Experiments

Small scale experiments were conducted to test the efficacy of potential biocontrol agents with and without combined HWT

against infection of the fungal pathogens *P. exopansum* ATCC 7861 (Origin: CBS 325.48) and *N. malicorticis* (Jacks) Nannfeld (Origin: DSMZ 62715), selected as representative for bull's eye rot-causing fungal pathogens. More than 800 bacterial strains, isolates from apples, were tested for antagonistic properties toward the two pathogens by dual-culture *in vitro* assay on Waksman agar (Berg et al., 2002). Bacterial isolates showing highest antagonistic properties toward both fungi were identified by 16S rRNA gene Sanger sequencing (LGC Genomics, Berlin, Germany) and using the NCBI BLAST alignment tool: *Pantoea vagans* 14E4, *Bacillus amyloliquefaciens* 14C9, and *Pseudomonas paralactis* 6F3. Preliminary tests showed *Pantoea vagans* 14E4 as well as a consortium of the three different bacterial strains on equal proportions to have the best control effect. For *in vivo* tests, 30 apples from the cultivar "Topaz" per treatment and pathogen were rinsed with water and four artificial wounds (1 cm in diameter and depth) were cut with a sterile knife around the radius of the fruits. Each apple was artificially infected with *N. malicorticis* (submerged in a 1.6×10^5 conidia/ml solution) or *P. expansum* (10 µl of a 5×10^4 spores/ml solution) and incubated for 24 h at 20°C. For both, the wound pathogen *P. expansum*, and the lenticel rot causing *N. malicorticis* this way an infection could be induced at the wanted locations. Overnight cultures in nutrient broth (Sifin, Berlin, Germany) of bacterial biocontrol strains were cultivated at 30°C and centrifuged at 5,000 rpm for 15 min. The supernatant was discarded and bacterial pellets were resuspended in sterile sodium chloride solution (0.85%). A consortium on equal proportions of all three biocontrol strains was prepared. Suspensions were diluted to an OD_{600} of 0.2 (approximately, 10^6 cells/ml). Apples, 24 h after inoculation with the fungal pathogens, were treated either with *P. vagans* 14E4 or the consortium by submerging the apples in the prepared solution for 5 s. HWT groups were previously submerged in 53°C hot water for 3 min and allowed to dry. Negative control samples were stored directly after wounding without pathogen infection and positive control samples were stored after infection with *N. malicorticis* and *P. expansum* without further treatment. Results were evaluated after 3 weeks (*P. expansum*) and 5 weeks (*N. malicorticis*) storage period under controlled conditions at 4°C. **Supplementary Figure S2** exemplifies the temporally disease progression of *P. expansum* infection, directly, 1 and 3 weeks after wounding. The diameter of infected areas as well as the length of the cuts was measured and statistical significance tested using a pairwise Wilcoxon test (Bonferroni correction) and visualized using ggplot2 in R version 3.5.1.

RESULTS

The Structure of the Core Postharvest Microbiota in Apples

After quality filtering and removing of chimeric sequences using the DADA2 algorithm and excluding mitochondrial and chloroplast sequences from the 16S rRNA gene fragments, the 16S rRNA and ITS datasets contained 1,071,751 and 880,909 paired reads, respectively. Sequences were assigned to 2,297 bacterial and 613 fungal features and the datasets were rarefied to 1,638 bacterial and 1,319 fungal sequences, according to the sample with the lowest amount of sequences. Core microbiota were defined for each sample group ("before storage," "HWT," "untreated healthy," and "untreated diseased"), by keeping only the features present in 50% of the replicates of the respective group. A 50% cutoff was used to keep enough features for the evaluation of the main features in all groups and to discard rarely occurring features. In total, 205 core bacterial and 89 core fungal features remained that were condensed to 60 and 44 genera, respectively. From those taxa, a network of co-occurring OTUs was constructed to visualize shared taxa and taxa being unique for a specific group (**Figure 1**). Among 104 bacterial and fungal genera, 23 were shared by all apples, while 22 genera were present in "HWT" and "untreated healthy" apples but absent in all other samples, probably indicating a health-related postharvest microbiome. Additionally, "HWT," "untreated healthy," and "before storage" samples hosted 13, 16, and 10 unique taxa, respectively, while no unique taxa were found for "untreated diseased" apples. *N. alba* was present in all apples, including "before storage" samples, whereas *P. expansum* only occurred in stored apples.

Taxonomic Changes Induced by Storage and Disease

In order to compare taxonomic composition of the four groups, **Figure 2** was constructed for the bacterial (**Figure 2A**) and fungal (**Figure 2B**) core microbiota of each group on genus level, where genera represented with less than 1% of the number of reads are clustered as "Other." The microbiota within the four different groups showed great taxonomic variability, especially when apples before storage were compared to stored apples. The bacterial microbiota within all samples was highly dominated by *Proteobacteria,* ranging from 65% in "before storage" samples up to 80% in "untreated healthy" apples. Apples "before storage" had additionally a high abundance of *Bacteroidetes* (32%) compared to the other groups (3–8%), whereas all stored apple samples prevailed in *Actinobacteria* abundance (9–20%) over "before storage" samples (1%). *Sphingomonas* was the most abundant genus in all groups (35–46%). *Hymenobacter* (31%) and *Massilia* (13%) were furthermore highly abundant in apples before storage. *Pseudomonas* (7–11%) and *Methylobacterium* (7%) were abundant in healthy apples after storage, whereas diseased apples after storage showed high abundances of *Methylobacterium* (12%) and *Frondihabitans* (11%) (**Figure 2A**). In total, the core microbiota of the four groups "before storage", "HWT", "untreated healthy" and "untreated diseased" contained 15, 50, 49, and 18 bacterial genera, respectively.

The fungal microbiota was dominated by *Ascomycota,* ranging from 72% in "untreated healthy" samples up to 97% in "untreated diseased" apples. *Basidiomycota* were more abundant in healthy apples before (19%) and after (11–26%) storage, compared to "untreated diseased" apples (3.5%). On genus level, *Mycosphaerella* dominated "before storage" samples (30%), followed by *Alternaria* (19%), *Vishniacozyma* (12%), *Cladosporium* (8%), and *Aureobasidium*

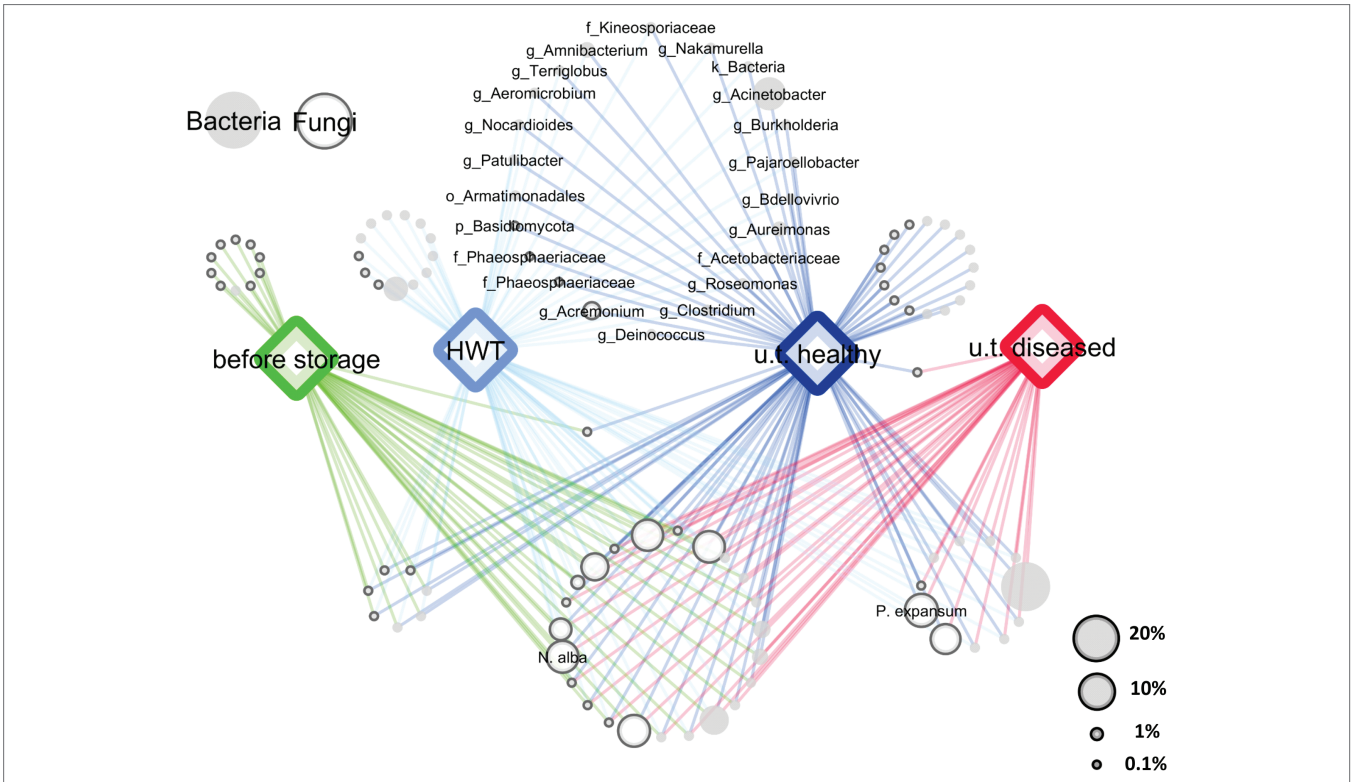

FIGURE 1 | Core and specific microbiota for the four apple groups. Core bacterial and fungal microbiota (taxa occurring in 50% of all replicates) of the four groups "before storage", "HWT", "untreated healthy" (u.t. healthy) and "untreated diseased" (u.t. diseased) were combined for network analysis. Node size corresponds to relative abundance in the dataset as described in the legend on the lower right. Node color indicates bacteria (filled light gray) and fungi (outlined dark gray), as shown in the legend on the upper left. Nodes of taxa shared by healthy stored apples, indicating the healthy postharvest microbiota, are labeled where the label prefixes k_, p_, o_, f_ and g_ denote for kingdom, phylum, order, family and genus, respectively. Taxonomy of the two postharvest pathogens *N. alba* and *P. expansum* was assigned on species level using the NCBI BLAST alignment tool.

(7%). Stored "HWT" samples were dominated by a not further assigned taxon of *Hypocreales* (20%), followed by *Cladosporium* (15%), *P. expansum* (11%), *Acremonium,* and *Didymellaceae* sp. (each 10%) and *Vishniacozyma* (9%). Almost the same fungal genera were highly abundant in stored "untreated healthy" samples, with *Vishniacozyma* (21%) being the main representative, except *P. expansum* featuring only 1% abundance. Stored "untreated diseased" apples were almost exclusively composed of the two postharvest pathogens *P. expansum* (45%) and *N. alba* (42%) (**Figure 2B**). Both fungi were present in "HWT" and "untreated healthy" apples, although with less relative abundance. "Before storage" apples contained 0.1% *N. alba*, while *P. expansum* was absent. The samples "before storage", "HWT", "untreated healthy" and "untreated diseased" contained 28, 27, 33, and 18 fungal core genera, respectively.

Diversity Changes Induced by Storage and Disease

The bacterial and fungal diversity within the apple samples was assessed by Shannon diversity index. Apples from the category "before storage" showed significantly the lowest bacterial diversity ($H' = 5.19 \pm 0.8$), followed by stored apples from the category "untreated diseased" ($H' = 5.72 \pm 0.3$). Both were significantly less diverse than stored "untreated healthy" ($H' = 6.46 \pm 0.6$) and "HWT" samples featuring highest bacterial diversity ($H' = 6.68 \pm 0.4$) (**Figure 3A**). Fungal diversity was highly decreased in stored "untreated diseased" apples ($H' = 1.93 \pm 0.8$), being significantly lower compared to all healthy apples: "before storage": $H' = 3.77 \pm 0.5$, "HWT": $H' = 3.87 \pm 0.6$ and "untreated healthy": $H' = 4.31 \pm 0.1$ (**Figure 3B**).

Beta diversity analyses, applied on the whole bacterial and fungal dataset and based on Bray Curtis distance matrix, indicated clear clustering between apples before and after storage in all cases (**Figures 3C,D**). Statistical significance in bacterial composition, assessed *via* pairwise ANOSIM (**Table 1**), revealed significant differences between all groups, except for the comparison of "HWT" and "untreated healthy" samples. Highest variability was found when "before storage" samples were compared to the remaining groups. The fungal composition was significantly different between all four groups, while difference between "HWT" and "untreated healthy" samples was lowest.

In order to identify bacterial and fungal taxa that potentially contribute to pathogen resistance in "untreated healthy" apples, significant differences in taxa abundance between "untreated healthy" and "untreated diseased" samples were calculated (**Supplementary Table S2**). A total of 42 bacterial and 28

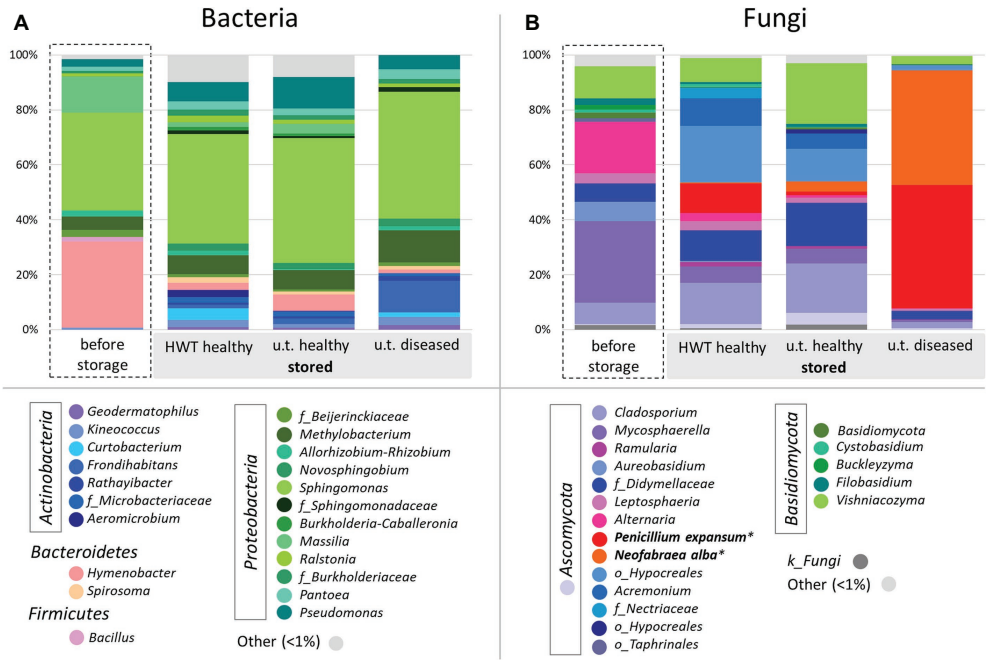

FIGURE 2 | Bacterial and fungal taxonomy of apples investigated. Core microbiomes were defined for taxa occurring in 50% of the replicates in the respective groups. Color-coded bacterial **(A)** and fungal **(B)** taxa are indicated in the bottom legend and are shown on genus level and grouped by phylum. Sequences of storage pathogens highlighted in bold were further identified on species level using NCBI BLAST alignment tool. Taxa occurring with less than 1% are shown as "Other".

fungal taxa were found significantly higher in "untreated healthy" apples as well as 2 fungal taxa (*P. expansum* and *N. alba*) being significantly increased in "untreated diseased" apples. Higher numbers of taxa in "untreated healthy" apples were found for e.g., *Sphingomonas*, *Pseudomonas,* and *Methylobacterium* as well as *Vishniacozyma*, *Cladosporium,* and *Acremonium*.

Additionally, the impact of HWT on the apple postharvest microbiota was evaluated as well, by calculating significant differences in taxa abundance between "HWT" and "untreated healthy" apples (**Supplementary Table S3**). A total of 25 bacterial and 22 fungal genera were found to be significantly different abundant between the two groups. Significantly increased in "HWT" were, e.g., *Hymenobacter*, *Rathayibacter* as well as *Filobasidium*; increased in "untreated healthy" were, e.g., *Curtobacterium*, *Rhodococcus* as well as *Penicillium* and *Alternaria*. However, as previous stated, the overall bacterial microbiome and diversity was not significantly different between the two groups only the fungal microbial composition was slightly changed.

Quantification of Bacteria, Fungi, *P. expansum,* and *Neofabraea* Sp. During Storage and Disease

A real time PCR was performed to quantify total bacterial 16S rRNA and fungal ITS gene copy numbers. Bull's eye rot-causing *Neofabraea* strains and *P. expansum* were specifically quantified as well (**Figure 4**). No significant differences in 16S rRNA gene copy abundance was observed between the four different apple groups; neither between apple "before storage" and all stored apples, nor within the stored groups (**Figure 4A**). Pathogen infection as well as HWT did accordingly not affect the bacterial abundance in apples. Regarding the total fungal ITS genes we found significantly higher abundances within "untreated diseased" apples compared to all other groups (**Figure 4B**), due to significant increase of both storage pathogens *Neofabraea* and *P. expansum* (**Figures 4C,D**, respectively). *Neofabraea* was already present in "before storage" apples in similar abundances as in "HWT" and "untreated healthy" apples while *P. expansum* was almost absent in apples "before storage." Overall, fungi were found to proliferate more efficiently compared to bacteria in stored apples, as showed *via* calculating the prokaryote to eukaryote ratio (**Figure 4E**). Whereas the ratio was almost balanced in apples before storage (58% bacteria and 42% fungi), fungal genes increased up to the two-fold in stored, healthy apples. A dramatic increase of fungal genes was however observed within stored, diseased apples; 99.4% of total microbial genes detected were fungal.

Efficiency of Hot Water Treatment and Biological Control Application Against Postharvest Diseases Determined in Small-Scale Storage Experiments

The efficacy of potential biocontrol strains (*P. vagans* 14E4, *B. amyloliquefaciens* 14C9 and *P. paralactis* 6F3) identified using

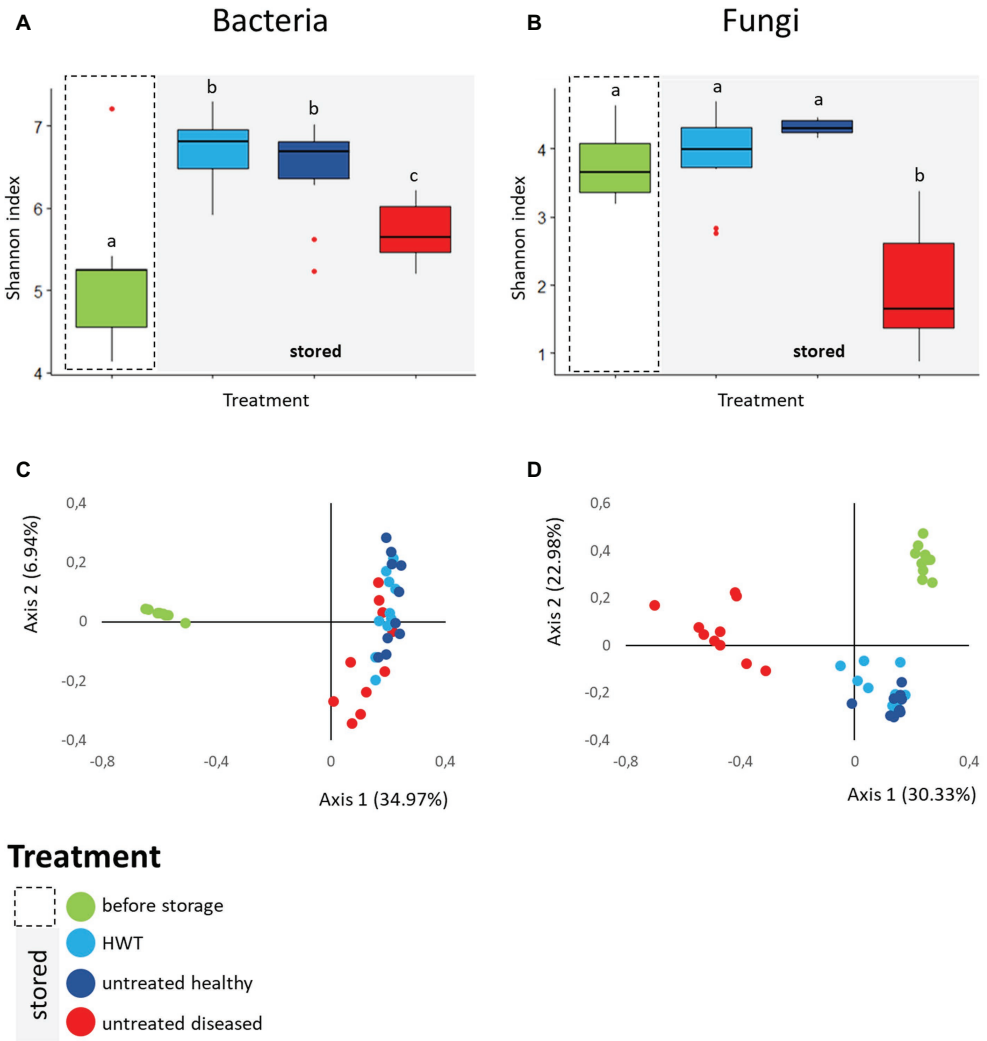

FIGURE 3 | Alpha- and Beta-diversity analyses on apple-associated bacterial and fungal structure. Box-and-Whiskers-plots visualize Shannon diversity index of the four different apple groups for bacteria **(A)** and fungi **(B)**. Significant differences ($p \leq 0.05$) were assessed by Kruskal Wallis test and are indicated by different lower case letters. Community clustering of bacterial **(C)** and fungal **(D)** composition of the samples is indicated by color-coded two dimensional Bray Curtis PCoA plots. Color code for the differentially treated apple samples is explained in the legend on the bottom left. Significant differences in bacterial and fungal composition was tested using ANOSIM pairwise test and can be looked up in **Table 1**.

antagonistic screening methods was tested in small-scale storage experiments with or without combined HWT against *N. malicorticis* and *P. expansum*. *P. vagans* E14 was applied as single agent as well as combined with the other potential biocontrol strains in form of a consortium. Negative control apples that were wounded artificially but not infected with fungal pathogens appeared to be unaffected after two as well as after 5 weeks of storage. Positive control apples that were inoculated with the fungal pathogens and untreated showed 100% infection rate for *N. malicorticis* and 96% for *P. expansum* (**Figure 5A**). Treatment using biocontrol strains slightly decreased infection rates, however, still up to 88% of apples were infected. HWT reduced infection rates of *N. malicorticis* and *P. expansum* to 58 and 75%, respectively. Overall, combining HWT and the biocontrol consortium reduced the total infection rates the most (up to 42%). Similar results were shown when the infection diameter was measured (**Figure 5B**). Here, no significant differences in infection diameter were found between positive control samples and apples treated with biocontrol strains that were not subjected to HWT. In contrast, HWT approved to be efficient in reducing pathogen infection rates, while the combined treatment of HWT and potential biocontrol strains resulted in even less infection.

DISCUSSION

The present study is the first to provide deeper insights into the taxonomic, diversity and abundance changes induced by

TABLE 1 | Pairwise ANOSIM results calculating significant differences in bacterial and fungal composition associated with differentially treated apple groups.

		Bacteria		Fungi	
Group 1	**Group 2**	***R***	***p***	***R***	***p***
HWT	Untreated diseased	0.21	0.002	0.79	0.001
HWT	Untreated healthy	0.06	0.136	0.41	0.001
HWT	Before storage	1.00	0.001	0.95	0.001
Untreated diseased	Untreated healthy	0.26	0.001	0.81	0.001
Untreated diseased	Before storage	1.00	0.001	0.85	0.001
Untreated healthy	Before storage	1.00	0.001	1.00	0.001

currently in-use HWT at industrial scale. The efficacy of HWT in reducing postharvest pathogens was demonstrated under commercial storage condition. The induced microbial shifts were observed by metabarcoding analysis and microbial quantification *via* qPCR. Small-scale storage experiments furthermore suggest the combination of highly effective HWT and a biological control consortium to be an alternative approach to prevent postharvest loss previously damaged apples.

HWT under commercial storage conditions was proven to be highly efficient as during long-term storage for 6 months, not a single fruit among 100 HW-treated apples was decayed. Among untreated and stored apples, 10% were infected and showed postharvest disease. We studied the induced changes in the microbiome comparing "HWT" and "untreated healthy" apples. The difference between the two groups was not statistically significant for bacteria on any level measured; Alpha and Beta diversity matrixes, as well as gene quantification revealed no significant differences between the two groups. The fungal composition was, however, slightly influenced. Accordingly, we hypothesize that the apple is protected by the previously suggested HWT-initiated transcription and translation of heat-shock proteins in the plant, where a subset of which comprise pathogenesis-related proteins (Fallik et al., 2001; Pavoncello et al., 2001; Maxin et al., 2014). The HWT as well as the plant response affects the present bacteria to a lesser extent than the fungi. However, still few bacterial and fungal taxa were found to be significantly different abundant between HW-treated and untreated healthy apples, which are therefore suggested to be directly affected by HWT. Whether this microbiota is heat-sensitive or diminished by HWT-induced plant response remains, however, unclear. Among others, also *Penicillium* was significantly reduced in HW-treated apples, which could also be due to the heat sensitivity of fungal spores and structures (Maxin et al., 2012a).

Overall, healthy apples (HWT or untreated) showed a distinct microbiome compared to diseased apples. A total of 18 bacterial and 4 fungal taxa were shared between HW-treated and untreated but healthy apples, while being absent in diseased apples. Explicitly selecting taxa from the healthy postharvest microbiome might provide promising opportunities for future applications to reduce postharvest decay of apples and other fruits.

The impact of pathogen infection on the bacterial and especially on the fungal microbiota of stored apples was severe. Microbial diversity was significantly reduced and the composition was clearly shifted. Even though each replicate consisted of one whole apple fruit and the infection observed was just 2.5 cm in diameter, almost 90% of all fungal sequences detected in diseased apples were composed by co-occurring *N. alba* (42% rel.) and *P. expansum* (45% rel.) and especially the low abundant taxa were almost outcompeted during pathogen infection.

Observing apples before storage, the ratio between bacteria and fungi was almost balanced (58 to 42% for bacteria and fungi, respectively). The ratio shifted toward 20% bacteria and 80% fungi in stored but healthy apples (both HW-treated and untreated samples) and climaxed in 99.4% fungal genes, out of all microbial genes detected, in diseased apples. This percentage was almost exclusively covered by pathogenic *Neofabrea* species and *P. expansum* as detected *via* specific gene quantification, coinciding significantly with the observations in microbiota taxonomy. Even though the infected spots on diseased apples reached a maximum of only 4 cm in diameter on one apple, this emphasizes even more the fast impact of pathogen infestation on the overall microbial composition. The results of this study suggest that the two pathogens are highly co-occurring; moreover, a mutualistic effect is suggested. Outbreaks of pathogenic *Neofabraea* species, known to infect the apple fruit already in the field (Snowdon, 1990), most likely facilitate infestation of rapidly proliferating *P. expansum,* which attacks the fruit through damaged tissues and wounds during storage (Amiri and Bompeix, 2005). After a 6-months storage period this results in a disease outbreak induced by both pathogens to an equal extent. For a significant reduction of *P. expansum* in stored fruits, prevention of *Neofabraea* infection might therefore be essential. The infectious cycles of the two pathogens was confirmed in the present study as well, as *N. alba* was detected already in apples before storage, whereas *P. expansum* was present only in apples stored for 6 months.

Overall, among stored apples, HWT and pathogen infection influenced the bacterial community to a lesser extent than the fungal. Surprisingly, the greatest effect on the bacterial microbiota was mediated by long-term storage. Apples before storage exhibited significantly lower bacterial diversity compared to all stored samples, including diseased apples. The bacterial microbiota was furthermore significantly shifted during storage, whereas bacterial abundance was unchanged across all samples investigated. Storage, therefore, seems to exhibit an even higher effect on the bacterial microbiota than pathogen infestation, whereas the opposite was observed for the fungal community. During storage significant shifts in fungal composition and slight, but not statistically significant increase in diversity was observed. Especially the bacterial genera *Hymenobacter* and *Massilia* and the fungi *Mycosphaerella*, *Alternaria* and *Aureobasidium,* featuring high abundances in apples before storage, were significantly reduced after the 6-months storage period; probably due to cold-sensitivity of those taxa.

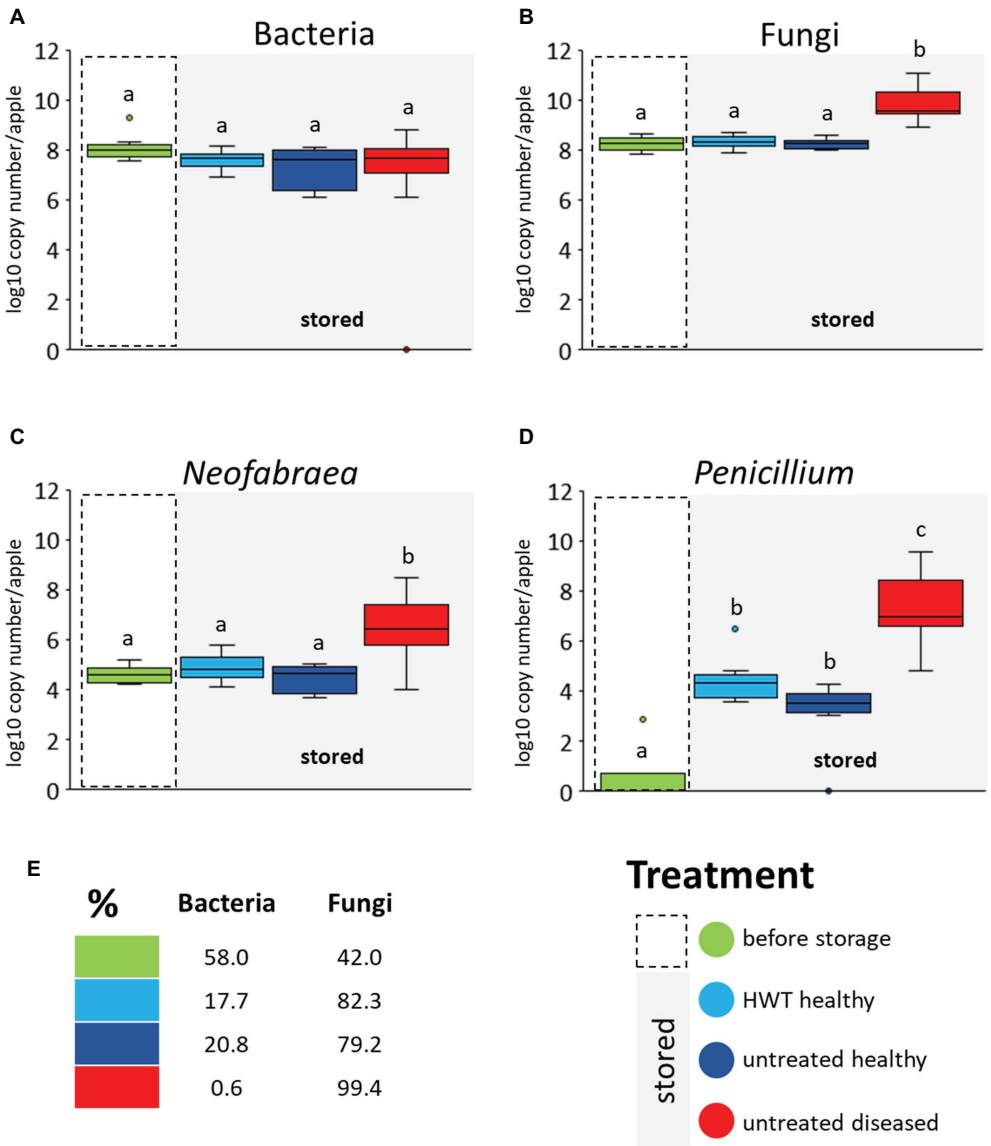

FIGURE 4 | Microbial gene copy numbers in apple groups determined by qPCR. Values are given by primers targeting bacterial 16S rRNA genes **(A)**, fungal ITS region **(B)** and genes of *N. alba* **(C)** and *P. expansum* **(D)**. Gene copy numbers are calculated per apple used for the microbiome analysis. Significant differences ($p \leq 0.05$) were assessed by Wilcoxon test (Bonferroni correction) and are indicated by different lower case letters. The prokaryote to eukaryote ratio within the total microbial gene copies detected in apples of the respective groups is shown **(E)**. Color code for apple groups is depicted in the legend on the bottom right.

Although HWT was shown to be highly efficient in this experiment, it was reported to cause heat damage to a fraction of the stored apples (Schloffer and Linhard, 2016). To prevent postharvest disease in those heat damaged as well as mechanically damaged fruits, biological control was previously suggested (Spadaro et al., 2004). Small-scale experiments demonstrated a significant reduction of symptoms caused by postharvest pathogens *N. malicorticis* and *P. expansum* when fruits were subjected to HWT with or without additional application of a biological control consortium, while the latter even enhanced the efficacy of the treatment. The efficiency was equally pronounced against both pathogens as determined by counting infected apples and measuring diameters of infection on apples artificially wounded and infected with the pathogens. The combined method of HWT and biological control consortium, previously isolated from apples, reduced infection rates up to 42%. Our experiment showed that the fungistatic effect was stable for at least 5 weeks as we evaluated fruit decay after 3 weeks for *P. expansum* and after 5 weeks for *N. malicorticis*. Efficacy of combined methods of HWT and biological control has already been proven successful for apple (Conway et al., 2004; Spadaro et al., 2004), citrus fruits (Porat et al., 2002; Obagwu and Korsten, 2003), pear (Zhang et al., 2008),

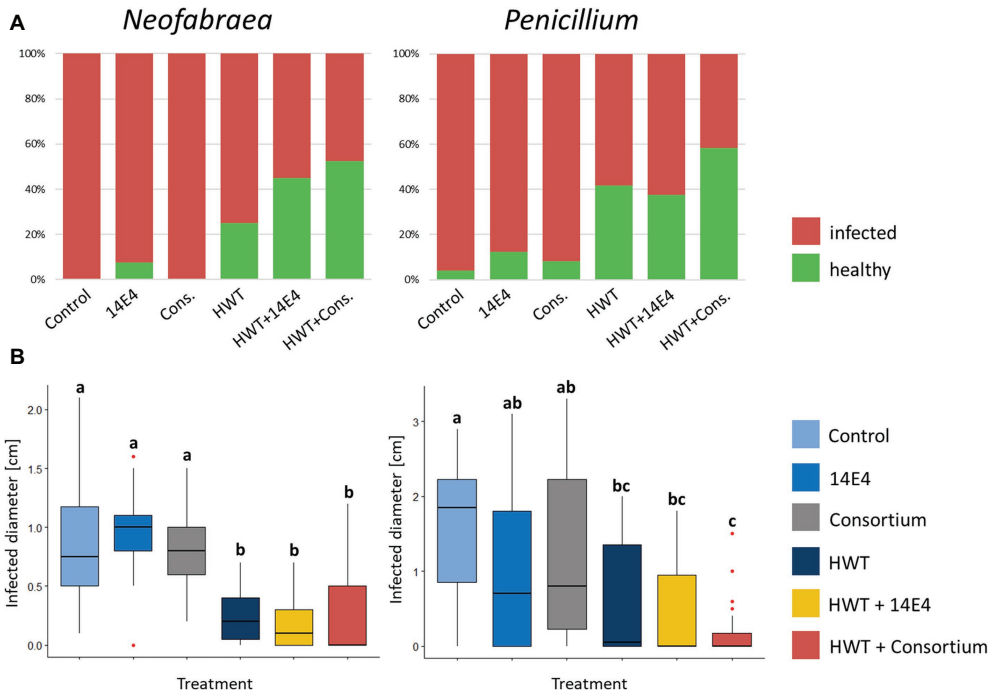

FIGURE 5 | Fraction of infected apples after storage **(A)** and analysis of infected diameter **(B)**. Apples were treated with fungal spores or conidia as well as bacterial strain *P. vagans* 14E4, a bacterial consortium and/or HWT. **(A)** Contrasts the total number of infected to healthy apples after treatment and **(B)** statistically evaluates the efficiency of the treatment based on the infection diameter. Statistical differences between differentially treated apple samples was assessed by Wilcoxon test (Bonferroni correction) and are indicated by lower case letters. Control samples were only inoculated with fungal spores and stored.

strawberry (Wszelaki, 2003), mandarin fruit (Hong et al., 2014) and tomato (Zong et al., 2010). However, the present study was the first to test microbial consortia in combination with HWT. Nevertheless, the efficacy of the combined method needs however to be confirmed on industrial scale and with naturally infected fruit.

Until now, only few studies have assessed the microbial dynamics during storage using metagenomic technologies. Investigations on the oomycete and fungal community of sugar beets infection by storage soft rot showed that the susceptibility to storage pathogens was rather conditioned by the cultivar than by the oomycete and fungal community present. Accordingly, plant-inherent but unspecific resistance mechanism was suggested to decrease the spread of pathogens, but without preventing the infection (Liebe et al., 2016). However, the bacterial community, which was not investigated in this study, could potentially contribute to disease expression as well. The dynamic changes of the endophytic bacterial community associated with potato tubers in response to bacterial storage pathogens was investigated by Kõiv et al. (2015). Here, pathogenesis is assumed to be initiated by the pathogen but complex contributions from the endophytic community are significantly involved. A crucial impact of endophytic bacteria and fungi on the development of postharvest stem-end rots was also observed for mango fruits (Diskin et al., 2017). In summary, and with reference to the present results, the severity of postharvest infestations may be rather mediated by the interactions of specific members of the total community than by one specific pathogen. High microbial diversity in plants was already described to determine abundance of pathogens (Berg et al., 2017).

CONCLUSION

The indigenous apple microbiome is important for health within the postharvest period and during storage. A healthy apple microbiome is characterized by high bacterial and fungal diversity and evenness, a balanced ratio between both groups and several health indicators, while diseased apples show dysbiosis, diversity loss and dominant fungal pathogens. HWT-induced plant response diminished pathogen infection at industrial scale, and showed an impact on the fungal composition. We suggest that the apple fruit is protected by either HWT or the inherent microbiome; however, presumable it is the combination of both, mediating disease resistance. Small-scale storage experiments applying HWT together with biological control agents provide further confirmation of the considerable potential of combining methods into one control strategy to reduce postharvest decay of apples. Moreover, harnessing the indigenous microbiota of fruits for a biological control approach is a promising and sustainable future strategy to prevent postharvest decay of fresh and stored produce.

DATA AVAILABILITY STATEMENT

The raw sequence files supporting the findings of this article are available from the European Nucleotide Archive (ENA) at study Accession Number PRJEB33672.

AUTHOR CONTRIBUTIONS

BW and PK performed the experiments, analyzed data, and wrote the manuscript. GB designed the study, discussed results, and wrote the manuscript. All authors read and approved the final manuscript.

FUNDING

This study was funded by Sparkling Science Research Program (grant No. SPA 06051) of the Federal Ministry of Education, Science and Research (BMBWF).

SUPPLEMENTARY MATERIAL

The Supplementary Material for this article can be found online at: https://www.frontiersin.org/articles/10.3389/fmicb.2019.02502/full#supplementary-material

REFERENCES

Amiri, A., and Bompeix, G. (2005). Diversity and population dynamics of Penicillium spp. on apples in pre- and postharvest environments: consequences for decay development. *Plant Pathol.* 54, 74–81. doi: 10.1111/j.1365-3059.2005.01112.x

Aulakh, J., and Regmi, A. (2013). *Post-harvest food losses estimation-development of consistent methodology*. Rome: FAO.

Berendsen, R. L., Pieterse, C. M. J., and Bakker, P. A. H. M. (2012). The rhizosphere microbiome and plant health. *Trends Plant Sci.* 17, 478–486. doi: 10.1016/j.tplants.2012.04.001

Berg, G. (2009). Plant–microbe interactions promoting plant growth and health: perspectives for controlled use of microorganisms in agriculture. *Appl. Microbiol. Biotechnol.* 84, 11–18. doi: 10.1007/s00253-009-2092-7

Berg, G., Köberl, M., Rybakova, D., Müller, H., Grosch, R., and Smalla, K. (2017). Plant microbial diversity is suggested as the key to future biocontrol and health trends. *FEMS Microbiol. Ecol.* 93. doi: 10.1093/femsec/fix050

Berg, G., Nicotte, R., Anette, S., Leo, E., Angela, Z., and Korndia, S. (2002). Plant dependent genotypic and phenotypic diversity of antagonistic rhizobacteria isolated from different verticillium host plants. *Appl. Environ. Microbiol.* 68, 3328–3338. doi: 10.1128/AEM.68.7.3328-3338.2002

Cao, D., Li, X., Cao, J., and Wang, W. (2013). PCR detection of the three Neofabraea pathogenic species responsible for apple Bull's eye rot. *Adv. Microbiol.* 3, 61–64. doi: 10.4236/aim.2013.31009

Conway, W. S., Leverentz, B., Janisiewicz, W. J., Blodgett, A. B., Saftner, R. A., and Camp, M. J. (2004). Integrating heat treatment, biocontrol and sodium bicarbonate to reduce postharvest decay of apple caused by *Colletotrichum acutatum* and *Penicillium expansum*. *Postharvest Biol. Technol.* 34, 11–20. doi: 10.1016/j.postharvbio.2004.05.011

Corke, A. T. K. (1956). Bitter rot of apples: II. Seasonal variations in the development and sporulation of cankers of Gloeosporium Spp. inoculated into apple branches. *J. Hortic. Sci.* 31, 272–283. doi: 10.1080/00221589.1956.11513877

Diskin, S., Feygenberg, O., Maurer, D., Droby, S., Prusky, D., and Alkan, N. (2017). Microbiome alterations are correlated with occurrence of postharvest stem-end rot in mango fruit. *Phytobiomes J.* 1, 117–127. doi: 10.1094/PBIOMES-05-17-0022-R

Droby, S., and Wisniewski, M. (2018). The fruit microbiome: a new frontier for postharvest biocontrol and postharvest biology. *Postharvest Biol. Technol.* 140, 107–112. doi: 10.1016/j.postharvbio.2018.03.004

Droby, S., Wisniewski, M., Macarisin, D., and Wilson, C. (2009). Twenty years of postharvest biocontrol research: is it time for a new paradigm? *Postharvest Biol. Technol.* 52, 137–145. doi: 10.1016/j.postharvbio.2008.11.009

Droby, S., Wisniewski, M., Teixidó, N., Spadaro, D., and Jijakli, M. H. (2016). The science, development, and commercialization of postharvest biocontrol products. *Postharvest Biol. Technol.* 122, 22–29. doi: 10.1016/j.postharvbio.2016.04.006

Fallik, E., Tuvia-Alkalai, S., Feng, X., and Lurie, S. (2001). Ripening characterisation and decay development of stored apples after a short pre-storage hot water rinsing and brushing. *Innov. Food Sci. Emerg. Technol.* 2, 127–132. doi: 10.1016/S1466-8564(01)00032-7

FAO (2015a). *Food loss and food waste*. Rome, Italy: Food and Agriculture Organisation. Available at: http://www.fao.org/food-loss-and-food-waste/en/ (Accessed May 5, 2019).

FAO (2015b). *Post-harvest losses along value and supply chains in the Pacific Island countries*. Vol. 1. Rome, Italy: Food and Agriculture Organisation, 0–5.

FAOSTAT (2017). *Food and agriculture Organization of the United Nations*. Rome, Italy: Food and Agriculture Organisation. Available at: http://www.fao.org/faostat/en/#data/QC (Accessed May 5, 2019).

Hong, P., Hao, W., Luo, J., Chen, S., Hu, M., and Zhong, G. (2014). Combination of hot water, *Bacillus amyloliquefaciens* HF-01 and sodium bicarbonate treatments to control postharvest decay of mandarin fruit. *Postharvest Biol. Technol.* 88, 96–102. doi: 10.1016/j.postharvbio.2013.10.004

Janisiewicz, W. J., and Korsten, L. (2002). Biological control of postharvest diseases of fruits. *Annu. Rev. Phytopathol.* 40, 411–441. doi: 10.1146/annurev.phyto.40.120401.130158

Johnston, J. W., Hewett, E. W., and Hertog, M. L. A. T. M. (2002). Postharvest softening of apple (*Malus domestica*) fruit: a review. *New Zeal. J. Crop Hortic. Sci.* 30, 145–160. doi: 10.1080/01140671.2002.9514210

Kader, A. A. (2003). A perspective on postharvest horticulture (1978-2003). *HortScience* 38, 1004–1008. doi: 10.21273/HORTSCI.38.5.1004

Kõiv, V., Roosaare, M., Vedler, E., Ann Kivistik, P., Toppi, K., Schryer, D. W., et al. (2015). Microbial population dynamics in response to Pectobacterium atrosepticum infection in potato tubers. *Sci. Rep.* 5:11606. doi: 10.1038/srep11606

Kõljalg, U., Nilsson, R. H., Abarenkov, K., Tedersoo, L., Taylor, A. F. S., Bahram, M., et al. (2013). Towards a unified paradigm for sequence-based identification of fungi. *Mol. Ecol.* 22, 5271–5277. doi: 10.1111/mec.12481

Konopacka, D., and Plocharski, W. J. (2004). Effect of storage conditions on the relationship between apple firmness and texture acceptability. *Postharvest Biol. Technol.* 32, 205–211. doi: 10.1016/j.postharvbio.2003.11.012

Liebe, S., Wibberg, D., Winkler, A., Pühler, A., Schlüter, A., and Varrelmann, M. (2016). Taxonomic analysis of the microbial community in stored sugar beets using high-throughput sequencing of different marker genes. *FEMS Microbiol. Ecol.* 92:fiw004. doi: 10.1093/femsec/fiw004

Lundberg, D. S., Yourstone, S., Mieczkowski, P., Jones, C. D., and Dangl, J. L. (2013). Practical innovations for high-throughput amplicon sequencing. *Nat. Methods* 10, 999–1002. doi: 10.1038/nmeth.2634

Lurie, S. (1998). Postharvest heat treatments. *Postharvest Biol. Technol.* 14, 257–269. doi: 10.1016/S0925-5214(98)00045-3

Maxin, P., Huyskens-Keil, S., Klopp, K., and Ebert, G. (2005). Control of postharvest decay in organic grown apples by hot water treatment. *Acta Hortic.* 682, 2153–2158. doi: 10.17660/ActaHortic.2005.682.294

Maxin, P., Weber, R. W. S., Lindhard Pedersen, H., and Williams, M. (2012a). Hot-water dipping of apples to control *Penicillium expansum*, *Neonectria galligena* and *Botrytis cinerea*: effects of temperature on spore germination and fruit rots. *Eur. J. Hortic. Sci.* 77, 1–9.

Maxin, P., Weber, R. W. S., Pedersen, H. L., and Williams, M. (2012b). Control of a wide range of storage rots in naturally infected apples by hot-water dipping and rinsing. *Postharvest Biol. Technol.* 70, 25–31. doi: 10.1016/j.postharvbio.2012.04.001

Maxin, P., Williams, M., and Weber, R. W. S. (2014). Control of fungal storage rots of apples by hot-water treatments: a northern European perspective. *Erwerbs-obstbau* 56, 25–34. doi: 10.1007/s10341-014-0200-z

Morales, H., Marín, S., Ramos, A. J., and Sanchis, V. (2010). Influence of post-harvest technologies applied during cold storage of apples in *Penicillium expansum* growth and patulin accumulation: a review. *Food Control* 21, 953–962. doi: 10.1016/j.foodcont.2009.12.016

Obagwu, J., and Korsten, L. (2003). Integrated control of citrus green and blue molds using *Bacillus subtilis* in combination with sodium bicarbonate or hot water. *Postharvest Biol. Technol.* 28, 187–194. doi: 10.1016/S0925-5214(02)00145-X

Pavoncello, D., Lurie, S., Droby, S., and Porat, R. (2001). A hot water treatment induces resistance to *Penicillium digitatum* and promotes the accumulation of heat shock and pathogenesis-related proteins in grapefruit flavedo. *Physiol. Plant.* 111, 17–22. doi: 10.1034/j.1399-3054.2001.1110103.x

Porat, R., Daus, A., Weiss, B., Cohen, L., and Droby, S. (2002). Effects of combining hot water, sodium bicarbonate and biocontrol on postharvest decay of citrus fruit. *J. Hortic. Sci. Biotechnol.* 77, 441–445. doi: 10.1080/14620316.2002.11511519

Quast, C., Pruesse, E., Yilmaz, P., Gerken, J., Schweer, T., Yarza, P., et al. (2013). The SILVA ribosomal RNA gene database project: improved data processing and web-based tools. *Nucleic Acids Res.* 41, D590–D596. doi: 10.1093/nar/gks1219

Schloffer, K., and Linhard, D. (2016). "Short time-high temperature hot water shower against Neofabraea rot" in *Ecofruit. 17th International Conference on Organic Fruit-Growing: Proceedings, 15–17 February 2016* (*Fördergemeinschaft Ökologischer Obstbau eV (FÖKO)*). ed. J. Kienzle (Hohenheim, Germany: FÖKO), 176–179.

Shannon, P., Markiel, A., Ozier, O., Baliga, N. S., Wang, J. T., Ramage, D., et al. (2003). Cytoscape: a software environment for integrated models of biomolecular interaction networks. *Genome Res.* 13, 2498–2504. doi: 10.1101/gr.1239303

Snowdon, A. L. (1990). *A colour atlas of post-harvest diseases and disorders of fruits and vegetables. Volume 1*. UK: Wolfe Scientific. Available at: https://www.cabdirect.org/cabdirect/abstract/19901142685 (Accessed July 2, 2019).

Spadaro, D., Garibaldi, A., and Gullino, M. L. (2004). Control of *Penicillium expansum* and *Botrytis cinerea* on apple combining a biocontrol agent with hot water dipping and acibenzolar-S-methyl, baking soda, or ethanol application. *Postharvest Biol. Technol.* 33, 141–151. doi: 10.1016/j.postharvbio.2004.02.002

Spadaro, D., and Gullino, M. L. (2005). Improving the efficacy of biocontrol agents against soilborne pathogens. *Crop Prot.* 24, 601–613. doi: 10.1016/j.cropro.2004.11.003

Tannous, J., Atoui, A., El Khoury, A., Kantar, S., Chdid, N., Oswald, I. P., et al. (2015). Development of a real-time PCR assay for *Penicillium expansum* quantification and patulin estimation in apples. *Food Microbiol.* 50, 28–37. doi: 10.1016/j.fm.2015.03.001

Thompson, A. K., Prange, R. K., Bancroft, R., and Puttongsiri, T. (2018) in *Controlled atmosphere storage of fruit and vegetables*. eds. A. K. Thompson, R. K. Prange, R. D. Bancroft, and T. Puttongsiri (Wallingford: CABI).

Trierweiler, B., Schirmer, H., and Tauscher, B. (2003). Hot water treatment to control Gloeosporium disease on apples during long-term storage. *J. Appl. Bot.* 77, 156–159.

Vandenkoornhuyse, P., Quaiser, A., Duhamel, M., Le Van, A., and Dufresne, A. (2015). The importance of the microbiome of the plant holobiont. *New Phytol.* 206, 1196–1206. doi: 10.1111/nph.13312

Wszelaki, A. L. (2003). Effect of combinations of hot water dips, biological control and controlled atmospheres for control of gray mold on harvested strawberries. *Postharvest Biol. Technol.* 27, 255–264. doi: 10.1016/S0925-5214(02)00095-9

Zhang, H., Wang, S., Huang, X., Dong, Y., and Zheng, X. (2008). Integrated control of postharvest blue mold decay of pears with hot water treatment and *Rhodotorula glutinis*. *Postharvest Biol. Technol.* 49, 308–313. doi: 10.1016/j.postharvbio.2008.01.004

Zong, Y., Liu, J., Li, B., Qin, G., and Tian, S. (2010). Effects of yeast antagonists in combination with hot water treatment on postharvest diseases of tomato fruit. *Biol. Control* 54, 316–321. doi: 10.1016/j.biocontrol.2010.06.003

Conflict of Interest: The authors declare that the research was conducted in the absence of any commercial or financial relationships that could be construed as a potential conflict of interest.

frontiers in Microbiology

ORIGINAL RESEARCH
published: 10 December 2019
doi: 10.3389/fmicb.2019.02694

The Impact of Soil-Applied Biochars From Different Vegetal Feedstocks on Durum Wheat Plant Performance and Rhizospheric Bacterial Microbiota in Low Metal-Contaminated Soil

Arianna Latini[1], Giovanni Bacci[2], Manuel Teodoro[3], Daniele Mirabile Gattia[1], Annamaria Bevivino[1] and Lukáš Trakal[3]*

[1] Italian National Agency for New Technologies, Energy and Sustainable Economic Development, ENEA Casaccia Research Centre, Rome, Italy, [2] Department of Biology, University of Florence, Florence, Italy, [3] Department of Environmental Geosciences, Faculty of Environmental Sciences, Czech University of Life Sciences Prague, Prague, Czechia

OPEN ACCESS

Edited by:
Feth-el-Zahar Haichar, Microbial Ecology, France

Reviewed by:
Haipeng Wu, Changsha University of Science and Technology, China
Thomas Ducey, Coastal Plain Soil, Water and Plant Conservation Research (USDA-ARS), United States

***Correspondence:**
Annamaria Bevivino
annamaria.bevivino@enea.it

Specialty section:
This article was submitted to Microbial Symbioses, a section of the journal Frontiers in Microbiology

Received: *31 July 2019*
Accepted: *06 November 2019*
Published: *10 December 2019*

Citation:
Latini A, Bacci G, Teodoro M, Mirabile Gattia D, Bevivino A and Trakal L (2019) The Impact of Soil-Applied Biochars From Different Vegetal Feedstocks on Durum Wheat Plant Performance and Rhizospheric Bacterial Microbiota in Low Metal-Contaminated Soil. Front. Microbiol. 10:2694. doi: 10.3389/fmicb.2019.02694

Biochar shapes the soil environment and plant growth. Nevertheless, the mechanisms associated with an improved plant biomass and soil microbiome in low metal-contaminated soils are still unclear. In this study, the influence of biochar on soil physico-chemical properties, plant performance, and rhizosphere microbiota in durum wheat was investigated at the above- and belowground levels. Two kinds of biochar from different feedstocks (wood chips and wheat straw pellets) and two Italian durum wheat varieties, Duilio and Marco Aurelio, were analyzed in a greenhouse using a low-nutrient gleyic fluvisol containing a very small amount of Pb and Zn. Four different treatments were performed: soil-only control (C), soil amended with woody biochar equilibrated with nutrient solution (B1+) and non-activated (B1−), and soil amended with non-activated (B2−) wheat straw biochar. Seven weeks after seed germination, (1) the physico-chemical properties of soil, biochars, and mixtures were assessed; (2) the fresh and dry weight of aboveground plant tissues and roots and other morphometric traits were measured; and (3) metabarcoding of the 16S rRNA bacterial gene was performed on rhizosphere soil samples. The results showed that the biochar from wheat straw had stronger impact on both durum varieties, with higher electrical conductivity, higher levels of available K and Na, and a substantial increase of dissolved Na^+, K^+, and Cl^- ions in pore water. Generally, biochar amendment decreased Zn availability for the plants. In addition, biochar improved plant growth in the early growth stage, and the more positive effect was achieved by combining wheat straw biochar with Marco Aurelio. Rhizosphere bacterial microbiota showed variation in alpha diversity only due to treatment; on the other hand, the differential analysis showed consistent variation among samples with significant effects on amplicon sequence variant (ASV) abundance due to the specific

biochar treatment as well as the genotype. The pure B1−, due to its scarce nutrient content with respect to the richer types (B1+ and B2−), had a negative impact on microbiota richness. Our study highlights that an appropriate combination of biochar feedstock and crop species may lead to superior yield.

Keywords: biochar, durum wheat, vegetal feedstock, rhizosphere bacterial microbiome, low-metal contaminated soil

INTRODUCTION

In the last decade, biochar has been focused upon due to its great potential for climate change mitigation, and its application to soil has emerged as an attractive strategy for sequestering carbon, reducing greenhouse gas (GHG) emissions, and improving soil quality (Lehmann, 2007; Atkinson et al., 2010; Agegnehu et al., 2016). Biochar may have variable effects on (i) soil properties, (ii) soil biota, including microbiota (Lehmann et al., 2011), (iii) plant growth and crop yield (Biederman and Harpole, 2013; Jefferey et al., 2015; Pandit et al., 2018; Sun et al., 2019), (iv) roots (Brennan et al., 2014; Prendergast-Miller et al., 2014; Xiang et al., 2017) and the rhizosphere microbiome (De Tender et al., 2016; Kolton et al., 2017), and (v) crop resistance to disease (Elad et al., 2011; Frenkel et al., 2017). Biochar has also been proved to be effective in the remediation of soils with both heavy metal and organic pollutants (Brennan et al., 2014; Zama et al., 2018), playing a critical role in reducing ecological and human health risks associated with heavy metal contamination.

The structure and function of biological communities within soils are complex, and the presence and variable abundance of individual members have a profound effect on soil function, plant health, and productivity (Atkinson et al., 2010). Several studies have reported that soil microorganisms are affected following biochar application, with it increasing or decreasing (Han et al., 2017; Kolton et al., 2017; Li et al., 2018) their biomass, while others have found that amendment with biochar had no significant effect (Lehmann et al., 2011). These variable microbial responses are controlled by multiple environmental factors like types and rates of biochar amendment, the initial edaphic conditions, land use and management regimes, and vegetation types. The results of next-generation sequencing across Europe have indicated that biochar has significant effects on soil microbial communities, even if these may be small with respect to the high microbiome variability in different soils (Jenkins et al., 2017). Very little is known about the mechanisms through which different types of biochar in the same soil environment affect the microbial abundance and community composition, and this has recently been reviewed by Palansooriya et al. (2019). Concerning microbial abundance and activities, pH is one of the soil chemical properties that have a major influence (Lehmann et al., 2011).

A comprehensive understanding of how soil microbial communities respond to different biochar amendments, taking into account the effects of different biochar feedstocks, pyrolysis protocols, concentrations in the soil, and so on, is still far off. Also, the cultivar-specific response of the bacterial community to soil-applied biochars in the rhizosphere of certain plant species needs to be further investigated. Choosing the best combination of cultivar and soil treatment could amplify the benefit of biochar-based practices and increase agricultural sustainability.

Durum wheat (*Triticum turgidum* L. subsp. *durum*), even though representing only 5% of total wheat, is an economically important crop due to its unique characteristics and end products, in particular pasta. It is better adapted to semiarid climates than bread wheat. Only a few experiments are reported in the literature that focus on durum wheat performance in the presence of biochar. Among the more noteworthy results on this topic, durum wheat showed a 10% increase in grain production after a biochar application of 10 t ha^{-1} in the field in Central Italy (Baronti et al., 2010). Vaccari et al. (2011) applied a large volume of biochar (30 and 60 t ha^{-1}) to the soil for durum wheat planting in the Mediterranean climate condition and obtained an increase of up to 30% on biomass production and yield. At the same time, they also evaluated the overall impact of biochar on soil microbial activity, which reached a minimum over the first 14 months after biochar incorporation (Castaldi et al., 2011). Moreover, biochar addition to a nutrient-poor, slightly acidic loamy sand pot soil had little effect on durum wheat yield in the absence of mineral fertilization, while it produced a 20–30% increase in grain yield at the highest mineralization rate (Albuquerque et al., 2013). The same team of researchers reported that durum wheat treated with biochar from olive-tree pruning in the field in the Mediterranean showed higher relative growth, aboveground biomass, and yield than control plants, in accordance with Vaccari et al. (2011). They also demonstrated that plants responded to biochar addition by increasing fine root proliferation (Olmo et al., 2014). Furthermore, the soil microbial community structure has been analyzed in a 2-year durum wheat field trial in Italy under two loads of woody biochar (30 and 60 t ha^{-1}), without any apparent effect on microbial biomass, activity, or diversity (Rutigliano et al., 2014).

Until now, the effect of soil-applied biochars from different stock biomasses on rhizosphere microbiota, durum wheat plant performance, and soil properties in low metal-contaminated soil has not been investigated. This study focused on soil originating from the vicinity of a mining/smelting district

Abbreviations: ASV, amplicon sequence variant; B1−, untreated wood chip biochar; B1+, wood chip biochar activated by incubation with nutrient-rich solution; B2−, untreated wheat straw biochar; C/N, carbon to nitrogen ration; CEC, cation exchange capacity; DW, dry weight; EC, electrical conductivity; FLL, flag leaf length; FW, fresh weight; mFLW, maximum flag leaf width; PH, plant height; SOM, soil organic matter; tAGFW and tAGDW, total aboveground fresh and dry weight; tBGFW and tBGDW, total belowground fresh and dry weight; TC, total carbon; TN, total nitrogen; TOC, total organic carbon; V1, Duilio durum wheat variety; V2, Marco Aurelio durum wheat variety; WHC, water holding capacity.

(Přibram, Czechia), 12 km distant from the heavily contaminated soil, and followed up several previous studies dealing with bulk metal contamination in this area (Zemanová et al., 2014; Jačka et al., 2018). In the present study, two different biochars (i.e., wood and wheat straw), both manufactured at a high pyrolysis temperature (700°C), and two durum wheat varieties exhibiting different behavior and traits, thus reflecting the level of influence of the plant genotype to the biochar treatment, were used with the aim of assessing the effect of biochar type and/or durum genotype on the diversity and composition of microbiota associated with rhizosphere soil, soil properties, and plant growth. This study was designed to establish the relationship of biochar-induced changes in rhizosphere bacterial community structure with soil nutrient composition and the growth promotion of durum wheat in a comprehensive fashion.

MATERIALS AND METHODS

Soil and Biochars

The soil used originated from a gleyic fluvisol coming from the alluvium of the Litavka river (Láz close to the Přibram mining/smelting district, Czechia). It had 2.2% SOM and a negligible amount of Pb and Zn, with a total content of both metals of up to 100 ppm; it is classified as sandy loam soil according to U.S.D.A. taxonomy. Soil samples were collected from the arable layer (0–25 cm), air-dried, sieved through a 2-mm stainless sieve, and homogenized. The soil texture was 8.7% clay (<2 μm), 34.8% silt (2–50 μm), and 56.5% sand (0.05–2 mm); the bulk density (ρ) was 1.21 g cm^{-3}, and the soil porosity was 0.58, as presented in Jačka et al. (2018).

Two types of biochars produced from different feedstocks were used for soil amendment; i.e., wood chip biochar (referred in this manuscript as B1) provided by Carbon Terra (Germany), and wheat straw pellet biochar (WSP700, referred here as B2) provided by the UK Biochar Research Center (2014) (University of Edinburgh, United Kingdom). Both biochars were produced at a high pyrolysis temperature of 700°C, as reported in **Supplementary Table S1** in **Supplementary Material S1** together with their other characteristics. These biochars are considered as standard; in fact, they have been widely investigated by several research teams (Wiedner et al., 2013; Kammann et al., 2015; Shen et al., 2017a,b; Kaetzl et al., 2018; Mašek et al., 2018; and several others) and were also used in this study for experimental reproducibility purposes.

Both untreated (B1−) and activated (B1+) woody biochars were employed; in this second form, biochar underwent conditioning incubation in full-nutrient Hoagland solution (Hoagland and Arnon, 1950) as fertilizer for 1 week. As the wheat straw biochar (B2) contained a sufficient quantity of nutrients (e.g., N, see **Supplementary Table S1** in **Supplementary Material S1**), activation by Hoagland solution was not performed for this case, and only the untreated (B2−) form was used.

Both soil and biochars were air-dried and finely ground (>2 mm) before soil mixture preparation. For samples different from controls, soil was mixed with the respective biochar (either as-such or previously activated) at a 3% *w/w* dosage.

Plants

Two Italian high-yielding durum wheat (*Triticum turgidum* L. subsp. *durum*) varieties, Duilio (V1) and Marco Aurelio (V2), chosen from among a panel of Italian elite genotypes previously analyzed[1] (unpublished results), were used. Their morpho-physiological characteristics, their tolerant/resistant behavior with respect to major biotic and abiotic stresses, and the main qualitative information regarding them are reported in **Supplementary Table S2** in **Supplementary Material S2**. These two varieties were chosen due to their different wheat biomass production in the early growth stage upon biochar addition: Duilio showed a positive effect on shoot biomass production in the presence of biochar from wood feedstock, while Marco Aurelio did not show improved performance in the presence of biochar from either wood or wheat straw feedstock (unpublished data).

Plant seeds were kindly provided by the Società Italiana Sementi (SIS), which describes Duilio as a good-yielding variety in most kinds of soil, an early and highly rustic wheat, very widespread, and reports for Marco Aurelio an excellent productivity, high protein content, high yellow index in semolina, wide adaptability, and tolerance to Septoria.

Greenhouse Experimental Design

A pot trial was carried out under greenhouse conditions in Prague at the Czech University of Life Science in March 2017. The climatic conditions set in the greenhouse during this experiment were: 24°C/18°C day/night temperature, 70% relative humidity, and a 16 h photoperiod. The experiment was laid out in a complete randomized block design with nine replicates in polyvinyl chloride (PVC) pots (12-cm top diameter, 10-cm bottom diameter, 10-cm height, with a volume of 1 L). Treatments were as follows: (i) soil-only control (C), (ii) soil plus untreated woody biochar (B1-), (iii) soil plus activated woody biochar (B1+), and (iv) soil plus untreated wheat straw biochar (B2−). This led to an experimental size of eight samples (2 plant varieties × 4 treatments), each of them with nine biological replicates, thus resulting in a total of 72 plants (1 plant/pot). Both soil and biochars were air-dried and finely ground (>2 mm) before soil mixture preparation. For samples different from controls, soil was mixed with the respective biochar (either as-such or previously activated) at a 3% *w/w* dosage. No further fertilization was applied to plants.

Before planting, seeds were surface-sterilized in 5% NaOCl for 2 min, then rinsed in three changes of sterile distilled water. Afterward, disinfected seeds were germinated onto filter paper (Whatman 1), moistened with 10 ml of sterile distilled water, in 100 × 10 mm Petri dishes. After 6 days, plantlets were transplanted into pots. In the beginning, three plantlets per pot were sown at a depth of 1 cm; then, after 10–12 days when

[1]https://www.plant-phenotyping-network.eu/lw_resource/datapool/systemfiles/elements/files/e4061064-d535-11e8-8a88-dead53a91d31/current/document/bioadd-mad-it-eat.pdf

most of the plants had emerged, only one plant was chosen and preserved. After planting, 100 g of the washed inert silica sand (>2 mm) was placed over the soil of each pot to minimize water evaporation.

Initial irrigation was realized gravitationally (using the counted weight of demi-water) in order to reach the given value of WHC = 60% (for a soil porosity of 0.58). Afterward, plants received irrigation three times per week by carefully pouring of deionized water onto the surface of the potting soil with a graduated cylinder. In each irrigation, each pot was weighed on a top-loading balance before watering to calculate the amount of water to be supplied. Considering that the pot and saucer weight was around 75 g, that each pot was filled with 900 g of dried soil or soil-biochar mixture, and that the approximate weight of water at 60% WHC was 300 g, varying slightly according to the particular soil treatment and the plant growth, the total pot weight was around 1,275 g (75 + 900 + 300 g), excluding the water-filled tube (explained hereinafter). Moreover, to ensure constant moisture (60% of WHC) from one watering time to another throughout the entire experiment duration, 15-ml Falcon tubes equipped with irrigation wicks were placed into the soil, with the volume of water in the tubes being regularly restored by filling (**Supplementary Material S3**).

Plants were checked regularly, and their phenological phases were assessed on the Feekes scale throughout the experiment. Six weeks after transplanting (final time, T_f), plants had grown enough for further analyses. First, bulk soil and soil-biochar mixtures were collected from all of the pots for their chemical-physical characterization at the final time of the experiment (T_f). In this case, pot soil samples were kept separated for the two plant varieties. Moreover, before harvesting (T_f), soil pore water was collected in each pot with 10-cm long rhizones (Eijkelkamp, Netherlands). Second, plant aboveground and belowground biomasses at T_f were evaluated for all 72 plants (9 replicates/condition) through their FW and DW measurement in order to estimate plant growth. Third, six biological replicates, randomly chosen out of the nine at the beginning of the experiment, were used for rhizosphere sampling for metagenomics analyses.

Biochar Microstructure Analysis

In order to ascertain the microstructure of the two biochars used, Scanning Electron Microscopy (SEM) has been performed with a Zeiss EVO MA15 operated at 20 kV. The samples were directly observed after supporting them on an aluminum stab covered with conductive carbon tape. X-ray diffraction was used in order to study the presence of crystalline phases in the biochar samples. A Rigaku SmartLab powder diffractometer, equipped with a monochromator in the diffracted beam and a Cu Kα radiation source (λ = 1.5405 Å), was operated at 40 kV and 30 mA in the range of 10–90 2θ, with a step size of 0.04, and 8 s per step. The biochars were reduced to a fine powder using an agate mortar and pestle.

Soil and Soil-Biochar Mixture Analysis

At time zero of the experiment (T_0) as well as at the end (T_f), the soil replicas for each variant were mixed together (V1C, V1B1−, V1B1+, and V1B2−; V2C, V2B1−, V2B1+, and V2B2−) and analyzed per treatment and per genotype in duplicate. Each soil sample was air dried, homogenized, and again sieved (<2 mm) to remove any residue of silica sand or plant roots. Determination of pH was measured in distilled water and a KCl suspension at a 1:5 (*w*/*v*) ratio (according to the ISO 10390:2005 standard for soil quality) using a pH meter (inoL^{a}b® pH 7310, WTW, Germany). Electric Conductivity (EC) was obtained from a 1:5 (*w*/*v*) H_2O suspension (USDA Soil Survey Staff, 2014) using a Multi 3420 (WTW, Germany) digital precision meter. CEC was determined using the 0.1 M $BaCl_2$ (1:5*0 w*/*v*) protocol (Carter and Gregorich, 2008). Total organic/inorganic C in soil was determined using a SSM-5000A (Shimadzu, Japan) carbon analyzer.

For the directly available metal pool, samples of 2 g of soil were treated with 20 ml of 0.01 M $CaCl_2$ (Quevauviller, 1998), shaken for 3 h at 300 rpm, centrifuged for 10 min at 3000 rpm, and filtered through a 0.45 μm nylon filter (VWR, Germany). Pseudo total concentrations of elements were extracted by adding 10 ml of *aqua regia* (2.5 ml HCl and 7.5 ml HNO_3) to 0.5 g of dry soil and were digested at 200°C under microwave conditions (SPD-Discover, CEM, United States). The samples were diluted in 25 ml of deionized water and filtered through a 0.45 μm nylon filter. The concentrations of elements in the solutions obtained were analyzed by inductively coupled plasma optical emission spectrometry (ICP-OES; 720ES, Varian Inc., Palo Alto, CA, United States). The standard reference materials 2710a Montana Soil I (NIST, United States) and CRM 483 (Institute for Reference Materials and Measurements, EU) were used.

Determinations of pH and EC in pore water were performed using standard equipment, as reported above. Major inorganic anions + cations were determined using a Dionex ICS-5000 ion chromatography system (Dionex, United States) and inductively coupled plasma optical emission spectrometry (ICP-OES).

Evaluation of Plant Performance in the Early Growth Stage

Fresh (FW) and dry weights (DW) were measured on an analytical balance at T_f. The aboveground part of each plant was kept separate from the roots. Before measuring the FW of the roots, they were washed in water and laid on filter paper to remove excess water. The values of DW of roots were recorded after 2 days of incubation at 75°C. At T_f, morphometric traits of the plants, namely the PH from the base of the stem up to the end of the emerging spike, FLL, and maximum width (FLMW), were measured in *cm*. Lastly, the number of plant leaves was also noted.

Rhizosphere Sampling for Metagenomics Analysis

After the removal of the silica sand on the soil surface with a spatula, pot plants (2 varieties × 4 treatments × 6 replicates, for a total of 48 plants) were turned upside down on filter paper. Each plant was carefully removed from the bulk soil and shaken vigorously to remove loosely adhered soil particles. Roots with adhering soil were covered in aluminum foil; then, in the lab, the plant was dissected. The entire root (belowground tissue) containing tightly adhering soil was put in a 15-ml Falcon

tube containing 10 ml autoclaved 0.9% (*w*/*v*) sodium chloride (NaCl) solution and then shaken at 50 rpm for 20 min at room temperature in a multirotator (multiRS-biosan) to free root-associated bacterial cells. Root tissue samples were then removed from the suspension, samples were centrifuged at 6,500 × *g* for 15 min, and the supernatant was decanted. The derived pellet was highly enriched in root-associated bacteria and stored at −80°C until DNA extraction.

DNA Extraction and PCR Amplification

DNA was extracted from 500 mg rhizosphere soil samples using a FastDNA® SPIN Kit for Soil in combination with a FastPrep-24™ 5G homogenizer (MP Biomedicals), according to the manufacturer's instructions. In order to optimize quality and A_{230} value, the extracted DNA was further diluted and concentrated by VIVASPIN 500 centrifugal concentrators (10,000 MWCO).

The extracted soil gDNA was run on a 1.0% agarose gel and quantified using both a Nanodrop ND-1000 spectrophotometer (NanoDrop Technologies, Wilmington, DE, United States) and a Qubit 4 Fluorometer (Invitrogen by Thermo Fisher Scientific Inc.) (**Supplementary Material S4**) for quality-quantity check. A PCR test with primers P0 and P6 for amplification and sequencing of bacterial 16S rDNA (Di Cello et al., 1997) was also performed on a few randomly chosen DNA samples.

For each of the 48 collected rhizosphere samples, we performed two independent DNA extractions, and then we pooled them in an equimolar ratio, obtaining a composite root-associated DNA sample for each plant.

Illumina 16S Library Construction and Sequencing

The DNA concentration of the samples was adjusted to 10 ng/μl and then diluted at 1:20 for the subsequent investigations. The sequencing protocol was performed at BMR Genomics Srl (Padua, Italy). Briefly, the V3-V4 regions of 16S rRNA gene were amplified using the following primers: Pro341F, 5′-CCTACGGGNBGCASCAG-3′, and Pro805R, 5′-GACTACN VGGGTATCTAATCC-3′ (Takahashi et al., 2014). Primers were modified with the forward and reverse overhangs (5′-TCGT CGGCAGCGTCAGATGTGTATAAGAGACAG-[locus-specific sequence]-3′ and 5′-GTCTCGTGGGCTCGGAGATGTGTAT AAGAGACAG-[locus-specific sequence]-3′, respectively) necessary for dual index library preparation. Amplicons were purified by 0.8x Agencourt AMPure XP magnetic beads (Beckman Coulter) and amplified with a short cycle with a Nextera XT Index (Illumina). They were then normalized by SequalPrep (Thermo Fisher) and multiplexed. The pool was purified by 1x Agencourt AMPure XP magnetic beads (Beckman Coulter), loaded on Illumina Miseq, and sequenced with a 300PE v3 chemistry strategy.

Amplicon Sequence Variant Inference

Sequences were clustered into ASVs using the DADA2 pipeline outlined at *https://benjjneb.github.io/dada2/tutorial.html* (Callahan et al., 2016). Before running the pipeline, PCR primers were removed with cutadapt (Martin, 2011) using the default settings. Sequences that were not trimmed by the software (namely those where the adapter was not found) were removed from the analysis (–discard-untrimmed option). If only one read of a pair was removed, the other one was also discarded to maintain the paired-end nature of the samples (–pair-filter = any option). Sequences were then filtered using the filterAndTrim function of DADA2 with a maximum error rate of 2. The truncLen option was set to 270 for forward reads and 200 for reverse reads in order to maintain more than 20 bp of overlap while removing low-quality tails. Trimmed sequences were used for error rate estimation (the learnErrors function with default parameters). Finally, sequences were denoised and merged, and variants were inferred using the DADA2 algorithm. Taxonomic annotation was carried out after chimera removal using the Silva training set 128 (Quast et al., 2012). The number of sequences retained in every step is reported in **Supplementary Material S5**, together with the resulting rarefaction analysis. Samples with a final number of reads lower than 10,000 were removed from subsequent analyses (five samples in total). Consistent ASVs were detected by comparing three technical replicates, as described in **Supplementary Material S6**, which provides additional information on the processing.

Differential Analysis and Taxonomic Distribution

Differential abundance analysis was performed on consistent ASVs using DESeq2 (Love et al., 2014). Fold changes were shrunk using the adaptive shrinkage estimator from the 'ashr' package (Stephens, 2016). All *p*-values were adjusted using the Benjamini and Hochberg correction (also known as the "false discovery rate"), and only contrasts reporting a *p*-value lower than 0.05 with an absolute log2-fold-change value higher than 1 have been considered.

For the taxonomic distribution of consistent ASVs, samples and taxa were clustered using the unweighted pair group method with arithmetic mean (UPGMA) based on the Bray–Curtis distance.

Statistical Analysis

Plant data were statistically analyzed by one-way ANOVA (with Tukey HSD *post hoc* test) with IBM SPSS Statistics 23 software, setting $p < 0.05$ as the significance level. The mean FW and DW values (in grams) proceeding from nine replicated samples were treated as the dependent variables, while the treatments and the two genotypes (V1C, V1B1−, V1B1+, and V1B2−; V2C, V2B1−, V2B1+, and V2B2−) as the independent variables. Before conducting one-way ANOVA, the normal distribution of the data was checked by Shapiro–Wilk test (Sig. > 0.05), and the homogeneity of variances was checked by Levene test (Sig. > 0.05; **Supplementary Materials S7, S8**).

Linear regression was carried out to inspect the relation between the abundance and persistence of bacterial ASVs, whereas one-way analysis of variance (ANOVA) was performed on alpha diversity to inspect the effect of genotype and treatment. Alpha diversity values were inspected without applying any transformation, whereas abundance data were

log-transformed before analysis. Consistent taxa (and samples) were clustered using the unweighted pair group method with arithmetic mean (UPGMA) based on the Bray–Curtis distance. Differential abundance analysis was performed using DESeq2 (Love et al., 2014). A model consisting of both genotype and treatment effect was used to test for differentially abundant ASVs. All statistical analyses on microbial community data were performed into the R environment, version 3.4.4 (R Core Team, 2018).

A Pearson correlation (bivariate) analysis was performed to determine the existence of a correlation among the average values of the Shannon and Inverse Simpson indexes and the chemical characteristics of the soil (pH, EC, CEC, TC, TOC, TN, and C/N). The two-tailed test ($p < 0.05$) was also completed by SPSS software.

RESULTS

The characteristics of the two biochars used - wood chip feedstock for B1 and wheat straw for B2 – are shown in **Table S1** in **Supplementary Material S1**, while the main features of the two durum wheat varieties analyzed – i.e., Duilio and Marco Aurelio – are listed in **Supplementary Table S1** in **Supplementary Material S2**. The results of our study confirm that biochar amendment influences several of the features analyzed related to soil properties, plant growth, and rhizosphere bacterial microbiota (**Figure 1**), as reported in detail in the three sections below.

Effect of Biochar Amendment on Soil Chemical Properties

As expected from the physical and chemical features reported in **Supplementary Table S1** in **Supplementary Material S1**, the two different biochars used exhibited different behavior. Indeed, when examined by scanning electron microscope, biochar from wood (i.e., B1) presented interconnected multi-directional channels with dimensions ranging from 5 to 50 microns, while biochar from wheat straw (i.e., B2) presented straight channels of 4–8 μm with pores of 3–4 μm (**Figure 2A**). On the other hand, they presented a very similar diffraction pattern, with broad peaks at about 3.85 Å, 2.09 Å, and 1.20 Å, which are generally associated with disordered carbons (Keiluweit et al., 2010). Some sharper peaks were also present in both biochar samples, mainly related to calcite ($CaCO_3$) and quartz (SiO_2) (**Figure 2B**).

The initial pH in water (5.17 at T_0 in the soil alone) showed more than a unit of increase in all of the samples at the end of the experiment (T_f) (**Supplementary Table S1** in **Supplementary Material S1**). EC showed important variations between the soil at the beginning of the experiment (T_0) and the soil and mixtures at the end (T_f), apart from B1− samples at T_f, where the EC value was similar to the initial control soil. In all other samples, EC showed an increase that was higher in B2- samples (**Table 1**). The CEC value increased in all samples at T_f with respect to the initial soil control, and a higher increase was related to the samples amended with activated wood chip biochar (average CEC value for B1+ samples was 6.02 ± 0.23 cmol/kg). The effect of biochar amendment on the carbon–nitrogen ratio (C/N) was remarkable,

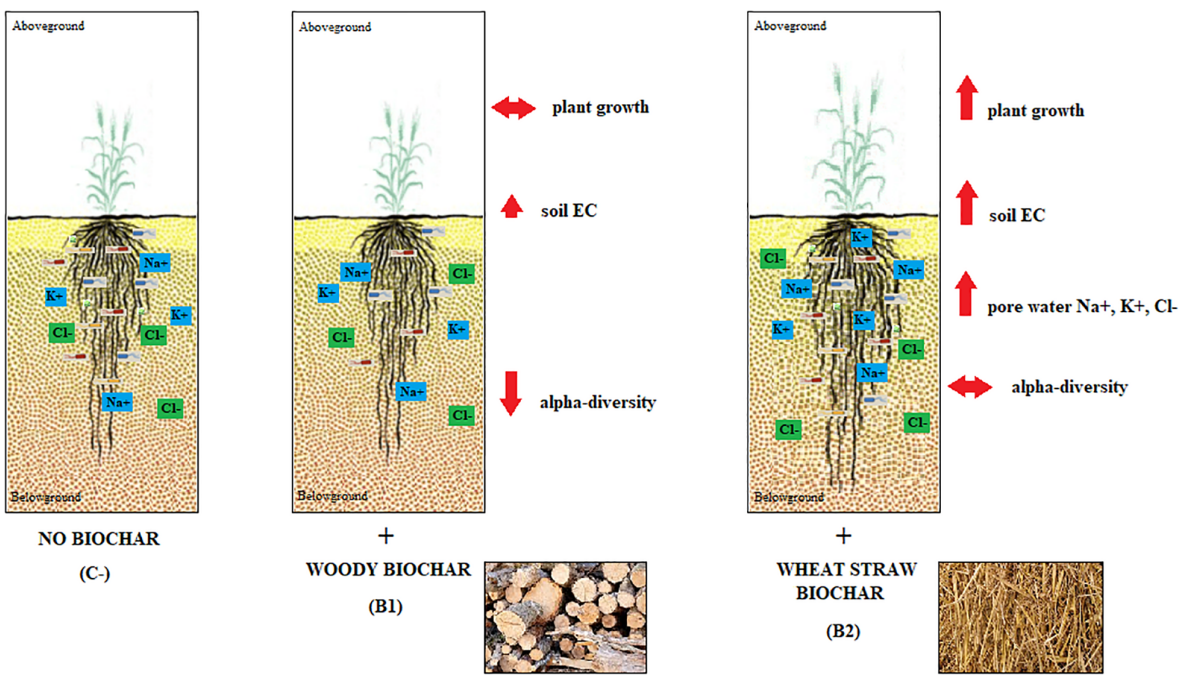

FIGURE 1 | Schematic representation of the main effects of the biochar amendment observed in soil properties, plant growth, and rhizosphere bacterial richness. The more significant outcomes from the two biochars used, i.e., that from wood and that from wheat straw feedstock, are expressed in comparison also with the soil-only control (no biochar).

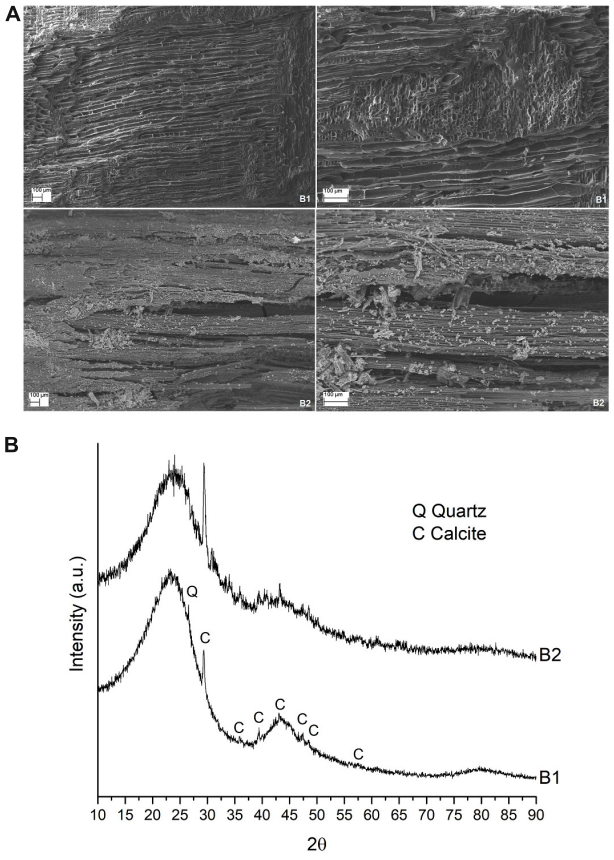

FIGURE 2 | (A) Microstructure of the two biochars used. a SEM images of biochar B1 (up) and B2 (down), 100X and 250X on the left and right side, respectively. **(B)** X-ray diffraction pattern of the two biochars.

where the ratio was ≥22.6 for all treated variants and ≤8.0 for both control variants (against 14.4 for the initial soil). The TC and TOC concentrations (*mg*/*g*) at T_f were both significantly higher for all biochar treated variants in comparison to control. TN at T_f with biochar was always equal or higher than in controls. Total phosphorus (TP) was not reported in **Table 1** because it was undetectable in all samples.

The total content of several elements in the soils was measured by the *aqua regia* extraction method (**Table 1**). In addition, the bioavailable content of these elements in the soils was determined by the $CaCl_2$ extraction method (**Table 1**, values in brackets). In summary, all of the total cation (Mg, Ca, K, and Na) contents increased slightly during the experiment, but at the same time, the available form of the cations decreased in a similar fashion, except Na. It is interesting that, at T_f, in the presence of B2−, K^+ ions in soil and particularly those available to the plant showed a substantial increase (close to 300 mg/Kg of usable potassium in B2-samples, ranging from 50 to 70 mg/Kg in B1 treated samples, and just over 20 mg/Kg in control samples without biochar). Total aluminum (Al) increased in all samples at T_f, while the available Al decreased, and the presence of biochar enhanced this Al decrease. Moreover, the presence of biochar resulted in a decrease of bioavailable Fe, Mn, and Ba. Concerning heavy metals, no lead usable by the plant was detected in any sample, either at T_0 or T_f, and a small increase in total Pb was seen due to the biochar amendment. Total zinc (Zn) showed an increase during the experiment, independently of the presence of biochar, whereas the Zn available to plants decreased substantially at the end of the experiment, and biochar-treated samples showed lower amounts.

Rhizones were used to collect pore water from soil pot samples at the end of the experiment. The values for pH and EC obtained from the pore water samples were comparable with those from the soil samples. Furthermore, the concentrations of several nutrient ions in the pore water samples were also determined (**Table 2**). Major variations were found in B2-treated samples showing significantly higher amounts of Na^+, K^+, and Cl^- ions. B1+ treated samples showed a slight increase in Mg^{2+} ions. Despite the improvement of B1+ by Hoagland solution, there were no significant differences between B1+ and the two untreated biochars through all of the nutrients analyzed in the final pore water. Moreover, the contents of dissolved phosphate anions in pore water were very low (**Table 2**).

Responses of Plant Growth and Biomass Production to the Presence of Biochar in Soil

At the final time of the experiment (T_f), the phenological stage for all plants according to the Feekes scale of wheat development was assessed at 10, corresponding to boot exposure at the end of stem extension and before heading. On average, each plant showed one tiller and 7–8 leaves.

The possible effect of the treatments applied (C, B1−, B1+, B2−) on plant growth and biomass was evaluated through the fresh (FW) and dry (DW) weights, specifically for the two durum wheat varieties under study, and for the aerial part of the plant and the rooting system. Concerning the plant total aboveground fresh weight (tAGFW), there was a significant difference ($p < 0.05$) between Duilio (3.468 ± 0.714 g) and Marco Aurelio (2.542 ± 0.691 g) control plants (**Figure 3**, V1C and V2C, black bars in the positive panel), as expected from previous experiments (unpublished data). This difference was not evident in the total aboveground dry weight (tAGDW) of the control plants (**Figure 3**, V1C and V2C, dark gray bars in the positive panel). Non-activated biochar 2 (B2−) exhibited a significant positive effect on both varieties ($p < 0.001$), with a tAGFW increase of up to 4.408 ± 0.620 g and 4.582 ± 0.612 g, respectively, in Duilio and Marco Aurelio (**Figure 3**, V1B2− and V2B2−, black bars in the positive panel). On the other hand, the effects of biochar 1, either activated or not, on the aerial plant FW were not significant (again **Figure 3**). Total aboveground dry weight (tAGDW) showed a similar trend, increasing in both varieties with B2−. The mean difference between control and B2− in Duilio was 0.095 g ($p < 0.01$) and in Marco Aurelio was 0.289 g ($p \geq 0.000$), with a Std. Error of 0.025 (**Figure 3**). In conclusion, B1 (activated or not) and B2 (not activated)

TABLE 1 | Chemical characteristics and total metal concentration in soil at the beginning of the experiment (T_0), and in soil and soil plus biochar mixtures at the end of the experiment (T_f).

	Sample	pH (–)		EC ($uS\ m^{-1}$)	CEC ($cmol\ kg^{-1}$)	TC (mg/g)	TOC (mg/g)	TN (mg/g)	C/N (–)	Total (available) element content ($mg\ kg^{-1}$)									
		H_2O	KCl							Mg	Ca	K	Na	Al	Fe	Mn	Ba	Pb	Zn
T_0	Soil	5.17***	4.08***	73.8***	3.53***	2.87***	2.31	0.20	14.4	2382 (111)	764*** (283[a])***	982*** (68)	84 (5)	13336** (11)***	10778 (17)***	610 (94)***	104 (11)***	53 (0)	48*** (7.1)***
T_f	V1C	6.56	6.37	93.6	5.70	1.20***	1.96	0.15	8.0***	2669 (99)	2590 (58[a])	1372 (22)***	88 (18)	17331 (1.2)	10847 (4.2)	709 (11.1)	97 (4.8)	58 (0)	69 (0.5)
	V2C	6.53	6.35	103.1	5.72	1.16***	1.94	0.16	7.3***	2664 (99)	2522 (33[a])	1633 (23)***	117 (18)	18356 (1.1)	10148 (2.2)	686 (9.5)	99 (4.9)	54 (0)	69 (0.4)
	V1B1−	6.44	6.32	66.8***	5.31	5.08	3.69	0.20	25.4	2512 (88)	2002** (35[a])	1488 (67)	92 (16)	17522 (0.2)	9606 (0.1)	762 (8.3)	94 (6.5)	61 (0)	69 (<0.1)
	V1B1+	6.73	6.52	95.1	5.86	4.18	3.10	0.18	23.2	2541 (94)	2507 (16[a])	1449 (51)	95 (21)	17175 (0.1)	9989 (0.2)	752 (4.9)**	96 (5.1)	58 (0)	68 (<0.1)
	V1B2−	6.51	6.40	123.2	5.60	4.30	2.60	0.19	22.6	2653 (84)	2073** (122[a])***	2044*** (292)***	107 (24)	19030** (0.2)	10284 (0.2)	779 (8.8)	100 (6.5)	62 (0)	73 (<0.1)
	V2B1−	6.40	6.26	74.6***	4.84**	4.94	3.97	0.18	27.4	2505 (88)	2044** (14[a])	1431 (66)	100 (19)	17878 (0.2)	9638 (0.1)	806 (9.5)	95 (6.7)	61 (0)	72 (0.1)
	V2B1+	6.73	6.55	91.5	6.18**	4.25	2.96	0.15	28.3	2537 (93)	2505 (22[a])	1538 (49)***	104 (21)	17533 (<0.1)	9661 (0.1)	763 (4.9)**	99 (4.7)	60 (0)	73 (0.1)
	V2B2-	6.56	6.34	129.6	4.91	3.77	3.52	0.17	26.9	2598 (84)	2046** (61[a])**	1887* (298)***	99 (24)	18132 (0.1)	10240 (0.1)	768 (8.1)	96 (6.5)	61 (0)	70 (0.1)

*Data shown are means ± SD (n = 2). Significant differences (p-value) *** < 0.001, ** < 0.01, * < 0.05. Values in brackets represent available form of the elements using 0.01 M $CaCl_2$; [a]values containing Ca coming from 0.01 M $CaCl_2$; EC is electrical conductivity; CEC is cation exchange capacity; TC is total (organic plus inorganic) carbon; TOC is total organic carbon; TN is total nitrogen; C/N is the ratio between carbon content and nitrogen content.*

TABLE 2 | Concentration of the main ions in pore water samples collected by rhizones at the end of the experiment.

	pH (-)	EC ($mS\ cm^{-1}$)	Dissolved ions in pore water ($mg\ L^{-1}$)							
			Na^+	Mg^{2+}	K^+	Ca^{2+}	Zn^{2+}	Cl^-	NO_2^-	NO_3^-	SO_4^{2-}
V1C	6.39 ± 0.01^{a}	0.17 ± 0.03^{bc}	$5.85 \pm 0.89a$	3.89 ± 1.14	1.31 ± 0.40^{a}	68.7 ± 8.67	0.88 ± 0.66	9.68 ± 7.86^{ab}	3.06 ± 1.16	79.1 ± 43.2	61.2 ± 35.6
V2C	6.57 ± 0.07^{a}	0.17 ± 0.02^{bc}	4.48 ± 0.30^{a}	4.44 ± 0.34	3.23 ± 2.94^{a}	67.5 ± 1.78	0.63 ± 0.08	5.46 ± 2.72^{a}	1.69 ± 0.70	67.3 ± 5.3	73.6 ± 3.3
V1B1−	6.47 ± 0.01^{a}	0.11 ± 0.04^{c}	5.85 ± 1.19^{a}	4.11 ± 1.55	5.10 ± 0.90^{a}	60.2 ± 20.29	1.04 ± 0.59	6.86 ± 8.13^{ab}	2.69 ± 1.03	112 ± 75	118 ± 100
V1B1+	6.58 ± 0.07^{a}	0.35 ± 0.11^{ab}	9.07 ± 0.75^{a}	7.14 ± 2.07	4.32 ± 0.78^{a}	103 ± 28.69	1.36 ± 0.99	9.76 ± 0.95^{ab}	4.87 ± 1.65	125 ± 47	79.8 ± 14.1
V1B2−	6.45 ± 0.07^{a}	0.36 ± 0.04^{a}	12.9 ± 1.3^{b}	5.36 ± 0.78	54.3 ± 9.98^{b}	65.8 ± 4.18	0.78 ± 0.22	37.8 ± 11.9^{abc}	4.47 ± 2.41	80.0 ± 31.9	76.8 ± 16.3
V2B1−	6.63 ± 0.09^{a}	0.16 ± 0.03^{bc}	6.66 ± 0.56^{a}	3.39 ± 0.19	14.2 ± 6.24^{a}	55.7 ± 10.34	0.78 ± 0.17	9.44 ± 6.82^{ab}	3.00 ± 1.26	73.4 ± 20.0	42.2 ± 15.6
V2B1+	6.96 ± 0.15^{b}	0.24 ± 0.08^{abc}	8.73 ± 1.36^{a}	5.59 ± 1.30	6.02 ± 1.71^{a}	75.6 ± 12.31	0.46 ± 0.29	13.5 ± 7.04^{ab}	5.11 ± 3.30	79.5 ± 14.2	93.9 ± 19.8
V2B2−	6.33 ± 0.10^{a}	0.43 ± 0.06^{ab}	12.9 ± 3.3^{b}	4.18 ± 1.62	53.9 ± 18.39^{b}	77.1 ± 14.38	1.15 ± 0.76	38.0 ± 15.5^{bc}	4.68 ± 2.11	133 ± 86	85.0 ± 42.8
p	<0.001	0.005	<0.001	0.188	<0.001	0.165	0.796	0.006	0.582	0.804	0.807

Data shown are means ± SD (n = 3). Different letters in a single column indicate a significant difference among the samples analyzed ($p < 0.05$).

behaved differently with respect to the aerial plant weight: the addition of B1 to soil did not result in any considerable change in the fresh or the dry weight of the plant aboveground fraction; in contrast, B2-addition to soil in its untreated form was found to be related to a statistically significant increase in these parameters.

Looking at the results related to the root system fresh weight (tBGFW), a positive effect of B2− on both Duilio and Marco Aurelio was again evident: here, the mean difference between control and B2− in Duilio was 0.246 g ($p \geq 0.000$), and that in Marco Aurelio was 0.172 g ($p < 0.01$), with a Std. Error 0.045. Moreover, exclusively for Marco Aurelio, the effect of B1− differed significantly from that of B1+ ($p \geq 0.000$), with a mean difference between V2B1− and V2B1+ equal to 0.232 g, and a Std. Error of 0.045 (**Figure 3**, black bars in the negative panel). Lastly, the total belowground dry weight (tBGDW) was significantly increased only in Marco Aurelio plants grown in B2− pots. More precisely, the average DW value of V2B2− in all replicated samples was significantly higher than in other treatments ($p < 0.01$), except for V2B1+, where this difference is not significant ($p = 0.113$) (**Figure 3**, dark gray bars in the negative panel). See **Supplementary Material S7** for the results of the statistical analysis carried out with the SPSS tool.

As additional traits for the evaluation of plant growth performance, PH, FLL, and maximum width (mFLW) were also measured at the end of the experiment (T_f). Concerning PH, even though exhibiting different heights in the control situation, lower in Duilio and higher in Marco Aurelio, both cultivars showed a similar positive influence from biochar treatment; indeed, the height increases resulting from B1− in a sharper fashion ($p < 0.003$ in V1 and $p < 0.004$ in V2) and B2− in a stronger fashion ($p < 0.000$ in both V1 and V2) were highly significant (**Figure 4**, black bars). The FLL trait was not significantly influenced by biochar in Duilio ($p > 0.05$), but was significantly altered by B1− (in a negative way; $p < 0.002$) and B2− (in a positive way; $p < 0.009$) in Marco Aurelio (**Figure 4**, gray bars; **Supplementary Material S8**). Lastly, the mFLW values were not normally distributed, so they were not considered for further statistical analysis; notwithstanding, in Marco Aurelio plants treated with B2−, flag leaf presented an increased width (data not shown).

The genotype influence on the plant response to biochar treatment (B1−, B1+, B2−) with respect to the control without biochar was also assessed. **Table 3** lists the plant response ("+" indicates a significant augmentation, "−" indicates no significant effect) in relation to the plant growth traits measured at the end of the experiment under the different treatments. The information reported in the table proceeds directly from the homogeneous subsets defined by Tukey HSD test (see **Figure 3** and related **Supplementary Material S7**, and **Figure 4** and related **Supplementary Material S8**). On the bases of the considered traits, the genotype-dependence is particularly evident in the case of B2−, where both V1 and V2 showed a general trend of plant growth increase, but their responses differentiate in relation to a few traits. In this case, tBGDW, FLL, and mFLW were kept

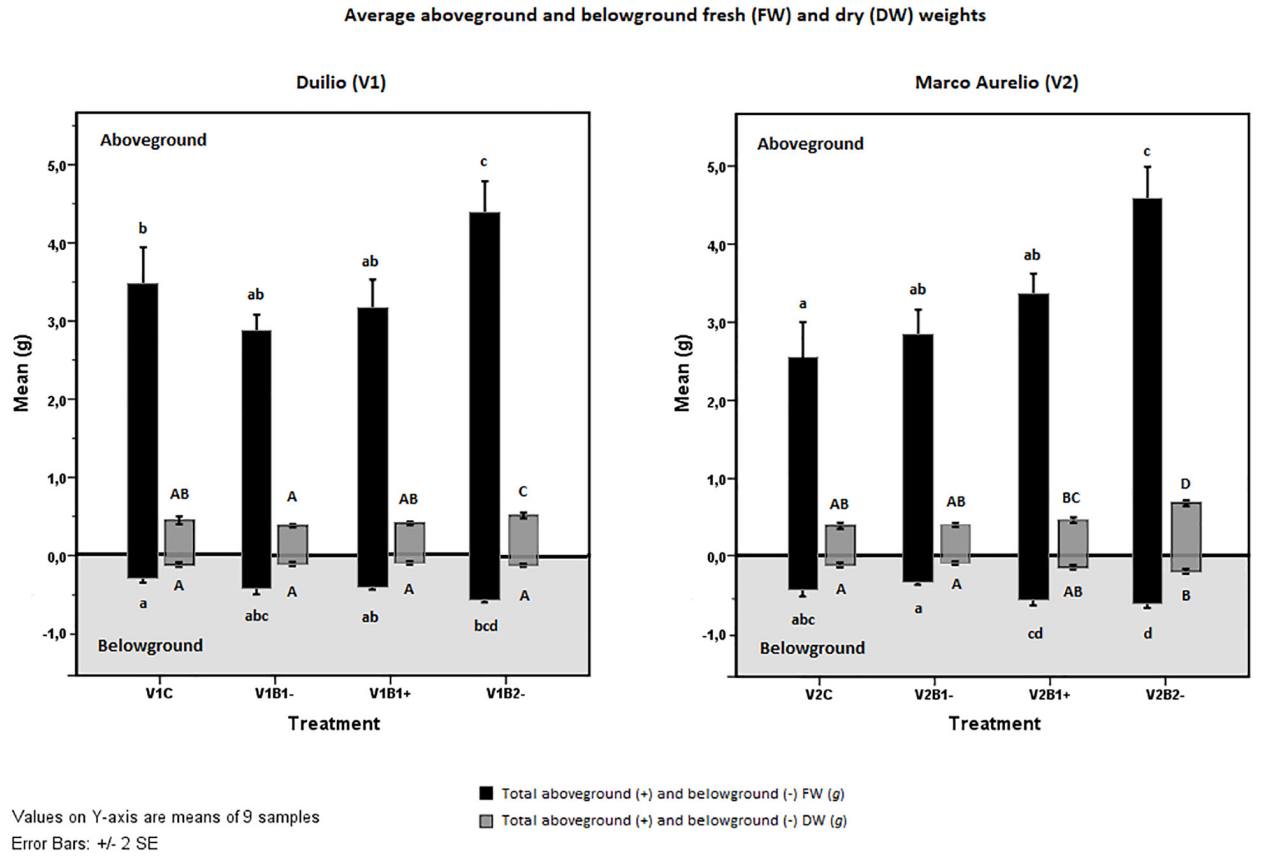

FIGURE 3 | Effect of genotype and treatment on fresh weight (FW, black bars) and dry weight (DW, dark gray bars) in the aboveground plant (upper part on white background) and in the belowground root system (lower part on the light gray background). Duilio data is on the **left**; Marco Aurelio data is on the **right**. Letters close to the error bars indicate the homogeneous subsets resulting from Tukey HSD *post hoc* test ($p < 0.05$). Lower case letters refer to FWs and upper case to DWs.

almost constant in V1 while they were positively affected in V2 (**Table 3**).

Effect of Biochar Soil Amendment on Rhizosphere Bacterial Community Structure and Diversity

To study the composition of bacterial communities in the rhizosphere samples, we used 16S rRNA amplicon sequencing. For a bacterial community, the number of specimens in which its members are detected (persistence) should be correlated to the abundance of those members, which is usually expressed as the normalized number of reads assigned to a given ASV (Shade and Handelsman, 2012; Bacci et al., 2015, 2018). In agreement with this definition, the abundance of all ASVs in different sampling sites was significantly correlated with the number of sites inhabited by those ASVs (linear regression on log-transformed abundance; $R^2 = 0.66$, $F(1, 6126) = 11{,}947.91$, $p < 0.001$) (**Supplementary Table S5** in **Supplementary Material S9** and **Figure 5A**). The ASVs of bacteria belonging to the phyla Proteobacteria, Verrucomicrobia, Acidobacteria, Bacterioides, Actinobacteria, and Firmicutes were the most commonly present, as reported in **Figure 5B**.

Alpha diversity was calculated to gain further insights into the complexity of the rhizosphere bacterial communities. It showed significant differences according to treatment but not according to genotype [two-way analysis of variance ANOVA; $F(3,27) = 3.22$, $MSE = 5{,}512.21$, $p = 0.039$ and $F(1,27) = 0.38$, $MSE = 5{,}512.21$, $p = 0.542$; **Supplementary Figure S5** in **Supplementary Material S9**). No significant effect was detected for the treatment-genotype interaction [$F(3,27) = 0.65$, $MSE = 5{,}512.21$, $p = 0.591$; **Supplementary Table S6** in **Supplementary Material S9**]. The inverse Simpson index was also used: alpha-diversity among treatments, independently on the genotypes, appears to be significantly lower under B1− treatment and to be kept almost stable under B1+ and B2− treatments, these last not varying with respect to the control (**Figure 6A**). In contrast, beta diversity showed a significant effect of treatment as well as genotype, with no significant interaction effect (permutational multivariate analysis of variance using distance matrices with 1000 permutations on the Bray–Curtis index; $p = 0.001$, $p = 0.0009$, $p = 0.054$, respectively). Despite the significant effect reported, the R^2 value is quite low, highlighting that the percentage of variance influenced by the treatment and genotype factors is, in turn, low ($R^2 = 0.19$ and 0.06, respectively) (**Supplementary Table S7** in **Supplementary Material S9**). This

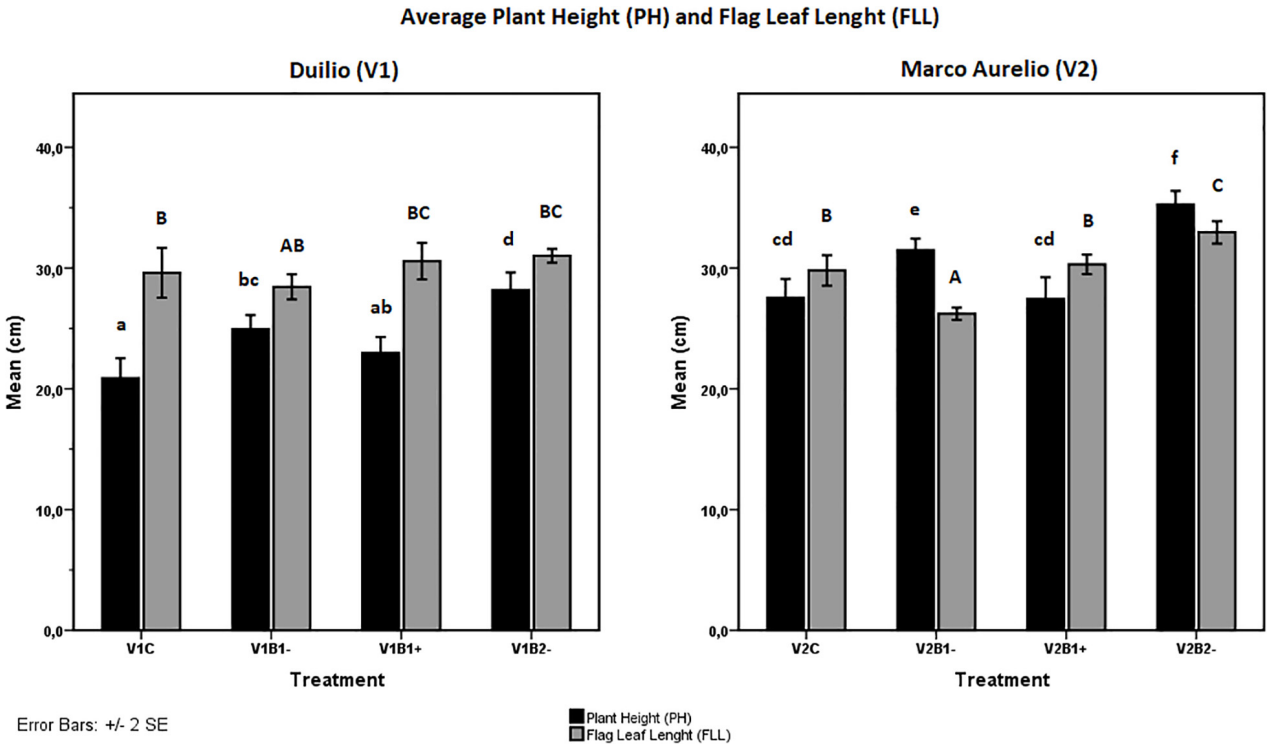

FIGURE 4 | Effect of genotype and treatment on plant height (PH, up) and flag leaf length (FLL, down) in Duilio (V1, on the **right**) and Marco Aurelio (V2, on the **left**). Letters close to the error bars indicate the homogeneous subsets resulting from Tukey HSD *post hoc* test ($p < 0.05$). Lower case letters refer to PH and upper case to FLL.

effect is clear looking at the principal component analysis (**Figure 6B**), where samples are difficult to group based on the treatment used.

Differential abundance analysis showed variation in the rhizosphere microbiome due to the treatment used (B1−, B1+, and B2−) with respect to the control as well as between plant genotypes (V2 *vs.* V1) (**Figure 7**). In particular, the biodiversity loss in B1− samples was confirmed by the reduction of numerous ASVs, especially those related to the classes of Alpha-, Beta-, and Gammaproteobacteria (Proteobacteria phylum), the classes of Cytophagia, Sphingobacteriia, and Flavobacteriia (Bacterioides phylum), and the class of Verrucomicrobiae (Verrucomicrobia phylum) (**Figure 7**, panel B1-/C). The details on the ASVs resulting from the differential analysis are provided in **Supplementary Material S10**.

The taxonomic distribution of the consistent ASVs is shown in **Figure 8**. Even though, by looking at the reported hierarchical clustering, samples could neither be grouped based on treatment nor on genotype, a shared set of ASVs can be detected.

The correlation analysis between the Shannon and the inverse Simpson index, chosen as biological indicators of the diversity of microbial communities in the soil rhizosphere (Kim et al., 2017), and the chemical properties of the sampled soils highlighted a few significant strong negative associations ($p < 0.05$). In particular, the rhizosphere α-diversity was inversely related to the TC content (Pearson r equals −0.735 with Shannon index and −0.801 with Inverse Simpson index), and also to the TN content (in this case, only with the Inverse Simpson index, Pearson r equals −0.755), as shown in **Supplementary Table S9** in **Supplementary Material S11**.

TABLE 3 | Genotype influence on the plant response to biochar treatment.

	B1−		BB1+		B1−V	
Measured plant growth traits	**V1**	**V2**	**V1**	**V2**	**V1**	**V2**
tAGFW	−	−	−	−	+	+
tAGDW	−	−	−	−	+	+
tBGFW	−	−	−	+	+	+
tBGDW	−	−	−	−	−	+
PH	+	+	−	−	+	+
FLL	−	+	−	−	−	+
mFLW	N.A.	N.A.	N.A.	N.A.	−*	+*

*"+" indicates a significant positive augmentation with respect to control at T_f, and "−" indicates no significant effect with respect to control; N.A. is not available: ANOVA statistics were applied to mFLW because the measured were not normally distributed; * results of ANOVA statistics for data that were not normally distributed.*

DISCUSSION

According to the research literature and also to experience, biochar amendment of soil may influence soil properties, plant

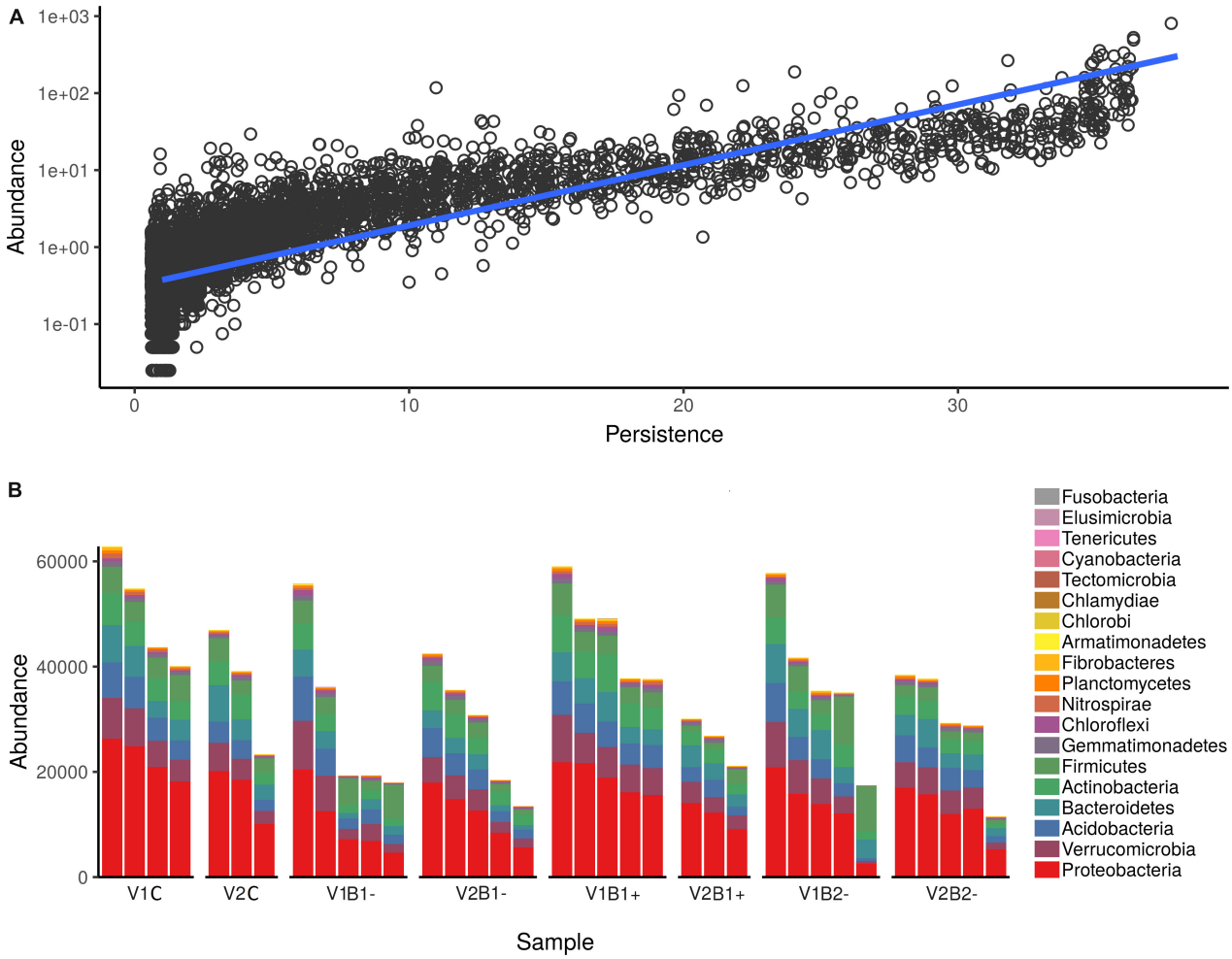

FIGURE 5 | Abundance of the 16S rRNA gene ASVs in the rhizosphere samples. **(A)** Persistence (on the *x*-axis) and abundance (on the *y*-axis) of ASVs detected in all samples. Persistence is expressed as the number of samples in which a given OTU (Operational Taxonomic Unit) was detected, whereas abundance is expressed as log-normalized number of reads assigned to a given ASV (linear regression is shown as a blue line; $R^2 = 0.66$, $F(1,6126) = 11{,}947.91$, $p < 0.001$). **(B)** Absolute abundance of ASVs. All ASVs were collapsed at the Phylum level and then plotted. Each bar reports the number of reads assigned for each sample colored according to the Phylum attribution. Plots are split according to treatment (top) and plant genotype (bottom).

physiology, and other environmental traits, including microbial composition at the levels of plant, soil, and rhizosphere. Here, we focused our attention on three main features – soil chemical composition, plant growth in the early growth stage, and rhizosphere bacterial microbiome – and hypothesized that the likely effects of biochar may be different depending on the biochar and the plant genotype. It is well established that the physicochemical properties of biochar and, for instance, its effects on the environment are strictly linked to the feedstock material used for its manufacture (Lei and Zhang, 2013; Shen et al., 2017b). Another very important factor is the temperature used during pyrolysis, even though Zhang et al. (2017) found that not all biochar properties change consistently with increasing temperature. Thus, to attain further information and determine to what extent the original vegetal source of the biochar could contribute to determining its overall effect, we used two biochars produced from two different feedstocks (wood and wheat straw) but at the same high pyrolysis temperature (around 700°C). Furthermore, the effects of biochar strongly depend on plant species and also on cultivars within a species, and even though their determination is fundamental for the most advantageous implementation of biochar in agriculture, they are still poorly known (Mollinedo et al., 2016; French and Iyer-Pascuzzi, 2018). Our results showed that the soil, plant, and rhizosphere microbiome are influenced by biochar addition, underlining the complexity of the effects of biochar and the resulting soil and plant reactions.

Biochar Amendment Increases Soil Carbon Content, pH, and CEC

Our results confirm that biochar amendment has a broad influence on the physical and chemical properties of the soil. As expected, we observed a remarkable effect of biochar on

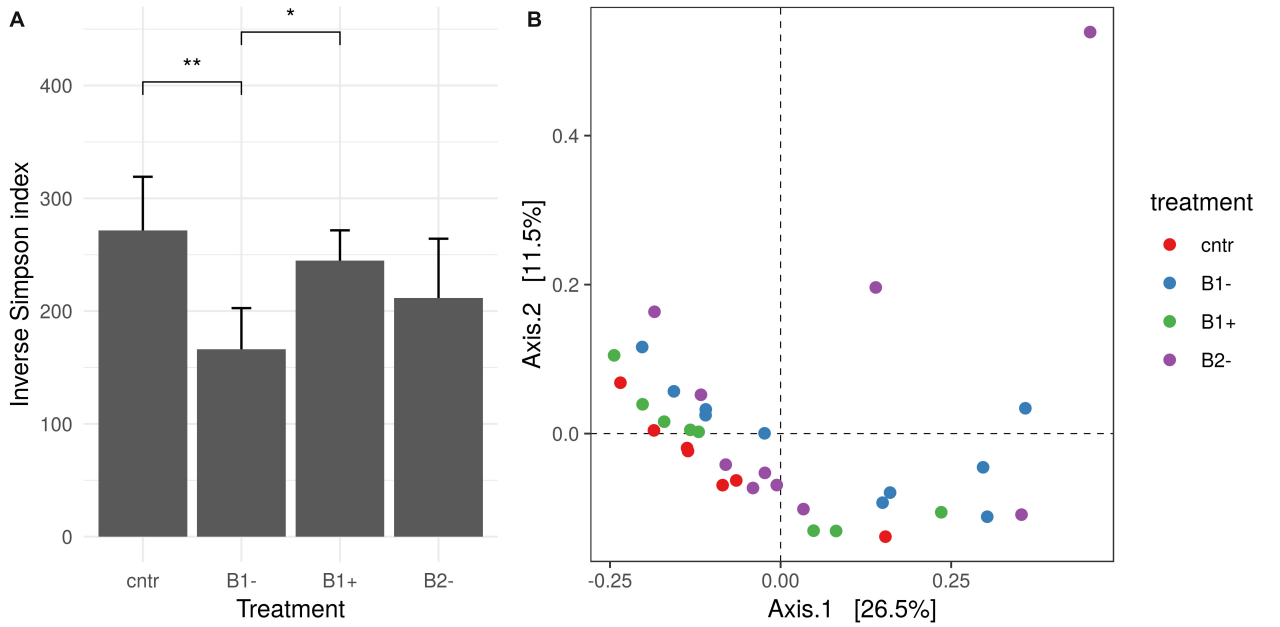

FIGURE 6 | Rhizosphere bacterial diversity analysis. **(A)** Inverse Simpson index distribution for different treatments. Treatments that showed a significant difference are marked with an asterisk (Wilcoxon test, adjusted *p*-value using a "false discovery rate" lower than 0.05). **(B)** Principal coordinate analysis (PCoA) based on the Bray–Curtis index. Different colors report different treatments.

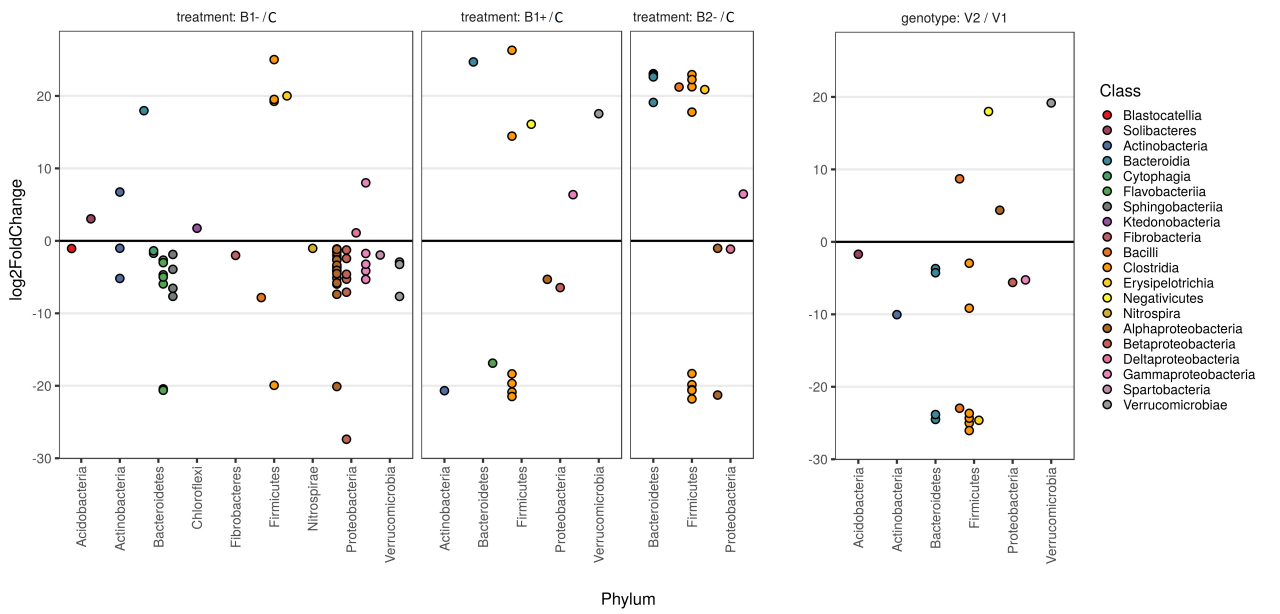

FIGURE 7 | Fold changes of differentially abundant ASVs. The first three panels represent the comparison of a particular treatment with the control, while the panel on the right is a comparison between the two genotypes used (V2 *vs*. V1), as reported at the top of the plots. Each dot represents an amplicon sequence variant (ASV). Fold changes were calculated according to the contrast reported on the top of each panel and transformed into log2. Log2 fold change values are reported in the vertical axis so that positive values represent ASVs that are more abundant in the treatment group and vice versa. Only contrasts with a *p*-value lower than 0.05 and with a |log2-fold-change| higher than 1 are reported in the plot (see **Supplementary Material S8**). The phylum attribution for each ASV is reported on the horizontal axis, whereas colors refer to the Class. Colors are ordered based on the Phylum attribution to help the plot to be understood correctly.

TC, TOC, and C/N, whose values were markedly higher in the biochar-treated samples than in the controls. In particular, the increased C/N ratio in biochar-treated variants is related to higher microbial activity (Wan et al., 2015), and, as was obvious from our results, application of biochar set up the conditions for an ideal microbial diet (C/N ≈ 24:1; USDA, 2011) during

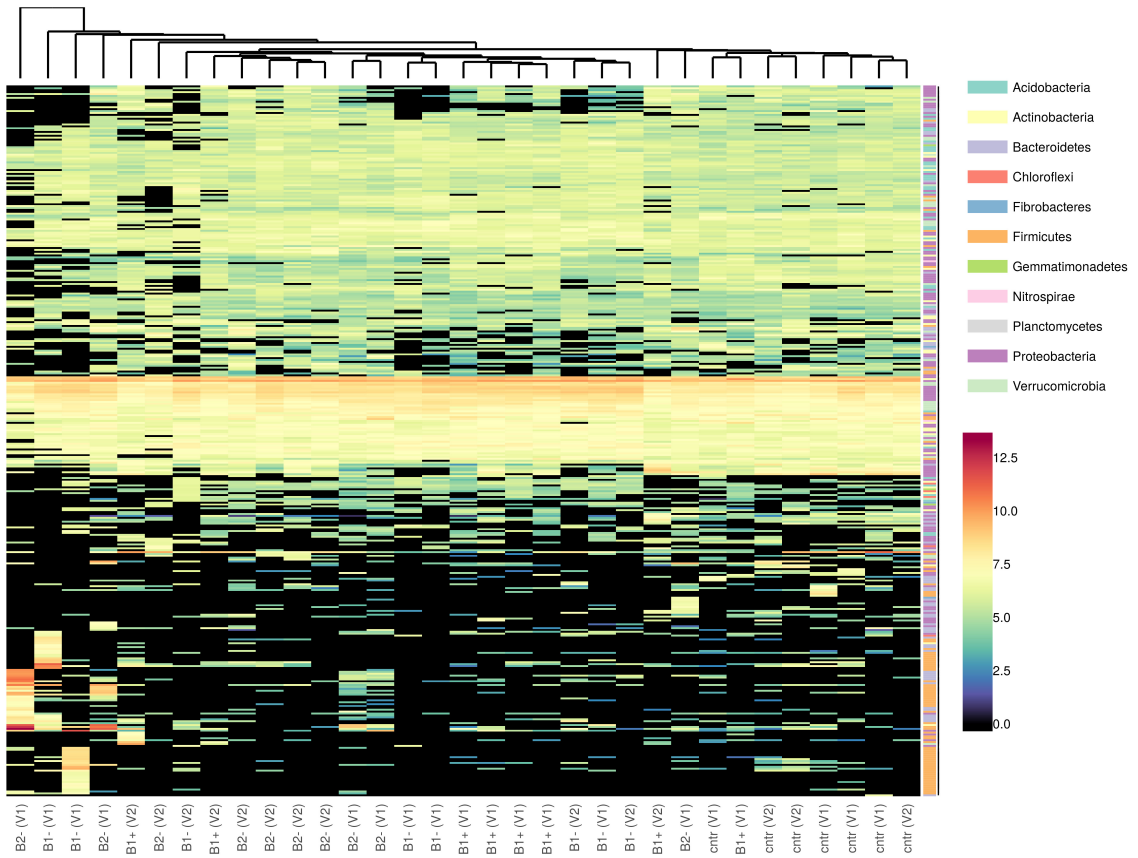

FIGURE 8 | Heatmap of the taxonomic distribution of consistent ASVs. Taxa (the rows on the heatmap) were marked with different colors according to Phylum attributions. Colors on the far left of the plot refer to the Phylum attribution of each ASV. Counts were variance-stabilized and log2-transformed before plotting using DESeq2 normalization.

the experiment, unlike in the control (C/N $\leq$ 8.0; see **Table 1**). On the other hand, we did not expect an increase in pH and CEC with respect to the sample soil in V1C and V2C, which are the control samples made of soil only, at the final time of the experiment (T_f). In fact, we foresaw such an increase exclusively for the samples treated with biochar. The difference in pH and CEC may be due to many factors that alter the soil under greenhouse conditions, including plant growth and local and root microorganisms that developed in the soil pot. We used demi-water for plant irrigation, and here we can speculate that root exudates caused a buffering effect (Trakal et al., 2017). It has been proved that root exudates affect the pH in the rhizosphere: Smiley (1974) found an increase in soil pH in the presence of crops; Romkens et al. (1999) found that the increase in pH was related to the excretion of OH^- by the roots during N and Ca uptake.

Biochar From Wheat Straw Increases EC and Nutrient Availability in Soil and Monovalent Element Ions in Pore Water

In particular, B2 coming from wheat straw feedstock is a biochar with a higher nutrient content with respect to B1 from wood, as shown in **Supplementary Table S1** (e.g., for total content of nitrogen and/or phosphorus). This is also the reason why we applied B2 directly to the soil without a previous "activation" in a nutrient solution (B2− treatment), as was additionally performed with B1 (both B1− and B1+ treatments were assayed). Looking at the total metal contents, and particularly at the bioavailable element contents (**Table 1**), which better represent the nutrient substrates that can directly benefit and sustain plant growth, B2− amendment showed a stronger impact on the pots in both the Duilio and Marco Aurelio varieties, leading to higher levels of available nutrients (mainly very high contents of usable K and Na with respect to all other soil pots). Furthermore, we used by rhizones to analyze the nutrient concentration in the soil solution occupying the interstitial spaces (**Table 2**), and B2− treatment resulted in a substantial increase in the concentration of sodium, potassium, and chloride ions dissolved in water, which explains the more nutrient-rich composition of the wheat straw biochar against the woody one. The biochemical functions of these elements used to be related to their osmotic potentials, controlling membrane permeability and regulating the cell osmotic tone and ionic balance. Surprisingly, there were no significant changes in nitrate (NO_3^-) concentrations among all variants [even between (non)activated biochars, B1+ *vs.* B1−], which could be explained

by individual N uptake into durum wheat through all variants (represented by very high SD).

It is worthy of note that our experiment gives an additional proof of the capability of biochar to decrease Zn availability for the plants (**Table 1**), thus supporting its application for the remediation of soils from zinc and other heavy metal pollutants (Zhang et al., 2013; Puga et al., 2015). The Zn concentration in pore water, nevertheless, does not fit this conclusion. This can probably be explained by significant dissolution of Zn by root exudates and consequent uptake into the biomass through all variants (during the whole period of the experiment). Indeed, zinc is needed by plants in small amounts, and it is crucial to plant development, playing an important role in a wide range of biochemical processes. Here, only a limited amount of the available Zn was then extracted by 0.01 M $CaCl_2$ from the final soils in which that Zn was: (*i*) already consumed by plants, and/or, most probably, (*ii*) Zn ions were most strongly bound to the biochar surface (Kiekens, 1995; Trakal et al., 2017).

Wheat Straw Biochar Enhances Durum Wheat Biomass

As broadly reported in literature, biochar amendment may also play an important role in plant growth, and the resulting effect is often augmentative [Baronti et al. (2010) and Vaccari et al. (2011) specifically for durum wheat; Solaiman et al. (2010) and Meng et al. (2019) for bread wheat; Kammann et al. (2015) for quinoa; and several others], but it may also be diminutive [as for example in Aguilar-Chávez et al. (2012) for bread wheat and Kammann et al. (2015) for quinoa] or even lead to no significant variation [as in Tammeorg et al. (2014) and Kelly et al. (2015) for bread wheat; and others].

In particular, in our experiment, biochar from wheat straw in its non-activated status (B2−) was related to a significant increase in plant fresh and dry weights, in both tested cultivars, with the only exception being Duilio root DW, which stayed almost constant among all treatments. This exception is not so unique, and indeed it has also been reported that aboveground productivity is one of the positive significant effects of biochar, while belowground productivity remains unaffected (Biederman and Harpole, 2013). To date, the effects of biochar application on root traits are still controversial, and results are highly variable (Xiang et al., 2017).

As reported in the results, B2− treatment markedly impacted soil nutrient status, and the major increase in soil potassium content was significant. Since potassium represents an element of huge importance to ensure healthy and well-sustained plant growth and participates in several metabolic pathways (Prajapati and Modi, 2012), one could hypothesize that the higher plant growth in the presence of wheat straw biochar was also attained thanks to the potassium increase directly determined by the biochar.

Long-Term Effects of Biochar on Plant Growth Need to Be Investigated

It is worthy of note that biochar from wood chips (B1) had no relevant effects on plant biomass (neither above- or belowground), independently of the way the biochar was supplied, i.e., pure, untreated, and coming directly from fresh production (B1−) or previously activated in a nutrient-rich solution (B1+). Concerning B1−, under greenhouse conditions and in the frame of the 6-week duration of our experiment, which may be considered a short time, one could expect that all of the biochar active sites, initially free at T_0, would have immediately bound to several nutrients; moreover, the use of a soil with a low SOM could even have led to plant starvation. In contrast, B1+ could be somewhat compared to co-composted biochar, and one could hypothesize this to determine a stronger effect on plant growth. In fact, it has been ascertained that co-composting improves the plant growth-promoting effects of biochar (Kammann et al., 2015). In our settings, we did not achieve the expected results, and a significant positive effect from either the B1− or B1+ treatments was lacking. In any case, the current experiment draws attention to the response of the durum wheat plant to biochar amendment during its first stages of development and growth. Thus, we designed pot experiments in a greenhouse under controlled conditions because this is easier to perform in order to infer preliminary results and avoids the complications that may arise due to the overlap of several environmental effects as happens in the field. It is possible that, in the field and with a longer experimental duration, with the aim of measuring the effects of durum wheat yield not only in terms of shoot and root biomass but particularly in terms of grain yield, the plants would have shown different behavior because of other factors not considered here.

Biochar From Straw-Based Feedstock Is More Suitable Then Woody Biochar for Improving Crop Yield

The significant effect of B2 on plant growth and the lack of effect of B1 is in perfect accordance with the results of the comparative study of the properties of biochar from wood material and crop residues performed by Wang et al. (2013), who showed that, despite high variability, biochars from crop straw may be more effective and desirable for improving soil fertility. In crop-residue-based biochars, including wheat straw-based biochar, they found a higher ash%, CEC, total contents of N, P, Ca, and Mg, pH, and wt% of C, Na, and K than in wood-based biochars. Many of these properties are comparable with the data reported in **Supplementary Table S1**. Moreover, they found that the BET surface area of straw-based biochars with a 700°C pyrolysis temperature, which is the same temperature used for the production of the two biochars analyzed in our experiment, may be wider than for other biochars (Wang et al., 2013). In this context, the scanning electron microscopy visualization of the biochar samples used (**Figure 2**) let us infer that the structure of B2, including its porous arrangement, distribution, and size, creates a larger surface area that improves the connections between plant and soil, allowing the plants to enhance their growth, at least in terms of fresh dry weight (with the only exception being Duilio tBGDW; **Figure 3**) but also in terms of average PH (**Figure 4**).

Durum Wheat Growth Response to Biochar Treatment Is Genotype-Dependent

In regard to a genotype dependence of plant response to the biochar treatments, there is proof that, for each treatment, both genotypes exhibited a general trend of response with some cultivar-specific exceptions. It is relevant that Marco Aurelio is more positively responsive to B2−. In fact, Marco Aurelio increases the magnitude of all measured traits (tAGFW, tAGDW, tBGFW, tBGDW, PH, FLL, and mFLW), while Duilio shows a significant increase due to B2− in most of these traits but not in all (tBGDW, FLL, and mFLW are not significantly influenced). As has emerged from other studies [Chen et al. (2016) and French and Iyer-Pascuzzi (2018) as examples], this result confirms that, where the aim is simultaneously improving soil fertility and increasing crop yield, for every target crop, the choice of the best cultivar genotype that better responds and adapts to a particular biochar is critical.

Biochar Treatment but Not Durum Wheat Genotype Has a Significant Influence on Rhizosphere α-Diversity

To assess the possible changes caused by biochar incorporation and/or the durum genotype to the soil microbiome, we specifically focused on the rhizosphere, which is the interface between plant roots and soil, since the microorganisms colonizing the rhizosphere may contribute to plant growth and health (Richter-Heitmann et al., 2016); moreover, different studies have already established that the rhizosphere corresponds to the plant-soil compartment harboring a higher richness (Qian et al., 2019).

Rhizosphere soil samples, like the soils, are very complex matrixes, and high-throughput 16S rRNA amplicon sequencing produced data that was difficult to analyze statistically, due in particular to the "background noise," which makes it hard to clearly distinguish what is really influenced by the treatment and by the genotype. Notwithstanding, bacterial species richness and their abundance levels, as may be inferred by the alpha diversity, showed influences due to the biochar treatment, while no significant change was encountered when assessing the effect due to the durum wheat variety (in contrast with our assessed genotype effects on plant growth). In the literature for bread wheat, it is reported that host genotype played a minor but significant role in the bacterial diversification of the rhizosphere (Mahoney et al., 2017); and, indeed, genotype is generally thought to have a minor role in shaping microbiota composition (Bulgarelli et al., 2012; Kwak et al., 2018). The bacterial phyla encountered in the rhizosphere samples analyzed and their abundances are consistent with those most commonly present in similar samples, as reported in different published research articles (Mahoney et al., 2017; Wang et al., 2019) and include Proteobacteria, Verrucomicrobia, Acidobacteria, Firmicutes, Bacterioidetes, and Actinobacteria. In agreement with Mahoney et al. (2017) and other previous studies on the wheat rhizosphere, we also found the Sphingobacteriia class as a dominant taxon.

Low-Nutrient Biochar Negatively Impacts Rhizosphere Microbiota Species Richness

In the rhizosphere of the untreated woody biochar (B1−) samples, a lower inverse Simpson index indicated a lower species richness and evenness, while in the other treatments (B1+ and B2−), the value of this index did not vary significantly (**Figure 6**). This outcome is worthy of note because it means that a nutrient rich biochar, such as B1+ and B2−, under the experimental conditions set up, does not negatively impact the rhizosphere bacterial species richness and keeps it stable. This result highlights the key role played by a biochar and a soil in shaping the microbiota, altering the number of species present and the relative abundance of each species, or keeping them stable and balanced. The outcome that a nutrient-rich source may favor the maintenance of a balanced bacterial microbiota status has also been shown in other studies; for example, Qiao et al. (2017) found, in cotton, that bacterial α-diversity in the rhizosphere of nutrient-rich soil was lower than in a soil from a continuous cropping field, while β-diversity was greater. In a different way, for bread wheat it has just been reported that wheat straw biochar increases the biodiversity of the soil microbiome and also the mycobiome of the seedlings' rhizosphere under herbicide stress, with the percentage of biochar application to the soil influencing the soil microbial community structure (Meng et al., 2019).

Both Biochar Treatment and Durum Wheat Genotype Influence the Overall Bacterial Composition of the Rhizosphere

In another way, our study highlighted a compositional difference of the bacterial microbiota expressed in terms of ASVs, as may be presumed by the beta-diversity, not only among the treatments but also between the two genotypes analyzed. The comparison among treatments and genotypes highlighted interesting variations related to the abundances of the different ASVs. In our experiment, we could not find any significant change attributable to a specific taxon (at least at the levels from Phylum to Genus), and the observed variation was due to several sequence variants that may represent single nucleotide variations, i.e., a particular strain of a species (**Figure 8** and **Supplementary Material S10**). This is also what we expected based on the fact that our pot samples were very similar with each other (same soil, same plant species, same irrigation level, same greenhouse conditions, etc.), with the only exception being the applied biochar, when comparing with the control to detect the effect of the treatment, or of the plant genotype, when comparing the two durum wheat varieties with each other. Moreover, concerning the different biochar applied, the bacterial input coming from both B1 and B2, both dried, was assumed to be very limited. In this case, one does not expect a big variation at the level of Phyla or

Class but may hypothesize that there will be much variation in species and/or within species.

From the higher C/N ratio detected in the bulk soil of the treated samples at the end of the experiment, we could expect an increased microbial activity. Our analysis of the rhizosphere does not allow us to confirm this occurrence, not only because we analyzed the rhizosphere compartment only but also because the degree of diversity could not necessarily be linked to the level of microbial activity, which should be measured spectrophotometrically through enzymatic activity or through soil respiration.

Influence of Soil Chemical Properties on the Diversity of Rhizosphere Bacterial Communities

In our study, Pearson's correlation analysis was adopted to estimate the associations between soil chemical characteristics and rhizosphere bacterial diversity indexes, revealing a strong negative correlation of microbiological indexes with soil TC and TN. Soil microorganisms, especially bacteria, which represent the most abundant group, play central roles in ecosystems. Even though several studies report that soil pH, TC, TOC, and TN are among the main abiotic factors structuring bacterial communities, they are not necessarily associated with the soil microbiota (Deng et al., 2018), particularly in rhizospheric soil; moreover, it is also well known that this relationship is very complex and should not be generalized (Celestina et al., 2019). The adding of "fresh biochar" to soil has been shown to induce short-term disturbance to the moisture equilibrium in soils due to the effect of capillary action, drawing moisture from soil pore spaces. In turn, this can cause negative effects on soil microbial communities and abundance through instantaneous desiccation (Dempster et al., 2012; Ameloot et al., 2013; Rex et al., 2015). However, soil pH and the other targeted traits were not significantly correlated with any bacterial diversity index.

CONCLUSION

Wheat straw biochar better adapted the soil for durum wheat plant growth than woody biochar, strongly increasing soil EC and the concentrations of important ions (Na^+, K^+, and Cl^-) available to plants. Biochar also enhanced plant growth, and the higher measured values of fresh and dry-weights, at both the above- and belowground levels, were for the samples treated with wheat straw biochar. From the rhizosphere microbiome analysis, it was evinced that untreated woody biochar led to a loss of bacterial strain richness, probably because of its nutrient deficiency, while more nutrient-rich biochars, such as wheat straw biochar and previously activated woody biochar, kept the bacterial alpha-diversity almost constant and stable. In addition, biochar showed a positive effect on the soil used, which was affected by light zinc and lead pollution, bringing a favorable decrease in the Zn available to plant, thus supporting its application in the remediation of soil with light contamination by heavy metals.

It is clear that, to attain the best advantages from the use of biochar, it is necessary to expend major efforts in the selection of the type of biochar used, with particular reference to the feedstock vegetal biomass and pyrolysis temperature, and the cultivar of the target crop to be cultivated in a specific agricultural soil. For durum wheat, in a low-organic matter soil, even with light heavy metal contamination, we suggest the combination of a straw-based-biochar with the Marco Aurelio variety. Of course, further comparative studies and, in particular, field trials have to be performed, aiming at choosing several pairs of biochar-cultivars that adapt and perform better in the various different wheat plantation regions.

DATA AVAILABILITY STATEMENT

The sequences have been submitted to the Sequence Read Archive (SRA) of the National Center for Biotechnology Information (NCBI) under the accession number PRJNA548437, referring to the BioProject entitled "Rhizospheric bacterial microbiota in durum wheat under biochar treatment."

AUTHOR CONTRIBUTIONS

AL conceived the study and planned the experimental greenhouse setup, performed the experiments, wrote the manuscript original draft, reviewed, and edited the final version. GB performed the bioinformatic analysis of the bacterial rhizosphere microbiota, wrote the manuscript, and prepared the figures and tables related to the microbiome section. MT provided substantial help in the pot experiment, collaborated in the plant data collection, performed all experimental analyses related to soil and pore water chemical composition, and provided the tables containing all soil data. DM was responsible for the scanning electron microscopy analysis of the biochar samples and provided critical comments on the study. AB conceived and designed the experiments, supervised the analyses, interpreted the data, made a fundamental contribution to funding acquisition, drafted the manuscript, reviewed, and edited the final version. LT allowed the greenhouse experiment to be performed and provided important advice, particularly on the biochars and the low contaminated soil used in this work, obtained the funding for soil analysis, and made a fundamental contribution to the manuscript writing and to the whole revision. All authors read and approved the final manuscript.

FUNDING

This work was possible thanks to COST Action FP1305 "Linking belowground biodiversity and ecosystem function in European forests (Biolink)," which granted an STSM to AL for carrying out the greenhouse experiment at the Czech University of Life Sciences Prague. This work was funded by the Ministry of Agriculture of the Czech Republic Project No. QK1910056, Ministry of Education, Youth and Sports of the Czech Republic Project No. CZ.02.1.01/0.0/0.0/16_026/0008403, and SIMBA (Sustainable Innovation of Microbiome Applications in Food System) project from the European Union H2020 Research and Innovation Programme under Grant Agreement No. 818431.

ACKNOWLEDGMENTS

The authors wish to thank Prof. M. Lukac (University of Reading, United Kingdom), coordinator of the above-mentioned COST Action, for his support and valuable suggestions on the experiment set up; M. Gamboni (Italian National Research Council, IT), leader of the WP3 Biolink Project (Belowground biodiversity in plantations and tree crops), for his valuable efforts; A. Mengoni (University of Florence, IT) for his criticisms, particularly in relation to the metagenomics analysis; S. Ravaglia (Società Italiana Sementi, S.I.S.) for providing seeds of the Duilio and Marco Aurelio durum wheat varieties; M. D'Erasmo and P. Venanzi (D.B.A. Italia S.r.l.) for allowing the use of the FastPrep-24^{TM} 5G instrument (MP Biomedicals) for DNA extraction from the rhizosphere samples.

SUPPLEMENTARY MATERIAL

The Supplementary Material for this article can be found online at: https://www.frontiersin.org/articles/10.3389/fmicb.2019.02694/full#supplementary-material

REFERENCES

Agegnehu, G., Bass, A. M., Nelson, P. N., and Bird, M. I. (2016). Benefits of biochar, compost and biochar-compost for soil quality, maize yield and greenhouse gas emissions in a tropical agricultural soil. *Sci. Total. Environ.* 543, 295–306. doi: 10.1016/j.scitotenv.2015.11.054

Aguilar-Chávez, Á, Díaz-Rojas, M., Cárdenas-Aquino, M. D., Dendooven, L., and Luna-Guido, M. (2012). Greenhouse gas emissions from a wastewater sludge-amended soil cultivated with wheat (*Triticum* spp. L.) as affected by different application rates of charcoal. *Soil Biol. Biochem.* 52, 90–94. doi: 10.1016/j.soilbio.2012.04.022

Albuquerque, J. A., Salazar, P., Barròn, V., Torrent, J., del Campillo, M. C., Gallardo, A., et al. (2013). Enhanced wheat yield by biochar addition under different mineralization levels. *Agron. Sustain. Dev.* 33, 475–484. doi: 10.1007/s13593-012-0128-3

Ameloot, N., De Neve, S., Jegajeevagan, K., Yildiz, G., Buchan, D., Funkuin, Y. N., et al. (2013). Short-term CO2 and N2O emissions and microbial properties of biochar amended sandy loam soils. *Soil Biol. Biochem.* 57, 401–410. doi: 10.1016/j.soilbio.2012.10.025

Atkinson, C. J., Fitzgerald, J. D., and Hipps, N. A. (2010). Potential mechanisms for achieving agricultural benefits from biochar application to temperate soil: a review. *Plant Soil* 337, 1–18. doi: 10.1007/s11104-010-0464-5

Bacci, G., Ceccherini, M. T., Bani, A., Bazzicalupo, M., Castaldini, M., Galardini, M., et al. (2015). Exploring the dynamics of bacterial community composition in soil: the pan-bacteriome approach. *Antonie Van Leeuwenhoek* 107, 785–797. doi: 10.1007/s10482-014-0372-4

Bacci, G., Cerri, M., Lastrucci, L., Ferranti, F., Ferri, V., Foggi, B., et al. (2018). Applying predictive models to decipher rhizobacterial modifications in common reed die-back affected populations. *Sci. Total. Environ.* 642, 708–722. doi: 10.1016/j.scitotenv.2018.06.066

Baronti, S., Alberti, G., Delle Vedove, G., Di Gennaro, F., Fellet, G., Genesio, L., et al. (2010). The biochar option to improve plant yields: first results from some field and pot experiments in Italy. *Ital. J. Agron.* 5, 3–11. doi: 10.4081/ija.2010.3

Biederman, L. A., and Harpole, W. S. (2013). Biochar and its effects on plant productivity and nutrient cycling: a meta-analysis. *GCB Bioener.* 5, 202–214. doi: 10.1111/gcbb.12037

Brennan, A., Jiménez, E. M., Puschenreiter, M., Albuquerque, J. A., and Switzer, C. (2014). Effects of biochar amendment on root traits and contaminant availability of maize plants in a copper and arsenic impacted soil. *Plant Soil* 379, 351–360. doi: 10.1007/s11104-014-2074-0

Bulgarelli, D., Rott, M., Schlaeppi, K., Ver Loren van Themaat, E., Ahmadinejad, N., Assenza, F., et al. (2012). Revealing structure and assembly cues for *Arabidopsis* root-inhabiting bacterial microbiota. *Nature* 488, 91–95. doi: 10.1038/nature11336

Callahan, B. J., McMurdie, P. J., Rosen, M. J., Han, A. W., Johnson, A. J. A., and Holmes, S. P. (2016). DADA2: high-resolution sample inference from Illumina amplicon data. *Nat. Methods* 13:581. doi: 10.1038/nmeth.3869

Carter, M. R., and Gregorich, E. G. (2008). *Soil Sampling and Methods of Analysis. 2nd Edition. Canadian Society of Soil Science*. Boca Raton: CRC Press, doi: 10.1201/9781420005271

Castaldi, S., Riondino, M., Baronti, S., Esposito, F. R., Marzaioli, R., Rutigliano, F. A., et al. (2011). Impact of biochar application to a Mediterranean wheat crop on soil microbial activity and green house gas fluxes. *Chemosphere* 85, 1464–1471. doi: 10.1016/j.chemosphere.2011.08.031

Celestina, C., Wood, J. L., Manson, J. B., Wang, X., Sale, P. W. G., Tang, C., et al. (2019). Microbial communities in top- and subsoil of repacked soil columns respond differently to amendments but their diversity is negatively correlated with plant productivity. *Sci. Rep.* 9:8890. doi: 10.1038/s41598-019-45368-9

Chen, D., Guo, H., Li, R., Li, L., Pan, G., Chang, A., et al. (2016). Low uptake affinity cultivars with biochar to tackle Cd-tainted rice – A field study over four rice seasons in Hunan. *China Sci. Total Environ.* 541, 1489–1498. doi: 10.1016/j.scitotenv.2015.10.052

De Tender, C., Haegeman, A., Vandecasteele, B., Clement, L., Cremelie, P., Dawyndt, P., et al. (2016). Dynamics in the strawberry rhizosphere microbiome in response to biochar and *Botrytis cinerea* leaf infection. *Front. Microbiol.* 7:2062. doi: 10.3389/fmicb.2016.02062

Dempster, D. N., Gleeson, D., Solaiman, Z., Jones, D. L., and Murphy, D. (2012). Decreased soil microbial biomass and nitrogen mineralisation with Eucalyptus biochar addition to a coarse textured soil. *Plant Soil* 354, 311–324. doi: 10.1007/s11104-011-1067-5

Deng, J., Yin, Y., Zhu, W., and Zhou, Y. (2018). Variations in soil bacterial community diversity and structures among different revegetation types in the Baishilazi Nature Reserve. *Front. Microbiol.* 9:2874. doi: 10.3389/fmicb.2018.02874

Di Cello, F., Bevivino, A., Chiarini, L., Fani, R., Paffetti, D., Tabacchioni, S., et al. (1997). Biodiversity of a *Burkholderia cepacia* population isolated from the maize rhizosphere at different plant growth stages. *Appl. Environ. Microbiol.* 63, 4485–4493.

Elad, Y., Cytryn, E., Meller Harel, Y., Lew, B., and Graber, E. R. (2011). The biochar effect: plant resistance to biotic stresses. *Phytopathol. Mediterr.* 50, 335–349. doi: 10.14601/Phytopathol_Mediterr-9807

French, E., and Iyer-Pascuzzi, A. S. (2018). A role for the gibberellins pathway in biochar-mediated growth promotion. *Sci. Rep.* 8:5389. doi: 10.1038/s41598-018-23677-9

Frenkel, O., Jaiswal, A. K., Elad, Y., Lew, B., Kammann, C., and Graber, E. R. (2017). The effect of biochar on plant diseases: what should we learn while designing biochar substrates? *J. Environ. Eng. Landsc. Manag.* 25, 105–113. doi: 10.3846/16486897.2017.1307202

Han, G., Lan, J., Chen, Q., Yu, C., and Bie, S. (2017). Response of soil microbial community to application of biochar in cotton soils with different continuous cropping years. *Sci. Rep.* 7:101184. doi: 10.1038/s41598-017-10427-6

Hoagland, D. R., and Arnon, D. I., eds. (1950). "The water-culture method for growing plants without soil," in *Circular and California Agricultural Experiment Station* (Berkeley, CA: College of Agriculture, University of California), 32.

Jačka, L., Trakal, L., Ouředníček, P., Pohořelý, M., and Šìpek, V. (2018). Biochar presence in soil significantly decreased saturated hydraulic conductivity due to swelling. *Soil Till. Res.* 184, 181–185. doi: 10.1016/j.still.2018.07.018

Jefferey, S., Abalos, D., Spokas, K., and Verheijen, F. G. A. (2015). "Biochar effects on crop yield," in *Biochar for environmental Management. Science, Technology and Implementation Chapter 12*, 2nd Edn, eds J. Lehmann, and S. Joseph, (London: Routledge).

Jenkins, J. R., Viger, M., Arnold, E. C., Harris, Z. M., Ventura, M., Miglietta, F., et al. (2017). Biochar alters the soil microbiome and soil function: results of next-generation amplicon sequencing across Europe. *GCB Bioenergy* 9, 591–612. doi: 10.1111/gcbb.12371

Kaetzl, K., Lübken, M., Gehring, T., and Wichern, M. (2018). Efficient low-cost anaerobic treatment of wastewater using biochar and woodchip filters. *Water* 10:818. doi: 10.3390/w10070818

Kammann, C. I., Schmidt, H.-P., Messerchmidt, N., Linsel, S., Steffens, D., Müller, C., et al. (2015). Plant growth improvement mediated by nitrate capture in co-composted biochar. *Sci. Rep.* 5:11080. doi: 10.1038/srep11080

Keiluweit, M., Nico, P. S., Johnson, M. G., and Kleber, M. (2010). Dynamic molecular structure of plant biomass derived black carbon (biochar). *Environ. Sci. Technol.* 44, 1247–1253. doi: 10.1021/es9031419

Kelly, C. N., Calderón, F. C., Acosta-Martínez, V., Mikha, M. M., Benjamin, J., Rutherford, D. W., et al. (2015). Switchgrass biochar effects on plant biomass and microbial dynamics in two soils from different regions. *Pedosphere* 25, 329–342. doi: 10.1016/S1002-0160(15)30001-1

Kiekens, L. (1995). "Zinc," in *Heavy Metals in Soils*, ed. B. J. Alloway, (New York, NY: Springer US), 284–305.

Kim, B.-R., Shin, J., Guevarra, R. B., Lee, J. H., Kim, D. W., Seol, K.-H., et al. (2017). Deciphering diversity indeces for a better understanding of microbial communities. *J. Microbiol. Biotechnol.* 27, 2089–2093. doi: 10.4014/jmb.1709.09027

Kolton, M., Graber, E. R., Tsehansky, L., Elad, Y., and Cytryn, E. (2017). Biochar-stimulated plant performance is strongly linked to microbial diversity and metabolic potential in the rhizosphere. *New Phytol.* 213, 1393–1404. doi: 10.1111/nph.14253

Kwak, M.-J., Kong, H. G., Choi, K., Kwon, S.-K., Song, J. Y., Lee, J., et al. (2018). Rhizosphere microbiome structure alters to enable wilt resistance in tomato. *Nat. Biotechnol.* 36, 1100–1109. doi: 10.1038/nbt.4232

Lehmann, J. (2007). Bio-energy in the black. *Front. Ecol. Environ.* 5:381–387. doi: 10.1890/1540-9295(2007)5[381:BITB]2.0.CO;2

Lehmann, J., Rillig, M. C., Thies, J., Masiello, C. A., Hockaday, W. C., and Crowley, D. (2011). Biochar effects on soil biota – a review. *Soil Biol. Biochem.* 43, 1812–1836. doi: 10.1016/j.soilbio.2011.04.022

Lei, O., and Zhang, R. (2013). Effects of biochar derived from different feedstock and pyrolysis temperatures on soil, physical and hydraulic properties. *J Soils Sediments* 13, 1561–1572. doi: 10.1007/s11368-013-0738-7

Li, Q., Lei, Z., Song, X., Zhang, Z., Ying, Y., and Peng, C. (2018). Biochar amendment decreases soil microbial biomass and increases bacterial diversity in Moso bamboo (*Phyllostachys edulis*) plantations under simulated nitrogen deposition. *Environ. Res. Lett.* 13:044029. doi: 10.1088/1748-9326/aab53a

Love, M. I., Huber, W., and Anders, S. (2014). Moderated estimation of fold change and dispersion for RNA-seq data with DESeq2. *Genom Biol.* 15:550. doi: 10.1186/s13059-014-0550-8

Mahoney, A. K., Yin, C., and Hulbert, S. H. (2017). Community structure, species variation, and potential functions of rhizosphere-associated bacteria of different winter wheat (*Triticum aestivum*) cultivars. *Front. Plant Sci.* 8:132. doi: 10.3389/fpls.2017.00132

Martin, M. (2011). Cutadapt removes adapter sequences from high-throughput sequencing reads. *EMBnet J.* 17, 10–12. doi: 10.14806/ej.17.1.200

Mašek, O., Buss, W., Roy-Poirier, A., Lowe, W., Peters, C., Brownsort, P., et al. (2018). Consistency of biochar properties over time and production scales: a characterisation of standard materials. *J. Anal. Appl. Pyrol.* 132, 200–210. doi: 10.1016/j.jaap.2018.02.020

Meng, L., Sun, T., Li, M., Saleem, M., Zhang, Q., and Wang, C. (2019). Soil-applied biochar increases microbial diversity and wheat plant performance under herbicide fomesafen stress. *Ecotox Environ. Safe* 171, 75–83. doi: 10.1016/j.ecoenv.2018.12.065

Mollinedo, J., Schumacher, T. E., and Chintala, R. (2016). Biochar effects on phenotypic characteristics of "*wild*" and "*sickle*". *Medicago truncatula* genotypes. *Plant Soil* 400, 1–4. doi: 10.1007/s11104-015-2708-x

Olmo, M. K., Albuquerque, J. A., Barròn, V., del Campillo, M. C., Gallardo, A., Fuentes, M., et al. (2014). Wheat growth and yield responses to biochar addition under Mediterranean climate conditions. *Biol. Fertil. Soils* 50, 1177–1187. doi: 10.1007/s00374-014-0959-y

Palansooriya, K. N., Wong, J. T. F., Hashimoto, Y., Huang, L., Rinklebe, J., Chang, S. C., et al. (2019). Response of microbial communities to biochar-amended soils: a critical review. *Biochar* 1, 3–22. doi: 10.1007/s42773-019-00009-2

Pandit, N. R., Mulder, J., Hale, S. E., Martinsen, V., Schmidt, H. P., and Cornelissen, G. (2018). Biochar improves maize growth by alleviation of nutrient stress in a moderately acidic low-input Nepalese soil. *Sci. Total Environ.* 625, 1380–1389. doi: 10.1016/j.scitotenv.2018.01.022

Prajapati, K., and Modi, H. A. (2012). The importance of potassium in plant growth – A review. *Indian J. Plant Sci.* 1, 177–186.

Prendergast-Miller, M. T., Duvall, M., and Sohi, S. P. (2014). Biochar-root interactions are mediated by biochar nutrient content and impacts on soil nutrient availability. *Eur. J. Soil Sci.* 65, 173–185. doi: 10.1111/ejss.12079

Puga, A. P., Abreu, C. A., Melo, L. C. A., and Beesley, L. (2015). Biochar application to a contaminated soil reduces the availability and plant uptake of zinc, lead and cadmium. *J. Environ. Manag.* 159, 86–93. doi: 10.1016/j.jenvman.2015.05.036

Qian, X., Li, H., Wang, Y., Wu, B., Wu, M., Chen, L., et al. (2019). Leaf and root endosphere harbor lower fungal diversity and less complex fungal co-occurrence patterns than rhizosphere. *Front. Microbiol.* 10:1015. doi: 10.3389/fmicb.2019.01015

Qiao, Q., Wang, F., Zhang, J., Chen, Y., Zhang, C., Liu, G., et al. (2017). Microbiome of cotton with soil type, genotype and developmental stage. *Sci. Rep.* 7:3940. doi: 10.1038/s41598-017-04213-7

Quast, C., Pruesse, E., Yilmaz, P., Gerken, J., Schweer, T., Yarza, P., et al. (2012). The SILVA ribosomal RNA gene database project: improved data processing and web-based tools. *Nucleic Acids Res.* 41, D590–D596. doi: 10.1093/nar/gks1219

Quevauviller, P. (1998). Operationally defined extraction procedures for soil and sediment analysis I. Standardization. *Trends Analyt. Chem.* 17, 289–298. doi: 10.1016/S0165-9936(97)00119-2

R Core Team (2018). *R: A Language and Environment for Statistical Computing*. Vienna: R Foundation for Statistical Computing.

Rex, D., Schimmelpfenning, S., Jansen-Willems, A., Moser, G., Kammann, C., and Müller, C. (2015). Microbial community shifts 2.6 years after top dressing of Miscanthus biochar, hydrochar and feedstock on a temperate grassland site. *Plant Soil* 397, 261–271. doi: 10.1007/s11104-015-2618-y

Richter-Heitmann, T., Eickhorst, T., Knauth, S., Friedrich, M. W., and Schmidt, H. (2016). Evaluation of strategies to separate root-associated microbial communities: a crucial choice in rhizobiome research. *Front. Microbiol.* 7:773. doi: 10.3389/fmicb.2016.00773

Romkens, P. F. A. M., Bouwman, L. A., and Boon, G. T. (1999). Effect of plant growth on copper solubility and speciation in soil solution samples. *Environ. Pollut.* 106, 315–321. doi: 10.1016/S0269-7491(99)00106-2

Rutigliano, F. A., Romano, M., Marzaioli, R., Baglivo, I., Baronti, S., and Miglietta, F. (2014). Effect of biochar addition on soil microbial community in a wheat crop. *Eur. J. Soil Biol.* 60, 9–15. doi: 10.1016/j.ejsobi.2013.10.007

Shade, A., and Handelsman, J. (2012). Beyond the Venn diagram: the hunt for a core microbiome. *Environ. Microbiol.* 14, 4–12. doi: 10.1111/j.1462-2920.2011.02585.x

Shen, Z., Zhang, Y., Jin, F., McMillan, O., and Al-Tabbaa, A. (2017a). Qualitative and quantitative characterisation of adsorption mechanisms of lead on four biochars. *Sci. Total Environ.* 609, 1401–1410. doi: 10.1016/j.scitotenv.2017.08.008

Shen, Z., Zhang, Y., McMillan, O., Jin, F., and Al-Tabbaa, A. (2017b). Characteristics and mechanisms of nickel adsorption on biochars produced from wheat straw pellets and rice husk. *Environ. Sci. Pollut. Res.* 24, 12809–12819. doi: 10.1007/s11356-017-8847-2

Smiley, R. W. (1974). Rhizosphere pH as influenced by plants, soils and nitrogen fertilizers". *Soil Sci. Soc. Am. J. Abstr.* 38, 795–799. doi: 10.2136/sssaj1974.03615995003800050030x

Solaiman, Z. M., Blackwell, P., Abbott, L. K., and Storer, P. (2010). Direct and residual effect of biochar application on mycorrhizal root colonisation, growth and nutrition of wheat. *Aust. J. Soil Res.* 48, 546–554. doi: 10.1071/SR10002

Stephens, M. (2016). False discovery rates: a new deal. *Biostatistics* 18:2. doi: 10.1093/biostatistics/kxw041

Sun, H., Shi, W., Zhou, M., Ma, X., and Zhang, H. (2019). Effect of biochar on nitrogen use efficiency, grain yield and amino acid content of wheat cultivated on saline soil. *Plant Soil Environ.* 65, 83–89. doi10.17221/525/2018-PSE

Takahashi, S., Tomita, J., Nishioka, K., Hisada, T., and Nishijima, M. (2014). Development of a prokaryotic universal primer for simultaneous analysis of

Bacteria and Archea using next-generation sequencing. *PLoS One* 9:e105592. doi: 10.1371/journal.pone.0105592

Tammeorg, P., Simojoki, A., Mäkelä, P., Stoddard, F. L., Alakukku, L., and Helenius, J. (2014). Biochar application to a fertile sandy clay loam in boreal conditions: effects on soil properties and yield formation of wheat, turnip rape and faba bean. *Plant Soil* 374, 89–107. doi: 10.1007/s11104-013-1851-5

Trakal, L., Raya-Moreno, I., Mitchell, K., and Beesley, L. (2017). Stabilization of metal(loid)s in two contaminated agricultural soils: comparing biochar to its non-pyrolysed source material. *Chemosphere* 181, 150–159. doi: 10.1016/j.chemosphere.2017.04.064

UK Biochar Research Center (2014). *WSP700 Standard Biochar Specification Sheet. (–)Version 1.0*.

USDA (2011). *Carbon to Nitrogen Rations in Cropping Systems*. Greensboro, NC: NRCS East National Technology Support Center.

USDA Soil Survey Staff (2014). "Soil survey field and laboratory methods manual," in *Soil Survey Investigations Report No. 51, Version 2.0*, eds R. Burt, and Soil Survey Staff, (Washington, DC: U.S. Department of Agriculture).

Vaccari, F. P., Baronti, S., Lugato, E., Genesio, L., Castaldi, S., Fornasier, F., et al. (2011). Biochar as a strategy to sequester carbon and increase yield in durum wheat. *Eur. J. Agron.* 34, 231–238. doi: 10.1016/j.eja.2011.01.006

Wan, X. H., Huang, Z. Q., He, Z. M., Yu, Z. P., Wang, M. H., Davis, M. R., et al. (2015). Soil C:N ratio is the major determinant of soil microbial community structure in subtropical coniferous and broadleaf forest plantations. *Plant Soil* 387, 103–116. doi: 10.1007/s11104-014-2277-4

Wang, R., Wei, S., Jia, P., Liu, T., Hou, D., Xie, R., et al. (2019). Biochar significantly alters rhizobacterial communities and reduces Cd concentration in rice grains grown on Cd-contaminated soils. *Sci. Total Environ.* 676, 627–638. doi: 10.1016/j.scitotenv.2019.04.133

Wang, Y., Hu, Y., Zhao, X., Wang, S., and Xing, G. (2013). Comparisons of biochar properties from wood material and crop residues at different temperatures and residence times. *Energy Fuels* 27, 5890–5899. doi: 10.1021/ef400972z

Wiedner, K., Rumpel, C., Steiner, C., Pozzi, A., Maas, R., and Glaser, B. (2013). Chemical evaluation of chars produced by thermochemical conversion (gasification, pyrolysis and hydrothermal carbonization) of agro-industrial biomass on a commercial scale. *Biomass Bioenergy* 59, 264–278. doi: 10.1016/j.biombioe.2013.08.026

Xiang, Y., Deng, Q., Duan, H., and Guo, Y. (2017). Effects of biochar application on root traits: a meta-analysis. *GCB Bioenergy* 9, 1563–1572. doi: 10.1111/gcbb.12449

Zama, E. F., Reid, B. J., Arp, H. P. H., Sun, G. X., Yuan, H. Y., and Zhu, Y. G. (2018). Advances in research on the use of biochar in soil for remediation: a review. *J. Soils Sediments* 18:2433. doi: 10.1007/s11368-018-2000-9

Zemanová, V., Trakal, L., Ochecová, P., Szaková, J., and Pavliková, D. (2014). A model experiment: competitive sorption of Cd, Cu, Pb and Zn by three different soils. *Soil Water Res.* 9, 97–103. doi: 10.17221/50/2013-SWR

Zhang, H., Chen, C., Gray, E. M., and Boyd, S. E. (2017). Effect of feedstock and pyrolysis temperature on properties of biochar governing end use efficacy. *Biomass Bioenergy* 105, 136–146. doi: 10.1016/j.biombioe.2017.06.024

Zhang, X., Wang, H., He, L., Lu, K., Sarmah, A., Li, J., et al. (2013). Using biochar for remediation of soils contaminated with heavy metals and organic pollutants. *Environ. Sci. Pollut. Res.* 20, 8472–8483. doi: 10.1007/s11356-013-1659-0

Conflict of Interest: The authors declare that the research was conducted in the absence of any commercial or financial relationships that could be construed as a potential conflict of interest.

frontiers in Plant Science

ORIGINAL RESEARCH
published: 28 February 2020
doi: 10.3389/fpls.2020.00203

Influences of Climate on Phyllosphere Endophytic Bacterial Communities of Wild Poplar

*Andrea Firrincieli[1], Mahsa Khorasani[1], A. Carolin Frank[2,3] and Sharon Lafferty Doty[1]**

[1] School of Environmental and Forest Sciences, College of the Environment, University of Washington, Seattle, WA, United States, [2] Life & Environmental Sciences School of Natural Sciences, University of California, Merced, Merced, CA, United States, [3] Sierra Nevada Research Institute, School of Natural Sciences, University of California, Merced, Merced, CA, United States

Plant-associated microbial communities play a central role in the plant response to biotic and abiotic stimuli, improving plant fitness under challenging growing conditions. Many studies have focused on the characterization of changes in abundance and composition of root-associated microbial communities as a consequence of the plant response to abiotic factors such as altered soil nutrients and drought. However, changes in composition in response to abiotic factors are still poorly understood concerning the endophytic community associated to the phyllosphere, the above-ground plant tissues. In the present study, we applied high-throughput 16S rDNA gene sequencing of the phyllosphere endophytic bacterial communities colonizing wild *Populus trichocarpa* (black cottonwood) plants growing in native, nutrient-limited environments characterized by hot-dry (xeric) riparian zones (Yakima River, WA), riparian zones with mid hot-dry (Tieton and Teanaway Rivers, WA) and moist (mesic) climates (Snoqualmie, Skykomish and Skagit Rivers, WA). From sequencing data, 587 Amplicon Sequence Variants (ASV) were identified. Surprisingly, our data show that a core microbiome could be found in phyllosphere-associated endophytic communities in trees growing on opposite sides of the Cascades Mountain Range. Considering only taxa appearing in at least 90% of all samples within each climatic zone, the core microbiome was dominated only by two ASVs affiliated *Pseudomonadaceae* and two ASVs of the *Enterobacteriaceae* family. Alpha-diversity measures indicated that plants colonizing hot-dry environments showed a lower diversity than those from mid hot-dry and moist climates. Beta-diversity measures showed that bacterial composition was significantly different across sampling sites. Accordingly, we found that specific ASV affiliated to *Pseudomonadaceae* and *Enterobacteriaceae* were significantly more abundant in the phyllosphere endophytic community colonizing plants adapted to the xeric environment. In summary, this study highlights that sampling site is the major driver of variation and that only a few ASV showed a distribution that significantly correlated to climate variables.

Keywords: Populus microbiome, endophytes, phyllosphere, plant bacterial microbiome, xeric environment

Abbreviations: aPPT30d, 30 days average precipitation; aPPT30y, 30 years average precipitation; ASV, amplicon sequence variant; TMAX30d, 30 days maximum temperature; TMAX30y, 30 years maximum temperature; VPDMAX30d, 30-days maximum pressure deficit; VPDMAX30y, 30 years maximum pressure deficit.

OPEN ACCESS

Edited by:
Tomislav Cernava, Graz University of Technology, Austria

Reviewed by:
Peter Kusstatscher, Graz University of Technology, Austria
Jie Xie, Southwest University, China

****Correspondence:***
Sharon Lafferty Doty
sldoty@uw.edu

Specialty section:
This article was submitted to Plant Abiotic Stress, a section of the journal Frontiers in Plant Science

Received: *30 October 2019*
Accepted: *11 February 2020*
Published: *28 February 2020*

Citation:
Firrincieli A, Khorasani M, Frank AC and Doty SL (2020) Influences of Climate on Phyllosphere Endophytic Bacterial Communities of Wild Poplar. Front. Plant Sci. 11:203. doi: 10.3389/fpls.2020.00203

INTRODUCTION

The bacterial plant microbiome is important for plant growth and health, increasing nutrient acquisition (Knoth et al., 2014; Pankievicz et al., 2015; Alori et al., 2017; Chhabra and Dowling, 2017), improving abiotic stress tolerances (Cura et al., 2017; Lata et al., 2018; Zhang et al., 2019), protecting against pathogens (Bulgarelli et al., 2013; Pandey et al., 2019), modulating plant hormones (Santoyo et al., 2016; Ali et al., 2017), and detoxifying environmental pollutants (Afzal et al., 2014; Hussain et al., 2018). There is a strong and steadily increasing interest in microbial endophytes of plants (Rho et al., 2017) and how they could be harnessed to improve sustainability in agriculture, forestry and bioenergy production (Busby et al., 2017; Doty, 2017). Endophytes from plants in high stress environments have strong impacts on plant stress tolerance (Timmusk et al., 1999; Rodriguez et al., 2004; Aghai et al., 2019). While shifts in microbiome composition has been observed to be cultivar/species-specific and possibly linked to plant physiology (Perez-Jaramillo et al., 2018; Liu et al., 2019), plants can select their microbiome (Jones et al., 2019), and under abiotic stress conditions such as in drought, they have a different microbiome (Xu et al., 2018; Cheng et al., 2019). A comprehensive plant microbiome analysis of perennial species in natural environments under challenging conditions may reveal the key microbial contributors to plant stress tolerance.

Poplar (*Populus*) and willow (*Salix*) trees of the Salicaceae have a wide global distribution, both in native riparian forests across the Northern Hemisphere and in planted forests, accounting for more than 95 million hectares globally (fao.org). Native poplar trees have a diverse microbiota, many with the ability to fix dinitrogen gas, solubilize phosphate, and promote plant growth and health especially under abiotic stresses such as drought and nutrient limitation (Doty et al., 2005, 2009; Xin et al., 2009; Khan et al., 2012, 2015, 2016; Kandel et al., 2015, 2017; Doty, 2016; Aghai et al., 2019). Beneficial microbiota have been isolated from hybrid poplar trees grown in contaminated sites, in field sites, or in tissue culture (Moore et al., 2006; Ulrich et al., 2008; Barac et al., 2009; Scherling et al., 2009; Taghavi et al., 2009). Several bacterial microbiome studies were conducted from hybrid poplar or planted poplar (Bonito et al., 2014; Hacquard and Schadt, 2015; Beckers et al., 2017) while few studies have been done on native poplar in natural environments (Gottel et al., 2011; Shakya et al., 2013). Consequently, the abiotic factors that drive the variation of the phyllosphere endophytic community are still poorly understood. To our knowledge, no comparisons of the phyllospheric, bacterial microbiome of the same poplar species across environmental gradients have been reported yet.

We chose to sample black cottonwood (*Populus trichocarpa*) trees from its natural habitat range from the western and eastern slopes of the Cascade Mountains in Washington State since the mountain range creates a natural barrier separating a maritime climate on the west from a continental climate on the east (Mathews, 2016). While black cottonwood (poplar) is present across this range, there are distinct phenotypic variations and productivity across this gradient from the cooler, moister (mesic) west side to the warmer, drier (xeric) east side of the Cascades (Dunlap and Stettler, 1996, 1998, 2001). Poplar trees from the maritime, mesic climate tend to grow larger, set leaf bud later and flush earlier, have larger leaf areas and higher rust resistance compared to poplar trees from the continental, xeric climate (Dunlap and Stettler, 2001). Poplar in the xeric Yakima river valley tend to be slower growing, have greater drought resistance, and have smaller and thinner leaves (Dunlap and Stettler, 2001). The riparian zones in these river valleys are characterized by nutrient-limitation, most dominated by primary substrate, cobble and sand, deposited from the natural flooding cycles of high alpine snow melt. To determine if a core bacterial microbiome is associated with a specific ecological niche, the phyllosphere endophytic community associated to poplar branches from six river valleys across the Cascade Range was characterized.

MATERIALS AND METHODS

Sampling and Climate Data Collection

In September 04–23, 2014, branch samples were collected from black cottonwood (*Populus trichocarpa* Torr. and Gray) trees inhabiting Yakima, Tieton, Teanaway, Snoqualmie, Skykomish and Skagit river valleys (**Supplementary Figure S1A**). The geographical coordinates and of each plant are reported in **Supplementary Table S1**. The Skagit, Snoqualmie, and Skykomish Rivers are located in the west side of the Cascade mountain range, at elevations of 45 to 200 meters. These three mesic sampling sites had cobble and sand substrates with no soil, with coniferous forest outside of the flood plain. The Tieton and Teanaway River sampling sites were on the east side of the Cascade mountain range at elevations of 567–740 m and 680 m, respectively. The Yakima River sampling sites, at an average elevation of 404 m, were distinctly xeric, with typical shrub-steppe as the accompanying vegetation. Thirty years climate, 30 days weather data and weather data at the sampling date were collected from the PRISM database[1]. Climate data are reported in **Supplementary Table S1**. Examples of the different environments of each river valley are shown in **Supplementary Figures S1B,C**.

Twig samples were placed in sterile 50 mL conical tubes and transported to the laboratory on ice and stored in a −80°C freezer. A total of 34 plants i.e., biological replicates were sampled; 6 biological replicates were collected from Skagit, 6 biological replicates were collected from the Skykomish, 3 biological replicates from the Snoqualmie, 4 biological replicates from the Teanaway, 5 biological replicates from the Tieton, and 10 biological replicates from the Yakima. For each plant, multiples twigs were collected from fully developed branches far from trunk at the 1–2 meter level from the ground.

DNA Extraction, Amplification and Sequencing

Leaves from branch cuttings were surface sterilized as described (Doty et al., 2016). Surface sterilized samples were ground with

[1]http://www.prism.oregonstate.edu/

mortar and pestle in liquid nitrogen to a fine powder. Total DNA was extracted from 100 milligrams of homogenized using the MasterPure Plant Leaf DNA Purification Kit (Epicentre). The quantity and purity of DNA extracts were determined with a Nanodrop ND-1000 Spectrophotometer (Thermo Fisher Scientific Inc.). Thirty ng of total DNA were used as template for PCR amplification (**Supplementary Table S2**) of the V4 region of the 16S rDNA gene using the primer set 515F (5′-GTGCCAGCMGCCGCGGTAA-3′) and 806rB (5′-GGACTACNVGGGTWTCTAAT-3′) (Caporaso et al., 2012), along with 100 μM of sequence-specific peptide nucleic acid (PNA) clamps for to reduce host-derived contaminations from chloroplast and mitochondria (Lundberg et al., 2012). The Exo-SAP-IT kit (Affimatrix) was used to clean the PCR products, and amplicons were tagged with Illumina sequencing primers following the standard Illumina protocol for amplicon library preparation. The libraries were then sequenced on the Illumina MiSeq sequencer using the v2 2 × 300 bp read kit by the Joint Genome Institute.

Sequencing Data Processing and Identification of Amplicon Sequence Variants (AVSs)

Adapter and primers were removed with Cutadapt v2.4 (Martin, 2011). To identify AVSs, paired-end reads were processed using dada2 as implemented in qiime2 v2019-08 (Callahan et al., 2016; Bolyen et al., 2019). Quality trimming, denoising, merging, and chimera detection were done using the qiime2 v2019-08 plugin "qiime dada2 denoise-paired" with default setting except for "–p-trunc-len-f" and "–p-trunc-len-r" which were set at 230 and 200, respectively. The resulting ASVs were taxonomically classified using the qiime2 v2019-08 plugin "*qiime feature-classifier classify-sklearn*" with the pre-trained Naive Bayes SILVA classifier v132 trimmed to the V4 region of the 16S rDNA gene (Quast et al., 2013). Finally, the plugins "*qiime taxa filter-seqs*" and "*qiime taxa filter-table*" were used to filter out ASVs taxonomically affiliated to "chloroplast" and "mitochondria."

Statistical Analysis

Core microbiome analysis were performed using the R package Microbiome v1.9.19[2]. For alpha diversity measures, each sample was rarefied down to 15,000 sequences. For analyses other than alpha diversity, a normalization method for zero-inflated sequencing data (GMPR) was used (Chen et al., 2018). The function "*estimate_richness*" from the R package "phyloseq v1.22.3" (McMurdie and Holmes, 2013) was used to estimate Chao1 and Shannon alpha-diversity measures. A non-parametric Wilcoxon sign rank test was used to compare alpha-diversity indices between sites. Differences across sites were considered significant for adjusted P-value < 0.1 (Benjamin-Hochberg method). A Principal-coordinate analysis (PCoA) based on Bray-Curtis dissimilarities was computed using the "ordinate" function implemented in "phyloseq v1.22.3". The function "adonis," from the package vegan 2.1-10, was used to perform a permutational univariate analysis of variance on Bray-Curtis dissimilarities and calculate the contribution of sampling site and climate variables using with 999 permutations. The constrained correspondence analysis (CCA) implemented in the R package Vegan 2.1-10 was used to evaluate how climate data shapes the microbial community (Oksanen, 2011). Finally, a Pearson correlation was used to find ASV whose abundance significantly correlate with climate variables.

[2]https://github.com/microbiome/microbiome/

RESULTS

Sampling Site Description

According to 30 years climate data i.e., maximum vapor pressure deficit (VPDMAX30y), maximum temperature (TMAX30y) and average precipitation (aPPT30Y), all variables equally contributed to the separation of sampling sites into three distinct climatic zones i.e., hot-dry (Yakima River), riparian zones with mid hot-dry (Tieton and Teanaway Rivers) and moist-cool (mesic) climates (Snoqualmie, Skykomish and Skagit Rivers) (**Figure 1A**). aPPT30y and VPDMAX30y reaching the highest values in moist-cool (Skykomish, Skagit, Snoqualmie) and hot-dry (Yakima) sites, respectively (**Figures 1B,C**) while TMAX30y reached the lowest values in mid hot-dry riparian zones (Teanaway and Tieton) (**Figure 1D**). Therefore, plant inhabiting hot-dry climates are subjected to drought conditions as a consequence of low precipitation and high temperature which causes high levels of vapor pressure deficit.

Microbial Composition and Alpha Diversity of the Endophytic Community

A total of 4,181,531 paired-end reads, with an average of 122,986.2 reads per sample, were generated. After quality filtering, denoising, merging and chimera screening an average of 97,664.5 reads per sample were obtained (**Supplementary Table S3**). Because bacterial 16S rDNA primers also target chloroplast and mitochondrial DNA, the actual number of amplicons per sample representing the phyllosphere community ranged from 15,739 to 100,397. After the removal sequences affiliated to chloroplast and mitochondria, 587 amplicon sequence variants (ASV) were identified (**Supplementary Table S4**). Despite a large fraction of amplicons assigned to plastid 16S rDNA, sequencing depth was high enough to capture the majority of observed ASV (**Supplementary Figure S2**).

Considering taxa with a relative abundance $> 1.0\%$ in at least 2 samples, the endophytic microbiota consisted of *Proteobacteria, Bacteroidetes, Firmicutes* and *Actinobacteria*. Proteobacteria was the dominant phylum, ranging from 69 to 99.9% of the total relative abundance, followed by *Bacteroidetes* (0.01–30%), *Firmicutes* (0.01–26%), and *Actinobacteria* (0.01–4%) (**Figure 2A** and **Supplementary Table S5**). Only few sequences, in total 148, were not assigned to any phylum. *Proteobacteria* were exclusively represented by *Gamma* and *Alphaproteobacteria*; *Bacteroidia* was the only class detected in *Bacteroidetes*, while Firmicutes were represented by *Bacilli* and *Clostridia* (**Figure 2B**). The latter were detected only in two samples. At finer taxonomic levels, only a few families occurred with relative abundance of more

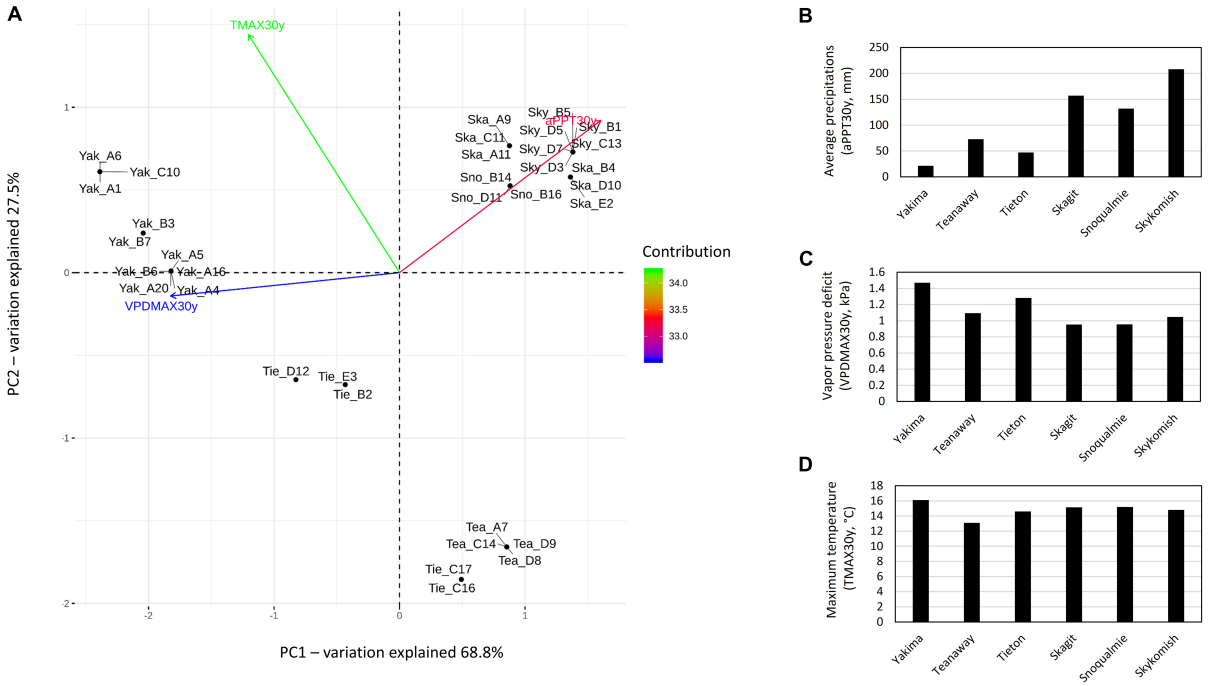

FIGURE 1 | Principal component analysis and trends on 30 year climate data, max temperature, average precipitations and max vapor pressure deficit in Yakima (Yak), Tieton (Tie), Teanaway (Tea), Snoqualmie (Sno), Skagit (Ska) and Skykomish (Sky) sampling sites. **(A)** Principal component analysis if 30 year climate data; the total contribution to PC1 and PC2 of max temperature (TMAX30y), average precipitations (aPPT30y) and maximum vapor pressure deficit (VPDMAX30y) on the first and second component are encoded in color scale. **(B–D)** trends of 30 year climate data, samples are grouped by sampling sites: Yakima, Teanaway, Tieton, Skagit, Snoqualmie and Skykomish.

than 1% across all samples. Among these, *Pseudomonadaceae* (*Gammaproteobacteria*) and *Enterobacteriaceae* (*Gammaproteobacteria*) dominated all samples, accounting all together for the 94 – 22% of the microbial community, followed by *Burkholderiaceae* (*Gammaproteobacteria*; aka *Betaproteobacteria*), *Sphingomonadaceae* (*Alphaproteobacteria*) and *Xanthomonadaceae* (*Gammaproteobacteria*) (**Figure 2C**). All *Pseudomonadaceae* ASV were affiliated to the *Pseudomonas* genus, while only few ASV belonging to *Enterobacteriaceae* were classified down to the genus level (**Supplementary Table S4**).

For each climatic zone, hot-dry, mid hot-dry and moist, a core microbiome was computed by selecting features with a relative abundance $\geq$1% within each sample and setting 50% occurrence as minimum threshold (**Table 1**). The most abundant core ASVs were affiliated to the genus *Pseudomonas* and *Enterobacteriaceae* family. At 90% threshold the core microbiome within each sampling site was dominated by ASV5 (*Pseudomonas*) and ASV17 (*Enterobacteriaceae*) (**Table 1**). We attempted to classify ASV17 and ASV5 down to species level by aligning the 16S sequences against all *Enterobacteriaceae* and *Pseudomonas* currently available in the Integrated Microbial Genome database. Interestingly, ASV17 generated significant alignment (100% sequence identity) with *Serratia*/*Yersinia*/*Rahnella* strains while ASV5 shared 100% identity with the 16S of *Pseudomonas viridiflava*. At lower threshold, 50–80% occurrence, other *Enterobacteriaceae* and *Pseudomonadaceae* ASVs were included part of the core members of each climatic zone. The only exceptions were represented by *Duganella*, *Xanthomonas* and *Sphingomonas* ASVs which occurred only in mid hot-dry and moist climatic zones (**Table 1**). Therefore, despite different climatic conditions, all samples shared ASVs mainly affiliated to *Enterobacteriaceae* and *Pseudomonas*.

Alpha Diversity Analysis

Shannon and Chao 1 indices were used to measure the Alpha diversity of the endophytic community (**Figure 3**). All diversity metrics tended to be significantly higher (adjusted *P*-value $<$ 0.1) for the phyllosphere community of plants colonizing moist-cool and mid hot-dry environments (**Figures 3A,B** and **Supplementary Table S6**). Similarly, although no significant differences were observed in microbiome diversity, when Shannon and Chao 1 indices were compared across sampling sites, phyllosphere community associated to plants inhabiting Tieton, Teanaway, Skagit, Skykomish and Snoqualmie river systems tended to show higher species richness and diversity compared to Yakima samples (**Figures 3C,D** and **Supplementary Table S6**).

Community Structure as a Function of Environmental Characteristics

The variation partitioning on Bray–Curtis dissimilarity was calculated to assess how sampling site, climate and

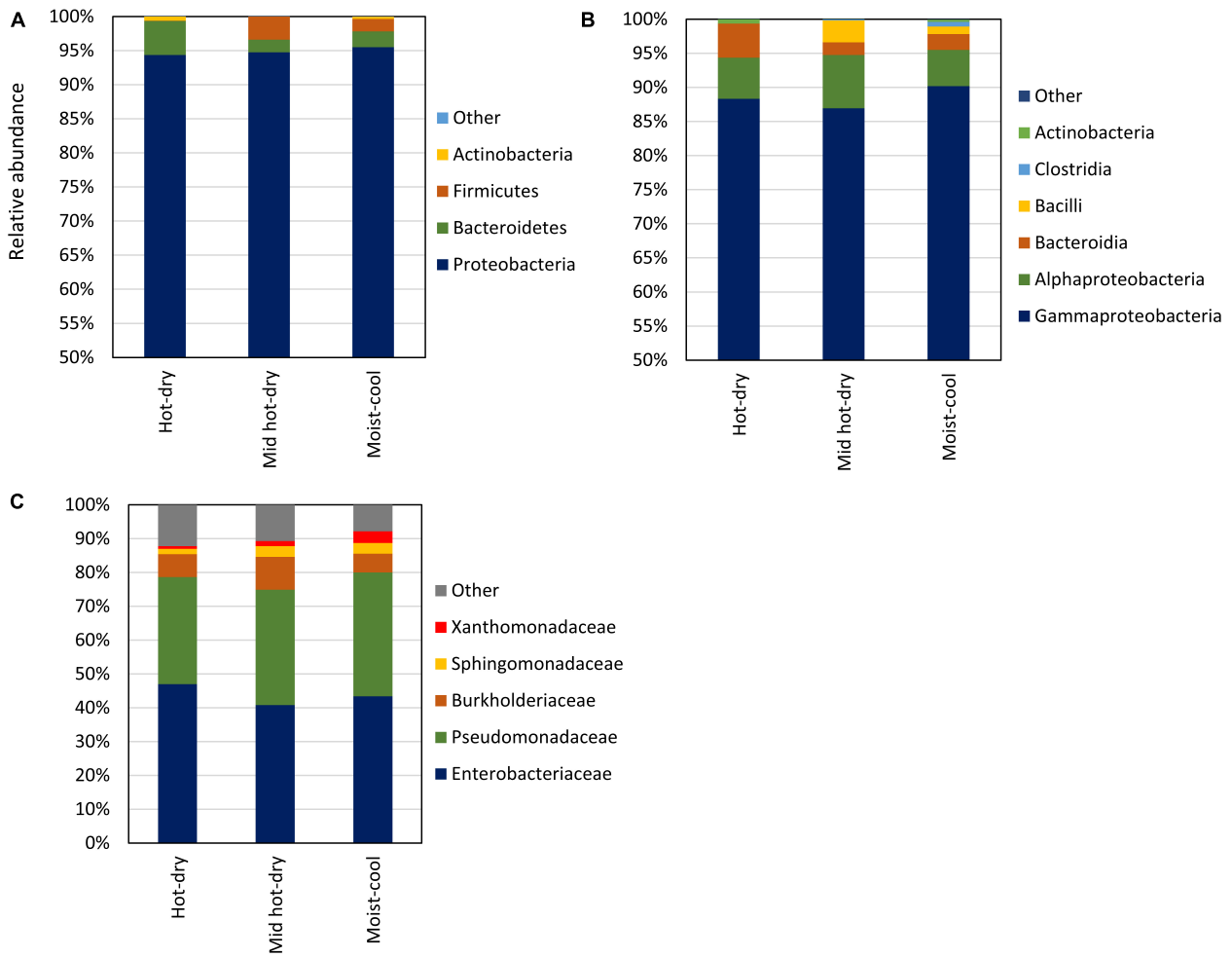

FIGURE 2 | Library composition based on the taxonomic classification of the 16S rDNA sequence variants of phyllosphere endophytic bacterial communities collected in hot-dry, mid hot-dry and moist-cool climatic zones. Taxonomy is displayed at Phylum **(A)**, Class **(B)**, and Family **(C)** level. Average values of relative abundance per climatic zone: hot-dry (n = 10), mid hot-dry (n = 9) and moist-cool (n = 15) are plotted. Relative abundance per samples are reported in **Supplementary Table S4**.

weather variables differentiated the phyllosphere endophytic community across sampling sites. As expected, from Bray–Curtis dissimilarity distances calculated on GMPR-normalized microbial abundance data (**Supplementary Table S4**), site was the strongest driver of bacterial community variation, explaining 29.01% of the variance (P = 0.001) (**Figure 4** and **Table 2**). Weather data collected at the sampling date had a low impact on community structure variation; precipitation and max temperatures explained, respectively the 6.1% (P = 0.025) and 6.2% (P = 0.02) of variation while the effect of vapor pressure deficit was not significant (P = 0.052). On the other hand, the effects of 30 days weather and 30 year climate variables on Bray–Curtis was greater compared to weather data measured at the sampling date (**Table 2**). Notably, among 30 days weather data vapor pressure deficit and max temperature showed comparable effects on variation in phyllosphere endophytic community, respectively 16.6% (P = 0.001) and 16.5% (P = 0.001), while among 30 years climate data vapor pressure deficit was the strongest driver of variation, explaining the 17% (P = 0.001) of the variance (**Table 2**).

To better capture the variation explained by those variables that mostly affected beta-diversity ($P < 0.0$; $R^2 > 0.1$), we performed a constrained correspondence analysis (CCA) on normalized abundance data. Accordingly, 7.3% was the total variance explained by those variables that had major effects on beta-diversity, contributing to the separation of phyllosphere community of plants growing in hot dry zones from those inhabiting mid hot-dry and moist climates (**Figure 5**). Therefore, we sought to determine which ASVs significantly correlated with these variables. As expected, due to the limited effect that climate/weather variables had on the distribution of ASVs across sites, very few of them moderately correlate with temperature, vapor pressure deficit and precipitation. Interestingly, a climate/weather-dependent distribution was observed for core ASVs. Specifically, ASV17 (*Enterobacteriaceae*), which is part of the core microbiome in mid hot-dry and moist-cool samples

TABLE 1 | Core microbiome ASVs detected in the phyllosphere endophytic community of poplar plants inhabiting hot-dry, mid hot-dry and moist-cool climatic zones.

Climatic zone	Sequence variant ID	Occurrence	Taxonomy[1]	Number of samples	Relative abundance (%)
Mid hot-dry (*n* = 9)	ASV5	1.00	*Pseudomonas*	9	2.11–12.65
	ASV428	1.00	*Pseudomonas*	9	1.33–12.26
	ASV17	1.00	*Enterobacteriaceae*	9	4.35–38.84
	ASV1	0.89	*Enterobacteriaceae*	8	0.56–51.09
	ASV11	0.67	*Pseudomonas*	6	0.09–29.55
	ASV2	0.67	*Pseudomonas*	6	0.1–4.71
	ASV8	0.67	*Duganella*	6	0.0–12.35
	ASV147	0.67	*Sphingobium*	6	0.0–4.42
	ASV233	0.55	*Pseudomonas*	5	0.0–19.07
Hot-dry (*n* = 10)	ASV5	0.90	*Pseudomonas*	9	0.72–45.67
	ASV1	0.80	*Enterobacteriaceae*	8	0.0–49.93
	ASV2	0.60	*Pseudomonas*	6	0.0–28.53
	ASV354	0.50	*Enterobacteriaceae*	5	0.0–22.56
Moist-cool (*n* = 15)	ASV17	1.00	*Enterobacteriaceae*	15	9.84–44.98
	ASV5	0.93	*Pseudomonas*	14	0.44–53.36
	ASV439	0.80	*Pectobacterium*	12	0.0–22.48
	ASV1	0.73	*Enterobacteriaceae*	11	0.0–15.10
	ASV41	0.73	*Xanthomonas*	11	0.07–12.72
	ASV233	0.67	*Pseudomonas*	10	0.0–16.08
	ASV8	0.53	*Duganella*	8	0.0–6.33

[1] *Full taxonomy lineage is reported in* ***Supplementary Table S4****.*

negatively correlate with vapor pressure deficit and temperature, while ASV1 (*Enterobacteriaceae*) and ASV2 (*Pseudomonas*), which are also part of the "core" of mid hot-dry and hot-dry samples, positively correlates with temperature and vapor pressure deficit (**Table 3**).

DISCUSSION

The plant microbiome plays a major role in the plant response to abiotic factors and mitigation of stresses through the induction of tolerance mechanisms via phytohormone production, improved water-use efficiency, nutrient uptake, and uptake/degradation of pollutants (e.g., heavy metals and organic pollutants) (Khare et al., 2018; Lata et al., 2018). In addition, the host could directly affect the composition of the plant-associated microbial community by modifying the chemical features of the surrounding environment (Gopal and Gupta, 2016). For instance, the ability of microbes to metabolize plant-derived metabolites e.g., root exudate, implies that the plant microbiome can vary greatly among hosts, as a consequence of plant metabolism/development, and in response to environmental cues/stressors (Naylor et al., 2017; Sasse et al., 2018). These mechanisms have been described in respect to the plant rhizobiome, the microbial community associated with rhizosphere, rhizoplane and root endosphere. Less is known about the drivers of microbiome variation in the aerial tree surface, which is characterized by being extremely poor in nitrogen and carbon sources, and subjected to more rapid fluctuations of physical conditions (Lindow and Brandl, 2003; Laforest-Lapointe et al., 2016; Remus-Emsermann and Schlechter, 2018). Environmental variables such as radiation, precipitation, temperature and humidity have a direct effect on stomata opening and, therefore, play a pivotal role in regulating CO_2 uptake for photosynthesis. In this respect, several studies have confirmed that endophytes can affect host fitness under drought conditions having a direct effect on stomata conductivity (Elmi and West, 1995; Arnold and Engelbrecht, 2007; Khan et al., 2016; Rho et al., 2018). While these studies have been conducted under controlled conditions, the importance of the phyllosphere microbial communities in natural ecosystems is still poorly understood (Laforest-Lapointe et al., 2016, 2017).

Our study characterized the structural features of the phyllosphere microbial communities collected from *Populus trichocarpa* plants inhabiting Yakima, Tieton, Teanaway, Snoqualmie, Skykomish and Skagit riparian zones, describing the impact of environmental factors, i.e., temperature, vapor pressure deficit and precipitation, to their composition. The sampling sites were characterized by different historical drought regimes as a consequence of differences in temperature, vapor pressure deficit and precipitations. In particular, based on the 30 years climate variables, the sampling sites can be pooled in three clusters characterized by hot-dry (Yakima, 10 plants), mid hot-dry (Tieton, 5 plants; Teanaway, 4 plants) and moist (Snoqualmie, 3 plants; Skagit, 6 plants; Skykomish, 6 plants) climates (**Figure 1A**). Such differences in temperature, precipitations and vapor pressure deficit indicates that plants inhabiting hot dry environments are subjected to drought conditions (Yuan et al., 2019).

By 16S rDNA sequencing the composition, alpha and beta diversity indices of phyllosphere-associated microbiome were characterized. The number of taxonomic groups dominating all

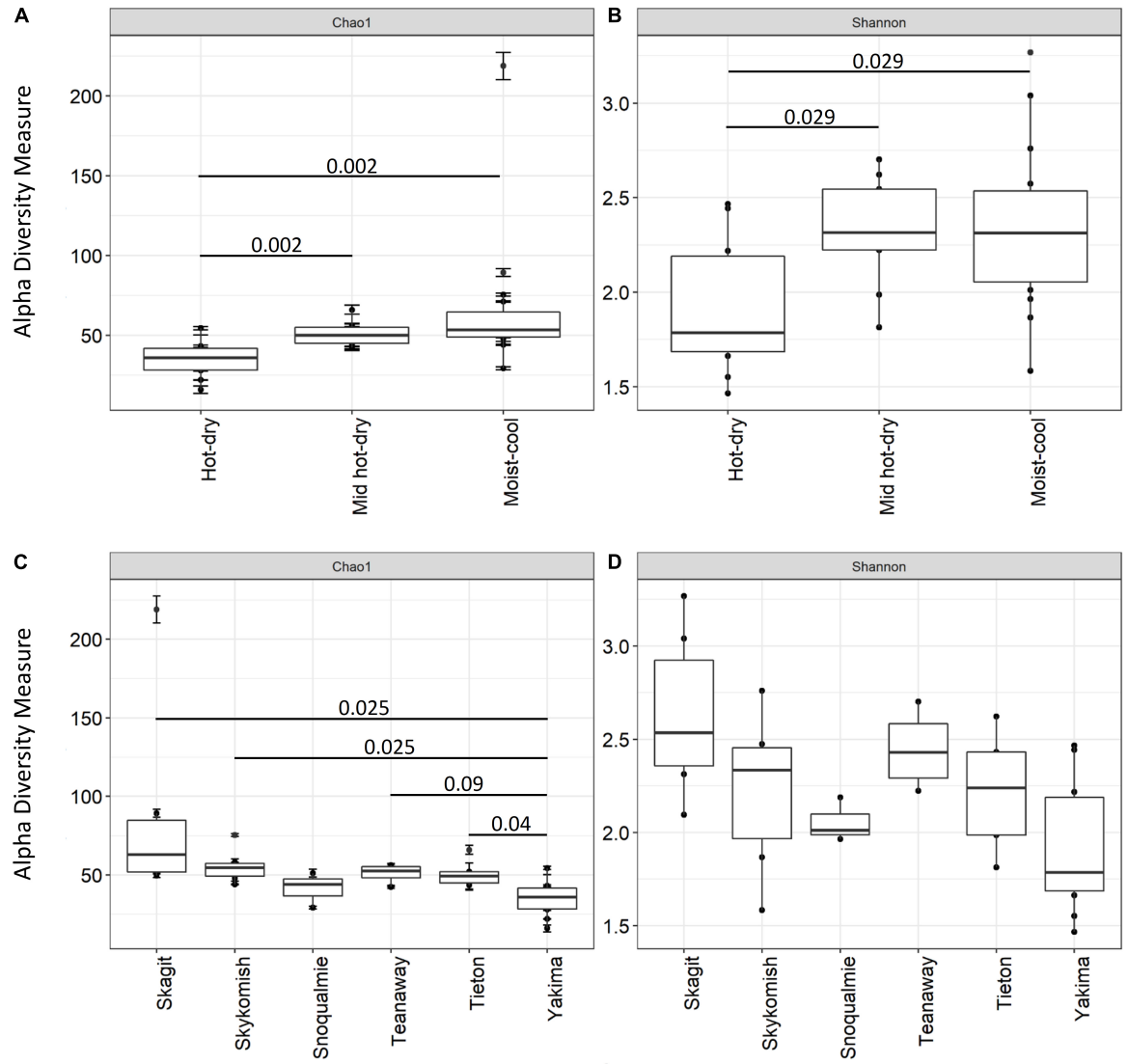

FIGURE 3 | Comparison of Alpha diversity indices Chao 1 and Shannon across hot-dry, mid hot-dry and moist-cool climatic zones **(A,B)** and between sampling sites **(C,D)**, i.e., Yakima, Skagit, Tieton, Teanaway, Snoqualmie, Skykomish. Only significant Benjamini–Hochberg adjusted *P*-values are shown. For completeness all adjusted *P*-value from pairwise comparison were added to **Supplementary Table S6**.

samples was relatively scarce. Only two families had a relative high abundance, *Enterobacteriaceae* and *Pseudomonadaceae* (**Figure 2C**). In addition, ASVs affiliated to these families were also part of the core microbiome of the phyllosphere endophytic community of each sampling site, confirming that members of the *Pseudomonadaceae* and *Enterobacteriaceae* are ubiquitous components of the plant microbiome (**Table 1**; Lindow and Brandl, 2003; Jun et al., 2016; Rufian et al., 2016; Cernava et al., 2019). All the ASVs affiliated to *Pseudomonadaceae* were exclusively represented by the genus *Pseudomonas* while only few *Enterobacteriaceae* ASV were taxonomically classified down to genus level (**Supplementary Table S4**); unfortunately, the most abundant *Enterobacteriaceae* ASV remained unidentified at lower taxonomic levels. This could be explained by the lack of power of the hypervariable region 4 in the taxonomical identification of the *Enterobacteriaceae* genera, making the 16S rDNA V4 region unsuitable for the downstream characterization of the members belonging of this family (Greay et al., 2019). However, the most dominant *Enterobacteriaceae*, i.e., ASV17 was indentified as a possible member of the genera *Serratia/Yersinia/Rahnella* which includes species recognized as plant/human pathogens and plant beneficial bacteria as well. Therefore, their identification as the most abundant ASVs might not be surprising. Similarly, the most dominant *Pseudomonas* ASV, i.e., ASV5, showed a significant hit with *Pseudomonas viridiflava*, a multi host plant pathogen (Sarris et al., 2012). None of the genera mentioned above have been recognized as pathogens in poplar, suggesting that outside its primary host, a phytopathogen could be a common inhabitant

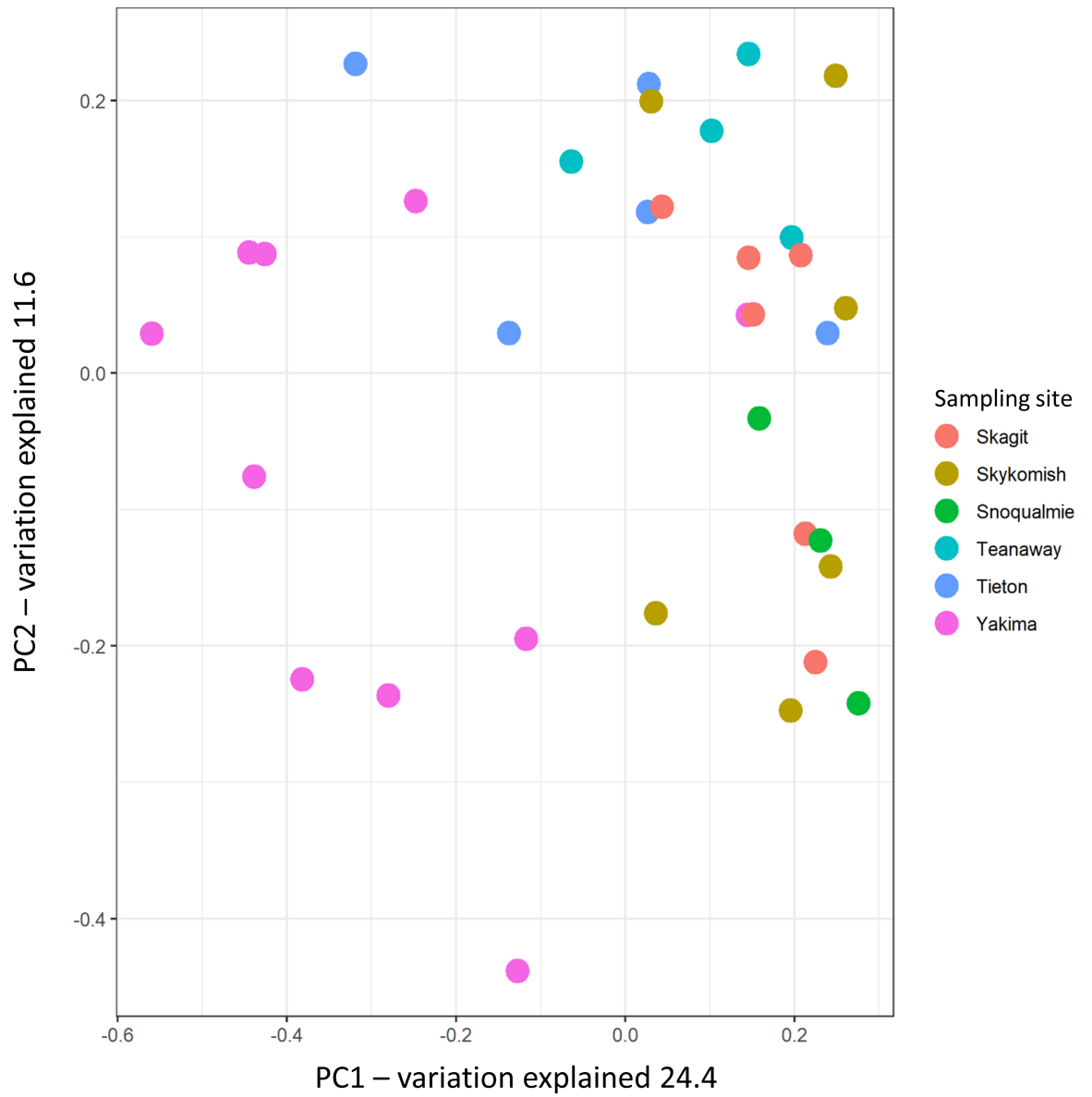

FIGURE 4 | Principal coordinate analysis of phyllosphere endophytic microbial communities using Bray-Curtis distances. Circles represent samples.

of the microbial community without contributing to plant fitness or, perhaps, acting as beneficial bacteria.

Alpha diversity indices, Shannon and Chao-1, indicates that the phyllosphere of plants inhabiting hot-dry environments had the lowest diversity. Decreases in alpha diversity as consequence of drought have been observed for microbial communities associated to plants under drought conditions before (Mendes et al., 2013; Naylor et al., 2017; Ullah et al., 2019). In our study, we found that the number of observed species (Chao-1) and the overall diversity (Shannon) tended to be lower in twigs collected from plants in hot-dry environments i.e., Yakima (**Figure 3**). However, from PERMANOVA analysis performed on Bray-Curtis distances, the sampling site was the major driver of variation while climate and weather data had only a limited effect on beta-diversity (**Table 2**). The limited effect weather and climate data on microbial community composition was also confirmed via CCA analysis (**Figure 4**). A possible explanation is that other environmental constraints such as chemical and physical characteristics of soil could participate to phyllosphere differentiation across sites (Verbon and Liberman, 2016; Ullah et al., 2019). However, the effect of soil composition on phyllosphere community structure could be negligible (Grady et al., 2019). Alternatively, host-specific traits that are positively selected as a result of adaptation mechanisms toward specific environmental constraints could be a major driver of variation. Indeed, as reported in

TABLE 2 | Bacterial community structure variation explained by weather and climate data, and sampling site (PERMANOVA on Bray-Curtis dissimilarities).

	Variables[1]	Df	*R* squared	*P*-value
Sampling date weather data	precipitation	1	0.06197	0.025
	max temperature	1	0.06208	0.02
	vapor pressure deficit	1	0.05223	0.052
30 days weather data	precipitation	1	0.08801	0.003
	max temperature	1	0.16602	0.001
	vapor pressure deficit	1	0.16523	0.001
30 years climate data	precipitation	1	0.1321	0.001
	max temperature	1	0.0986	0.001
	vapor pressure deficit	1	0.17099	0.001
Sampling site	–	5	0.29012	0.001

[1] *Each variable was tested individually.*

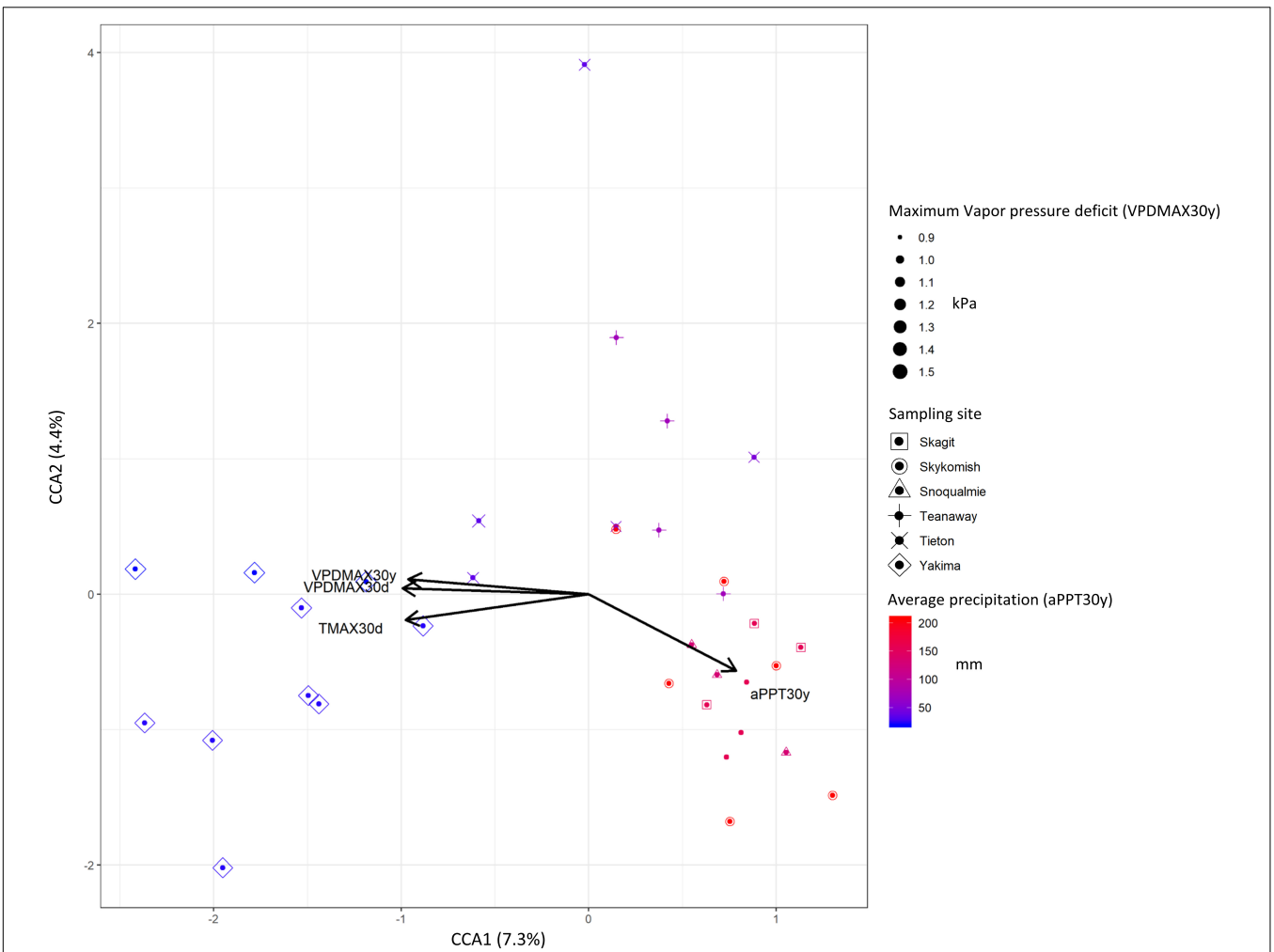

FIGURE 5 | Canonical constrained analysis (CCA) biplot relating community composition to climate and weather variables. The percent of variation explained by each axis is indicated in parentheses. Symbols size and color gradient represents 30 years climate data maximum vapor (VPDMAX30y) pressure deficit and average precipitations (aPPT30y).

Laforest-Lapointe et al. (2016), functional traits characteristic of tree ecological strategy explained the differences in leaf community structure observed across sites.

Most of the information we have regarding the molecular mechanisms behind the beneficial role of phyllosphere-associated bacteria have been obtained from studies examining the

TABLE 3 | Correlation of ASV abundance data with the 30 year climate and 30 days weather data.

Amplicon sequence variant ID	Taxonomy	30 days		30 years	
		Maximum temperature	Maximum vapor pressure deficit	Average precipitation	Maximum vapor pressure deficit
ASV41	*Xanthomonas*	−0.48**	−0.57***	0.56***	−0.61***
ASV17	*Enterobacteriaceae*	−0.49**	−0.49**	ns	−0.54***
ASV1	*Enterobacteriaceae*	0.44**	0.46**	−0.52**	0.52**
ASV2	*Pseudomonas*	0.63***	0.46**	ns	0.48**
ASV417	*Allorhizobium-Neorhizobium-Pararhizobium-Rhizobium*	ns	Ns	0.51***	ns
ASV19	*Allorhizobium-Neorhizobium-Pararhizobium-Rhizobium*	ns	ns	0.48**	ns
ASV40	*Burkholderiaceae*	ns	0.46**	ns	ns

*Numbers represent correlation coefficient (Pearson); Significance levels for each variable are given by: **P < 0.01; ***P < 0.001; ns, P > 0.05.*

interaction between the host plant and single strains. As mentioned before, the effect of drought on the leaf gas exchange involves a strict regulation of stomata opening, which directly affects the photosynthetic capacity of the plant (Urban et al., 2017). In this respect, volatile organic compounds produced by plant growth promoting bacteria enhance stomatal closure and reduce water loss under drought conditions (Cho et al., 2008). Such aspects have been also studied at the community level, using a well-defined microbial consortium composed exclusively by plant growth-promoting bacteria (Rho et al., 2017). We found that only few ASV showed a positive and significant correlation with vapor pressure deficit which trigger stomatal closure due to the high evaporative demand of the air (Carnicer et al., 2013; Yuan et al., 2019). As mentioned before, *Enterobacteriaceae* and *Pseudomonadaceae* ASVs, which were identified as common inhabitants of our phyllopshere microbial community, have been extensively studied for their capability to improve plant tolerance toward abiotic stresses (Kang et al., 2015; Asaf et al., 2016). *Enterobacteriaceae* and *Pseudomonadaceae* are capable of secreting secondary metabolites or produce enzymes that enhance drought tolerance. For instance, volatile organic compounds such as acetoin and butanediol elicits stomatal closure, helping the plant prevent water loss from transpiration (Cho et al., 2008) and improving drought tolerance (Saha and Bothast, 1999; Celińska and Grajek, 2009; Ji et al., 2011; Khalifa et al., 2016). In addition, *Pseudomonas, Klebsiella, Erwinia, Serratia* and *Pantoea* species are known to be ACC deaminase-producing bacteria and therefore able to regulate plant ethylene levels inducing tolerance to drought stress (Li et al., 2015; Saikia et al., 2018; Danish and Zafar-ul-Hye, 2019). Therefore, while climate and weather data had a limited impact on microbial community composition, community ASVs significantly correlated with environmental constraints such as vapor pressure deficit could enhance drought tolerance in plant inhabiting hot-dry environments.

CONCLUSION

Overall, this study highlights that the phyllosphere microbial community is dominated by relatively few species and that bacterial diversity decreases in plants inhabiting hot-dry environments. However, climate and weather variables related to drought such as temperature vapor pressure deficit and precipitation had a low impact of microbial community differentiation across sampling sites as only few ASVs significantly correlated with these environmental variables. Therefore, the variation in microbial community composition observed across sites opens up the possibility that host-specific effects as a result of the adaptation to extreme environment could be the major drivers of variation observed between hot-dry, mid hot-dry and moist-cool climates. Finally, the question whether these taxa that significantly correlate with climate and weather variables are real plant helpers still remain, and a metagenome level analysis would be more informative to better differentiate from a functional point of view those ASVs that, within the same family, show different degrees of correlation with temperature and precipitation.

DATA AVAILABILITY STATEMENT

The datasets generated for this study can be found in NCBI BioProject ID PRJNA589182.

AUTHOR CONTRIBUTIONS

SD and MK conceived, designed, and performed the experiments. ACF and AF analyzed the data. SD, ACF, and AF contributed reagents, materials, and analysis tools, and wrote the manuscript.

FUNDING

The sequencing aspects of the project were conducted by the United States Department of Energy Joint Genome Institute, a DOE Office of Science User Facility supported by the Office of Science of the United States Department of Energy under Contract No. DE-AC02-05CH11231. MK was supported by the Agriculture and Food Research Initiative Competitive Grant No. 2011-68005-30407. AF was supported by the Washington Research Foundation.

ACKNOWLEDGMENTS

The authors sincerely thank Andrew Ko for his assistance in plant sample processing.

SUPPLEMENTARY MATERIAL

The Supplementary Material for this article can be found online at: https://www.frontiersin.org/articles/10.3389/fpls.2020.00203/full#supplementary-material

FIGURE S1 | Location of the six sites sampled during in September 2014 across the state of Washington **(A)** and representative photographs of the mesic (**B**, Skykomish River) and xeric (**C**, Yakima River) environments. Nearby vegetation in the mesic environment included the climate indicator species, western hemlock (*Tsuga heterophylla*), sitka spruce (*Picea sitchensis*) and western redcedar (*Thuja plicata*). Accompanying vegetation in the xeric environment included included sagebrush (*Chrysothamnus nauseosus* and *Artemisia tridentata*), bitterbrush (*Purshia tridentata*), wildroses (*Rosa* sp.), grasses (hordeae), Saskatoon serviceberry (*Amelanchier alnifolia*), and ponderosa pine (*Pinus ponderosa*).

FIGURE S2 | Rarefaction curves of sequence variants for each sample. Lines are colored by sampling sites: Yakima (purple), Teanaway (dark red), Tieton (orange), Skagit (blue), Snoqualmie (dark green), Skykomish (Cyan).

TABLE S1 | Sampling site, geographical coordinates, and climate data associated to each sample.

TABLE S2 | PCR reaction conditions.

TABLE S3 | DADA2 denoising and taxonomy filtering stats.

TABLE S4 | Taxonomic affiliation of 16S rDNA sequence variants with relative and GMPR-normalized abundance data.

TABLE S5 | Relative abundance of major taxonomic groups identified in phyllosphere microbial communities of Poplars inhabiting hot-dry, mid hot-dry and moist-cool climates.

TABLE S6 | Benjamin-Hochberg adjusted P-value from pairwise comparisons using Wilcoxon rank sum test.

REFERENCES

Afzal, M., Khan, Q. M., and Sessitsch, A. (2014). Endophytic bacteria: prospects and applications for the phytoremediation of organic pollutants. *Chemosphere* 117, 232–242. doi: 10.1016/j.chemosphere.2014.06.078

Aghai, M. M., Khan, Z., Joseph, M. R., Stoda, A. M., Sher, A. W., Ettl, G. J., et al. (2019). The effect of microbial endophyte consortia on *Pseudotsuga menziesii* and *Thuja plicata* survival, growth, and physiology across edaphic gradients. *Front. Microbiol.* 10:1353. doi: 10.3389/fmicb.2019.01353

Ali, S., Charles, T. C., and Glick, B. R. (2017). "Endophytic phytohormones and their role in plant growth promotion," in *Functional Importance of the Plant Microbiome: Implications for Agriculture, Forestry and Bioenergy*, ed. S. L. Doty, (Cham: Springer), 89–106.

Alori, E. T., Glick, B. R., and Babalola, O. O. (2017). Microbial phosphorus solubilization and its potential for use in sustainable agriculture. *Front. Microbiol.* 8:971. doi: 10.3389/fmicb.2017.00971

Arnold, A. E., and Engelbrecht, B. M. J. (2007). Fungal endophytes nearly double minimum leaf conductance in seedlings of a neotropical tree species. *J. Trop. Ecol.* 23, 369–372. doi: 10.1017/s0266467407004038

Asaf, S., Khan, M. A., Khan, A. L., Waqas, M., Shahzad, R., Kim, A. Y., et al. (2016). Bacterial endophytes from arid land plants regulate endogenous hormone content and promote growth in crop plants: an example of *Sphingomonas* sp. and *Serratia marcescens*. *J. Plant Interact.* 12, 31–38. doi: 10.1080/17429145.2016.1274060

Barac, T., Weyens, N., Oeyen, L., Taghavi, S., van der Lelie, D., Dubin, D., et al. (2009). Field note: hydraulic containment of a BTEX plume using poplar trees. *Int. J. Phytoremediation* 11, 416–424. doi: 10.1080/15226510802655880

Beckers, B., Op De, B. M., Weyens, N., Boerjan, W., and Vangronsveld, J. (2017). Structural variability and niche differentiation in the rhizosphere and endosphere bacterial microbiome of field-grown poplar trees. *Microbiome* 5:25. doi: 10.1186/s40168-017-0241-2

Bolyen, E., Rideout, J. R., Dillon, M. R., Bokulich, N. A., Abnet, C. C., Al-Ghalith, G. A., et al. (2019). Reproducible, interactive, scalable and extensible microbiome data science using QIIME 2. *Nat. Biotechnol.* 37, 852–857.

Bonito, G., Reynolds, H., Robeson, M. S., Nelson, J., Hodkinson, B. P., Tuskan, G., et al. (2014). Plant host and soil origin influence fungal and bacterial assemblages in the roots of woody plants. *Mol. Ecol.* 23, 3356–3370. doi: 10.1111/mec.12821

Bulgarelli, D., Schlaeppi, K., Spaepen, S., van Ver Loren, T. E., and Schulze-Lefert, P. (2013). Structure and functions of the bacterial microbiota of plants. *Annu. Rev. Plant Biol.* 64, 807–838. doi: 10.1146/annurev-arplant-050312-120106

Busby, P. E., Soman, C., Wagner, M. R., Friesen, M. L., Kremer, J., Bennett, A., et al. (2017). Research priorities for harnessing plant microbiomes in sustainable agriculture. *PLoS Biol.* 15:e2001793. doi: 10.1371/journal.pbio.2001793

Callahan, B. J., McMurdie, P. J., Rosen, M. J., Han, A. W., Johnson, A. J., and Holmes, S. P. (2016). DADA2: high-resolution sample inference from Illumina amplicon data. *Nat. Methods* 13, 581–583. doi: 10.1038/nmeth.3869

Caporaso, J. G., Lauber, C. L., Walters, W. A., Berg-Lyons, D., Huntley, J., Fierer, N., et al. (2012). Ultra-high-throughput microbial community analysis on the Illumina HiSeq and MiSeq platforms. *ISME J.* 6, 1621–1624. doi: 10.1038/ismej.2012.8

Carnicer, J., Barbeta, A., Sperlich, D., Coll, M., and Penuelas, J. (2013). Contrasting trait syndromes in angiosperms and conifers are associated with different responses of tree growth to temperature on a large scale. *Front. Plant Sci.* 4:409. doi: 10.3389/fpls.2013.00409

Celińska, E., and Grajek, W. (2009). Biotechnological production of 2,3-butanediol—current state and prospects. *Biotechnol. Adv.* 27, 715–725. doi: 10.1016/j.biotechadv.2009.05.002

Cernava, T., Erlacher, A., Soh, J., Sensen, C. W., Grube, M., and Berg, G. (2019). *Enterobacteriaceae* dominate the core microbiome and contribute to the resistome of arugula (*Eruca sativa* Mill.). *Microbiome* 7:13. doi: 10.1186/s40168-019-0624-7

Chen, L., Reeve, J., Zhang, L., Huang, S., Wang, X., and Chen, J. (2018). GMPR: a robust normalization method for zero-inflated count data with application to microbiome sequencing data. *PeerJ* 6:e4600. doi: 10.7717/peerj.4600

Cheng, Y. T., Zhang, L., and He, S. Y. (2019). Plant-microbe interactions facing environmental challenge. *Cell Host Microbe* 26, 183–192. doi: 10.1016/j.chom.2019.07.009

Chhabra, S., and Dowling, D. N. (2017). "Endophyte-promoted nutrient acquisition: phosphorus and iron," in *Functional Importance of the Plant Microbiome*, ed. S. L. Doty, (Cham: Springer), 21–42. doi: 10.1007/978-3-319-65897-1_3

Cho, S. M., Kang, B. R., Han, S. H., Anderson, A. J., Park, J. Y., Lee, Y. H., et al. (2008). 2R,3R-butanediol, a bacterial volatile produced by *Pseudomonas* chlororaphis O6, is involved in induction of systemic tolerance to drought in *Arabidopsis thaliana*. *Mol. Plant Microbe Interact.* 21, 1067–1075. doi: 10.1094/MPMI-21-8-1067

Cura, J. A., Franz, D. R., Filosofia, J. E., Balestrasse, K. B., and Burgueno, L. E. (2017). Inoculation with *Azospirillum* sp. and *Herbaspirillum* sp. bacteria increases the tolerance of maize to drought stress. *Microorganisms* 5:41. doi: 10.3390/microorganisms5030041

Danish, S., and Zafar-ul-Hye, M. (2019). Co-application of ACC-deaminase producing PGPR and timber-waste biochar improves pigments formation, growth and yield of wheat under drought stress. *Sci. Rep.* 9:5999. doi: 10.1038/s41598-019-42374-9

Doty, S. L. (2016). Key roles of the poplar microbiome. *Poplar Willow News* 6, 2–4. doi: 10.1007/s00442-014-3063-y

Doty, S. L. (2017). "Functional importance of the plant microbiome: implications for agriculture, forestry and bioenergy," in *Functional Importance of the Plant Microbiome: Implications for Agriculture, Forestry and Bioenergy*, ed. S. L. Doty, (Cham: Springer), 1–6.

Doty, S. L., Dosher, M. R., Singleton, G. L., Moore, A. L., van Aken, B., Stettler, R. F., et al. (2005). Identification of an endophytic *Rhizobium* in stems of *Populus*. *Symbiosis* 39, 27–36.

Doty, S. L., Oakely, B., Xin, G., Kang, J. W., Singleton, G., Khan, Z., et al. (2009). Diazotrophic endophytes of native black cottonwood and willow. *Symbiosis* 47, 23–33. doi: 10.1007/bf03179967

Doty, S. L., Sher, A. W., Fleck, N. D., Khorasani, M., Bumgarner, R., Khan, Z., et al. (2016). Variable nitrogen fixation in wild *Populus*. *PLoS One* 11:e0155979. doi: 10.1371/journal.pone.0155979

Dunlap, J. M., and Stettler, R. F. (1996). Genetic variation and productivity of *Populus trichocarpa* and its hybrids, IX. Phenology and Melampsora rust incidence of native black cottonwood clones from four river valleys in Washington. *For. Ecol. Manag.* 87, 233–256. doi: 10.1016/s0378-1127(96)03774-7

Dunlap, J. M., and Stettler, R. F. (1998). Genetic variation and productivity of *Populus trichocarpa* and its hybrids X. Trait correlations in young black cottonwood from four river valleys in Washington. *Trees* 13, 28–39. doi: 10.1007/pl00009735

Dunlap, J. M., and Stettler, R. F. (2001). Variation in leaf epidermal and stomatal traits of *Populus trichocarpa* from two transects across the Washington Cascades. *Can. J. Bot.* 79, 528–536. doi: 10.1139/b01-029

Elmi, A. A., and West, C. P. (1995). Endophyte infection effects on stomatal conductance, osmotic adjustment and drought recovery of tall fescue. *New Phytol.* 131, 61–67. doi: 10.1111/j.1469-8137.1995.tb03055.x

Gopal, M., and Gupta, A. (2016). Microbiome selection could spur next-generation plant breeding strategies. *Front. Microbiol.* 7:1971. doi: 10.3389/fmicb.2016.01971

Gottel, N. R., Castro, H. F., Kerley, M., Yang, Z., Pelletier, D. A., Podar, M., et al. (2011). Distinct microbial communities within the endosphere and rhizosphere of Populus deltoides roots across contrasting soil types. *Appl. Environ. Microbiol.* 77, 5934–5944. doi: 10.1128/AEM.05255-11

Grady, K. L., Sorensen, J. W., Stopnisek, N., Guittar, J., and Shade, A. (2019). Assembly and seasonality of core phyllosphere microbiota on perennial biofuel crops. *Nat. Commun.* 10:4135. doi: 10.1038/s41467-019-11974-4

Greay, T. L., Gofton, A. W., Zahedi, A., Paparini, A., Linge, K. L., Joll, C. A., et al. (2019). Evaluation of 16S next-generation sequencing of hypervariable region 4 in wastewater samples: an unsuitable approach for bacterial enteric pathogen identification. *Sci. Total Environ.* 670, 1111–1124. doi: 10.1016/j.scitotenv.2019.03.278

Hacquard, S., and Schadt, C. W. (2015). Towards a holistic understanding of the beneficial interactions across the Populus microbiome. *New Phytol.* 205, 1424–1430. doi: 10.1111/nph.13133

Hussain, I., Aleti, G., Naidu, R., Puschenreiter, M., Mahmood, Q., Rahman, M. M., et al. (2018). Microbe and plant assisted-remediation of organic xenobiotics and its enhancement by genetically modified organisms and recombinant technology: a review. *Sci. Total Environ.* 62, 1582–1599. doi: 10.1016/j.scitotenv.2018.02.037

Ji, X.-J., Huang, H., and Ouyang, P.-K. (2011). Microbial 2,3-butanediol production: a state-of-the-art review. *Biotechnol. Adv.* 29, 351–364. doi: 10.1016/j.biotechadv.2011.01.007

Jones, P., Garcia, B. J., Furches, A., Tuskan, G. A., and Jacobson, D. (2019). Plant host-associated mechanisms for microbial selection. *Front. Plant Sci.* 10:862. doi: 10.3389/fpls.2019.00862

Jun, S. R., Wassenaar, T. M., Nookaew, I., Hauser, L., Wanchai, V., Land, M., et al. (2016). Diversity of *Pseudomonas* genomes, including populus-associated isolates, as revealed by comparative genome analysis. *Appl. Environ. Microbiol.* 82, 375–383. doi: 10.1128/AEM.02612-15

Kandel, S., Firrincieli, A., Joubert, P. M., Okubara, P. A., Leston, N., McGeorge, K., et al. (2017). An *in vitro* study of bio-control and plant growth promotion potential of Salicaceae endophytes. *Front. Microbiol.* 8:386. doi: 10.3389/fmicb.2017.00386

Kandel, S., Herschberger, N., Kim, S.-H., and Doty, S. L. (2015). Diazotrophic endophytes of poplar and willow promote growth of rice plants in nutrient-limited conditions. *Crop Sci.* 55, 1765–1772. doi: 10.2135/cropsci2014.08.0570

Kang, S.-M., Khan, A. L., Wagas, M., You, Y.-H., Hamayun, M., Joo, G.-J., et al. (2015). Gibberellin-producing *Serratia nematodiphila* PEJ1011 ameliorates low temperature stress in *Capsicum annum* L. *Eur. J. Soil Biol.* 68, 85–93. doi: 10.1016/j.ejsobi.2015.02.005

Khalifa, A. Y. Z., Alsyeeh, A.-M., Almalki, M. A., and Saleh, F. A. (2016). Characterization of the plant growth promoting bacterium, *Enterobacter cloacae* MSR1, isolated from roots of non-nodulating *Medicago sativa*. *Saudi J. Biol. Sci.* 23, 79–86. doi: 10.1016/j.sjbs.2015.06.008

Khan, Z., Guelich, G., Phan, H., Redman, R. S., and Doty, S. L. (2012). Bacterial and yeast endophytes from poplar and willow promote growth in crop plants and grasses. *ISRN Agron.* 2012:890280. doi: 10.5402/2012/890280

Khan, Z., Kandel, S., Ramos, D., Ettl, G. J., Kim, S.-H., and Doty, S. L. (2015). Increased biomass of nursery-grown Douglas-fir seedlings upon inoculation with diazotrophic endophytic consortia. *Forests* 6, 3582–3593. doi: 10.3390/f6103582

Khan, Z., Rho, H., Firrincieli, A., Luna, V., Hung, S. H., Kim, S.-H., et al. (2016). Growth enhancement and drought tolerance of hybrid poplar upon inoculation with endophyte consortia. *Curr. Plant Biol.* 6, 38–47. doi: 10.1016/j.cpb.2016.08.001

Khare, E., Mishra, J., and Arora, N. K. (2018). Multifaceted interactions between endophytes and plant: developments and prospects. *Front. Microbiol.* 9:2732. doi: 10.3389/fmicb.2018.02732

Knoth, J. L., Kim, S. H., Ettl, G. J., and Doty, S. L. (2014). Biological nitrogen fixation and biomass accumulation within poplar clones as a result of inoculations with diazotrophic endophyte consortia. *New Phytol.* 201, 599–609. doi: 10.1111/nph.12536

Laforest-Lapointe, I., Messier, C., and Kembel, S. W. (2016). Host species identity, site and time drive temperate tree phyllosphere bacterial community structure. *Microbiome* 4:27. doi: 10.1186/s40168-016-0174-1

Laforest-Lapointe, I., Paquette, A., Messier, C., and Kembel, S. W. (2017). Leaf bacterial diversity mediates plant diversity and ecosystem function relationships. *Nature* 546, 145–147. doi: 10.1038/nature22399

Lata, R., Chowdhury, S., Gond, S. K., and White, J. F. Jr. (2018). Induction of abiotic stress tolerance in plants by endophytic microbes. *Lett. Appl. Microbiol.* 66, 268–276. doi: 10.1111/lam.12855

Li, Z., Chang, S., Ye, S., Chen, M., Lin, L., Li, Y., et al. (2015). Differentiation of 1-aminocyclopropane-1-carboxylate (ACC) deaminase from its homologs is the key for identifying bacteria containing ACC deaminase. *FEMS Microbiol. Ecol.* 91:fiv112. doi: 10.1093/femsec/fiv112

Lindow, S. E., and Brandl, M. T. (2003). Microbiology of the phyllosphere. *Appl. Environ. Microbiol.* 69, 1875–1883. doi: 10.1128/aem.69.4.1875-1883.2003

Liu, F., Hewezi, T., Lebeis, S. L., Pantalone, V., Grewal, P. S., and Staton, M. E. (2019). Soil indigenous microbiome and plant genotypes cooperatively modify soybean rhizosphere microbiome assembly. *BMC Microbiol.* 19:201. doi: 10.1186/s12866-019-1572-x

Lundberg, D. S., Lebeis, S. L., Paredes, S. H., Yourstone, S., Gehring, J., Malfatti, S., et al. (2012). Defining the core *Arabidopsis thaliana* root microbiome. *Nature* 488, 86–90. doi: 10.1038/nature11237

Martin, M. (2011). Cutadapt removes adapter sequences from high-throughput sequencing reads. *EMBnet J* 17, 10–12.

Mathews, D. (2016). *Natural History of the Pacific Northwest Mountains*. Portland, OR: Timber Press, Inc.

McMurdie, P. J., and Holmes, S. (2013). phyloseq: an R package for reproducible interactive analysis and graphics of microbiome census data. *PLoS One* 8:e61217. doi: 10.1371/journal.pone.0061217

Mendes, R., Garbeva, P., and Raaijmakers, J. M. (2013). The rhizosphere microbiome: significance of plant beneficial, plant pathogenic, and human pathogenic microorganisms. *FEMS Microbiol. Rev.* 37, 634–663. doi: 10.1111/1574-6976.12028

Moore, F. P., Barac, T., Borremans, B., Oeyen, L., Vangronsveld, J., van der, L. D., et al. (2006). Endophytic bacterial diversity in poplar trees growing on a BTEX-contaminated site: the characterisation of isolates with potential to enhance phytoremediation. *Syst. Appl Microbiol.* 29, 539–556. doi: 10.1016/j.syapm.2005.11.012

Naylor, D., DeGraaf, S., Purdom, E., and Coleman-Derr, D. (2017). Drought and host selection influence bacterial community dynamics in the grass root microbiome. *ISME J.* 11, 2691–2704. doi: 10.1038/ismej.2017.118

Oksanen, J. (2011). *Multivariate Analysis of Ecological Communities in R: Vegan Tutorial*. Oulu: University of Oulu.

Pandey, P. K., Samanta, R., and Yadav, R. N. S. (2019). Inside the plant: addressing bacterial endophytes in biotic stress alleviation. *Arch. Microbiol.* 201, 415–429. doi: 10.1007/s00203-019-01642-y

Pankievicz, V. C., do Amaral, F. P., Santos, K. F., Agtuca, B., Xu, Y., Schueller, M. J., et al. (2015). Robust biological nitrogen fixation in a model grass-bacterial association. *Plant J.* 81, 907–919. doi: 10.1111/tpj.12777

Perez-Jaramillo, J. E., Carrion, V. J., de, H. M., and Raaijmakers, J. M. (2018). The wild side of plant microbiomes. *Microbiome* 6:143.

Quast, C., Pruesse, E., Yilmaz, P., Gerken, J., Schweer, T., Yarza, P., et al. (2013). The SILVA ribosomal RNA gene database project: improved data processing and web-based tools. *Nucleic Acids Res.* 41, D590–D596. doi: 10.1093/nar/gks1219

Remus-Emsermann, M. N. P., and Schlechter, R. O. (2018). Phyllosphere microbiology: at the interface between microbial individuals and the plant host. *New Phytol.* 218, 1327–1333. doi: 10.1111/nph.15054

Rho, H., Hsieh, M., Kandel, S. L., Cantillo, J., Doty, S. L., and Kim, S. H. (2017). Do endophytes promote growth of host plants under stress? A meta-analysis on plant stress mitigation by endophytes. *Microb. Ecol.* 75, 407–418. doi: 10.1007/s00248-017-1054-3

Rho, H., Van, E. V., Wegley, N., Doty, S. L., and Kim, S. H. (2018). Salicaceae endophytes modulate stomatal behavior and increase water use efficiency in rice. *Front. Plant Sci.* 9:188. doi: 10.3389/fpls.2018.00188

Rodriguez, R. J., Redman, R. S., and Henson, J. M. (2004). The role of fungal symbioses in the adaptation of plants to high stress environments. *Mitig. Adapt. Strateg. Glob. Chang.* 9, 261–272. doi: 10.1023/b:miti.0000029922.31110.97

Rufian, J. S., Sanchez-Romero, M. A., Lopez-Marquez, D., Macho, A. P., Mansfield, J. W., Arnold, D. L., et al. (2016). *Pseudomonas syringae* differentiates into phenotypically distinct subpopulations during colonization of a plant host. *Environ. Microbiol.* 18, 3593–3605. doi: 10.1111/1462-2920.13497

Saha, B. C., and Bothast, R. J. (1999). Production of 2,3-butanediol by newly isolated *Enterobacter cloacae*. *Appl. Microbiol. Biotechnol.* 52, 321–326. doi: 10.1007/s002530051526

Saikia, J., Sarma, R. K., Dhandia, R., Yadav, A., Bharali, R., Gupta, V. K., et al. (2018). Alleviation of drought stress in pulse crops with ACC deaminase producing rhizobacteria isolated from acidic soil of Northeast India. *Sci. Rep*. 8:3560. doi: 10.1038/s41598-018-21921-w

Santoyo, G., Moreno-Hagelsieb, G., Del, C. O.-M., and Glick, B. R. (2016). Plant growth-promoting bacterial endophytes. *Microbiol. Res.* 183, 92–99.

Sarris, P. F., Trantas, E. A., Mpalantinaki, E., Ververidis, F., and Goumas, D. E. (2012). *Pseudomonas viridiflava*, a multi host plant pathogen with significant genetic variation at the molecular level. *PLoS One* 7:e36090. doi: 10.1371/journal.pone.0036090

Sasse, J., Martinoia, E., and Northen, T. (2018). Feed your friends: do plant exudates shape the root microbiome? *Trends Plant Sci.* 23, 25–41. doi: 10.1016/j.tplants.2017.09.003

Scherling, C., Ulrich, K., Ewald, D., and Weckwerth, W. (2009). A metabolic signature of the beneficial interaction of the endophyte *Paenibacillus* sp. isolate and *in vitro*-grown poplar plants revealed by metabolomics. *Mol. Plant Microbe Interact.* 22, 1032–1037. doi: 10.1094/MPMI-22-8-1032

Shakya, M., Gottel, N., Castro, H., Yang, Z. K., Gunter, L., Labbe, J., et al. (2013). A multifactor analysis of fungal and bacterial community structure in the root microbiome of mature *Populus deltoides* trees. *PLoS One* 8:e76382. doi: 10.1371/journal.pone.0076382

Taghavi, S., Garafola, C., Monchy, S., Newman, L., Hoffman, A., Weyens, N., et al. (2009). Genome survey and characterization of endophytic bacteria exhibiting a beneficial effect on growth and development of poplar trees. *Appl. Environ. Microbiol.* 75, 748–757. doi: 10.1128/AEM.02239-08

Timmusk, S., Nicander, B., Granhall, U., and Tillberg, E. (1999). Cytokinin production by *Paenobacillus polymyxa*. *Soil Biol. Biochem.* 31, 1847–1852. doi: 10.1007/s12088-009-0008-y

Ullah, A., Akbar, A., Luo, Q., Khan, A. H., Manghwar, H., Shaban, M., et al. (2019). Microbiome diversity in cotton rhizosphere under normal and drought conditions. *Microb. Ecol.* 77, 429–439. doi: 10.1007/s00248-018-1260-7

Ulrich, K., Ulrich, A., and Ewald, D. (2008). Diversity of endophytic bacterial communities in poplar grown under field conditions. *FEMS Microbiol. Ecol.* 63, 169–180. doi: 10.1111/j.1574-6941.2007.00419.x

Urban, J., Ingwers, M. W., McGuire, M. A., and Teskey, R. O. (2017). Increase in leaf temperature opens stomata and decouples net photosynthesis from stomatal conductance in *Pinus taeda* and *Populus deltoides* x *nigra*. *J. Exp. Bot.* 68, 1757–1767. doi: 10.1093/jxb/erx052

Verbon, E. H., and Liberman, L. M. (2016). Beneficial microbes affect endogenous mechanisms controlling root development. *Trends Plant Sci.* 21, 218–229. doi: 10.1016/j.tplants.2016.01.013

Xin, G., Zhang, G., Kang, J. W., Staley, J. T., and Doty, S. L. (2009). A diazotrophic, indole-3-acetic acid-producing endophyte from wild cottonwood. *Biol. Fertil. Soils* 45, 669–674. doi: 10.1007/s00374-009-0377-8

Xu, L., Naylor, D., Dong, Z., Simmons, T., Pierroz, G., Hixson, K. K., et al. (2018). Drought delays development of the sorghum root microbiome and enriches for monoderm bacteria. *Proc. Natl. Acad. Sci U.S.A.* 115, E4284–E4293. doi: 10.1073/pnas.1717308115

Yuan, W., Zheng, Y., Piao, S., Ciais, P., Lombardozzi, D., Wang, Y., et al. (2019). Increased atmospheric vapor pressure deficit reduces global vegetation growth. *Sci. Adv.* 5:eaax1396. doi: 10.1126/sciadv.aax1396

Zhang, Y., Yu, X., Zhang, W., Lang, D., Zhang, X., Cui, G., et al. (2019). Interactions between endophytes and plants: beneficial effect of endophytes to ameliorate biotic and abiotic stresses in plants. *J. Plant Biol.* 62, 1–13. doi: 10.1007/s12374-018-0274-5

Conflict of Interest: The authors declare that the research was conducted in the absence of any commercial or financial relationships that could be construed as a potential conflict of interest.

frontiers in Plant Science

ORIGINAL RESEARCH
published: 26 March 2020
doi: 10.3389/fpls.2020.00348

Alleviation of Salt Stress in Upland Rice (*Oryza sativa* L. ssp. *indica* cv. Leum Pua) Using Arbuscular Mycorrhizal Fungi Inoculation

*Rujira Tisarum[1], Cattarin Theerawitaya[1], Thapanee Samphumphuang[1], Kanyamin Polispitak[2], Panarat Thongpoem[2], Harminder Pal Singh[3] and Suriyan Cha-um[1]**

[1] National Center for Genetic Engineering and Biotechnology (BIOTEC), National Science and Technology Development Agency, Khlong Luang, Thailand, [2] Devision of Biology, Faculty of Science and Technology, Rajamangala University of Technology Thanyaburi, Khlong Hok, Thailand, [3] Department of Environment Studies, Faculty of Science, Panjab University, Chandigarh, India

Arbuscular mycorrhizal fungi (AMF) symbionts not only promote the growth of host plant but also alleviate abiotic stresses. This study aimed to investigate the putative role of AMF in salt stress regulation of upland pigmented rice cv. Leum Pua (LP) comparing with Pokkali salt tolerant (positive check). In general, LP is a variety of glutinous rice that contains anthocyanin pigment in the black pericarp, due to which it possesses high antioxidant activities compared to non-pigmented rice. Pot experiment was conducted to evaluate the impact of inoculated AMF, *Glomus etunicatum* (GE), *Glomus geosporum* (GG), and *Glomus mosseae* (GM) strains, in the LP plantlets subjected to 0 (control) or 150 mM NaCl (salt stress) for 2 weeks in comparison with Pokkali (a salt tolerant rice cultivar), which was maintained as a positive check. Root colonization percentage under NaCl conditions ranged from 23 to 30%. Na^+ content in the flag leaf tissues was increased to 18–35 mg g^{-1} DW after exposure to 150 mM NaCl for 14 days in both inoculated and un-inoculated LP plants, whereas Na:K ratio was very low in cv. Pokkali. Interestingly, sucrose content in the flag leaf tissues of un-inoculated LP plants under salt stress was increased significantly by 50 folds over the control as an indicator of salt stress response, whereas it was unchanged in all AMF treatments. Fructose and free proline in GE inoculated plants under salt stress were accumulated over control by 5.75 and 13.59 folds, respectively, for osmotic adjustment of the cell, thereby maintaining the structure and functions of chlorophyll pigments, F_v/F_m, Φ_{PSII}, and stomatal function. Shoot height, flag leaf length, number of panicles, panicle length, panicle weight, and 100-grain weight in GE inoculated plants of cv. LP under salt stress were maintained similar to cv. Pokkali. Interestingly, cyanidin-3-glucoside (C3G) and peonidin-3-glucoside (P3G) in the pericarp of cv. LP were regulated by GE inoculation under salt stress conditions. In summary, AMF-inoculation in rice crop is a successful alternative approach to reduce salt toxicity, maintain the yield attributes, and regulate anthocyanins enrichment in the pericarp of grains.

Keywords: AMF-inoculation, anthocyanins, cyanidin-3-glucoside, peonidin-3-glucoside, photosynthetic abilities, salt stress, yield attributes

OPEN ACCESS

Edited by:
Collin M. Timm, Johns Hopkins University, United States

Reviewed by:
Shaozhen He, China Agricultural University, China
Melissa Cregger, Oak Ridge National Laboratory (DOE), United States

****Correspondence:***
Suriyan Cha-um
suriyanc@biotec.or.th

Specialty section:
This article was submitted to Plant Abiotic Stress, a section of the journal Frontiers in Plant Science

Received: *25 July 2019*
Accepted: *09 March 2020*
Published: *26 March 2020*

Citation:
Tisarum R, Theerawitaya C, Samphumphuang T, Polispitak K, Thongpoem P, Singh HP and Cha-um S (2020) Alleviation of Salt Stress in Upland Rice (Oryza sativa L. ssp. indica cv. Leum Pua) Using Arbuscular Mycorrhizal Fungi Inoculation. Front. Plant Sci. 11:348. doi: 10.3389/fpls.2020.00348

INTRODUCTION

Saline soil affects agricultural productivity in several regions of the world including United States, Argentina, Australia, China, Egypt, India, Iran, Iraq, Pakistan, and Thailand (i.e., an area > 800 million ha; Rengasamy, 2010). It is estimated that 5% or 3.85 million ha of the total cultivated area in the world (77 million ha) is affected by salt stress (Sheng et al., 2008), accounting by nearly 50% of arable land (Wang et al., 2003). By the year 2050, salt affected soil is predicted to be increased up to 16.2 million ha, which may result in food insecurity for world's population (Yadav et al., 2017). In Southeast Asia, 5.8 million ha arable land has been identified as salt affected (Shrestha, 2006). In Thailand, the problem of saline soil is widely distributed in Northeastern region (1.84 million ha), classifying the agricultural areas as slightly, moderately, and severely salt-affected (Arunin and Pongwichian, 2015).

Arbuscular mycorrhizal fungi (AMF) is one of the symbiotic microorganisms that regulate phosphorus (P) content, growth, and yield of the host plant (Gosling et al., 2006). AMF colonizes with root organs of the host plant, and regulates its photosynthetic abilities, growth characteristics, and abiotic stress tolerance (Panneerselvam et al., 2017; Basu et al., 2018; Mbodj et al., 2018). *Glomus mosseae* (GM), *Glomus geosporum* (GG), *Glomus intraradices*, *Acaulospora* sp., and *Scutellospora* sp. are AMF species that generally colonize with rice (Gosling et al., 2006; Maiti et al., 2013; Zhang et al., 2014; Tisarum et al., 2019). Previous studies have reported a positive relationship between AMF symbiosis and salt defense mechanisms of the host plants (Ruiz-Lozano and Azcón, 2000). For example, ion homeostasis (influx/efflux), compartmentalization (vacuolar storage), and Na^+ translocation from root to shoot via apoplastic and/or symplastic routes have been regulated by AMF-inoculation (Evelin et al., 2009; Porcel et al., 2012; He and Huang, 2013; Porcel et al., 2016; Yadav et al., 2017; Evelin et al., 2019). Better defense responses in terms of the higher production of free proline, glycine betaine, and soluble sugars in AMF inoculated plants against salt stress have also been reported (Campanelli et al., 2013; Evelin et al., 2013; Garg and Baher, 2013; Talaat and Shawky, 2014). The regulation of proline biosynthesis [pyrroline-5-carboxylate synthetase (P5CS)] and inhibition of proline degradation [proline dehydrogenase (PDH)] are evidently observed when AMF-inoculated plants are exposed to salt stress (Jahromi et al., 2008; Garg and Baher, 2013). Similarly, several antioxidant enzymes, i.e., superoxide dismutase (SOD), catalase (CAT), peroxidase (POD), and ascorbate peroxidase (APX), are upregulated as salt defense responses in AMF inoculated plants under salt stress (Borde et al., 2011; Ruiz-Lozano et al., 2012; Evelin and Kapoor, 2014; Chang et al., 2018).

Rice is an important carbohydrate crop providing a staple food to more than half of the world's population (Khush, 2005). The crop is highly susceptible to salt stress and its productivity declines even at very low concentrations of salt (Zeng and Shannon, 2000; Grattan et al., 2002). Pokkali cultivar of rice is a salt tolerant cultivar, which is used as a positive check in the screening of salt tolerant rice cultivars (Senadhira et al., 2002) and as a parental line in rice breeding programs conducted to develop salt tolerant traits (de Leon et al., 2016). In Thailand, rice is one of the major cultivating crops, and premium rice varieties with high antioxidant capacities, good cooking quality, and better fragrance are produced and exported globally (Vanavichit et al., 2018). Leum Pua (LP) is one such upland cultivar of glutinous rice with black pericarp, good cooking qualities, fine aroma, excellent flavor, high nutritional values, soft texture, and high antioxidant activities (Kerdphol et al., 2015; Nakaew and Sungthong, 2018; Piyawanitpong et al., 2018; Pornputtapitak et al., 2018; Sansenya et al., 2018; Seekhaw et al., 2018). Upland aerobic rice is known for AMF colonization (Maiti et al., 2011); however, studies investigating salt tolerance ability of AMF colonized upland rice are still lacking. Moreover, the physiological adaptations, i.e., photosynthetic pigments, chlorophyll fluorescence, net photosynthetic rate, stomatal conductance and transpiration rate, morphological responses, and yield attributes, in AMF colonized upland rice under salt stress are critically evaluated as major parameters to investigate salt toxicity (Dodd and Pérez-Alfocea, 2012; Hameed et al., 2014; Latef and Miransari, 2014; Muthukumar et al., 2017; Bhattacharjya et al., 2018). Therefore, the objective of this investigation was to evaluate the potential of three *Glomus* spp. in alleviating the salt stress in pigmented pericarp upland rice (cv. LP) based on physiological and biochemical changes, and yield traits. To the best of our knowledge, this is the first study reporting regulation of salt tolerant abilities in LP using AMF-colonization under salt stress conditions.

MATERIALS AND METHODS

Plant Material, AMF-Inoculation, and Water Deficit Treatment

Seeds of pigmented upland rice cv. "LP (salt sensitive)" and positive check cv. Pokkali (Pok; salt tolerant) were sown in the mixed soil (EC = 2.69 dS m^{-1}; pH = 5.5; organic matter = 10.36%; total nitrogen = 0.17%; total phosphorus = 0.07%, and total potassium = 1.19%) for 4 weeks. Healthy seedlings were transplanted into plastic bags containing 2 kg mixed soil in two groups: (a) sterilized soil without AMF and (b) sterilized soil with AMF species: *Glomus etunicatum* (GE; synonym *Claroideoglomus etunicatum*), GG (synonym *Funneliformis geosporum*), and GM (synonym *Funneliformis mosseae*) @ 10 g or 250 spores per plastic bag. Arbuscular mycorrhizal fungus powder was provided by Maejo University, Chiang Mai, Thailand. The powder was inoculated in the soil following the method of Pitaktamrong et al. (2018). The rice plants were grown in a net house under 500–1000 μmol m^{-2} s^{-1} photosynthetic photon flux density (PPFD) with a 10 h d^{-1} photoperiod, 35 ± 2°C (day time)/28 ± 2°C (night time) temperature, and 80 ± 5% RH until booting stage. Thereafter, Pok without AMF (Pok), LP without AMF (LP), and LP with AMF (LP + GE; LP + GG; and LP + GM) were exposed to 0 mM NaCl (control) or 150 mM NaCl (salt stress) for 14 days. Morphological characters, AMF colonization percentage, inorganic ions (Na^+, K^+, and Ca^{2+}), total phosphorus, osmotic potential, free proline, soluble sugar,

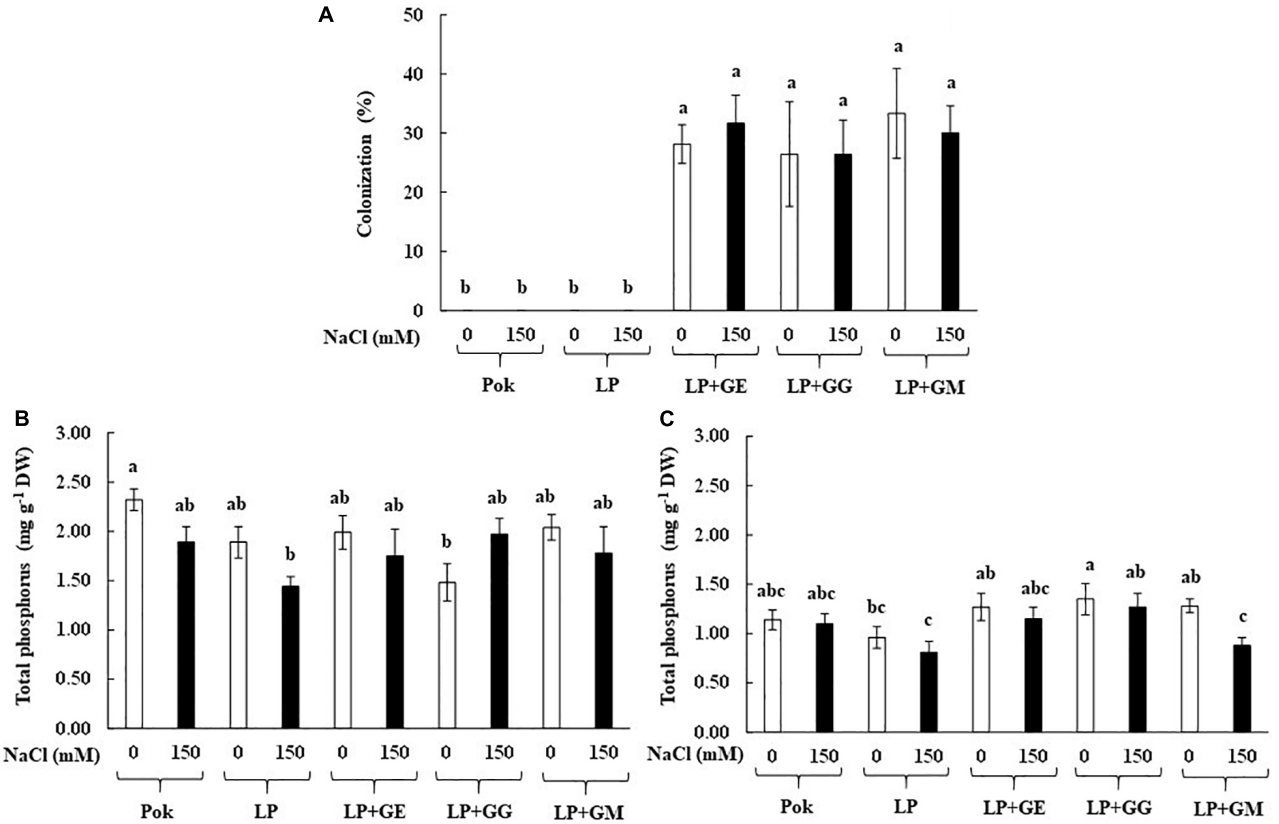

FIGURE 1 | Root AMF colonization **(A)**, total phosphorus in roots **(B)**, and flag leaf tissues **(C)** of "Leum Pua" (LP) plants inoculated with AMF (GE; *Glomus etunicatum*, GG; *G. geosporum*, and GM; *G. mosseae*) at booting stage, and subsequently exposed to salt stress conditions for 14 days. Error bar in each treatment represents by ± SE (n = 6). Different letters in each bar represent significant difference at $p \leq 0.01$ according to Tukey's HSD.

chlorophyll content, chlorophyll fluorescence, net photosynthetic rate, stomatal conductance, and transpiration rate were measured in these 10 sets of observations. In addition, the grain yield traits, number of panicles, panicle length, grain fertility percentage, panicle weight, total grain yield per clump, 100-grain weight, and anthocyanin content of cyanidin-3-glucoside (C3G) and peonidin-3-glucoside (P3G) were evaluated in the pericarp of LP rice at the time of harvest.

AMF Colonization Assay

Fresh roots (3.0 ± 0.5 cm in length) were collected from each set of observations, washed with distilled water, cut into 1.0 cm length and kept in 60% ethanol (used as a storage solution). Roots were washed thrice with distilled water, transferred to 10% KOH, and incubated at 95°C for 30 min. Cleaned roots were again washed with distilled water and stained using 0.05% (*w/v*) Trypan blue for 15 min. AMF-colonization in the roots was observed under light microscope (Zeiss, Germany) to count the arbuscules, vesicles, and mycorrhizal hyphae (**Supplementary Figure S1**), according to the method of Brundrett et al. (1996).

Plant Biochemical Analysis

Na^+, K^+, and Ca^{2+} were assayed following the modified method of Tanaka et al. (1999) and Hossain et al. (2006). In brief, flag leaf tissues were collected and washed by deionized water to remove surface contaminating ions. The tissue was ground into a powder in liquid nitrogen, extracted with boiling distilled water, and centrifuged at 10,000 × g for 10 min. The supernatant was filtered through a 0.45 μm membrane filter (VertiPure^{TM}, Vertical®). Cellular Na^+, K^+, and Ca^{2+} concentrations were determined using Waters HPLC coupled with 432 Conductivity Detector and WATER IC-PACK^{TM} ion-exclusion column (Waters Associates, Millford, MA, United States). Mobile phase, a mixed solution of 0.012 μM nitric acid and 71.73 μM Na-EDTA (ethylene diamine tetraacetic acid disodium salt dehydrate) in deionized water, was used at 0.6 mL min^{-1} flow rate. Na^+, K^+, and Ca^{2+} (Sigma, United States) were used as standards.

Available phosphorus (P) was extracted and determined spectrophotometrically as blue molybdate–phosphate complexes under partial reduction with ascorbic acid (Jackson, 1958). Briefly, 100 mg of dried root and flag leaf samples in each treatment were ground, transferred to 1 mL digestion mixture (0.42 g Se, 14 g $LiSO_4 \cdot 2H_2O$ added to 350 mL H_2O_2, and 420 mL H_2SO_4), and then placed on the hot plate (gradually increased from 50 to 150°C) until the mixture turned back. Five-hundred microliters of 72% $HClO_4$ was added to each sample and heated until the material became colorless. After cooling, the samples were diluted with equal

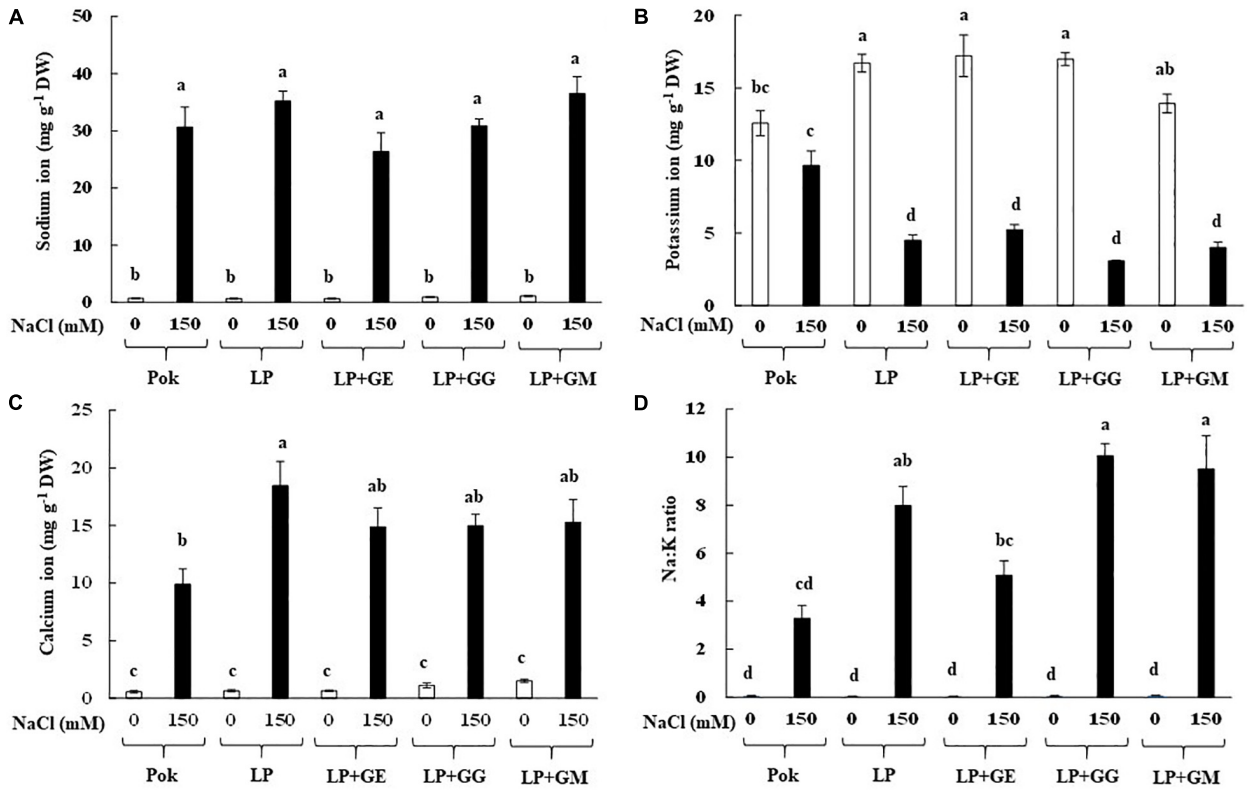

FIGURE 2 | Sodium **(A)**, potassium **(B)**, calcium **(C)** ions, and Na:K ratio **(D)** in flag leaf tissues of "Leum Pua" (LP) plants inoculated with AMF (GE; *Glomus etunicatum*, GG; *G. geosporum*, and GM; *G. mosseae*) at booting stage, and subsequently exposed to salt stress conditions for 14 days. Error bar in each treatment represents by ± SE (n = 6). Different letters in each bar represent significant difference at $p \leq 0.01$ according to Tukey's HSD.

volume of $HClO_4$, filtered (Whatman #42, United Kingdom) and then mixed with 0.5 mL of Barton's reagent [25 g ammonium molybdate (400 mL), 1.25 g ammonium meta-vanadate (350 mL), and HNO_3 (250 mL)] for 10 min. Total P (mg g^{-1} DW) was measured at 420 nm by UV-spectrophotometer (HACH DR/4000; Model 48,000, HACH Company, Loveland, CO, United States) using KH_2PO_4 as a calibration standard.

Free proline in the flag leaf tissues was extracted and analyzed according to the method of Bates et al. (1973). Fifty milligrams of fresh material was ground with liquid nitrogen in a mortar. The homogenate powder was mixed with 1 mL of aqueous sulfosalicylic acid (3%, *w/v*) and filtered through filter paper (Whatman#1, United Kingdom). The extracted solution was reacted with an equal volume of glacial acetic acid and ninhydrin reagent (1.25 mg ninhydrin in 30 mL glacial acetic acid and 20 mL 6 M H_3PO_4) and incubated at 95°C for 1 h. The reaction was terminated by placing the container in an ice bath. The reaction mixture was mixed vigorously with 2 mL of toluene. After cooling to 25°C, the chromophore was measured at 520 nm by UV–Vis spectrophotometer using L-proline as a calibration standard.

Soluble sugars (sucrose, glucose, and fructose) in the flag leaf tissues were assayed following the method of Karkacier et al. (2003). In brief, 50 mg of flag leaf sample was ground in a mortar with liquid nitrogen. One milliliter of nanopure water was added and centrifuged at 10,000 × g for 15 min. The supernatant was collected and filtered through a 0.45 μm membrane filter (VertiPure^{TM}, Vertical®). Twenty microliters of the filtrate was

TABLE 1 | Sucrose, glucose and fructose contents in "Leum Pua" (LP) plants inoculated with AMF (GE; *Glomus etunicatum*, GG; *G. geosporum*, and GM; *G. mosseae*) of rice cv. at booting stage, and subsequently exposed to salt stress conditions for 14 days.

Treatment	NaCl (mM)	Sucrose (mg g^{-1} DW)	Glucose (mg g^{-1} DW)	Fructose (mg g^{-1} DW)
Pok	0	4.67b	88.03b	139.70ab
	150	23.21b	104.97ab	159.16ab
LP	0	2.36b	97.77b	112.32bc
	150	146.72a	115.91a	166.78a
LP + GE	0	14.81b	53.80c	6.72d
	150	26.52b	58.31c	91.34bc
LP + GG	0	44.94b	47.29c	77.46c
	150	52.31b	88.02b	113.11bc
LP + GM	0	50.27b	77.76bc	121.53b
	150	55.25b	96.13b	120.41b
Significant level		**	**	**

*Pok: Pokkali, salt tolerant genotype, positive check. ** represents highly significant difference at $p \leq 0.01$. Different letters in each column show significant difference at $p \leq 0.01$ according to Tukey's HSD.*

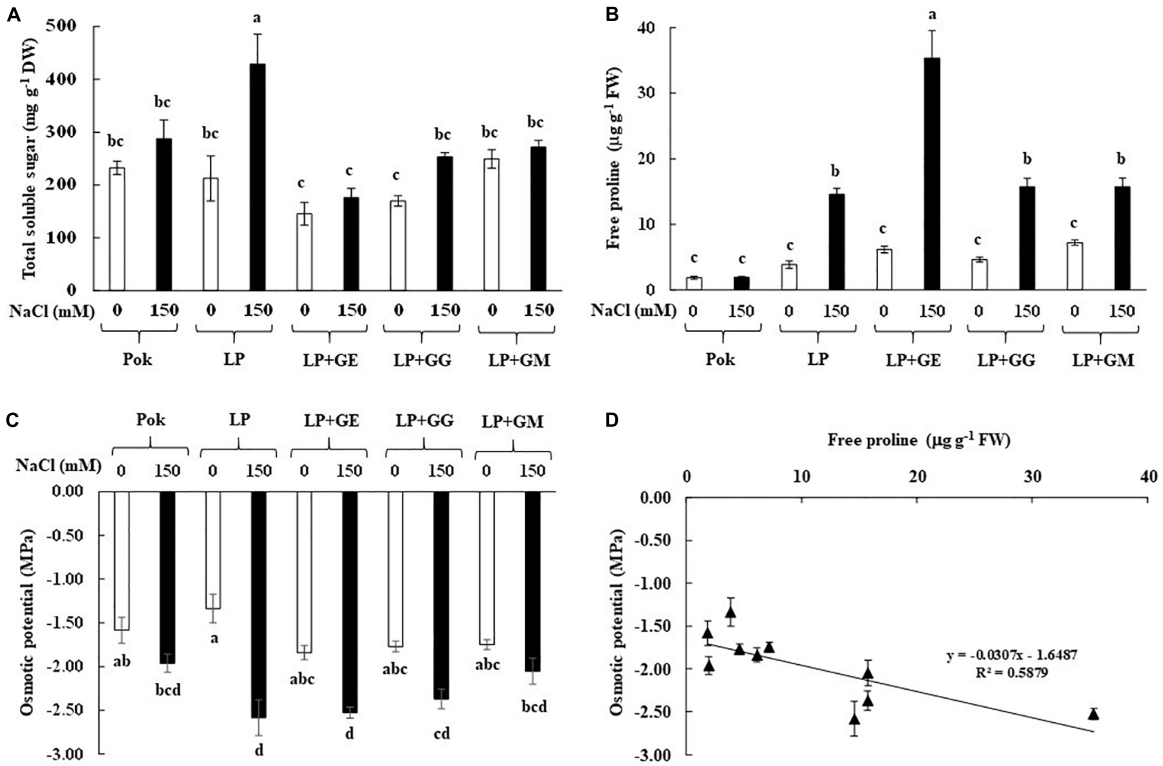

FIGURE 3 | Total soluble sugar **(A)**, free proline **(B)**, osmotic potential in flag leaf **(C)**, and relationship between free proline and osmotic potential in flag leaf **(D)** of "Leum Pua" (LP) plants inoculated with AMF (GE; *Glomus etunicatum*, GG; *G. geosporum*, and GM; *G. mosseae*) at booting stage, and subsequently exposed to salt stress conditions for 14 days. Error bar in each treatment represents by ± SE (n = 6). Different letters in each bar represent significant difference at $p \leq 0.01$ according to Tukey's HSD.

injected into a Waters HPLC equipped with a MetaCarb 87C column and a guard column. Deionized water was used as the mobile phase at a flow rate of 0.5 mL min^{-1}. The online detection was performed using a Waters 410 differential refractometer detector and the data were analyzed by Empower® software. Sucrose, glucose, and fructose (Fluka, United States) were used as the standards.

Total anthocyanins (C3G and P3G) were assayed following the method of Chandra et al. (2001). Hand-dehusked seeds (2 g) were weighed and transferred in capped glass vials and then 1.5 mL of 1% HCl in methanol were added (**Supplementary Figure S2**). Extracted solution was vortexed and kept in the dark on the shaker (150 r/min) for 12 h in the cold room (8°C). Supernatant was collected and filtered through a 0.45 µm PTFE filter (VertiPure, Vertical Chromatography). Each sample was analyzed by Waters HPLC equipped with a Waters 2998 photodiode array detector set at 520 nm, and fitted with an ODS C_{18} Hypersil column (250 mm × 4.6 mm; 5 µm, Thermo Fisher Scientific Inc., CA, United States). The mobile phase comprised of: Solvent A (0.5% aqueous phosphoric acid, *v/v*), and solvent B (water/acetonitrile/glacial acetic acid/phosphoric acid, 50: 48.5: 1: 0.5, *v/v/v/v*) used as following gradient: 0 min, 20% B (i.e., 80% solvent A and 20% solvent B); 1–26 min, 60% B, 27–30 min, 20% B, 31–35 min, 20% B (80%). Flow rate was set at 0.8 mL min^{-1}. Column temperature was set at 30°C and injection volume was 20 µL. C3G and P3G (Sigma–Aldrich, United States) were injected as standards (**Supplementary Figure S3**).

Plant Physiological Assay

Osmotic potential in the flag leaf of "LP" rice was measured according to Lanfermeijer et al. (1991). In brief, 100 mg of fresh tissue were chopped into small pieces, transferred to 1.5 mL micro tube, and then crushed using a glass rod. The 20 µL of extracted solution was dropped directly onto a filter paper in an osmometer chamber (5520 Vapro®, Wescor, UT, United States) and subsequently, the data were collected. Then, the osmolarity (mmol kg^{-1}) was converted to osmotic potential (MPa) using conversion factor of osmotic potential measurement.

Chlorophyll a (Chl_a), chlorophyll b (Chl_b), and total chlorophyll (TC) in the flag leaf tissues were analyzed according to the method of Shabala et al. (1998), whereas total carotenoid (C_{x+c}) content was assayed following the method of Lichtenthaler (1987). One hundred milligrams of leaf tissue was homogenized in glass vials using 10 mL of 99.5% acetone and blended using a homogenizer (model T25 Ultra Turrax®, IKA, Malaysia). The glass vials were sealed with Parafilm® to prevent evaporation, and then stored at 4°C for 48 h. Chl_a and Chl_b concentrations were measured at 662 and 644 nm, whereas

C_{x+c} concentration was measured at 470 nm using UV–Vis spectrophotometer against acetone (99.5%) as a blank.

Chlorophyll fluorescence emission was measured from the adaxial surface of flag leaf using a fluorescence monitoring system (model FMS 2; Hansatech Instruments Ltd., Norfolk, United Kingdom) in the pulse amplitude modulation mode (Loggini et al., 1999). A leaf, kept in dark for 30 min, was initially exposed to the modulated measuring beam of far-red light (LED source) with typical peak at wavelength 735 nm. Original (F_0) and maximum (F_m) fluorescence yields were measured under weak modulated red light (<85 μmol m^{-2} s^{-1}) with 1.6 s pulses of saturating light (>1500 μmol m^{-2} s^{-1} PPFD) and calculated using FMS software for Windows®. The variable fluorescence yield (F_v) was calculated using the equation: $F_v = F_m - F_0$. The ratio of variable to maximum fluorescence (F_v/F_m) was calculated as the maximum quantum yield of PSII photochemistry. The photon yield of PSII (Φ_{PSII}) in the light was calculated as: $F_{PSII} = (F_m'-F)/F_m'$ after 45 s of illumination, when steady state was achieved (Maxwell and Johnson, 2000).

Net photosynthetic rate (P_n; μmol m^{-2} s^{-1}), transpiration rate (E; mmol H_2O m^{-2} s^{-1}), and stomatal conductance (g_s; mmol m^{-2} s^{-1}) were measured using a Portable Photosynthesis System fitted with an Infra-red Gas Analyzer (IRGA, Model LI 6400, LI-COR® Inc., Lincoln, NE, United States). All parameters were measured continuously by monitoring the content of the air entering and exiting in the IRGA headspace chamber, according to Cha-um et al. (2007).

Plant Morphological Characterization and Yield Traits

Shoot height, number of leaves, leaf length, leaf width, and number of tillers were measured in LP rice at booting stage (**Supplementary Figure S4**). Total grain yield, number of panicles, panicle dry weight, panicle length, seed fertility, and 100-grain weight were also evaluated at harvesting stage.

TABLE 2 | Chlorophyll a (Chl_a), chlorophyll b (Chl_b), and total carotenoids (C_{x+c}) contents in "Leum Pua" (LP) plants inoculated with AMF (GE; *Glomus etunicatum*, GG; *G. geosporum*, and GM; *G. mosseae*) of rice cv. at booting stage, and subsequently exposed to salt stress conditions for 14 days.

Treatment	NaCl (mM)	Chlorophyll a (μg g^{-1} FW)	Chlorophyll b (μg g^{-1} FW)	Total carotenoids (μg g^{-1} FW)
Pok	0	63.49c	52.88c	7.46bc
	150	58.75c	51.26c	7.05bc
LP	0	233.70a	118.72a	12.60ab
	150	82.99c	76.71bc	6.24c
LP + GE	0	209.94ab	133.76a	16.66a
	150	98.88bc	88.79abc	13.39ab
LP + GG	0	214.61ab	133.82a	16.89a
	150	70.35c	66.22c	6.73c
LP + GM	0	217.01ab	135.36a	19.00a
	150	72.69c	68.10c	7.91*bc*
Significant level		**	**	**

*Pok: Pokkali, salt tolerant genotype, positive check. ** represents highly significant difference at $p \leq 0.01$. Different letters in each column show significant difference at $p \leq 0.01$ according to Tukey's HSD.*

Statistical Analysis

The experiment was arranged as Completely Randomized Design (CRD) with six biological replicates ($n = 6$) in each treatment. The mean values obtained from 10 set of observations were compared using Tukey's HSD and analyzed by SPSS software (version 11.5 for Window®).

RESULTS AND DISCUSSION

AMF Colonization and Total P Assay

Arbuscular mycorrhizal fungi colonization percentage in the root tissues of rice cv. LP inoculated with GE, GG, and GM was found to be >26%, irrespective of the salt treatment (**Figure 1A**). Total P content in the root tissues was greater than that of leaf tissues. Under salt stress, total P content in the root tissues was nearly same in the inoculated and un-inoculated plants. In addition, P content in the root tissues of rice cv. Pokkali (Pok) under control was greater than cv. LP as well as LP + GG (**Figure 1B**). On the other hand, P content in leaf tissues of LP + GG (1.35 mg g^{-1} DW) was greater than LP (0.81 mg g^{-1} DW) by 1.67 folds (**Figure 1C**). Moreover, P content in the leaf tissues of LP + GM under salt stress declined by 31.25% over the control.

In the present study, root colonization of AMF inoculated plants was evidently demonstrated in both control and salt stress conditions, whereas it was undetected in un-inoculated plants. As per a previous report inoculation of AM fungus isolated from salt affected soil (Cabo de Gata Natural Park, Spain) showed a positive relation between degree of salt treatments (75 and 150 mM NaCl) and root colonization, and also increased the total P in both shoots and roots (Porcel et al., 2016). Interestingly, root colonization of Rhizophagus *intraradices* (collected), *C. etunicatum*, and *Septoglomus constrictum* was alleviated by salt-treated (66 and 100 mM NaCl) maize plants (Estrada et al., 2013a). In contrast, when *Glomus* spp. collected from rhizosphere of maize plants was inoculated in wheat plants, and subsequently exposed to salt stress, a decline in AM-fungal colonization, especially at high salinity levels (4.7 and 9.4 dS m^{-1}) was observed (Talaat and Shawky, 2014). Similarly, in alfalfa, colonization percentage of AMF (*Glomus viscosum*) was sharply declined, in relation to the degree of salt treatments (100–150 mM NaCl) (Campanelli et al., 2013). Colonization percentage of *R. intraradices*, *Massilia* sp. RK4, and their mixtures (collected from rhizosphere of the *Phragmites* sp., Saemangeum reclamation land, South Korea) in maize plants was significantly dropped when subjected to 40 and 80 mM NaCl for 22 days (Krishnamoorthy et al., 2016). In *Leymus chinensis* seedlings, AM root colonization was only detected in AMF inoculation under salt stress (100–200 mM NaCl), whereas it was undetected in un-inoculated plants (Lin et al., 2017).

Na^+, K^+, Ca^{2+}, and Na: K Ratio

Na^+ levels in the flag leaf tissues of rice cvs. Pok (30.66 mg g^{-1} DW) and LP (35.20 mg g^{-1} DW) were increased in response

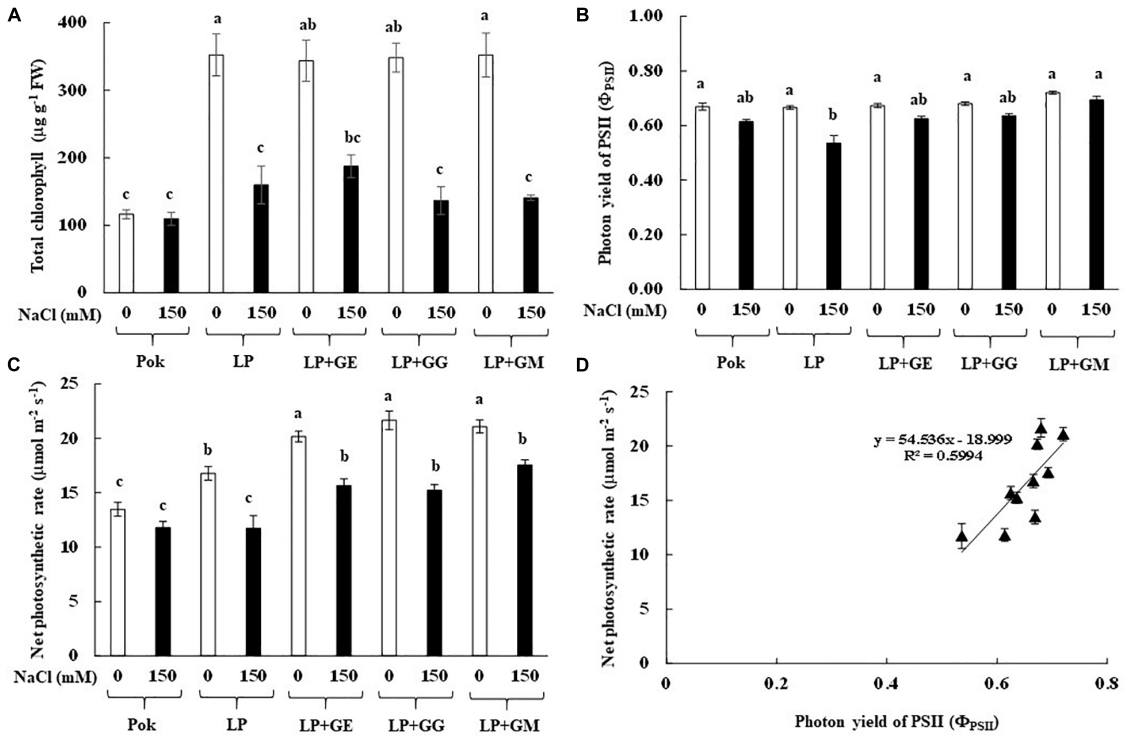

FIGURE 4 | Total chlorophyll content **(A)**, photon yield of PSII **(B)**, net photosynthetic rate **(C)**, and relationship between photon yield of PSII and net photosynthetic rate in flag leaf **(D)** of "Leum Pua" (LP) plants inoculated with AMF (GE; *Glomus etunicatum*, GG; *G. geosporum*, and GM; *G. mosseae*) at booting stage, and subsequently exposed to salt stress conditions for 14 days. Error bar in each treatment represents by ± SE (n = 6). Different letters in each bar represent significant difference at $p \leq 0.01$ according to Tukey's HSD.

to 150 mM NaCl treatment over the control by 43.20 and 52.50 folds, respectively (**Figure 2A**). Compared to control, 32.90–40.60 folds increase in Na^+ level in AMF inoculated plants (GE, GG, and GM) in LP under salt stress was observed. Interestingly, K^+ in LP was significantly decreased when plants, both with and without AMF, were exposed to 150 mM NaCl salt stress for 14 days, while it was maintained in cv. Pok (**Figure 2B**). Ca^{2+} was found to be 18.47 mg g^{-1} DW in LP without AMF under salt stress (28.4 folds over control), whereas it was 9.89 mg g^{-1} DW in Pok under salt stress (17.7 folds over control) (**Figure 2C**). Na:K ratio in salt stressed LP plants, both with and without AMF, was significantly increased; however, it was maintained in cv. Pok (**Figure 2D**).

Na^+ and Ca^{2+} were accumulated (by > 10 folds) in the flag leaf tissues of rice cvs. Pok and LP under 150 mM NaCl for 14 days irrespective of AMF-inoculation, whereas K^+ in LP declined, leading to greater Na^+:K^+ ratio. Therefore, Na^+ enrichment in LP with GE, GG, or GM was lower than that of LP without AMF inoculation. Na^+ in AMF (*R. intraradices*, *Massilia* sp. RK4, and their mixtures) inoculated maize (cv. Shrunken-2) plants grown under 40 mM NaCl for 17 days was lower than that in the plants without AMF-inoculation (Krishnamoorthy et al., 2016). Similarly, Na^+ in shoots of AMF (*R. intraradices*, *C. etunicatum*, and *S. constrictum*) inoculated maize plants under 66 and 100 mM NaCl was lower than that in the plants without AMF (Estrada et al., 2013a). In wheat cv. Henta, Na^+ in shoots of AMF (GM and *Glomus deserticola*) inoculated plants was significantly lesser than in un-inoculated plants and *Gigaspora gergaria* inoculated plants (Abdel-Fattah and Asrar, 2012). In

TABLE 3 | Maximum quantum yield of PSII (F_v/F_m), stomatal conductance (g_s), and transpiration rate (E) in AMF-inoculated plants (GE; *Glomus etunicatum*, GG; *G. geosporum*, and GM; *G. mosseae*) of rice cv. "Leum Pua" (LP) at booting stage subsequently exposed to salt stress conditions for 14 days.

Treatment	NaCl (mM)	F_v/F_m	g_s (mmol H_2O m^{-2} s^{-1})	E (mmol H_2O m^{-2} s^{-1})
Pok	0	0.865a	0.42a	4.28ab
	150	0.793ab	0.32ab	3.60b
LP	0	0.839ab	0.29b	3.98ab
	150	0.629c	0.20c	2.83c
LP + GE	0	0.858a	0.40ab	4.98a
	150	0.818ab	0.32ab	4.13ab
LP + GG	0	0.842ab	0.39ab	4.77a
	150	0.812ab	0.32ab	4.09ab
LP + GM	0	0.844ab	0.35ab	5.01a
	150	0.818ab	0.31ab	4.20ab
Significant level		**	**	**

*Pok: Pokkali, salt tolerant genotype, positive check. ** represents highly significant difference at p ≤ 0.01. Different letters in each column show significant difference at p ≤ 0.01 according to Tukey's HSD.*

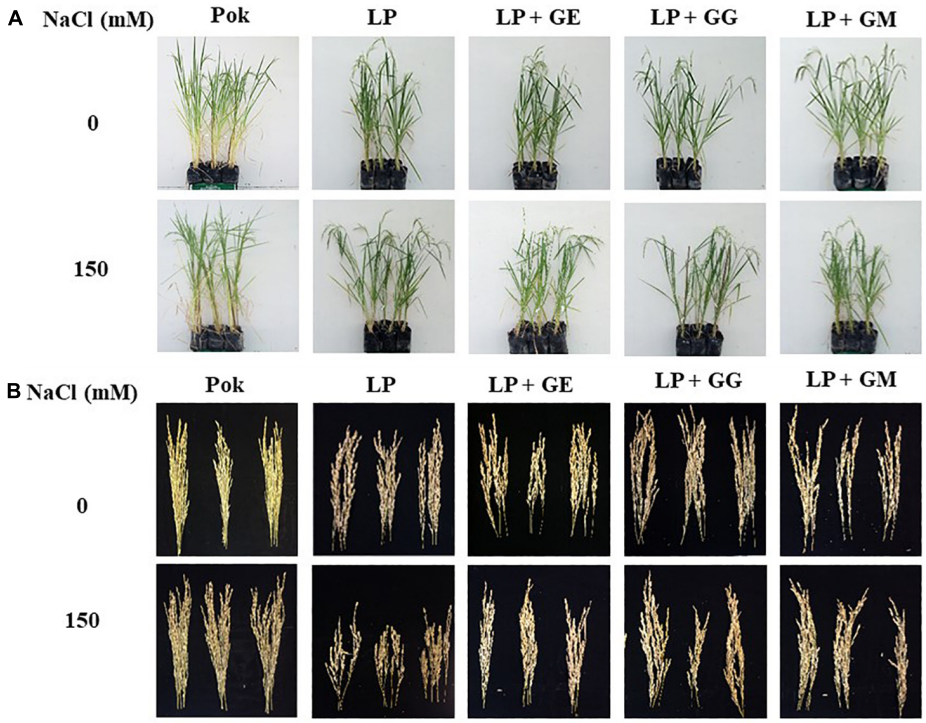

FIGURE 5 | Overall growth performances **(A)** and panicles **(B)** of "Leum Pua" (LP) plants inoculated with AMF (GE; *Glomus etunicatum*, GG; *G. geosporum*, and GM; *G. mosseae*) at booting stage, and subsequently recovered until grain harvesting process.

alfalfa cv. icon, low levels of Na^+ in AMF inoculated plants were demonstrated when compared with the control (Campanelli et al., 2013). In citrus (red tangerine) seedlings, Na^+ enrichment is generally antagonist with K^+ when subjected to 100 mM NaCl for 60 days and also, Na^+ in AMF inoculated plants (GM and *Paraglomus occultum*) was significantly lower than in un-inoculated plants (Wu et al., 2010). Moreover, Na^+ in AMF inoculated wheat cv. Sids 1 was unchanged, whereas it was increased in cv. Giza 168 over AMF un-inoculated plants, in response to the degree of salinity levels (Talaat and Shawky, 2014). Interestingly, Na^+ in the shoots of rice cv. Puntal with AMF-inoculation (*C. etunicatum*) was similar to that of the un-inoculated plants, whereas Na^+ levels in the root tissues of AMF-inoculated plants were higher than control and this involved upregulation of plasma membrane Na^+/H^+ antiporter (*OsSOS1*) and high affinity potassium transporter (*OsHKT2;1*) (Porcel et al., 2016). In addition, it was confirmed that expression of vacuolar Na^+/H^+ antiporter gene (*LeNHX1*) in the root tissues of salt-stressed tomato was upregulated by AMF (GM) inoculation (He and Huang, 2013).

Soluble Sugar, Free Proline, Osmotic Potential, and Their Relationship

Sucrose, glucose, and fructose contents in flag leaf tissues were increased when subjected to 150 mM NaCl. Sucrose, glucose and fructose contents in LP plants without AMF under salt stress were peaked at 147.2, 115.9, and 166.7 mg g^{-1} DW and enriched by 62.17, 1.19, and 1.48 folds over the control, respectively (**Table 1**). Interestingly, fructose in GE-pretreated plants and glucose in GG-pretreated plants of cv. LP exposed to 150 mM NaCl were increased by 13.59 and 1.86 folds over control, respectively (**Table 1**). Total soluble sugar in LP without AMF was found to be the maximum (2.02 folds over control) when exposed to salt stress. It was maintained at low levels in AMF-pretreated plants similar to that of salt tolerant rice, Pok (**Figure 3A**). Free proline in Pok was observed to be similar in both control and salt stressed plants. In contrast, it was significantly high in salt stressed plants of cv. LP by 3.79 folds, LP + GM by 2.19 folds, LP + GG by 3.39 folds, and LP + GE by 5.74 folds over control (**Figure 3B**). Osmotic potential in salt stressed flag leaf of cv. Pok was maintained, whereas it was significantly declined in LP (1.93 folds over control) and LP + GE (1.37 folds over control). Interestingly, it was retained in LP + GG and LP + GM under 150 mM NaCl (**Figure 3C**). Moreover, a negative relationship between free proline content and osmotic potential was demonstrated ($R^2 = 0.5879$; **Figure 3D**).

In rice crop, flag leaf at booting stage is reported to be very sensitive to salt stress (Wankhade et al., 2013). In general, total soluble carbohydrates in the leaf tissues of AMF-colonized plants of trifoliate orange (Zou and Wu, 2011) and chickpea (Garg and Bharti, 2018) were upregulated. In trifoliate orange (*Poncirus trifoliata*), only sucrose was accumulated in the leaves of plants grown under 100 mM NaCl for 7 weeks, whereas glucose and fructose were unchanged even in the plants inoculated with GM and *Glomus versiforme* (Zou and

TABLE 4 | Shoot height, flag leaf length, number of panicles, and panicle length in "Leum Pua" (LP) plants inoculated with AMF (GE; *Glomus etunicatum*, GG; *G. geosporum*, and GM; *G. mosseae*) of rice cv. at booting stage, and subsequently exposed to salt stress conditions for 14 days.

Treatment	NaCl (mM)	Shoot height (cm)	Flag leaf length (cm)	Number of panicles	Panicle length (cm)
Pok	0	126.3a	49.5a	5.3a	27.1a
	150	115.3a	48.7a	4.2ab	26.8a
LP	0	87.4b	29.7b	3.5b	22.6ab
	150	82.1b	26.8b	3.0b	18.8b
LP + GE	0	86.3b	22.0b	3.0b	23.8ab
	150	82.3b	20.8b	3.0b	21.1ab
LP + GG	0	88.2b	27.9b	3.0b	22.4ab
	150	84.0b	24.0b	2.3b	21.4ab
LP + GM	0	88.2b	28.3b	3.2b	24.8a
	150	87.3b	26.7b	2.5b	21.7ab
Significant level		**	**	**	**

*Pok: Pokkali, salt tolerant genotype, positive check. ** represents highly significant difference at $p \leq 0.01$. Different letters in each column show significant difference at $p \leq 0.01$ according to Tukey's HSD.*

Wu, 2011). In contrast, sucrose in chickpea cvs. PBG 5 (salt tolerant) and BG 256 (salt sensitive), inoculated with *R. intraradices*, was declined in response to the degree of salt stress. Glucose and total soluble sugar in salt tolerant PBG 5 (both with or without AMF-inoculation) were gradually increased when subjected to salt stress (Garg and Bharti, 2018). Total soluble sugars in several plants, i.e., wheat, fenugreek, and two legumes (soybean and cluster bean) grown under salt stress were found to vary in accordance to the degree of salt stress, AMF species, and the symbiotic interactions (Evelin et al., 2013; Datta and Kulkarni, 2014a; Talaat and Shawky, 2014). Interestingly, free proline content in salt tolerant cv. Pok was maintained at low levels, whereas it was enriched by 5.74-folds in salt stressed LP with GE inoculation, over the control. An increasing rate of free proline accumulation in the salt stressed plants has been reported in wheat genotypes, tomato cultivars, and mustard plants in relation to salt-tolerant abilities (Hajiboland et al., 2010; Talaat and Shawky, 2014; Sarwat et al., 2016). On the other hand, free proline enrichment varies according to different species of AMF as seen from the differences observed between GM, *Glomus fasciculatum* (GF), and mixed GM + GF inoculation in *Acacia arabica* (Datta and Kulkarni, 2014b); *R. intraradices*, *C. etunicatum*, and *Septoglomus conicatum* inoculation in maize (Estrada et al., 2013a); and *GM*, *G. deserticola*, and *G. gergaria* inoculation in wheat (Abdel-Fattah and Asrar, 2012). It was confirmed that the P5CS plays a major role in proline biosynthesis under salt stress in both salt tolerant PBG-5 and salt sensitive CSG-9505 genotypes of chickpea (Jahromi et al., 2008; Garg and Baher, 2013). Free proline and total soluble sugars are the major osmolytes in AMF-inoculated plants under salt stress that control the osmotic potential at the cellular level, leading to enhanced salt tolerant ability (Campanelli et al., 2013; Yang et al., 2014; Evelin et al., 2019). Free proline enrichment in the salt stressed plants with AMF inoculation plays a key role as osmotic adjustment (Chun et al., 2018), which confirmed the function as osmolytes by mitigation of NaCl stress in mustard plant (Sarwat et al., 2016).

Physiological Responses to Salt Stress

Chl_a, Chl_b, and C_{x+c} degradation in cv. Pok under salt stress was low as compared to the cv. LP, where these declined by 64.49, 35.39, and 44.05% over the control, respectively (**Table 2**). In LP + GE, Chl_a, Chl_b, and C_{x+c} in flag leaf tissues were maintained when subjected to salt stress. In contrast, those parameters in LP + GG and LP + GM under salt stress were sharply dropped by ≥50% (**Table 2**). In addition, TC content in salt stressed plants of cv. Pok was maintained, whereas it was significantly degraded in LP (54.68% over control), LP + GE (45.39% over control), LP + GG (60.79% over control), and LP + GM (60.04% over control) (**Figure 4A**). F_v/F_m, Φ_{PSII}, g_s, and E in the flag leaf of cv. Pok under salt stress were retained, while these were lowered in cv. LP by 25.03, 19.52, 31.03, and 28.89%, respectively (**Table 3** and **Figure 4B**). However, these parameters were maintained by GE, GG, and GM inoculation even when exposed to salt stress (**Table 3**). P_n is a very sensitive parameter to salt stress; however, it was maintained in cv. Pok even under salt stress. In AMF inoculated plants, it was significantly declined by 30.10, 22.31, 29.64, and 16.75% over the control in cv. LP, LP + GE, LP + GG, and LP + GM, respectively (**Figure 4C**). A positive relation between Φ_{PSII} and P_n was also established ($R^2 = 0.5994$; **Figure 4D**).

In the present study, chlorophyll pigments: Chl_a, Chl_b, and C_{x+c}, in GE-inoculated LP plants under salt stress were unchanged, leading to stabilized F_v/F_m, Φ_{PSII}, and P_n, whereas these were degraded by >50% over the control in LP without AMF inoculation. Previously, Chl_a and Chl_b in rice crop cv. Puntal with AMF-inoculation (*C. etunicatum*, isolate EEZ 163) were elevated when compared with non-AMF inoculated crop, both subjected to 150 mM NaCl for 4 weeks (Porcel et al., 2015). Chl_a and Chl_b in AMF-inoculated plants of false wheatgrass (*L. chinensis* symbiont with GM) and wheat (*Triticum aestivum* L. cvs. Sids 1 and Giza 168 symbiont with a mixture of *Glomus* spp.), were alleviated under both normal and salt stressed conditions (Talaat and Shawky, 2014; Lin et al., 2017). Moreover, plant–microbe interactions are another factor that regulates the salt tolerant abilities in the host plants. For example, Chl_a, Chl_b, and C_{x+c} in AMF-inoculated wheat grown with GM under saline soil (860 mg kg^{-1} Na^+) for 8 and 12 weeks were observed to be higher than those in un-inoculated plants and AMF-inoculated plants with *G. deserticola* and *G. gergaria* (Abdel-Fattah and Asrar, 2012). Consequently, F_v/F_m, Φ_{PSII}, P_n, g_s, and E in AMF-inoculated rice cv. Puntal were promoted under both control and salt stressed conditions (Porcel et al., 2015). In maize, F_v/F_m and g_s in plants inoculated with *C. etunicatum*, *R. intraradices*, and *Septoglomus claroideum* under 100 mM NaCl for 30 days were alleviated compared to the un-inoculated plants (Estrada et al., 2013b). In rice crop cv. Puntal, efficiency of PSII and g_s in salt stressed plants (75 and 150 mM NaCl for 4 weeks) were significantly improved using *C. etunicatum* isolate EEZ 163 (Porcel et al., 2016). Based on this evidence, it can be suggested

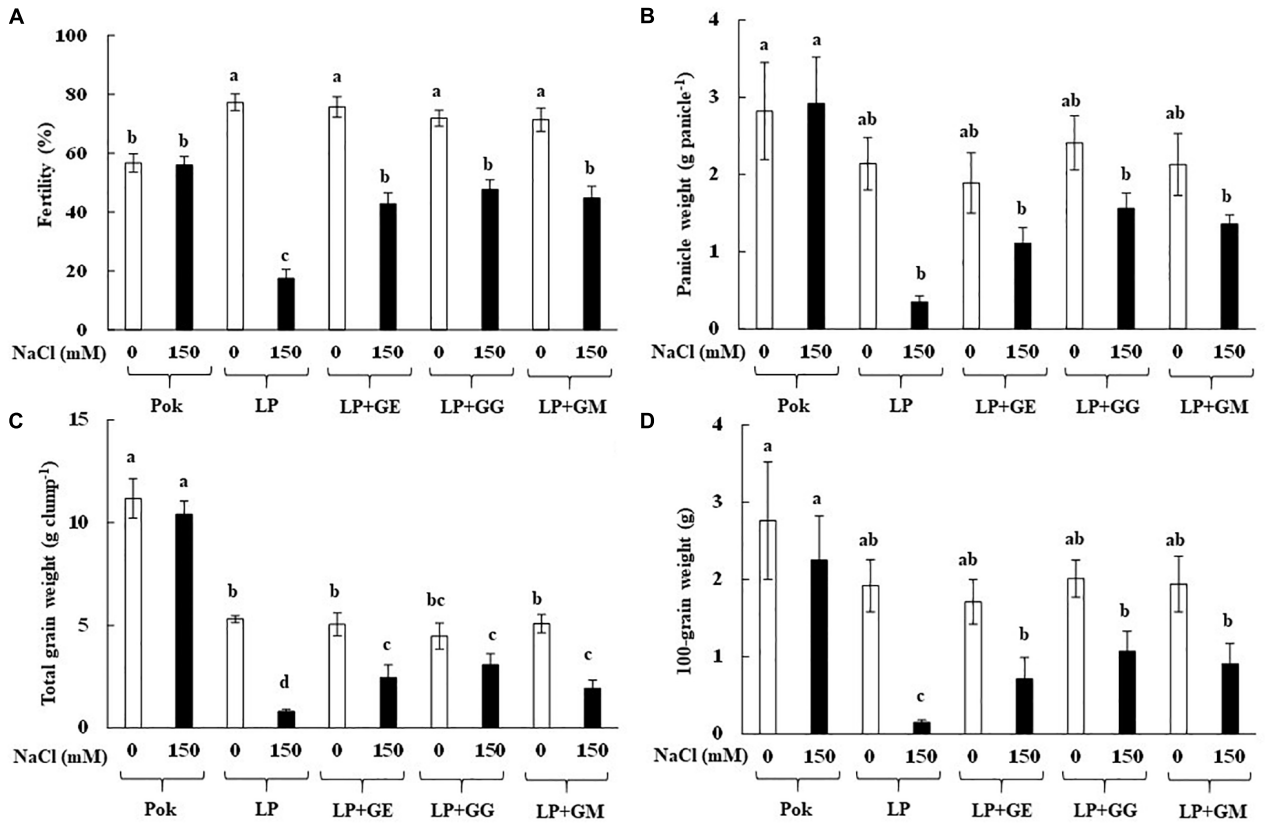

FIGURE 6 | Grain fertility **(A)**, panicle weight **(B)**, total grain weight **(C)**, and 100 grain weight **(D)** of "Leum Pua" (LP) plants inoculated with AMF (GE; *Glomus etunicatum*, GG; *G. geosporum*, and GM; *G. mosseae*) at booting stage, and subsequently recovered until grain harvesting process. Error bar in each treatment represents by ± SE (n = 6). Different letters in each bar represent significant difference at $p \leq 0.01$ according to Tukey's HSD.

that the regulation of osmolytes and antioxidant activities in AMF-inoculated plant grown under salt stress plays a major role in salt defense mechanisms and reduction of electrolyte leakage at the cellular level (Estrada et al., 2013b). Moreover, the photosynthetic efficiencies in AMF-inoculated plants under salt stress are found to be dependent on type of plant species, genotypic variations, AMF genus/species/strain, degree of salt stress, and their interactions (Wu et al., 2010). A positive relationship between Φ_{PSII} and P_n with a high correlation coefficient has been observed in rice crop ($R^2 = 0.691$; Porcel et al., 2015) and black locust ($R^2 = 0.789$; Zhu et al., 2014), leading to retain the yield attributes.

Morphological Changes

Morphological and phenological characters in cvs. Pok and LP under control and salt stress were also observed (**Figure 5**). Shoot height, flag leaf length, number of panicle, and panicle length were greater in cv. Pok than in cv. LP. Moreover, these parameters were unchanged when plants were subjected to 150 mM NaCl for 14 days (**Table 4**). Fertility percentage in cv. Pok under salt stress was unchanged, whereas it was sharply declined by 77.39, 43.48, 33.68, and 37.31% over control in LP, LP + GE, LP + GG, and LP + GM, respectively (**Figure 5A**). Panicle weight, total grain weight, and 100-grain weight were unchanged in salt stressed rice cv. Pok and LP + GG (**Figures 6B–D**). In contrast, panicle weight, total grain weight, and 100-grain weight in salt stressed rice cv. LP were significantly declined by 83.65, 84.91, and 92.19%, respectively, over the control. It was confirmed that LP is a salt susceptible variety of rice crop. However, yield attributes such as fertility, panicle weight, total grain weight, and 100-grain weight in AMF-inoculated plants of LP salt stressed rice showed significant improvement compared with un-inoculated plants (**Figure 6**).

In the present study, shoot height in LP plants exposed to salt stress was unchanged irrespective of the AMF inoculation. In general, shoot height improves by AMF inoculation, but is subsequently inhibited by salt concentrations (Yano-Melo et al., 2003; Campanelli et al., 2013) and different AMF species (GM, *G. deserticola*, and *G. gergaria*) (Abdel-Fattah and Asrar, 2012). In rice crop cv. Puntal, shoot fresh weight and shoot dry weight of AMF-inoculated plants (*C. etunicatum*) under salt stress (75 and 150 mM NaCl) were greater than those in un-inoculated plants (Porcel et al., 2015, 2016). Likewise, number of panicles, panicle weight, grain yield, and 1000-grain weight in rice crop inoculated with AMF (*Sebacina vermifera*) and subjected to salt stress (3, 6, and 9 dS m^{-1} EC_e NaCl)

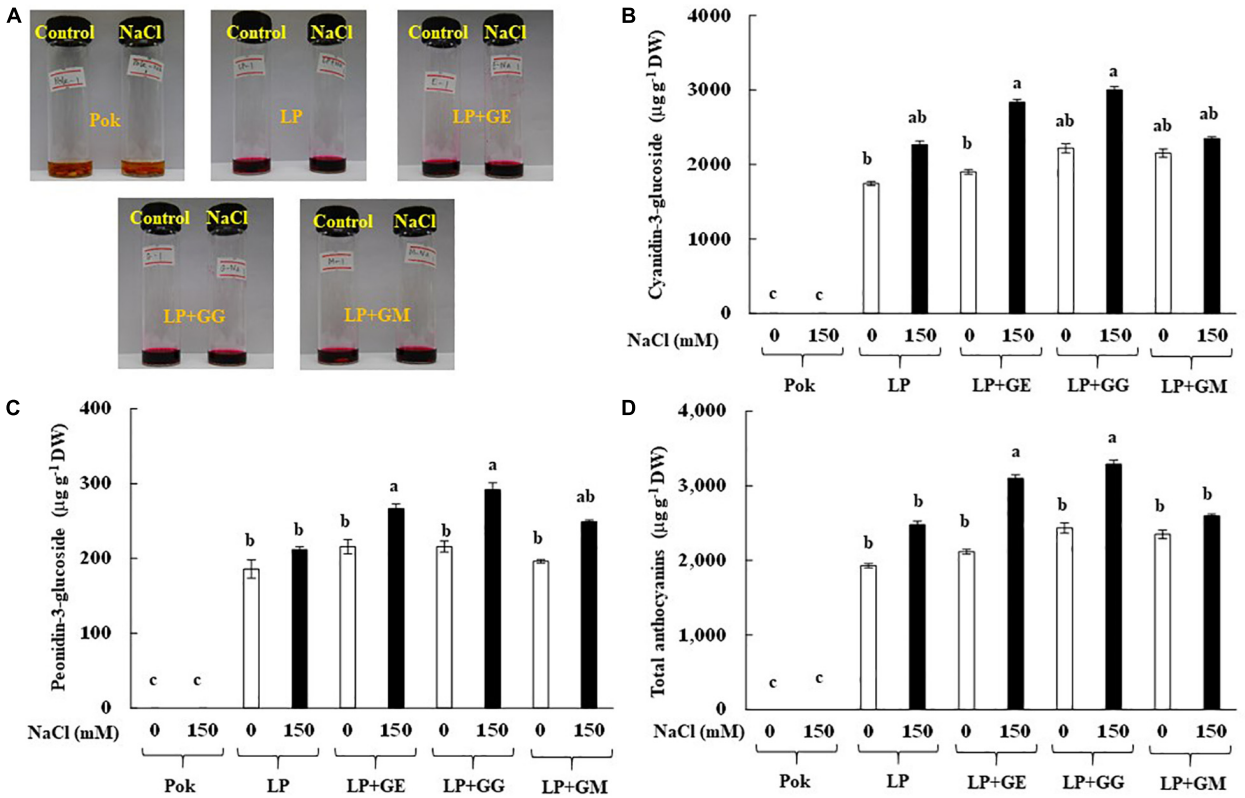

FIGURE 7 | HCl-methanolic extracted solution of rice grain **(A)**, cyanidin-3-glucoside (C3G; **B**), peonidin-3-glucoside (P3G; **C**), and total anthocyanins **(D)** of "Leum Pua" (LP) plants inoculated with AMF (GE; *Glomus etunicatum*, GG; *G. geosporum*, and GM; *G. mosseae*) at booting stage, and subsequently recovered until grain harvesting process. Error bar in each treatment represents by ± SE (n = 6). Different letters in each bar represent significant difference at $p \leq 0.01$ according to Tukey's HSD.

performed better than that of un-inoculated plants, but again depending on the degree of salt stress (Pirdashti et al., 2012). In wheat cvs. Sids 1 and Giza 168, number of grains per plant and grain yield per plant were significantly improved by AMF-inoculation (mixed *Glomus* spp.) under salt stress [4.7 and 9.4 dS m^{-1} (a mixture of NaCl, $CaCl_2$ and $MgSO_4$ at molar ratio of 2:2:1)] (Talaat and Shawky, 2014). In maize, the salt tolerant abilities (66 and 100 mM NaCl) in terms of shoot dry weight of plants subjected to different AMF strains, *R. intraradices* and *C. etunicatum*, were significantly improved than in plants without AMF and those inoculated with *S. claroideum* (Estrada et al., 2013a,b). Moreover, yield per pot, 1000-grain weight, and grains per ear of AMF-inoculated (*Piriformospora indica*) barley cvs. Ingrid and Annabell grown under salt stress were greater than that of the un-inoculated plants (Waller et al., 2005).

Anthocyanin Analysis

Extracted solution of anthocyanins using 1% HCl in methanol solvent is presented in **Figure 7A**. Interestingly, C3G, P3G, and total anthocyanins in cv. Pok were absent, whereas these were accumulated in the pericarp of cv. LP, especially in the AMF-inoculated plants subjected to salt stress (**Figures 7B–D**). In LP + GE, C3G, P3G, and total anthocyanins in salt stressed pericarp of rice grains were increased by 1.49, 1.24, and 1.47 folds over the control, respectively (**Figures 7B–D**). P3G and total anthocyanins in LP + GG under salt stress were significantly increased by 1.35 and 1.35% over the control, respectively (**Figures 7C,D**). In addition, the regulation of C3G and P3G chromatogram profiles in LP rice cultivar under salt stress was evidently demonstrated (**Figure 8**).

Total anthocyanin enrichment in the pericarp of rice grain depends on genotype and the biotic and/or abiotic environmental elicitors. In the present study, anthocyanins in the red pericarp of Pok were absent, whereas two species of anthocyanins, C3G and P3G, were present in cv. LP. In lettuce, anthocyanins in the inner and outer leaves of cv. Maravilla de Verano (MV) were accumulated in higher amounts than Batavia RubiaMurguia (BRM) (Baslam et al., 2011). Anthocyanins were evidently dominated in the stem and whole plant of basil varieties, i.e., Cinnamon, Siam Queen, Sweet Dani, and Red Rubin, whereas these were undetected in the roots (Seagel, 2012). In addition, anthocyanin accumulation in pericarp of rice grain inoculated by AMF and exposed to NaCl salt elicitor was clearly observed. In strawberry fruits, C3G, P3G, and pelagonidin-3-rutinoside (P3R) were alleviated in plants grown under AMF (*Glomus* sp.) + *Pseudomonas* bacteria + 70% fertilization

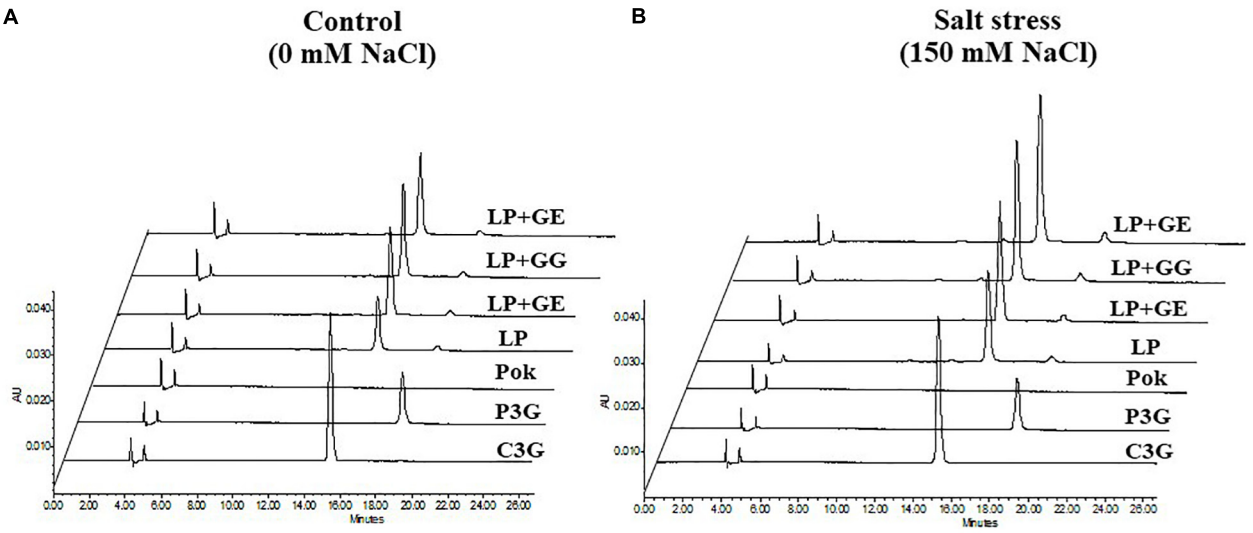

FIGURE 8 | HPLC profiles of cyanidin-3-glucoside (C3G) and peonidin-3-glucoside (P3G) of "Leum Pua" (LP) plants inoculated with AMF (GE; *Glomus etunicatum*, GG; *G. geosporum*, and GM; *G. mosseae*) at booting stage exposed to control **(A)** and salt stress **(B)** conditions for 14 days, and subsequently recovered until grain harvesting process.

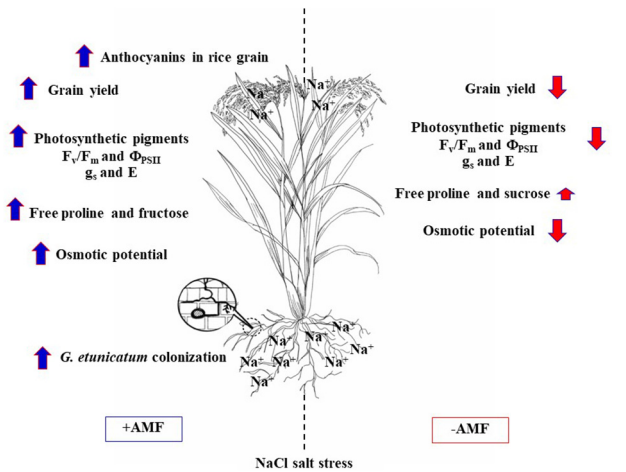

FIGURE 9 | A summary of GE (*Glomus etunicatum*) regulation on salt tolerant ability of "Leum Pua" (LP) plants at booting stage and subsequently recovered until grain harvesting process.

(Lingua et al., 2013). Total anthocyanins were increased in lettuce in AMF (commercial inoculation; mixed *G. intraradices* and GM) inoculated plants compared to plants without AMF (Baslam et al., 2011). It is possible that AMF and NaCl salt may regulate the anthocyanin biosynthesis pathway, via targeting several enzymes, i.e., phenylalanine ammonialyase (PAL), chalcone synthase (CHS), and flavonol synthase (FLS) (Abdallah et al., 2016; Battini et al., 2016). In contrast, proanthocyanidins in the leaves of AMF (*Gigaspora albida* and *Acaulospora longula*) inoculated "Aroeira-do-sertão" were unchanged when compared to plants without inoculation (da Silva and Maia, 2018). Likewise, total anthocyanins declined in the leaves of *Cicer arietinum* cvs. PGB5 (salt tolerant) and BG256 (salt susceptible), inoculated with AMF (*R. intraradices*) in response to the degree of NaCl salt treatments (Garg and Bharti, 2018). Moreover, accumulation of anthocyanins in rice grain varies with the species of *Glomus* genus, as seen from the greater accumulation of anthocyanins in grains-derived from GG and GE pretreated plants compared to plants with GM inoculation. In lettuce cvs. Cogollos de Tudela, BRM, and Maravia de Verano, GF, *G. intraradices*, and GM evidently regulated carotenoids (neoxanthin, violaxanthin, antheraxanthin, zeaxanthin, lutein, lactucaxanthin, and β-carotene) and tocopherols (α-, β-, and γ-tocopherols), thereby demonstrating their role as biotic elicitors (Baslam et al., 2013).

CONCLUSION

Root colonization by GE, GG, and GM was detected irrespective of the salt treatment. GG inoculation leads to high level of phosphorus accumulation in flag leaf of rice crop cv. LP, whereas Na^+ was trend to increase in salt-treated plants similar to cv. Pok (salt tolerant). Photosynthetic abilities, chlorophyll pigments, Chl_a fluorescence, and stomatal function in flag leaf of LP inoculated with GE grown under salt stress were stabilized by the production of total soluble sugars and free proline that acted as osmolytes to reduce salt toxicity. Therefore, the yield attributes were maintained, and anthocyanins content was enhanced in the pericarp of rice cv. LP inoculated with GE (**Figure 9**).

DATA AVAILABILITY STATEMENT

All datasets for this study are included in the article/**Supplementary Material**.

AUTHOR CONTRIBUTIONS

SC carried out the experiment, data analysis, a draft of manuscript preparation, and played a role as corresponding author. RT analyzed anthocyanins (C3G and P3G) and physiological data. CT did soluble sugar analysis and data analysis. TS assayed free proline and overall growth performances. KP conducted the experiment, AMF-colonization and total phosphorus analysis, and yield attributes. PT played a role as project coordinator and a discussion on manuscript preparation. HS performed a critical reading, comments, suggestion, and grammatical checking before submission.

FUNDING

The authors would like to sincerely thank The Thailand Research Fund (TRF) for funding support (Grant No. SRI5920201) and National Science and Technology Development Agency (NSTDA) for partial support to CT as post-doctoral scholarship and Young Scientist and Technologist Program (YSTP) for partial support to KP.

ACKNOWLEDGMENTS

Also, we would like to thank Dr. Supatida Aumtong, Maejo University, Chiang Mai, Thailand, for providing three species of *Glomus* AMF.

SUPPLEMENTARY MATERIAL

The Supplementary Material for this article can be found online at: https://www.frontiersin.org/articles/10.3389/fpls.2020.00348/full#supplementary-material

REFERENCES

Abdallah, S. B., Aung, B., Amyot, L., Lalin, I., Lachâal, M., Karray-Bouraoui, N., et al. (2016). Salt stress (NaCl) affects plant growth and branch pathways of carotenoid and flavonoid biosynthesis in *Solanum nigrum*. *Acta Physiol. Plant* 38:72. doi: 10.1007/s11738-016-2096-8

Abdel-Fattah, G. M., and Asrar, A. W. A. (2012). Arbuscular mycorrhizal fungal application to improve growth and tolerance of wheat (*Triticum aestivum* L.) plants grown in saline soil. *Acta Physiol. Plant* 34, 267–277. doi: 10.1007/s11738-011-0825-6

Arunin, S., and Pongwichian, P. (2015). Salt-affected soils and management in Thailand. *Bull. Soc. Sea Water Sci.* 69, 319–325. doi: 10.11457/swsj.69.319

Baslam, M., Esteban, R., García-Plazaola, J. I., and Goicoechea, N. (2013). Effectiveness of arbuscular mycorrhizal fungi (AMF) for inducing the accumulation of major carotenoids, chlorophylls and tocopherol in green and red leaf lettuces. *Appl. Microbiol. Biotechnol.* 97, 3119–3128. doi: 10.1007/s00253-012-4526-x

Baslam, M., Pascual, I., Sánchez-Díaz, M., Erro, J., García-Mina, J. M., and Goicoechea, N. (2011). Improvement of nutritional quality of greenhouse-grown lettuce by arbuscular mycorrhizal fungi is conditioned by the source of phosphorus nutrition. *J. Agric. Food Chem.* 59, 11129–11140. doi: 10.1021/jf202445y

Basu, S., Rabara, R. C., and Negi, S. (2018). AMF: the future prospect for sustainable agriculture. *Physiol. Mol. Plant Pathol.* 102, 36–45. doi: 10.1016/j.pmpp.2017.11.007

Bates, L. S., Waldren, R. P., and Teare, I. D. (1973). Rapid determination of free proline for water-stress studies. *Plant Soil* 39, 205–207. doi: 10.1007/BF00018060

Battini, F., Bernardi, R., Turrini, A., Agnolucci, M., and Giovannetti, M. (2016). *Rhizophagus intraradices* or its associated bacteria affect gene expression of key enzymes involved in the rosmarinic acid biosynthetic pathway of basil. *Mycorrhiza* 26, 699–707. doi: 10.1007/s00572-016-0707-2

Bhattacharjya, S., Bhaduri, D., and Sahu, A. (2018). Arbuscular mycorrhizal fungi: a potential tool for enhancing crop productivity in salt affected soil. *Inter. J. Agric. Environ. Biotechnol.* 11, 871–880. doi: 10.30954/0974-1712.12.2018.8

Borde, M., Dudhane, M., and Jite, P. (2011). Growth photosynthetic activity and antioxidant responses of mycorrhizal and non-mycorrhizal bajra (*Pennisetum glaucum*) crop under salinity stress condition. *Crop Prot.* 30, 265–271. doi: 10.1016/j.cropro.2010.12.010

Brundrett, M., Bougher, N., Dell, B., Grove, T., and Malajczuk, N. (1996). *Working with Mycorrhizas in Forestry and Agriculture. ACIAR Monograph 32*. Canberra, ACT: Australian Centre for International Agricultural Research, 373.

Campanelli, A., Ruta, C., de Mastro, G., and Morone-Fortunato, I. (2013). The role of arbuscular mycorrhizal fungi in alleviating salt stress in *Medicago sativa* L. var. icon. *Symbiosis* 59, 65–76. doi: 10.1007/s13199-012-0191-1

Chandra, A., Rana, J., and Li, Y. (2001). Separation, identification, quantification, and method validation of anthocyanins in botanical supplement raw materials by HPLC and HPLC-MS. *J. Agric. Food Chem.* 49, 3515–3521. doi: 10.1021/jf010389p

Chang, W., Sui, X., Fan, X. X., Jia, T. T., and Song, F. Q. (2018). Arbuscular mycorrhizal symbiosis modulates antioxidant response and ion distribution in salt-stressed *Elaeagnus angustifolia* seedlings. *Front. Microbiol.* 9:652. doi: 10.3389/fmicb.2018.00652

Cha-um, S., Supaibulwatana, K., and Kirdmanee, C. (2007). Glycinebetaine accumulation, physiological characterizations and growth efficiency in salt-tolerant and salt-sensitive lines of indica rice (*Oryza sativa* L. ssp. *indica*) in response to salt stress. *J. Agron. Crop Sci.* 193, 157–166. doi: 10.1111/j.1439-037X.2007.00251.x

Chun, S. C., Paramasivan, M., and Chandrasekaran, M. (2018). Proline accumulation influenced by osmotic stress in arbuscular mycorrhizal symbiotic plants. *Front. Microbiol.* 9:2525. doi: 10.3389/fmicb.2018.02525

da Silva, F. S. B., and Maia, L. C. (2018). Mycorrhization and phosphorus may be an alternative for increasing the production of metabolites in *Myracrodruon urundeuva*. *Theor. Exp. Plant Physiol.* 30, 297–302. doi: 10.1007/s40626-018-0123-4

Datta, P., and Kulkarni, M. (2014b). Arbuscular mycorrhizal colonization improves growth and biochemical profile in *Acacia arabica* under salt stress. *J. Biosci. Biotechnol.* 3, 235–245.

Datta, P., and Kulkarni, M. V. (2014a). Arbuscular mycorrhizal colonization enhances biochemical status and mitigates adverse salt effect on two legumes. *Not. Sci. Biol.* 6, 381–393. doi: 10.15835/nsb639250

de Leon, T. B., Linscombe, S., and Subudhi, P. K. (2016). Molecular dissection of seedling salinity tolerance in rice (*Oryza sativa* L.) using a high-density GBS-based SNP linkage map. *Rice* 9:52. doi: 10.1186/s12284-016-0125-2

Dodd, I. C., and Pérez-Alfocea, F. (2012). Microbial amelioration of crop salinity stress. *J. Exp. Bot.* 63, 3415–3428. doi: 10.1093/jxb/ers033

Estrada, B., Aroca, R., Barea, J. M., and Ruiz-Lozano, J. M. (2013b). Native arbuscular mycorrhizal fungi isolated from a saline habitat improved maize antioxidant systems and plant tolerance to salinity. *Plant Sci.* 201, 42–51. doi: 10.1016/j.plantsci.2012.11.009

Estrada, B., Aroca, R., Maathuis, F. J., Barea, J. M., and Ruiz−Lozano, J. M. (2013a). Arbuscular mycorrhizal fungi native from a Mediterranean saline area enhance maize tolerance to salinity through improved ion homeostasis. *Plant Cell Environ.* 36, 1771–1782. doi: 10.1111/pce.12082

Evelin, H., Devi, T. S., Gupta, S., and Kapoor, R. (2019). Mitigation of salinity stress in plants by arbuscular mycorrhizal symbiosis: current understanding and new challenges. *Front. Plant Sci.* 10:470. doi: 10.3389/fpls.2019.00470

Evelin, H., Giri, B., and Kapoor, R. (2013). Ultrastructural evidence for AMF mediated salt stress mitigation in *Trigonella foenum-graecum*. *Mycorrhiza* 23, 71–86. doi: 10.1007/s00572-012-0449-8

Evelin, H., and Kapoor, R. (2014). Arbuscular mycorrhizal symbiosis modulates antioxidant response in salt-stressed *Trigonella foenum-graecum* plants. *Mycorrhiza* 24, 197–208. doi: 10.1007/s00572-013-0529-4

Evelin, H., Kapoor, R., and Giri, B. (2009). Arbuscular mycorrhizal fungi in alleviation of salt stress: a review. *Ann. Bot.* 104, 1263–1280. doi: 10.1093/aob/mcp251

Garg, N., and Baher, A. (2013). Role of arbuscular mycorrhizal symbiosis in proline biosynthesis and metabolism of *Cicer arietinum* L. (chickpea) genotypes under salt stress. *J. Plant Growth Regul.* 32, 767–778. doi: 10.1007/s00344-013-9346-4

Garg, N., and Bharti, A. (2018). Salicylic acid improves arbuscular mycorrhizal symbiosis, and chickpea growth and yield by modulating carbohydrate metabolism under salt stress. *Mycorrhiza* 28, 727–746. doi: 10.1007/s00572-018-0856-6

Gosling, P., Hodge, A., Goodlass, G., and Bending, G. D. (2006). Arbuscular mycorrhizal fungi and organic farming. *Agric. Ecosyst. Environ.* 113, 17–35. doi: 10.1016/j.agee.2005.09.009

Grattan, S., Zeng, L., Shannon, M., and Roberts, S. (2002). Rice is more sensitive to salinity than previously thought. *California Agric.* 56, 189–198. doi: 10.3733/ca.v056n06p189

Hajiboland, R., Aliasgharzadeh, N., Laiegh, S. F., and Poschenrieder, C. (2010). Colonization with arbuscular mycorrhizal fungi improves salinity tolerance of tomato (*Solanum lycopersicum* L.) plants. *Plant Soil* 331, 313–327. doi: 10.1007/s11104-009-0255-z

Hameed, A., Dilfuza, E., Abd-Allah, E. F., Hashem, A., Kumar, A., and Ahmad, P. (2014). "Salinity stress and arbuscular mycorrhizal symbiosis in plants," in *Use of Microbes for the Alleviation of Soil Stresses*, ed. M. Miransari (New York, NY: Springer), 139–159.

He, Z., and Huang, Z. (2013). Expression analysis of *LeNHX1* gene in mycorrhizal tomato under salt stress. *J. Microbiol.* 51, 100–104. doi: 10.1007/s12275-013-2423-3

Hossain, G. S., Waditee, R., Hibino, T., Tanaka, Y., and Takabe, T. (2006). Root specific expression of Na^+/H^+ antiporter gene from *Synechocystis* sp. PCC6803 confers salt tolerance of tobacco plant. *Plant Biotechnol.* 23, 275–281. doi: 10.5511/plantbiotechnology.23.275

Jackson, M. L. (1958). *Soil Chemical Analysis*. Englewood Cliffs, NJ: Prentice Hall.

Jahromi, F., Aroca, R., Porcel, R., and Ruiz-Lozano, J. M. (2008). Influence of salinity on the *in vitro* development of *Glomus intraradices* and on the *in vivo* physiological and molecular responses of mycorrhizal lettuce plants. *Microbiol. Ecol.* 55, 45–53. doi: 10.1007/s00248-007-9249-7

Karkacier, M., Ebras, M., Uslu, M. K., and Aksu, M. (2003). Comparison of different extraction and detection methods for sugars using amino-bonded phase HPLC. *J. Chromatog. Sci.* 41, 331–333. doi: 10.1093/chromsci/41.6.331

Kerdphol, R., Sreewongchai, T., Sripichitt, P., Uckarach, S., and Worede, F. (2015). Obtaining a black pericarp and improved aroma using genetic resources from Leum Pua rice. *Sci. Asia* 41, 93–96. doi: 10.2306/scienceasia1513-1874.2015.41.093

Khush, G. S. (2005). What it will take to feed 5.0 billion rice consumers in 2030. *Plant Mol. Biol.* 59, 1–6.

Krishnamoorthy, R., Kim, K., Subramanian, P., Senthilkumar, M., Anandham, R., and Sa, T. (2016). Arbuscular mycorrhizal fungi and associated bacteria isolated from salt-affected soil enhances the tolerance of maize to salinity in coastal reclamation soil. *Agric. Ecosyst. Environ.* 231, 233–239. doi: 10.1016/j.agee.2016.05.037

Lanfermeijer, F. C., Koerselman-Kooij, J. W., and Borstlap, A. C. (1991). Osmosensitivity of sucrose uptake by immature pea cotyledons disappears during development. *Plant Physiol.* 95, 832–838. doi: 10.1104/pp.95.3.832

Latef, A. A. H. A., and Miransari, M. (2014). "The role of arbuscular mycorrhizal fungi in alleviation of salt stress," in *Use of Microbes for the Alleviation of Soil Stresses*, ed. M. Miransari (New York, NY: Springer), 23–38.

Lichtenthaler, H. K. (1987). Chlorophylls and carotenoids: pigments of photosynthetic biomembranes. *Method Enzymol.* 148, 350–380.

Lin, J., Wang, Y., Sun, S., Mu, C., and Yan, X. (2017). Effects of arbuscular mycorrhizal fungi on the growth, photosynthesis and photosynthetic pigments of *Leymus chinensis* seedlings under salt-alkali stress and nitrogen deposition. *Sci. Total Environ.* 576, 234–241. doi: 10.1016/j.scitotenv.2016.10.091

Lingua, G., Bona, E., Manassero, P., Marsano, F., Todeschini, V., Cantamessa, S., et al. (2013). Arbuscular mycorrhizal fungi and plant growth-promoting pseudomonads increases anthocyanin concentration in strawberry fruits (*Fragaria*×*ananassa* var. Selva) in conditions of reduced fertilization. *Inter. J. Mol. Sci.* 14, 16207–16225. doi: 10.3390/ijms140816207

Loggini, B., Scartazza, A., Brugnoli, E., and Navari-Izzo, F. (1999). Antioxidant defense system, pigment composition, and photosynthetic efficiency in two wheat cultivars subjected to drought. *Plant Physiol.* 119, 1091–1100. doi: 10.1104/pp.119.3.1091

Maiti, D., Singh, C. V., Variar, M., Mandal, N. P., and Anantha, M. S. (2013). Impact of rainfall pattern on native arbuscular-mycorrhizal activity influencing phosphorus utilization by direct seeded rainfed upland rice (*Oryza sativa* L.). *Proc. Nat. Acad. Sci. U.S.A.* 83, 159–162. doi: 10.1007/s40011-012-0132-z

Maiti, D., Variar, M., and Singh, R. K. (2011). Optimizing tillage schedule for maintaining activity of the arbuscular mycorrhizal fungal population in a rainfed upland rice (*Oryza sativa* L.) agro-ecosystem. *Mycorrhiza* 21, 167–171. doi: 10.1007/s00572-010-0324-4

Maxwell, K., and Johnson, G. N. (2000). Chlorophyll fluorescence-a practical guide. *J. Exp. Bot.* 51, 659–668. doi: 10.1093/jexbot/51.345.659

Mbodj, D., Effa-Effa, B., Kane, A., Manneh, B., Gantet, P., Lapaze, L., et al. (2018). Arbuscular mycorrhizal symbiosis in rice: establishment, environmental control and impact on plant growth and resistance to abiotic stresses. *Rhizosphere* 8, 12–26. doi: 10.1016/j.rhisph.2018.08.003

Muthukumar, T., Bagyaraj, D. J., and Ashwin, R. (2017). "Arbuscular mycorrhizal fungi: Role in alleviating salt stress in crop plants," in *Microbes for Plant Stress Management*, eds D. J. Bagyaraj and Jamaluddin (New Delhi: New India Publishing Agency), 221–243.

Nakaew, N., and Sungthong, R. (2018). Seed phytochemicals shape the community structures of cultivable actinobacteria—inhabiting plant interiors of Thai pigmented rice. *Microbiol. Open* 7:e00591. doi: 10.1002/mbo3.591

Panneerselvam, P., Kumar, U., Sugitha, T. C. K., Parameswaran, C., Sahoo, S., Binodh, A. K., et al. (2017). "Arbuscular mycorrhizal fungi (AMF) for sustainable rice production," in *Advances in Soil Microbiology: Recent Trends and Future Prospects, Microorganisms for Sustainable*, Vol. 4, eds T. Adhya, B. Mishra, K. Annapurna, D. Verma, U. Kumar (Singapore: Springer), 99–126.

Pirdashti, H., Yaghoubian, Y., Goltapeh, E., and Hosseini, S. (2012). Effect of mycorrhiza-like endophyte (*Sebacina vermifera*) on growth, yield and nutrition of rice (*Oryza sativa* L.) under salt stress. *J. Agric. Technol.* 8, 1651–1661.

Pitaktamrong, P., Kingkaew, J., Yooyongwech, S., Cha-um, S., and Phisalaphong, M. (2018). Development of arbuscular mycorrhizal fungi-organic fertilizer pellets encapsulated with alginate film. *Eng. J.* 22, 65–79. doi: 10.4186/ej.2018.22.6.65

Piyawanitpong, C., Therdthai, N., and Ratphitagsanti, W. (2018). Effect of precooking and superheated steam treatment on quality of black glutinous rice. *J. Food Qual.* 2018, 1–9. doi: 10.1155/2018/8496723

Porcel, R., Aroca, R., Azcón, R., and Ruiz-Lozano, J. M. (2016). Regulation of cation transporter genes by the arbuscular mycorrhizal symbiosis in rice plants subjected to salinity suggests improved salt tolerance due to reduced Na^+ root-to-shoot distribution. *Mycorrhiza* 26, 673–684. doi: 10.1007/s00572-016-0704-5

Porcel, R., Aroca, R., and Ruiz-Lozano, J. M. (2012). Salinity stress alleviation using arbuscular mycorrhizal fungi. A review. *Agron. Sustain. Dev.* 32, 181–200. doi: 10.1007/s13593-011-0029-x

Porcel, R., Redondo-Gómez, S., Mateos-Naranjo, E., Aroca, R., Garcia, R., and Ruiz-Lozano, J. M. (2015). Arbuscular mycorrhizal symbiosis ameliorates the optimum quantum yield of photosystem II and reduces non-photochemical quenching in rice plants subjected to salt stress. *J. Plant Physiol.* 185, 75–83. doi: 10.1016/j.jplph.2015.07.006

Pornputtapitak, W., Pantakitcharoenkul, J., Panpakdee, R., Teeranachaideekul, V., and Sinchaipanid, N. (2018). Development of γ-oryzanol rich extract from Leum Pua glutinous rice bran loaded nanostructured lipid carriers for topical delivery. *J. Oleo Sci.* 67, 125–133. doi: 10.5650/jos.ess17113

Rengasamy, P. (2010). Soil processes affecting crop production in salt-affected soils. *Funct. Plant Biol.* 37, 613–620. doi: 10.1071/FP09249

Ruiz-Lozano, J. M., and Azcón, R. (2000). Symbiotic efficiency and infectivity of an autochthonous arbuscular mycorrhizal *Glomus* sp. from saline soils and *Glomus deserticola* under salinity. *Mycorrhiza* 10, 137–143. doi: 10.1007/s005720000075

Ruiz-Lozano, J. M., Porcel, R., Azcón, C., and Aroca, R. (2012). Regulation by arbuscular mycorrhizae of the integrated physiological response to salinity in plants: new challenges in physiological and molecular studies. *J. Exp. Bot.* 63, 4033–4044. doi: 10.1093/jxb/ers126

Sansenya, S., Hua, Y., and Chumanee, S. (2018). The correlation between 2-acetyl-1-pyrroline content, biological compounds and molecular characterization to the aroma intensities of Thai local rice. *J. Oleo Sci.* 67, 893–904. doi: 10.5650/jos.ess17238

Sarwat, M., Hashem, A., Ahanger, M. A., Abd-Allah, E. F., Alqarawi, A. A., Alyemeni, M. N., et al. (2016). Mitigation of NaCl stress by arbuscular mycorrhizal fungi through the modulation of osmolytes, antioxidants and secondary metabolites in mustard (*Brassica juncea* L.) plants. *Front. Plant Sci.* 7:869. doi: 10.3389/fpls.2016.00869

Seagel, C. F. (2012). Phenolic composition of basil plants differentially altered by plant nutrient status and inoculation with mycorrhizal fungi. *HortScience* 47, 660–671. doi: 10.21273/HORTSCI.47.5.660

Seekhaw, P., Mahatheeranont, S., Sookwong, P., Luangkamin, S., Neonplab, A. N. L., and Puangsombat, P. (2018). Phytochemical constituents of Thai dark purple glutinous rice bran extract [cultivar LuemPua (*Oryza sativa* L.)]. *Chiang Mai J. Sci.* 45, 1383–1395.

Senadhira, D., Zapata-Arias, F. J., Gregorio, G. B., Alejar, M. S., de la Cruz, H. C., Padolina, T. F., et al. (2002). Development of the first salt-tolerant rice cultivar through indica/indica anther culture. *Field Crop. Res.* 76, 103–110. doi: 10.1016/S0378-4290(02)00032-1

Shabala, S. N., Shabala, S. I., Martynenko, A. I., Babourina, O., and Newman, I. A. (1998). Salinity effect on bioelectric activity growth, Na^+ accumulation and chlorophyll fluorescence of maize leaves: a comparative survey and prospects for screening. *Aust. J. Plant Physiol.* 25, 609–616. doi: 10.1071/PP97146

Sheng, M., Tang, M., Chen, H., Yang, B., Zhang, F., and Huang, Y. (2008). Influence of arbuscular mycorrhizae on photosynthesis and water status of maize plants under salt stress. *Mycorrhiza* 18, 287–296. doi: 10.1007/s00572-008-0180-7

Shrestha, R. P. (2006). Relating soil electrical conductivity to remote sensing and other soil properties for assessing soil salinity in Northeast Thailand. *Land Degrad. Dev.* 17, 677–689. doi: 10.1002/ldr.752

Talaat, N. B., and Shawky, B. T. (2014). Protective effects of arbuscular mycorrhizal fungi on wheat (*Triticum aestivum* L.) plants exposed to salinity. *Environ. Exp. Bot.* 98, 20–31. doi: 10.1016/j.envexpbot.2013.10.005

Tanaka, K., Ohta, K., Haddad, P. R., Fritz, J. S., Lee, K. P., Hasebe, K., et al. (1999). Acid-rain monitoring in East Asia with a portable-type ion-exclusion-cation-exchange chromatographic analyzer. *J. Chromatog. A* 850, 311–317. doi: 10.1016/S0021-9673(99)00286-1

Tisarum, R., Theerawitaya, C., Samphumphuang, T., Phisalaphong, M., Singh, H. P., and Cha-um, S. (2019). Promoting water deficit tolerance and anthocyanin fortification in pigmented rice cultivar (*Oryza sativa* L. subsp. *indica*) using arbuscular mycorrhizal fungi inoculation. *Physiol. Mol. Biol. Plant.* 25, 821–835. doi: 10.1007/s12298-019-00658-4

Vanavichit, A., Kamolsukyeunyong, W., Siangliw, M., Siangliw, J. L., Traprab, S., Ruengphayak, S., et al. (2018). Thai Hom Mali Rice: origin and breeding for subsistence rainfed lowland rice system. *Rice* 11:20. doi: 10.1186/s12284-018-0212-7

Waller, F., Achatz, B., Baltruschat, H., Fodor, J., Becker, K., Fischer, M., et al. (2005). The endophytic fungus *Piriformospora indica* reprograms barley to salt-stress tolerance, disease resistance, and higher yield. *Proc. Nat. Acad. Sci. U.S.A.* 102, 13386–13391. doi: 10.1073/pnas.0504423102

Wang, W., Vinocur, B., and Altman, A. (2003). Plant responses to drought, salinity and extreme temperatures: towards genetic engineering for stress tolerance. *Planta* 218, 1–14. doi: 10.1007/s00425-003-1105-5

Wankhade, S. D., Cornejo, M. J., Mateu-Andrés, I., and Sanz, A. (2013). Morpho-physiological variations in response to NaCl stress during vegetative and reproductive development of rice. *Acta Physiol. Plant.* 35, 323–333. doi: 10.1007/s11738-012-1075-y

Wu, Q. S., Zou, Y. N., and He, X. H. (2010). Contributions of arbuscular mycorrhizal fungi to growth, photosynthesis, root morphology and ionic balance of citrus seedlings under salt stress. *Acta Physiol. Plant.* 32, 297–304. doi: 10.1007/s11738-009-0407-z

Yadav, R. S., Mahatma, M. K., Thirumalaisamy, P. P., Meena, H. N., Bhaduri, D., Arora, S., et al. (2017). "Arbuscular mycorrhizal fungi (AMF) for sustainable soil and plant health in salt-affected soils," in *Bioremediation of Salt Affected Soils: An Indian Perspective*, eds S. Arora, A. K. Singh, and Y. P. Singh (Cham: Springer), 133–156.

Yang, S. J., Zhang, Z. L., Xue, Y. X., Zhang, Z. F., and Shi, S. Y. (2014). Arbuscular mycorrhizal fungi increase salt tolerance of apple seedlings. *Bot. Stud.* 55:70. doi: 10.1186/s40529-014-0070-6

Yano-Melo, A. M., Saggin, O. J. Jr., and Maia, L. C. (2003). Tolerance of mycorrhized banana (*Musa* sp. cv. Pacovan) plantlets to saline stress. *Agric. Ecosyst. Environ.* 95, 343–348. doi: 10.1016/S0167-8809(02)00044-0

Zeng, L., and Shannon, M. C. (2000). Salinity effects on seedling growth and yield components of rice. *Crop Sci.* 40, 996–1003. doi: 10.2135/cropsci2000.404996x

Zhang, S., Wang, L., Ma, F., Bloomfield, K. J., Yang, J., and Atkin, O. K. (2014). Is resource allocation and grain yield of rice altered by inoculation with arbuscular mycorrhizal fungi? *J. Plant Ecol.* 8, 436–448. doi: 10.1093/jpe/rtu025

Zhu, X. Q., Wang, C. Y., Chen, H., and Tang, M. (2014). Effects of arbuscular mycorrhizal fungi on photosynthesis, carbon content, and calorific value of black locust seedlings. *Photosynthetica* 52, 247–252. doi: 10.1007/s11099-014-0031-z

Zou, Y. N., and Wu, Q. S. (2011). Sodium chloride stress induced changes in leaf osmotic adjustment of trifoliate orange (*Poncirus trifoliata*) seedlings inoculated with mycorrhizal fungi. *Not. Bot. Horti Agrobo. Cluj Napoca* 39, 64–69. doi: 10.15835/nbha3926243

Conflict of Interest: The authors declare that the research was conducted in the absence of any commercial or financial relationships that could be construed as a potential conflict of interest.

frontiers in Microbiology

ORIGINAL RESEARCH
published: 25 May 2020
doi: 10.3389/fmicb.2020.01052

Unraveling the Complexity of Soil Microbiomes in a Large-Scale Study Subjected to Different Agricultural Management in Styria

Martina Köberl[1], Philipp Wagner[1], Henry Müller[1], Robert Matzer[2], Hans Unterfrauner[3], Tomislav Cernava[1] and Gabriele Berg[1]*

[1] Institute of Environmental Biotechnology, Graz University of Technology, Graz, Austria, [2] ARGE obst.wein, Association of Weinbauverband Steiermark and Verband Steirischer Erwerbsobstbauern, Graz, Austria, [3] TB Unterfrauner GmbH, Vienna, Austria

Healthy soil microbiomes are crucial for achieving high productivity in combination with crop quality, but our understanding of microbial diversity is still limited. In a large-scale study including 116 composite samples from vineyards, orchards and other crops from all over Styria (south-east Austria), agricultural management as well as distinct soil parameters were identified as drivers of the indigenous microbial communities in agricultural soils. The analysis of the soil microbiota based on microbial profiling of prokaryotic 16S rRNA gene fragments and fungal ITS regions revealed high bacterial and fungal diversity within Styrian agricultural soils; 206,596 prokaryotic and 53,710 fungal OTUs. Vineyards revealed a significantly higher diversity and distinct composition of soil fungi over orchards and other agricultural soils, whereas the prokaryotic diversity was unaffected. Soil pH was identified as one of the most important edaphic modulators of microbial community structure in both, vineyard and orchard soils. In general, the acid-base balance, disorders in the soil sorption complex, content and quality of organic substance as well as individual nutrients were identified as important drivers of the microbial community structure of Styrian vineyard and orchard soils. However, responses to distinct parameters differed in orchards and vineyards, and prokaryotic and fungal community responded differently to the same abiotic factor. In comparison to orchards, the microbiome of vineyard soils maintained a higher stability when herbicides were applied. Orchard soils exhibited drastic shifts within community composition; herbicides seem to have a substantial impact on the bacterial order *Chthoniobacterales* as well as potential plant growth promoters and antagonists of phytopathogens (*Flavobacterium*, *Monographella*), with a decreased abundance in herbicide-treated soils. Moreover, soils of herbicide-treated orchards revealed a significantly higher presence of potential apple pathogenic fungi (*Nectria*, *Thelonectria*). These findings provide the basis to adapt soil management practices in the future in order to maintain a healthy microbiome in agricultural soils.

Keywords: soil microbiome, vineyards, orchards, edaphic parameters, herbicide usage

OPEN ACCESS

Edited by:
David William Waite, Ministry for Primary Industries, New Zealand

Reviewed by:
Syrie Maria Hermans, The University of Auckland, New Zealand
Johanna Nelkner, Bielefeld University, Germany

****Correspondence:***
Martina Köberl
martina.koeberl@tugraz.at

Specialty section:
This article was submitted to Microbial Symbioses, a section of the journal Frontiers in Microbiology

Received: *29 January 2020*
Accepted: *28 April 2020*
Published: *25 May 2020*

Citation:
Köberl M, Wagner P, Müller H, Matzer R, Unterfrauner H, Cernava T and Berg G (2020) Unraveling the Complexity of Soil Microbiomes in a Large-Scale Study Subjected to Different Agricultural Management in Styria. Front. Microbiol. 11:1052. doi: 10.3389/fmicb.2020.01052

INTRODUCTION

Soil is a non-renewable natural bio-resource involved in important ecosystem functions and biogeochemical cycles on earth. One of the most important characteristics of a soil ecosystem is soil health, which is the result of biotic as well as abiotic processes and connected to various interactions within the system. These interactions have strong impact on the microbial activity, supporting many central processes in soil (Frąc et al., 2018). The cycling of carbon and other nutrients or the promotion of plant growth are found among a broad variety of functions ascribed to soil microorganisms (Jansson and Hofmockel, 2018). Soil health is also fundamental for food security and safety as well as carbon storage (FAO and ITPS, 2015). Microbial communities as well as other organisms which reside in soils are extremely complex and diverse. Millions of species and billions of individual organisms can be found in various soils ranging from microorganisms such as bacteria, archaea, fungi, and protists to larger organism like ants and earthworms. Moreover, 1,000s of individual taxa including members of all three domains of life can live in one gram of soil (Fierer, 2017). Bacterial species form the biggest group by number and also by diversity (Gagelidze et al., 2018). Biotic and abiotic factors, including soil pH, temperature, soil type, geographic and climatic conditions, shape the microbiome of bulk and rhizospheric soil (Santoyo et al., 2017). Plant species influence soil microbial diversity (Berg and Smalla, 2009) and *vice versa* (Bardgett and van der Putten, 2014). Soils are characterized by a high degree of spatial structuring; they are composed of micro-aggregates (< 0.25 mm), which bind soil organic carbon and protect it from removal by erosion, and of macro-aggregates (0.25 to 2 mm), which limit oxygen diffusion and regulate water flow; each of the aggregates provides a unique ecological niche with its characteristic microbiome structure (Wilpiszeski et al., 2019). In fact, it has been suggested that soils are the ecosystems with the most diverse composition of microbiota on earth as a consequence of so many different niches being present at small spatial scales (Jansson, 2011; Prosser, 2015). However, this microbial biodiversity is largely understudied, and regional or global overviews are rare. The first global atlas of soil bacterial taxa revealed a region-specific composition (Delgado-Baquerizo et al., 2018), but regional studies are barely available, e.g., for Austria.

Styria is a region in south-east Austria and characterized by a uniquely high diversity of soil types. Together with the Mediterranean-influenced climate, the hilly area provides excellent conditions for cultivation of a large variety of grape and pome (mainly apple) cultivars, including the indigenous 'Schilcher' grape and 'Kronprinz Rudolf' apple. Both crops are therefore of economic importance for the Styrian agriculture but also world-wide (FAOSTAT, 2016, 2017; International Organisation of Vine and Wine, 2016). Compared to international standards, Austria has a small-scaled agriculture. Austria counted in 2015 a total of 14,133 viticulture holdings, of which 2,085 holdings were located in Styria. The total area of Styrian grapevine (*Vitis vinifera* L.) production is 4,329.22 hectares in size, which also includes non-productive vineyards. Most of this area (3,337.37 hectares) is attributed to the production of white wine, while the remaining area is used for red wine production. Apple (*Malus domestica* Borkh.) is due to its climatic adaption the most planted tree fruit of the temperate zone and one of the most cultivated in the world (Ahmed et al., 2011; Eccher et al., 2014). Austria's apple production covers a total area of 7,700 hectares, managed by 3,909 commercial fruit producers. The largest part of this area is located in the state of Styria with 5,900 hectares, which corresponds to 77% of Austria's total apple production area. The quantity of harvested apples in Styria is close to 100,000 tons per year. In 2017, the Styrian area for organic apple production amounted to 1,195 hectares, corresponding to 20% (all data for Austria/Styria were obtained from STATISTIK AUSTRIA[1]).

A recent study on the microbiome of vineyard soils in the Italian province of Trentino highlighted the need to characterize bacterial and fungal communities of the soil microbiota to fully understand the factors that drive their variability. It was found that while the bacterial component of the microbiome had a core of conserved species that accounted for more than 60% of the reads of each sample, and that was shaped both by location and land use, the core fungal microbiome was smaller and determined by geographic factors that dominated differences due to land management (Coller et al., 2019). The rhizospheric microbiome of grapevines is also strongly influenced by host genetic control, namely by the rootstock genotype. This was recently confirmed for vineyards in Spain (Berlanas et al., 2019) and Italy (Marasco et al., 2018). Interestingly, despite these host-related differences in the taxonomic structure of the microbiome, Marasco et al. (2018) observed a homeostatic effect on the distribution of plant growth-promoting abilities. The impact of the rootstock genotype on the microbiome structure has been reported for apple trees as well (Liu et al., 2018). However, a greater number of significant effects in apple orchards were observed due to different soil management practices such as soil amendment with *Brassica* seed meal (Mazzola et al., 2015) or varying manure ratios (Zhang et al., 2013).

The focus of the present study was the detailed assessment of the soil microbiome of vineyards and orchards in Styria/Austria subjected to different agricultural practices. Altogether, 116 soil samples were collected in a large-scale approach and analyzed in terms of their prokaryotic and fungal diversity and community composition. Complementary cultivation-independent and statistical analyses were performed to identify prevalent taxa and characterize the soil microbiome. In order to determine the impact of abiotic soil parameters, physico-chemical parameters were ascertained in detail by fractional analysis, separating water-soluble, exchangeable, and subsequently deliverable (reserve) fractions. Microbiome shifts resulting from the usage of herbicides were investigated based on the treatment history of each cultivation site.

[1]https://www.statistik.at

MATERIALS AND METHODS

Sampling and Metagenomic DNA Extraction

Soil samples were collected in early spring (March/April) 2017 in nine different regions of Styria in Austria: Feldbach (6 samples), Gleisdorf (24), Hartberg (16), Kitzeck (9), Leibnitz (8), Leutschach (23), Südoststeiermark (14), Südsteiermark (5), and Weststeiermark (11). Altogether, 116 composite soil samples consisting of five sub-samples each were collected in a horizon of 10–30 cm depth, which are assigned to three general sample groups: vineyards (73 samples), orchards (32; 28 apple orchards, 3 pear orchards, and 1 quince orchard), and other agricultural soils (11) of diverse usage (grassland, soy bean, rye, oat).

In order to isolate total community DNA, 5 g of soil were mixed with 15 ml of sterile 0.85% NaCl and placed for 10 min on a shaking platform. Subsequently, 3 ml of the suspensions were centrifuged (20 min, 16,000 × *g*, 4°C) and the resulting pellets were stored at −70°C until further processing. This approach enables the usage of a greater amount of input soil material comprising micro- and macro-aggregates. DNA was extracted using the FastDNA SPIN Kit for Soil (MP Biomedicals, Solon, OH, United States) and quantified using a NanoDrop 2000c spectrophotometer (Thermo Scientific, Waltham, MA, United States).

Edaphic Parameters and Herbicide Usage

Physico-chemical soil parameters were assessed through fractional analysis according to ÖNORM S 2122-1 by TB Unterfrauner (Vienna, Austria). This analysis separates water-soluble, exchangeable, and subsequently deliverable (reserve) fraction by considering the different bond types of elements in soil impacting their accessibility for plants. Water-soluble elements define the concentrations of substances in the soil solution, the most important source for plant nutrition. Organic and mineral parts in soil build the sorption complex; their negatively charged surfaces adsorb cations, which can be exchanged to become available for roots, e.g., through root excretion or fertilization – those elements are referred to as exchangeable. Water-soluble and exchangeable elements are considered as plant-available, whereas the subsequently deliverable (reserve) fraction will become accessible to plants by natural weathering processes within 10 to 15 years. Soil pH was determined in water (soil–water saturation extract) as well as in neutral salt solution (1M KCl). Soil texture (KH), electrical conductivity (EC) and water-soluble elements were analyzed based on soil–water saturation extracts. Exchangeable elements were assessed from LiCl extracts and the subsequently deliverable elements (reserve fraction) from HCl extracts. Total contents of C, N and S were determined by dry combustion. Lime content was calculated as $CaCO_3$ using a Scheibler calcimeter. More details about the fractional analysis can be found under https://www.bodenoekologie.com/en/. Information about treatment history was gathered from the farmers by a questionnaire.

PCR-Based Barcoding

Microbial profiling was performed according to the standards of the Earth Microbiome Project[2]. The hypervariable V4–V5 region of the 16S rRNA gene was amplified with the primers 515F-Y/926R (Quince et al., 2011; Parada et al., 2016), which carried sequence pads for later extension with sample specific tags. The reaction mixture for the first PCR (10 μl) contained 1 × Taq-&GO (MP Biomedicals, Solon, OH, United States), 0.1 μM of each primer, and 1 μl of template DNA (95°C, 3 min; 35 cycles of 95°C, 45 s; 55°C, 45 s; 72°C, 90 s; and elongation at 72°C, 5 min). Individual golay_12 barcodes (Caporaso et al., 2012) were attached in a second PCR (30 μl) comprising 1 × Taq-&GO, 0.2 μM of each primer, and 1 μl of the first PCR mixtures (95°C, 5 min; 15 cycles of 95°C, 30 s; 53°C, 30 s; 72°C, 30 s; and elongation at 72°C, 5 min). For the fungal community, the ITS1 region was amplified with the primer pair ITS1f/ITS2 (White et al., 1990; Gardes and Bruns, 1993) carrying the sequence pads for later golay_12 barcode extension. The first PCR (10 μl) consisted of 1 × Taq-&GO, 3 mM $MgCl_2$, 0.1 μM of each primer, and 1 μl of template DNA (94°C, 5 min; 30 cycles of 94°C, 30 s; 58°C, 35 s; 72°C, 40 s; and elongation at 72°C, 10 min). The second PCR (30 μl) comprised 1 × Taq-&GO, 0.2 μM of each primer, and 1.8 μl of the first PCR mixtures (95°C, 5 min; 15 cycles of 95°C, 30 s; 53°C, 30 s; 72°C, 30 s; and elongation at 72°C, 5 min). For the prokaryotic and for the fungal community, PCR products of three independent reactions were pooled in equal volumes and purified by employing the Wizard SV Gel and PCR Clean-Up System (Promega, Madison, WI, United States). Paired-end Illumina HiSeq sequencing (2 × 300 bp) was conducted by GATC Biotech (Konstanz, Germany).

Data Analysis

Data analysis was performed by employing QIIME 1.9.1 (Caporaso et al., 2010a). Joined paired-end reads with more than three consecutive low-quality base calls (Phred quality score ≤ 25) were truncated at the position where their quality began to drop, and only reads with > 75% consecutive high-quality base calls, without any ambiguous characters, and longer than 200 nucleotides in length were retained for further analyses. Demultiplexed high-quality 16S rRNA gene fragments were *de novo* clustered into operational taxonomic units (OTUs) with uclust (Edgar, 2010), using a 97% similarity threshold. For each OTU, the most abundant sequence was selected as representative, and the taxonomy was assigned with the uclust-based consensus taxonomy assigner against the Greengenes database (version 13.8). The representative sequence set was aligned with PyNAST (Caporaso et al., 2010b), and potential chimeric sequences were discarded based on a check with ChimeraSlayer. Joined, quality-filtered and demultiplexed ITS reads were cleaned from chimeras using the usearch7 algorithm and open-reference picked into OTUs with uclust against the dynamic UNITE database (version 7.1). The taxonomy of the representative ITS sequences was assigned with blast against the same reference database. OTU tables were constructed and singletons, doubletons, and reads for

[2]http://press.igsb.anl.gov/earthmicrobiome/protocols-and-standards

which taxonomy could not be assigned were removed from the datasets. The prokaryotic dataset was further filtered to remove cyanobacterial and mitochondrial sequences, and fungal dataset was filtered to remove bacterial and archaeal reads. When joining paired-end reads from the ITS regions, there is a bias against species with long ITS regions which exceed the sequencing length and are therefore discarded during the joining process (Hoggard et al., 2018). We examined this effect by comparing the results of merging read pairs to analysis using only the forward reads (**Supplementary Table 1**).

For alpha and beta diversity analyses, OTU tables were rarefied to the lowest number of reads per sample (all samples: 1,847 reads for 16S rRNA genes and 7,992 reads for ITS; herbicide impact: 10,653 reads for 16S rRNA genes and 74,662 reads for ITS). For metadata-based comparisons, only soil samples from vineyards and orchards were considered. The impact of herbicide usage was analyzed on a subset of samples with known treatment history (5 samples per treatment for vineyards and orchards, respectively). Organic sites have been under this management since at least two years. Alpha diversity was evaluated based on Shannon, Chao1 and the observed_otus metric; significant differences were calculated using the non-parametric two-sample *t*-test with 999 Monte Carlo permutations. Beta diversity was analyzed based on Bray–Curtis dissimilarities; ANOSIM and adonis tests with 999 permutations were used for corresponding statistics. Significances for differences in the abundances of taxa were determined based on the Bonferroni-corrected Kruskal–Wallis test with 1,000 permutations. Differences in OTU abundances between herbicide-treated and organic sites were assessed with the non-parametric *t*-test with 1,000 Monte Carlo permutations. Heat maps were visualized in Heatmapper (Babicki et al., 2016). Fungal communities were classified according their predicted trophic mode using FUNGuild (Nguyen et al., 2016); significant differences between herbicide-treated and organic sites were calculated with SPSS Statistics 26 (SPSS, Inc., Chicago, IL, United States) using the independent samples *t*-test. PICRUSt (version 1.1.1; Langille et al., 2013) analyses were performed to predict metabolic functions of the prokaryotic communities. Closed-reference picked (Greengenes version 13.8) rarefied OTU tables were used as input material, and the KO (KEGG orthology) database served as reference database. Predicted metagenome tables were analyzed with STAMP (Statistical Analysis of Metagenomic Profiles; version 2.1.3; Parks et al., 2014), the two-sided Welch's *t*-test was used for statistical comparisons.

RESULTS

The Soil Microbiome of Styrian Vineyards and Orchards

The analysis of the soil microbiome based on high-throughput amplicon sequencing of 16S rRNA gene fragments and the fungal internal transcribed spacer (ITS) 1 region revealed high bacterial and fungal diversity within Styrian agricultural soils. Overall, 206,596 prokaryotic OTUs were identified with a total of 10,808,936 reads. The fungal dataset revealed 53,710 OTUs and a total read count of 23,927,374.

Alpha diversity indicated significant differences ($p \leq 0.05$) in relation to soil usage (vineyards, orchards, and other agricultural soils) for the fungal diversity, whereas the prokaryotic diversity was unaffected by this factor (**Figure 1A**). Fungal diversity was detected to be highest in vineyard soils. Non-metric multidimensional scaling (NMDS) analyses based on Bray–Curtis dissimilarity matrices revealed a clustering of vineyard and orchard samples for the fungal community (**Figure 1B**; $R = 0.26$, $p = 0.001$). The prokaryotic community showed no significant separation of soil samples originating from vineyards and orchards ($R = 0.02$, $p = 0.263$). Soil usage was responsible for only 1.7% ($p = 0.006$) of prokaryotic and 6.0% ($p = 0.001$) of fungal community variation between vineyards or orchards. The sample group with other agricultural soils revealed broad scattering in both datasets, which reflects different agricultural usage (grassland, soy bean, rye, oat). One outlier within agricultural soil samples, which clearly separated from all the others in the prokaryotic and in the fungal dataset, originated from a recently cleared woodland currently under green manuring.

Proteobacteria were identified as the most dominant bacterial phylum in vineyards, orchards, and other agricultural soils, encompassing 27.7, 27.4, and 27.8%, respectively. At the class level, they could be affiliated to *Alpha-*, *Beta-*, *Gamma-*, and *Delta proteobacteria* (**Figure 1C**), whereby *Alphaproteobacteria* were the most prevalent (vineyards 12.3%, orchards 12.0%, and other agricultural soils 13.0%). Besides *Proteobacteria*, *Acidobacteria* (classes *Acidobacteria*-6, *Acidobacteriia*, [*Chloracidobacteria*], DA052 and *Solibacteres*), *Verrucomicrobia* ([*Pedosphaerae*] and [*Spartobacteria*]), *Actinobacteria* (*Thermoleophilia* and *Actinobacteria*), *Bacteroidetes* ([*Saprospirae*], *Flavobacteriia* and *Sphingobacteriia*), *Planctomycetes* (*Planctomycetia* and *Phycisphaerae*), and *Chloroflexi* (*Anaerolineae* and *Chloroflexi*) were found as dominant soil inhabitants. Additionally, *Gemmatimonadetes* (*Gemmatimonadetes* and Gemm-1), *Nitrospirae* (*Nitrospira*), and WS3 (PRR-12) were found in an overall relative abundance over 1%. The fungal soil community was dominated by *Ascomycota* (vineyards 43.8%, orchards 45.0%, and other agricultural soils 44.8%), which could be divided into *Sordariomycetes*, *Dothideomycetes*, *Leotiomycetes*, *Eurotiomycetes* and unidentified *Ascomycota*. High abundances were also observed for *Zygomycota* (*Mortierellomycotina*_cls_*Incertae_sedis*), *Basidiomycota* (*Tremellomycetes* and *Agaricomycetes*) and unidentified *Fungi*. Significant differences ($p \leq 0.05$) in relation to soil usage were observed for the bacterial class *Gemmatimonadetes* (also for the phylum *Gemmatimonadetes*) and the fungal class *Tremellomycetes*, both with highest abundances in orchard soils.

Impact of Edaphic Parameters on Soil Microbiomes

Abiotic soil parameters were ascertained in detail by fractional analysis, separating water-soluble, exchangeable, and subsequently deliverable (reserve) fractions. For vineyard soils, the parameters mostly affecting prokaryotic and fungal community variation are highly similar, while orchard soils revealed a generally higher complexity within their community

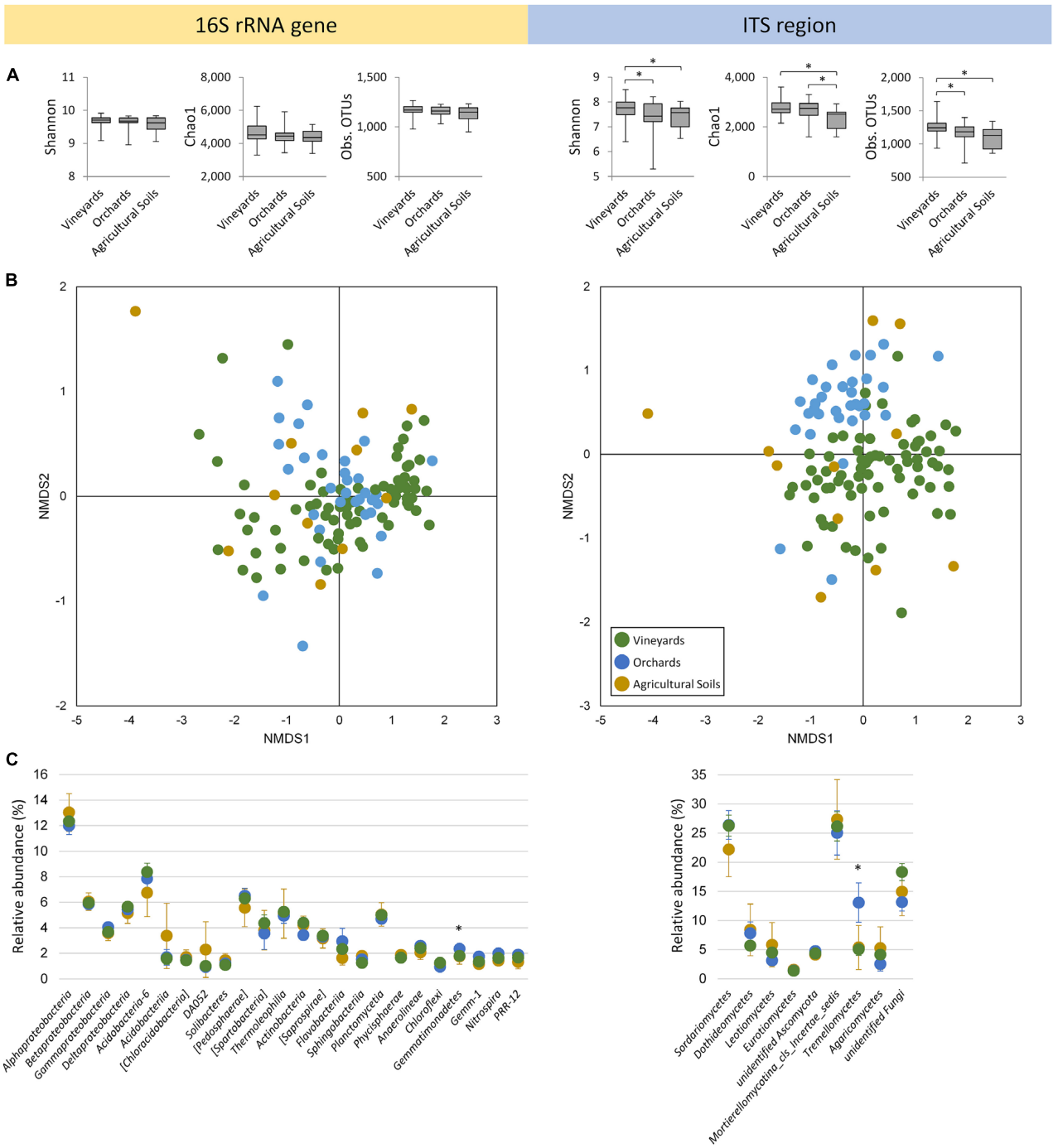

FIGURE 1 | Microbial soil communities colonizing vineyards, orchards, and other agricultural soils in Styria/Austria. **(A)** Alpha diversity determined by Shannon, Chao1 index, and observed OTUs in the rarefied datasets. Significant differences (non-parametric two-sample *t*-test, $p \leq 0.05$) are indicated by asterisks. **(B)** Non-metric multidimensional scaling (NMDS) plots based on Bray–Curtis dissimilarities. The corresponding 2D stress values are 0.1 and 0.2, respectively for 16S rRNA genes and ITS regions. **(C)** Taxonomic composition visualizing classes with > 1% of overall relative abundance. Data are mean values ± confidences; asterisks indicate significant differences (Bonferroni-corrected Kruskal–Wallis test, $p \leq 0.05$) in relation to soil usage.

drivers with divergent importance for prokaryotes and fungi (**Figure 2**). The parameter with the most significant influence on all microbial communities was the soil pH (vineyards: 14% for prokaryotes, 13% for fungi; orchards: 8% for prokaryotes, 8% for fungi). Vineyard communities were also affected by calcium concentrations – within all fractions, but especially in the sorption complex (13% for both communities) – and consequently base saturation (13% for both communities).

Potential acids in the sorption complex also substantially influenced community variation in vineyard soils (13% for both communities). The proportions of variance explained by those parameters were in general higher for the vineyard than for the orchard microbiomes. The prokaryotic orchard communities were in addition to soil pH (8%) and calcium in the sorption complex (6%) most significantly affected by water-soluble manganese (6%), whereas the fungal variation within orchard soils was in addition to soil pH (8%) mostly driven by sodium concentrations – sorption complex (9%) and exchangeable fraction (8%).

Impact of Herbicide Usage on Soil Microbiomes

The microbial alpha diversity (Shannon index) was not significantly impacted ($p > 0.05$) by recent applications of herbicides (**Figure 3A**). However, for vineyards, a trend to higher microbial soil diversity after several years of organic management could be observed. In orchards, organic management revealed an overall tendency to a lower diversity within the fungal community, however with high variability within the organic sample group and without statistical significance.

In comparison to vineyards under organic management, herbicide-treated vineyard soils revealed significantly lower ($p \leq 0.05$) relative abundances of unclassified *Lasiosphaeriaceae* (*Sordariales*, *Ascomycota*), *Ilyonectria* (*Hypocreales*, *Ascomycota*), and *Candidatus Solibacter* (*Solibacterales*, *Acidobacteria*). Conversely, herbicide-treated vineyards showed a significant increase in unclassified *Gemmatimonadetes* (phylum *Gemmatimonadetes*) and a group of unclassified *Fungi* (**Figure 3B**). Herbicide application had a substantial impact on the microbial community composition in orchard soils: 19 out of 209 taxa (genus level, > 0.1% of overall abundance) were significantly shifted. Among those, 12 taxa showed a significantly higher relative abundance in soils of organically managed sites, while for seven taxa the relative abundance was higher in herbicide-treated orchards (**Figure 3B**).

The herbicide-related shifts at taxonomic level were further verified by analyzing the trophic modes of the fungal community (**Supplementary Figure 1**). Thereby, no statistically significant shifts ($p > 0.05$) were observed, neither for the mycobiome of vineyard soils nor for orchard soils. However, organically managed orchards showed a trend, although not significant, to a higher abundance of patotrophic-saphrotrophic fungi (2 versus 11% in herbicide-treated orchard soils; $p = 0.1$). The trophic modes of the fungal microbiome inhabiting vineyard soils revealed high stability to herbicide application and remained stable also after 9 years of organic management (maximum ± 2%). Overall, the fraction of pathotrophic fungi was found to be higher in organically managed soils, for both vineyards and orchards (V: 8 vs. 5%, O: 15 vs. 6%). Just for the soils of orchards, the inferred functional composition of the prokaryotic microbiome did show significant differences ($p \leq 0.05$) in relation to herbicide application, whereby 10 predicted functional categories (KEGG orthology level 3)

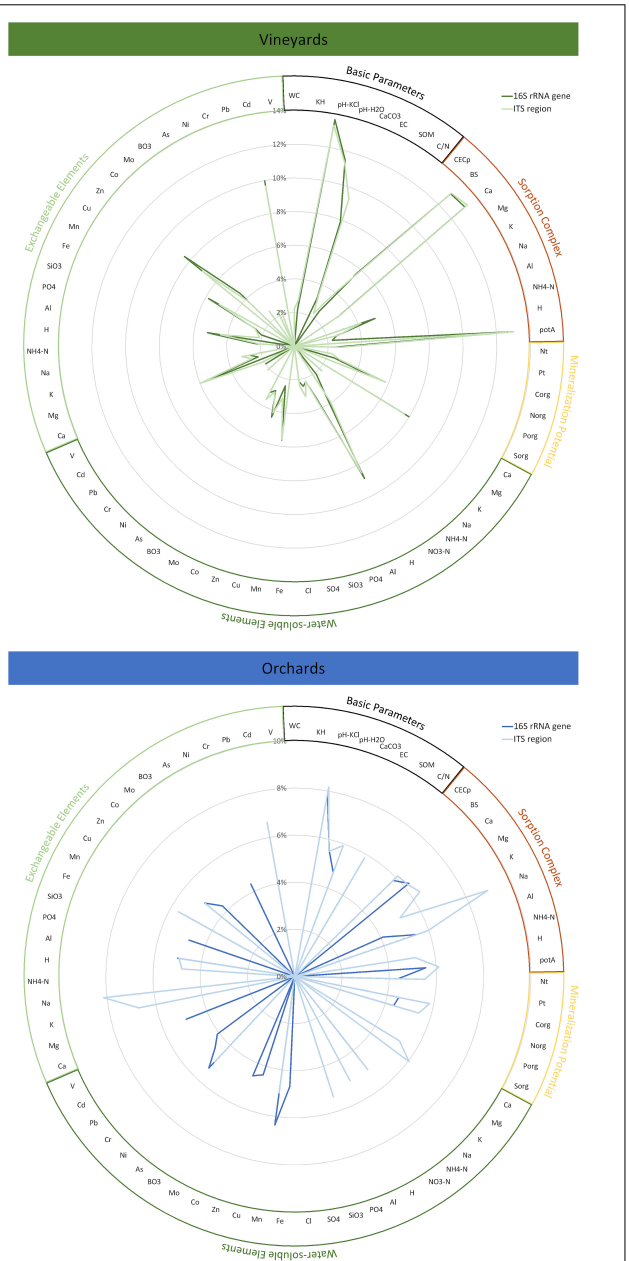

FIGURE 2 | Variance within the prokaryotic (16S rRNA gene) and fungal (ITS region) community inhabiting Styrian vineyard and orchard soils explained by the individual edaphic parameters. Significant variations ($p \leq 0.05$) were determined with adonis based on Bray–Curtis dissimilarities. Abiotic soil parameters were ascertained in detail by fractional analysis, whereby the currently not available reserve fraction was not considered in the analysis of community impact. Basic parameters: WC = water content, KH = soil texture, pH-KCl = pH in neutral KCl solution, pH-H_2O = pH in water, $CaCO_3$ = lime content, EC = electrical conductivity, SOM = soil organic matter, C/N = C/N ratio of SOM; Sorption complex: CECp = potential cation exchange capacity, BS = base saturation, substance ratios in the sorption complex (Ca, Mg, K, Na, Al, NH_4-N, H, potA = potential acids); Mineralization potential: Nt, Pt = total content of N and P, Corg, Norg, Porg, Sorg = organic pool of C, N, P, S; Water-soluble elements: Ca, Mg, K, Na, NH_4-N, NO_3-N, H, Al, PO_4, SiO_3, SO_4, Cl, Fe, Mn, Cu, Zn, Co, Mo, BO_3, As, Ni, Cr, Pb, Cd, V; Exchangeable elements: Ca, Mg, K, Na, NH_4-N, H, Al, PO_4, SiO_3, Fe, Mn, Cu, Zn, Co, Mo, BO_3, As, Ni, Cr, Pb, Cd, V.

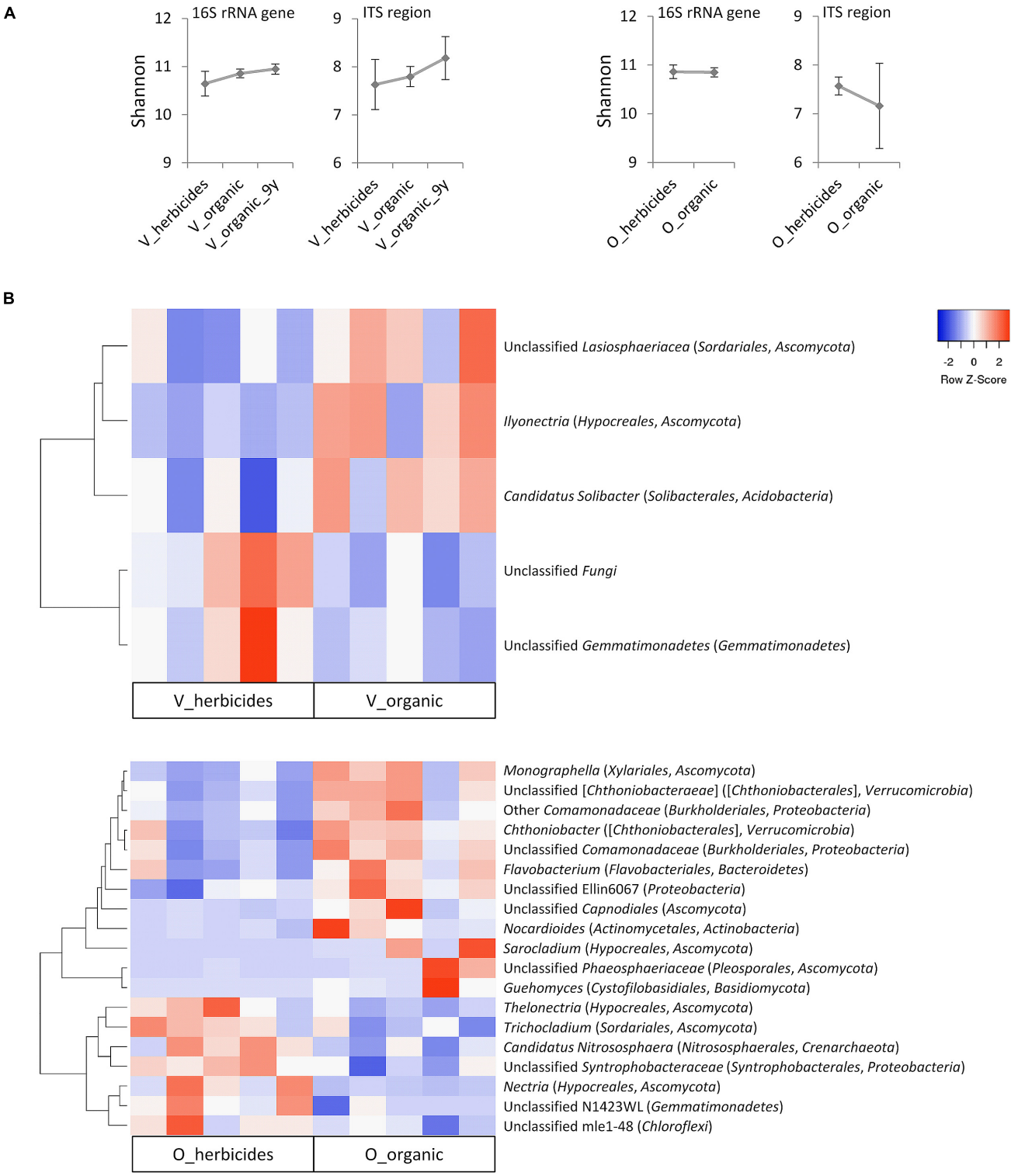

FIGURE 3 | Impact of herbicide application on the soil microbiome of vineyards (V) and orchards (O) in Styria/Austria. **(A)** Alpha diversity determined by Shannon index. Data are mean values ± confidences. Vineyard soils which were knowingly treated organically since the last 9 years were assessed as separate group (V_organic_9y). **(B)** Heat maps displaying the relative abundance of taxa at genus level (>0.1% of overall abundance) with significant difference (non-parametric *t*-test, $p \leq 0.05$) between herbicide-treated and organic sites. The dendrograms are based on average linkage clustering and Pearson distances.

revealed higher presence in organic soils and only four in herbicide-treated ones (**Supplementary Figure 2**).

DISCUSSION

The analysis of the soil microbiota of Styrian agricultural soils revealed an outstanding high bacterial and fungal diversity. Today we know that microbial diversity is a key factor for soil health and in preventing diseases (van Elsas et al., 2012; Berg et al., 2017). Agricultural management as well as distinct soil parameters were identified as drivers of the indigenous microbial communities of Styrian soils, whereby the prokaryotic and fungal community responded differently, and responses differed in orchard and vineyard soils. A detailed understanding of these community responses and interactions can provide the basis to enable the management of vineyards and orchards in a more environmentally friendly and resource-saving way.

Comparative analyses of microbial profiling of prokaryotic 16S rRNA gene fragments and fungal ITS regions revealed several common responses regarding the microbial community composition across all investigated sample groups, especially at higher taxonomic levels. *Proteobacteria* was the most dominant bacterial phylum in Styrian vineyards, orchards, and other agriculturally used soils. This was previously also shown for agricultural soils of the Mediterranean region (Bevivino et al., 2014). Likewise, Janssen (2006) reported *Proteobacteria* to make up the majority (on average 39%) of libraries derived from soil bacterial communities with diverse origin, among those – in accordance with the present study – also *Alphaproteobacteria* were identified as the most dominant. *Alphaproteobacteria* harbor several bacterial lineages that are common plant-associated microorganisms and contribute to plant health and productivity (Wasai and Minamisawa, 2018). Agricultural soils are an important reservoir for these microorganisms that can be attracted and enriched in the rhizosphere of cultivated plants (Sessitsch et al., 2002). *Acidobacteria* was identified as the second highest abundant bacterial phylum in Styrian vineyard and orchard soils. This is as well in accordance with other studies, where *Acidobacteria* were reported to own an average share of 20% of soil bacteria (Janssen, 2006; Naether et al., 2012). Third most represented in the present study was the bacterial phylum *Verrucomicrobia*, which is known as dominant phylum in many soils across the globe (Bergmann et al., 2011). In contrary to the results of Janssen (2006), *Verrucomicrobia* outnumber the abundance of *Actinobacteria* in Styrian vineyard and orchard soils. *Ascomycota* represented the most dominant fungal phylum over all samples, followed by *Zygomycota*, and *Basidiomycota*. Klaubauf et al. (2010) showed similar result for agricultural soils from Lower Austria, whereby in their study the presence of *Ascomycota* was remarkably higher (∼80%).

Vineyards revealed a significantly higher diversity of soil fungi over orchards and other agricultural soils, whereas the prokaryotic diversity was unaffected by soil usage. Also, the community structure differed significantly between vineyard and orchard mycobiomes, while there was a negligible effect for prokaryotes. The most distinct difference was a significantly higher abundance of the fungal class *Tremellomycetes* in orchard soils. This was due to the occurrence of the genus *Solicoccozyma*, a basidiomycetous yeast commonly found in soils with high salt content (Mokhtarnejad et al., 2016; Zajc et al., 2017). Although all investigated soils were classified as non-saline, orchard soils revealed on average higher salinity (mean EC = 0.40 mS cm^{-1}) than vineyards (mean EC = 0.28 mS cm^{-1}) and other agricultural soils (mean EC = 0.25 mS cm^{-1}). This is most probably a result of the fertilization management; application rates in orchards are generally higher.

The acid-base balance, disorders in the sorption complex, content and quality of organic substance as well as individual nutrients (such as zinc and manganese) were identified as important drivers of the microbial community structure of Styrian vineyard and orchard soils. Soil pH was one of the most important edaphic modulators in both, vineyard and orchard soils. In a continental-scale study, Fierer and Jackson (2006) found that diversity and richness of soil bacterial communities was strongly correlated with soil pH. Bacterial diversity was highest in neutral soils and lower in acidic soils (Fierer and Jackson, 2006). Similarly, Wu et al. (2017) reported that bacterial diversity in arable soils is strongly related to soil pH, with lower diversity under acidic and higher diversity under neutral pH conditions. On an experimental farm maintaining a pH gradient from 4.5 to 7.5, shifts were observed even at higher taxonomic levels (phylum, class) across the gradient (Bartram et al., 2014). The pH values (in water) from soils of vineyards ranged from 5.5 to 7.9. Soils of orchards had a slightly narrower pH range from 5.9 to 7.6. In the same environment, soil fungi commonly show a growth optimum of one to two pH units lower than bacteria (Piña and Cervantes, 1996), where soil pH causes a physiological limitation on fungal survival and growth (Zhang et al., 2016). Both in vineyards and orchards, the acid-base ratio and the sorption complex played a major role in shaping microbial communities. The relationship to the quantity and quality of organic matter seems to be stronger within the orchards than in vineyards. Individual sampling sites with a combination of different suboptimal edaphic factors showed a particularly strong effect on microbial diversity and composition, this could be referred to as soil fatigue.

The impact of herbicide application on the microbial soil community was assessed based on the sites' treatment history. Soils of vineyards and orchards were analyzed based on the information if they were treated with herbicides during the last two years or managed organically, independent from herbicide type, application form and period. In comparison to orchards, the microbiome of vineyard soils maintained a higher stability in terms of taxonomy and inferred functionality when herbicides were applied. In contrast to vineyards, where the application of herbicides tends to be associated with a general reduction in microbial soil diversity, orchard soils exhibited drastic shifts within community composition at taxonomic and predicted functional level. For example, in orchards, herbicides seem to have a substantial impact on the bacterial order *Chthoniobacterales* (genus *Chthoniobacter* and others), with a decreased abundance in herbicide-treated soils. *Chthoniobacterales* are rod-shaped or pleomorphic cells, which

are common in soil but not well-studied so far (Sangwan et al., 2004). Hirsch et al. (2017) described them as rapid responders to soil management changes, with highest abundance in grassland, followed by arable soil, and least in bare fallow soil. According to genomic data, *Spartobacteria* (*Chthoniobacterales*) contribute to the cycling of carbon by the degradation of various complex carbohydrates, such as cellulose and xylan (Herlemann et al., 2013). In the microbiome of lichens, transcriptomics suggest their involvement in the metabolism of aromatic compounds (degradation of phenolic substances), production of various vitamins, and defense against antibiotics (fluoroquinolones) and oxidative stress (Cernava et al., 2017). Other identified genera with increased abundance in herbicide-free orchard soils comprise potential plant growth promoters and antagonists of phytopathogens, including *Flavobacterium* (Soltani et al., 2010) and *Monographella* (Berg et al., 2005). Moreover, soils of herbicide-treated orchards revealed a significantly higher presence of the potential apple pathogenic fungus *Nectria*, the causal agent of apple canker, and also of the closely related genus *Thelonectria*. Contrarily, vineyards revealed higher abundances of the potentially pathogenic genus *Ilyonectria* (black-foot disease) in organic soils. It was also evident from our data that a lack of greening in the plant strip through the regular use of herbicides led to humus degradation over years. A perceived reduction in fruit quality and yield can potentially lead to anthropogenic over-fertilization. However, this has generally negative effects by inducing additional acidification. That is in turn linked to a decrease in available carbon (Högberg et al., 2007) and microbial, in particular bacterial, diversity (Fierer and Jackson, 2006; Wu et al., 2017) – a downward spiral of which it is difficult to re-escape.

In the end, the limitations of marker gene-based approaches, as applied in the present study, should be briefly discussed. In particularly mentioned should be a possible bias toward certain microbial groups incorporated with the initial amplification step (Caporaso et al., 2012; Klindworth et al., 2013). In order to minimize this bias and for comparability reasons, the protocol applied in the present study was following the latest guidelines recommended by the Earth Microbiome Project (Gilbert et al., 2014, 2018). A critical point in the analysis of fungi is that ITS regions can vary drastically in length for different taxa. In some cases they may be longer than the possible merged read length of paired-end reads and will be discarded in the data analysis workflow (Hoggard et al., 2018). To rule this out as far as possible, in the present study, longest possible paired-end reads were sequenced (2 × 300 bp). However, also this length can far be exceeded by the ITS1 region of some taxa. Therefore, an additional comparison of the data using merged paired-end reads vs. analyzing only forward reads was performed, whereby a momentous bias resulting from exceeding the ITS1 read length could be excluded (**Supplementary Table 1**). In general, microbial profiling based on rRNA genes or ITS regions is limited to measurements of taxonomy and diversity and allows no direct inference to the metabolic potential of a microbial community (White et al., 2017). Tools like PICRUSt (Langille et al., 2013) predict functional profiles of microbial communities by linking marker genes with the nearest organism for which a whole genome sequence is available. This can be problematic, especially when studying microbiomes containing large proportions of not well-characterized taxa. FUNGuild (Nguyen et al., 2016) classifies fungal taxa by their probable ecological guild. An important caution about the accuracy of this assignment is the fact that some fungi do not fall exclusively into a single guild. Taxonomy-based functional predictions should therefore be interpreted cautiously.

The overall findings of our large-scale study indicate that certain agricultural management practices as well as distinct soil parameters have a substantial effect on indigenous microbial communities in agricultural soils. Moreover, we could show that responses to distinct parameters differed in orchards and vineyards as well as that bacterial and fungal community showed different responses to the same abiotic factor. These findings provide the basis to adapt soil management practices in the future in order to maintain a healthy microbiome in agricultural soils.

DATA AVAILABILITY STATEMENT

The datasets generated and analyzed for this study can be found in the European Nucleotide Archive (www.ebi.ac.uk/ena) under the BioProject accession number PRJEB36740.

AUTHOR CONTRIBUTIONS

RM (sampling design), MK, and GB (experimental design) conceived and designed the study. MK, PW, HM, and HU analyzed the data. GB, RM, and HU contributed reagents, materials, and analysis tools. MK, PW, TC, and GB wrote the manuscript.

FUNDING

This study was supported by the European Commission through the LEADER project "Ressourcenschonende Technik im steirischen Obst- und Weinbau." MK acknowledges support from the Austrian Science Fund FWF (T 847).

ACKNOWLEDGMENTS

We want to thank Regina Lind, Christian Darnhofer, Patrick Taucher (Fachgruppe Technik), and Barbara Fetz (TU Graz) for their valuable support. We are grateful to all farmers who were involved in this project.

SUPPLEMENTARY MATERIAL

The Supplementary Material for this article can be found online at: https://www.frontiersin.org/articles/10.3389/fmicb.2020.01052/full#supplementary-material

REFERENCES

Ahmed, R. A., El-Shehawy, M. A., and Lutang, L. (2011). The structure and competitiveness of China's apple exports. *World J. Agric. Sci.* 7, 678–683.

Babicki, S., Arndt, D., Marcu, A., Liang, Y., Grant, J. R., Maciejewski, A., et al. (2016). Heatmapper: web-enabled heat mapping for all. *Nucleic Acids Res.* 44, W147–W153. doi: 10.1093/nar/gkw419

Bardgett, R. D., and van der Putten, W. H. (2014). Belowground biodiversity and ecosystem functioning. *Nature* 515, 505–511.

Bartram, A. K., Jiang, X., Lynch, M. D., Masella, A. P., Nicol, G. W., Dushoff, J., et al. (2014). Exploring links between pH and bacterial community composition in soils from the craibstone experimental farm. *FEMS Microbiol. Ecol.* 87, 403–415. doi: 10.1111/1574-6941.12231

Berg, G., Köberl, M., Rybakova, D., Müller, H., Grosch, R., and Smalla, K. (2017). Plant microbial diversity is suggested as the key to future biocontrol and health trends. *FEMS Microbiol. Ecol.* 93:fix050. doi: 10.1093/femsec/fix050

Berg, G., and Smalla, K. (2009). Plant species and soil type cooperatively shape the structure and function of microbial communities in the rhizosphere. *FEMS Microbiol. Ecol.* 68, 1–13. doi: 10.1111/j.1574-6941.2009.00654.x

Berg, G., Zachow, C., Lottmann, J., Götz, M., Costa, R., and Smalla, K. (2005). Impact of plant species and site on rhizosphere-associated fungi antagonistic to *Verticillium dahliae* Kleb. *Appl. Environ. Microbiol.* 71, 4203–4213. doi: 10.1128/AEM.71.8.4203-4213.2005

Bergmann, G. T., Bates, S. T., Eilers, K. G., Lauber, C. L., Caporaso, J. G., Walters, W. A., et al. (2011). The under-recognized dominance of *Verrucomicrobia* in soil bacterial communities. *Soil Biol. Biochem.* 43, 1450–1455. doi: 10.1016/j.soilbio.2011.03.012

Berlanas, C., Berbegal, M., Elena, G., Laidani, M., Cibriain, J. F., Sagües, A., et al. (2019). The fungal and bacterial rhizosphere microbiome associated with grapevine rootstock genotypes in mature and young vineyards. *Front. Microbiol.* 10:1142. doi: 10.3389/fmicb.2019.01142

Bevivino, A., Paganin, P., Bacci, G., Florio, A., Pellicer, M. S., Papaleo, M. C., et al. (2014). Soil bacterial community response to differences in agricultural management along with seasonal changes in a Mediterranean region. *PLoS One* 9:e105515. doi: 10.1371/journal.pone.0105515

Caporaso, J. G., Bittinger, K., Bushman, F. D., DeSantis, T. Z., Andersen, G. L., and Knight, R. (2010a). PyNAST: a flexible tool for aligning sequences to a template alignment. *Bioinformatics* 26, 266–267. doi: 10.1093/bioinformatics/btp636

Caporaso, J. G., Kuczynski, J., Stombaugh, J., Bittinger, K., Bushman, F. D., Costello, E. K., et al. (2010b). QIIME allows analysis of high-throughput community sequencing data. *Nat. Methods* 7, 335–336. doi: 10.1038/nmeth.f.303

Caporaso, J. G., Lauber, C. L., Walters, W. A., Berg-Lyons, D., Huntley, J., Fierer, N., et al. (2012). Ultra-high-throughput microbial community analysis on the Illumina HiSeq and MiSeq platforms. *ISME J.* 6, 1621–1624. doi: 10.1038/ismej.2012.8

Cernava, T., Erlacher, A., Aschenbrenner, I. A., Krug, L., Lassek, C., Riedel, K., et al. (2017). Deciphering functional diversification within the lichen microbiota by meta-omics. *Microbiome* 5:82. doi: 10.1186/s40168-017-0303-5

Coller, E., Cestaro, A., Zanzotti, R., Bertoldi, D., Pindo, M., Larger, S., et al. (2019). Microbiome of vineyard soils is shaped by geography and management. *Microbiome* 7:140. doi: 10.1186/s40168-019-0758-7

Delgado-Baquerizo, M., Oliverio, A. M., Brewer, T. E., Benavent-González, A., Eldridge, D. J., Bardgett, R. D., et al. (2018). A global atlas of the dominant bacteria found in soil. *Science* 359, 320–325. doi: 10.1126/science.aap9516

Eccher, G., Ferrero, S., Populin, F., Colombo, L., and Botton, A. (2014). Apple (*Malus domestica* L. Borkh) as an emerging model for fruit development. *Plant Biosyst.* 148, 157–168.

Edgar, R. C. (2010). Search and clustering orders of magnitude faster than BLAST. *Bioinformatics* 26, 2460–2461. doi: 10.1093/bioinformatics/btq461

FAO, and ITPS, (2015). *Status of the World's Soil Resources (SWSR) – Main Report. Food and Agriculture Organization of the United Nations and Intergovernmental Technical Panel on Soils*. Rome: FAO.

FAOSTAT, (2016). Statistical Database of the Food and Agriculture Organization of the United Nations. Available: http://www.fao.org/faostat/en/#data/TP (accessed November 19, 2019).

FAOSTAT, (2017). *Statistical Database of the Food and Agriculture Organization of the United Nations*. Available: http://www.fao.org/faostat/en/#data/QC (accessed November 19, 2019).

Fierer, N. (2017). Embracing the unknown: disentangling the complexities of the soil microbiome. *Nat. Rev. Microbiol.* 15, 579–590. doi: 10.1038/nrmicro.2017.87

Fierer, N., and Jackson, R. B. (2006). The diversity and biogeography of soil bacterial communities. *Proc. Natl. Acad. Sci. U.S.A.* 103, 626–631. doi: 10.1073/pnas.0507535103

Frąc, M., Hannula, S. E., Bełka, M., and Jędryczka, M. (2018). Fungal biodiversity and their role in soil health. *Front. Microbiol.* 9:707. doi: 10.3389/fmicb.2019.0707

Gagelidze, N. A., Amiranashvili, L. L., Sadunishvili, T. A., Kvesitadze, G. I., Urushadze, T. F., and Kvrivishvili, T. O. (2018). Bacterial composition of different types of soils of Georgia. *Ann. Agrar. Sci.* 16, 17–21.

Gardes, M., and Bruns, T. D. (1993). ITS primers with enhanced specificity for basidiomycetes – application to the identification of mycorrhizae and rusts. *Mol. Ecol.* 2, 113–118. doi: 10.1111/j.1365-294x.1993.tb00005.x

Gilbert, J. A., Jansson, J. K., and Knight, R. (2014). The Earth Microbiome Project: successes and aspirations. *BMC Biol.* 12:69. doi: 10.1186/s12915-014-0069-1

Gilbert, J. A., Jansson, J. K., and Knight, R. (2018). Earth Microbiome Project and global systems biology. *mSystems* 3:e0217-17. doi: 10.1128/mSystems.00217-17

Herlemann, D. P., Lundin, D., Labrenz, M., Jürgens, K., Zheng, Z., Aspeborg, H., et al. (2013). Metagenomic *de novo* assembly of an aquatic representative of the verrucomicrobial class *Spartobacteria*. *mBio* 4:e0569-12. doi: 10.1128/mBio.00569-12

Hirsch, P. R., Jhurreea, D., Williams, J. K., Murray, P. J., Scott, T., Misselbrook, T. H., et al. (2017). Soil resilience and recovery: rapid community responses to management changes. *Plant Soil* 412, 283–297. doi: 10.1007/s11104-016-3068-x

Högberg, M. N., Högberg, P., and Myrold, D. D. (2007). Is microbial community composition in boreal forest soils determined by pH, C-to-N ratio, the trees, or all three? *Oecologia* 150, 590–601. doi: 10.1007/s00442-006-0562-5

Hoggard, M., Vesty, A., Wong, G., Montgomery, J. M., Fourie, C., Douglas, R. G., et al. (2018). Characterizing the human mycobiota: a comparison of small subunit rRNA, ITS1, ITS2, and large subunit rRNA genomic targets. *Front. Microbiol.* 9:2208. doi: 10.3389/fmicb.2019.02208

International Organisation of Vine and Wine, (2016). *World Vitiviniculture Situation – OIV Statistical Report on World Vitiviniculture*. Available: http://www.oiv.int/public/medias/5029/world-vitiviniculture-situation-2016.pdf (accessed November 19, 2019).

Janssen, P. H. (2006). Identifying the dominant soil bacterial taxa in libraries of 16S rRNA and 16S rRNA genes. *Appl. Environ. Microbiol.* 72, 1719–1728. doi: 10.1128/AEM.72.3.1719-1728.2006

Jansson, J. K. (2011). Towards "Tera-Terra": terabase sequencing of terrestrial metagenomes. *Microbe* 6, 309–315.

Jansson, J. K., and Hofmockel, K. S. (2018). The soil microbiome – from metagenomics to metaphenomics. *Curr. Opin. Microbiol.* 43, 162–168.

Klaubauf, S., Inselsbacher, E., Zechmeister-Boltenstern, S., Wanek, W., Gottsberger, R., Strauss, J., et al. (2010). Molecular diversity of fungal communities in agricultural soils from Lower Austria. *Fungal Divers.* 44, 65–75. doi: 10.1007/s13225-010-0053-1

Klindworth, A., Pruesse, E., Schweer, T., Peplies, J., Quast, C., Horn, M., et al. (2013). Evaluation of general 16S ribosomal RNA gene PCR primers for classical and next-generation sequencing-based diversity studies. *Nucleic Acids Res.* 41:e1. doi: 10.1093/nar/gks808

Langille, M. G., Zaneveld, J., Caporaso, J. G., McDonald, D., Knights, D., Reyes, J. A., et al. (2013). Predictive functional profiling of microbial communities using 16S rRNA marker gene sequences. *Nat. Biotechnol.* 31, 814–821. doi: 10.1038/nbt.2676

Liu, J., Abdelfattah, A., Norelli, J., Burchard, E., Schena, L., Droby, S., et al. (2018). Apple endophytic microbiota of different rootstock/scion combinations suggests a genotype-specific influence. *Microbiome* 6:18. doi: 10.1186/s40168-018-0403-x

Marasco, R., Rolli, E., Fusi, M., Michoud, G., and Daffonchio, D. (2018). Grapevine rootstocks shape underground bacterial microbiome and networking but not potential functionality. *Microbiome* 6:3. doi: 10.1186/s40168-017-0391-2

Mazzola, M., Hewavitharana, S. S., and Strauss, S. L. (2015). *Brassica* seed meal soil amendments transform the rhizosphere microbiome and improve apple production through resistance to pathogen reinfestation. *Phytopathology* 105, 460–469. doi: 10.1094/PHYTO-09-14-0247-R

Mokhtarnejad, L., Arzanlou, M., Babai-Ahari, A., Di Mauro, S., Onofri, A., Buzzini, P., et al. (2016). Characterization of basidiomycetous yeasts in hypersaline soils of the Urmia Lake National Park. Iran. *Extremophiles* 20, 915–928. doi: 10.1007/s00792-016-0883-1

Naether, A., Foesel, B. U., Naegele, V., Wüst, P. K., Weinert, J., Bonkowski, M., et al. (2012). Environmental factors affect acidobacterial communities below the subgroup level in grassland and forest soils. *Appl. Environ. Microbiol.* 78, 7398–7406. doi: 10.1128/AEM.01325-12

Nguyen, N. H., Song, Z., Bates, S. T., Branco, S., Tedersoo, L., Menke, J., et al. (2016). FUNGuild: an open annotation tool for parsing fungal community datasets by ecological guild. *Fungal Ecol.* 20, 241–248.

Parada, A. E., Needham, D. M., and Fuhrman, J. A. (2016). Every base matters: assessing small subunit rRNA primers for marine microbiomes with mock communities, time series and global field samples. *Environ. Microbiol.* 18, 1403–1414. doi: 10.1111/1462-2920.13023

Parks, D. H., Tyson, G. W., Hugenholtz, P., and Beiko, R. G. (2014). STAMP: statistical analysis of taxonomic and functional profiles. *Bioinformatics* 30, 3123–3124. doi: 10.1093/bioinformatics/btu494

Piña, R. G., and Cervantes, C. (1996). Microbial interactions with aluminium. *Biometals* 9, 311–316. doi: 10.1007/BF00817932

Prosser, J. I. (2015). Dispersing misconceptions and identifying opportunities for the use of 'omics' in soil microbial ecology. *Nat. Rev. Microbiol.* 13, 439–446. doi: 10.1038/nrmicro3468

Quince, C., Lanzen, A., Davenport, R. J., and Turnbaugh, P. J. (2011). Removing noise from pyrosequenced amplicons. *BMC Bioinform.* 12:38.

Sangwan, P., Chen, X., Hugenholtz, P., and Janssen, P. H. (2004). Chthoniobacter flavus gen. nov., sp. nov., the first pure-culture representative of subdivision two, *Spartobacteria* classis nov., of the phylum *Verrucomicrobia*. *Appl. Environ. Microbiol.* 70, 5875–5881. doi: 10.1128/AEM.70.10.5875-5881.2004

Santoyo, G., Hernández-Pacheco, C., Hernández-Salmerón, J., and Hernández-León, R. (2017). The role of abiotic factors modulating the plant-microbe-soil interactions: toward sustainable agriculture – a review. *Span J. Agric. Res.* 15:e03R01.

Sessitsch, A., Howieson, J. G., Perret, X., Antoun, H., and Martínez-Romero, E. (2002). Advances in *Rhizobium* research. *Crit. Rev. Plant Sci.* 21, 323–378.

Soltani, A., Khavazi, K., Asadi-Rahmani, H., Omidvari, M., Dahaji, P. A., and Mirhoseyni, H. (2010). Plant growth promoting characteristics in some *Flavobacterium* spp. isolated from soils of Iran. *J. Agric. Sci.* 2, 106–115.

van Elsas, J. D., Chiurazzi, M., Mallon, C. A., Elhottova, D., Kristufek, V., and Salles, J. F. (2012). Microbial diversity determines the invasion of soil by a bacterial pathogen. *Proc. Natl. Acad. Sci. U.S.A.* 109, 1159–1164. doi: 10.1073/pnas.1109326109

Wasai, S., and Minamisawa, K. (2018). Plant-associated microbes: from rhizobia to plant microbiomes. *Microb. Environ.* 33, 1–3. doi: 10.1264/jsme2.ME3301rh

White, R. A. III, Rivas-Ubach, A., Borkum, M. I., Köberl, M., Bilbao, A., Colby, S. M., et al. (2017). The state of rhizospheric science in the era of multi-omics: a practical guide to omics technologies. *Rhizosphere* 3, 212–221.

White, T. J., Bruns, T., Lee, S., and Taylor, J. W. (1990). "Amplification and direct sequencing of fungal ribosomal RNA genes for phylogenetics," in *PCR Protocols: A Guide To Methods And Applications*, eds M. A. Innis, D. H. Gelfand, J. J. Sninsky, and T. J. White, (New York, NY: Academic Press), 315–322.

Wilpiszeski, R. L., Aufrecht, J. A., Retterer, S. T., Sullivan, M. B., Graham, D. E., Pierce, E. M., et al. (2019). Soil aggregate microbial communities: towards understanding microbiome interactions at biologically relevant scales. *Appl. Environ. Microbiol.* 85:e0324-19. doi: 10.1128/AEM.00324-19

Wu, Y., Zeng, J., Zhu, Q., Zhang, Z., and Lin, X. (2017). pH is the primary determinant of the bacterial community structure in agricultural soils impacted by polycyclic aromatic hydrocarbon pollution. *Sci. Rep.* 7:40093. doi: 10.1038/srep40093

Zajc, J., Zalar, P., and Gunde-Cimerman, N. (2017). "Yeasts in hypersaline habitats," in *Yeasts in Natural Ecosystems: Diversity*, eds P. Buzzini, M. A. Lachance, and A. Yurkov, (Berlin: Springer), 293–329.

Zhang, Q., Sun, J., Liu, S., and Wei, Q. (2013). Manure refinement affects apple rhizosphere bacterial community structure: a study in sandy soil. *PLoS One* 8:e76937. doi: 10.1371/journal.pone.076937

Zhang, T., Wang, N. F., Liu, H. Y., Zhang, Y. Q., and Yu, L. Y. (2016). Soil pH is a key determinant of soil fungal community composition in the Ny-Ålesund Region, Svalbard (High Arctic). *Front. Microbiol.* 7:227. doi: 10.3389/fmicb.2019.0227

Conflict of Interest: HU is founder and CEO of the company TB Unterfrauner GmbH.

The remaining authors declare that the research was conducted in the absence of any commercial or financial relationships that could be construed as a potential conflict of interest.

frontiers in Plant Science

ORIGINAL RESEARCH
published: 28 May 2020
doi: 10.3389/fpls.2020.00599

Drought Drives Spatial Variation in the Millet Root Microbiome

*Tuesday Simmons[1], Alexander B. Styer[1], Grady Pierroz[1], Antonio Pedro Gonçalves[1], Ramji Pasricha[1], Amrita B. Hazra[1], Patricia Bubner[1] and Devin Coleman-Derr[1,2]**

[1] Department of Plant & Microbial Biology, University of California, Berkeley, Berkeley, CA, United States, [2] Plant Gene Expression Center, United States Department of Agriculture–Agriculture Research Service, Albany, CA, United States

Efforts to boost crop yield and meet global food demands while striving to reach sustainability goals are hindered by the increasingly severe impacts of abiotic stress, such as drought. One strategy for alleviating drought stress in crops is to utilize root-associated bacteria, yet knowledge concerning the relationship between plant hosts and their microbiomes during drought remain under-studied. One broad pattern that has recently been reported in a variety of monocot and dicot species from both native and agricultural environments, is the enrichment of Actinobacteria within the drought-stressed root microbiome. In order to better understand the causes of this phenomenon, we performed a series of experiments in millet plants to explore the roles of drought severity, drought localization, and root development in provoking *Actinobacteria* enrichment within the root endosphere. Through 16S rRNA amplicon-based sequencing, we demonstrate that the degree of drought is correlated with levels of *Actinobacterial* enrichment in four species of millet. Additionally, we demonstrate that the observed drought-induced enrichment of *Actinobacteria* occurs along the length of the root, but the response is localized to portions of the root experiencing drought. Finally, we demonstrate that *Actinobacteria* are depleted in the dead root tissue of Japanese millet, suggesting saprophytic activity is not the main cause of observed shifts in drought-treated root microbiome structure. Collectively, these results help narrow the list of potential causes of drought-induced *Actinobacterial* enrichment in plant roots by showing that enrichment is dependent upon localized drought responses but not root developmental stage or root death.

Keywords: plant microbiome, abiotic stress, root endosphere, drought, plant microbe interaction

OPEN ACCESS

Edited by:
Collin M. Timm, Johns Hopkins University, United States

Reviewed by:
Sarah Lydia Lebeis, The University of Tennessee, Knoxville, United States
Parvathi Madathil Sreekumar, Kerala Agricultural University, India
Ramona Marasco, King Abdullah University of Science and Technology, Saudi Arabia

***Correspondence:**
Devin Coleman-Derr
colemanderr@berkeley.edu

Specialty section:
This article was submitted to Plant Abiotic Stress, a section of the journal Frontiers in Plant Science

Received: *07 December 2019*
Accepted: *20 April 2020*
Published: *28 May 2020*

Citation:
Simmons T, Styer AB, Pierroz G, Gonçalves AP, Pasricha R, Hazra AB, Bubner P and Coleman-Derr D (2020) Drought Drives Spatial Variation in the Millet Root Microbiome. Front. Plant Sci. 11:599. doi: 10.3389/fpls.2020.00599

INTRODUCTION

Drought is a major obstacle to agricultural productivity. It is currently the climate phenomenon with the greatest negative impact on cereal production (Lesk et al., 2016), and the severity and frequency of drought is expected to increase in the coming decade (Vicente-Serrano and Lopez-Moreno, 2014; Spinoni et al., 2018). As such, it represents one of the largest challenges to food security (Kogan et al., 2019), especially considering the anticipated increases in food production that will be needed to feed the growing world population (Ray et al., 2013). Historically, crop breeding has helped select for drought resistant cultivars, but such efforts are often time and labor intensive (Coleman-Derr and Tringe, 2014). For these reasons, development of alternative

strategies of protection against drought's negative impacts on crop fitness are needed (Kang et al., 2009; Lesk et al., 2016).

Microbially mediated crop fortification is currently touted as an attractive strategy for mitigating drought stress (Naylor and Coleman-Derr, 2018). Additionally, it has been shown that plant growth promoting microorganisms (PGPM) have a greater effect on plant growth during drought compared to well-watered conditions (Rubin et al., 2017), and it is well established that crops grown in arid desert ecosystems act as "resource islands" for cultivating known PGPM in the surrounding soil (Köberl et al., 2011; Marasco et al., 2012). Recent work has demonstrated that drought has a strong impact on the structure and activity of the root microbiome, and is correlated with a significant enrichment in lineages of monoderm bacteria within the root and rhizosphere that is not observed in the surrounding soil (Naylor et al., 2017; Santos-Medellín et al., 2017; Edwards et al., 2018; Fitzpatrick et al., 2018; Xu et al., 2018). It should be noted that within these studies, those that investigated single host species (Santos-Medellín et al., 2017; Edwards et al., 2018; Xu et al., 2018) reported an enrichment of primarily *Actinobacteria*, *Firmicutes* to a lesser degree, and some lineages of *Chloroflexi*. Other studies that looked at multiple host species (Naylor et al., 2017; Fitzpatrick et al., 2018) reported that *Actinobacteria* were the enriched taxa across hosts, and additional studies have noted that *Actinobacteria* dominate portions of the root microbiome for desert-adapted plants (Marasco et al., 2018). For this reason, the primary focus of this research is on understanding the causes of the *Actinobacterial* enrichment in the endosphere.

It has been shown that applications of *Actinobacteria*, in particular *Streptomyces spp.*, may benefit host fitness under drought (Yandigeri et al., 2012; Xu et al., 2018); many strains are antagonistic toward pathogens (Millard and Taylor, 1927; Newitt et al., 2019; Suárez-Moreno et al., 2019), produce beneficial secondary metabolites, and assist in nutrient acquisition (Sathya et al., 2017). However, the spatial-temporal dynamics of drought-induced enrichment of *Actinobacteria* remains largely uncharacterized, and it is unclear if this restructuring occurs in all roots – and all parts of each root – within the root system. Water availability is known to vary within the root zone, both at the macro scale (due to the falling water table) and the micro scale (due to the heterogeneous nature of soil composition) (D'odorico and Porporato, 2006). Whether the resulting variability in the degree of water stress that is likely to occur across a drought-stressed root system corresponds with differential recruitment of microbes is also currently unknown.

A better understanding of the underlying spatial organization of the observed *Actinobacterial* enrichment may help identify the underlying causes of this phenomenon. At present, it is unknown if the enrichment is driven by local or systemic changes in host physiology or metabolism. If the drought-induced shifts in the root microbiome are limited to roots that directly perceive a lack of water, then localized responses to drought stress could serve as a signal for *Actinobacteria* enrichment. For example, perhaps root tissue death (Liu et al., 2009) triggers the proliferation of saprophytic lineages within *Actinobacteria*. Alternatively, if the observed enrichment also occurs in the relatively few roots of drought stressed plants with access to water, this phenomenon may instead be driven by systemic processes, such as above-ground, vasculature-mediated changes in plant metabolism that are translocated throughout all root tissue.

In addition, physiological and functional properties of root tissue differ along the root's longitudinal axis even within the context of a single root (Petricka et al., 2012). Older root tissue closer to the stem is responsible for root hair and lateral root development, while the youngest tissue at the tip is responsible for active growth, cell division, and is the site of the majority of root exudation (Canarini et al., 2019). Whether the drought-induced enrichment in *Actinobacteria* occurs across the entirety of an individual root's length, or is specific to older or younger tissue types, is currently unknown.

To address these knowledge gaps, we have conducted a series of field and greenhouse-based experiments to allow for spatially resolved measurements of the compositional shifts within the millet root microbiome that occur in response to drought. Millets are a polyphyletic group of cereal crops that provide a primary source of food and fodder for hundreds of millions of people in the dry regions of Africa and Asia (Patil, 2017). They are often grown on marginal lands where irrigation is rain fed and sporadic, and as such are among the crops most exposed to water stress during periods of drought (Kumar et al., 2018). In this study, we worked with five different members of the Paniceae tribe: *Setaria italica* (foxtail millet), *Pennisetum glaucum* (pearl millet), *Panicum miliaceum* (proso millet), and *Echinochloa esculenta* (Japanese barnyard millet), which are all millets, and *Sorghum bicolor,* a related cereal crop. We set out to test whether millets, like other cereal crops, are enriched with *Actinobacteria* when drought stressed, and whether this enrichment is correlated with the severity of drought. We also tested whether this pattern is specific to a particular root tissue age, and if enrichment occurs at similar levels from the actively growing root tip to older and more mature root tissue basal to the stem. This would demonstrate whether recently reported drought-induced changes in the plant root microbiome are driven by root specific factors that are independent of the root tissue's developmental stage. Additionally, using a split-pot experimental design, we test whether observed enrichment of *Actinobacteria* is localized to drought-stressed roots, or systemically throughout the root system. Finally, we investigate localized root death as a potential primary driver of the observed bacterial community shifts.

MATERIALS AND METHODS

Drought Gradient and Multi-Species Field Design

Four species of millet – all members of the *Paniceae* tribe – were planted on May 19th, 2015 at the University of California at Berkeley's Gill Tract research field in Albany, California (37°53′12.3″N 122°18′00.3″W): *Setaria italica* (foxtail millet), *Pennisetum glaucum* (pearl millet), *Panicum miliaceum* (proso millet), and *Echinochloa esculenta* (Japanese millet). Seeds were planted directly in the field with 8–10 seeds per hill and hills 25–30 cm apart. The four species were subjected to three different watering regimes: control (watered on the day of planting then

weekly until maturity), moderate drought (watered on the day of planting, weekly for the next 5 weeks, and water then withheld until maturity), and severe drought (watered on the day of planting, once the following week, then withheld until maturity). Watering treatments were applied for 6 h using drip irrigation tape with 1.89 L/h rate flow emitters. Tissue and soil samples were harvested 24 weeks post-germination, after each species had reached maturity. Root systems for each species are structurally similar; they all are fibrous and lack a tap root, typical of monocotyledons. Bulk soil samples were taken 30 cm from the base of the plant at the same time point; root/rhizosphere were collected as detailed in Simmons et al. (2018) and stored in phosphate buffer at −80°C until further processing.

Sub-Sectioned Root Field Experimental Design

Sorghum bicolor was chosen for this experiment due to its larger root structure, which allowed for increased precision during root system dissection. *S. bicolor* seeds were planted on June 21, 2017 at the USDA Gill Tract research field in Albany, California under a sheet of plastic mulch to reduce weed growth. Plants were watered weekly for the first 3 weeks after planting. For each application, water was administered for 6 h using drip irrigation tape with 1.89 L/h rate flow emitters. Samples were taken for whole root systems and three single roots after 1 week. After 2, 3, 9, and 11 weeks, we collected whole root systems and six single roots, three of which were further partitioned into 3 approximately equal length subsections. At each time point, a single bulk soil sample was collected for each plant, approximately 30 cm from the base of the plant. When collecting root samples, the single roots were collected first, and the remaining roots were pooled and considered to be the whole root system (**Supplementary Figure S1**). The single roots were selected from the system by: presence of root tip and minimal lateral root growth. After sample collection, roots were placed into sterile conical tubes with phosphate buffer and stored at −20°C until further processing.

Split-Pot Experimental Design

Fifteen *E. esculenta* seeds were planted in sterile pots filled with sifted field soil and grown for 2 weeks before transferring 12 plants to a split-pot design (**Supplementary Figure S2**). The split-pot design consisted of two 1-L square sterile pots connected together with adhesive and filled with field soil pre-sifted through a 1 cm sieve; transplanted seedling roots were partitioned such that half of the root system was located on each side of the split-pot system. After a 1 week acclimation period, three different watering regimes were initiated: full water (W; water was applied on both sides), full drought (D; drought was applied on both sides), and half-water/half-drought (W/D; water was applied only on one side) with four plants per treatment. A plastic sheath was applied to the outside of the pot on the drought side of the W/D plants to prevent water from moving up through the base of the pot from the water reservoir below. Plants were grown for an additional 10 days before collecting bulk soil from both sides of the pot; root/rhizosphere samples were collected as described above and stored in phosphate buffer at −20°C until further processing.

Live-Dead Root Community Profiling Design

Five *E. esculenta* seeds were planted per pot in 0.25L sterilized pots (13) in a greenhouse. After 1 week, the pots were thinned to one plant each, and 1 week later the plants were transplanted to sterile 4 L pots filled with sifted (1 cm sieve) field soil. They were grown for an additional week before initiating drought stress on half of the plants (28 days post-germination). One day after the start of drought treatment, a subsection of roots was severed from the rest of the plant by connecting a razor blade to the end of a wooden stake and pushing it at a 45° angle through the root zone, starting at the base of the plant (**Supplementary Figure S3**). The blade was then removed, and the wooden stake replaced within the soil to identify the location of separated tissue. After 10 days of drought, root and rhizosphere samples were collected from both living and dead roots and placed into conical tubes with phosphate buffer. Samples were stored at −20°C until further processing. Additional severed and live root samples were collected from replicate plants to perform cell viability assays on the roots. These assays were performed on roots collected on the day of root detachment, 3 days later, and on the day samples were collected for community profiling (9 days post-detachment). To assay cell death, we used the Plant Cell Viability Assay kit (Sigma-Aldrich, Darmstadt, Germany) according to the manufacturer's instructions.

Root/Rhizosphere Processing and DNA Extraction

The methods used here are modifications of what is described in Simmons et al. (2018). Roots frozen in phosphate buffer solution were thawed at 4°C and washed by sonication in a Bioruptor Plus ultrasonicator (Diagenode, Denville, NJ, United States) at 4°C for 10 min. Roots were removed from vials and rinsed twice with autoclaved water. For each plant in the subsectioning experiment, three of the clean individual roots were then cut into three sections of equal length. Roots not being processed immediately were placed in fresh sterile phosphate buffer and frozen at −80°C. Rhizosphere soil samples from the sonicated vials were centrifuged (10 min at 4 °C, 4,000 × *g*), and DNA was extracted by processing approximately 250 mg of each sample with MoBio's PowerSoil kit (prior to Qiagen purchasing MoBio). DNA was extracted from root samples by grinding to a powder with liquid nitrogen, mixing 600–700 mg powder with CTAB buffer, and washing with phenol chloroform-isoamyl alcohol. For individual and sectioned roots in the subsectioning experiment, DNA was extracted using approximately 50 mg of tissue in MoBio's PowerPlant kit. Bulk soil DNA was extracted with MoBio's PowerSoil kit.

16S Amplification and Sequencing

All samples were amplified in triplicate using barcoded universal primers (180 s at 98 °C, 30 cycles of: 98 °C for 45 s, 78°C for 10 s, 55°C for 60 s, and 72°C for 90 s, then

600 s at 72°C followed by a 4°C hold) for the v3-v4 region (341 F, 5′-CCTACGGGNBGCASCAG-3′ and 785 R, 5′-GACTACNVGGGTATCTAATCC-3′) of the 16S rRNA gene according to Simmons et al. (2018). Additionally, PNAs matching chloroplast and mitochondrial 16S sequences were spiked into PCRs (2.28 μM final concentration) to prevent amplification of these unwanted reads. Replicate PCR products were pooled and quantified using Qubit HS assay; 100 ng from each sample was pooled together and cleaned using AMPureXP magnetic beads before a final quantification and dilution to 10 nM for sequencing at the UC Berkeley Vincent Coates Sequence Facility via Illumina MiSeq (v3 chemistry, 300 bp paired-end sequencing). Reads were demultiplexed in QIIME2 (Bolyen et al., 2018) and then passed to DADA2 (Callahan et al., 2016) where sequences were trimmed to ensure minimum median Phred Q-scores of 30 or greater at any given base pair position prior to denoising and Amplicon Sequence Variant (ASV) inference; 500,000 reads were used to train error-rate models, but otherwise all other pipeline default settings were used. A taxonomy classifier was trained to the V3-V4 region of sequences from the August 2013 version of GreenGenes 16S rRNA gene database via Naive Bayesian methods in QIIME2 and used to assign taxonomic associations to ASVs. All subsequent statistical analyses were completed in R; scripts and datasets can be found at https://github.com/colemanderr-lab. The phylogenetic tree of indicator species was generated using the online tool: Interactive Tree Of Life (iTOL) v5 (Letunic and Bork, 2019). All raw reads are deposited in the NCBI Short Read Archive at accession PRJNA607579.

RESULTS

Bacterial Root Microbiome Is Driven by Host Species and Degree of Drought

Recent work has shown that drought leads to enrichment of *Actinobacteria* within the root microbiome of a wide variety of angiosperms, including many cereal crops (Naylor et al., 2017; Fitzpatrick et al., 2018). To establish whether drought produced similar enrichment patterns in millets, as well as explore whether such enrichments are correlated with the severity of drought treatment, we conducted a field experiment in which four millet species (see section "Materials and Methods") were subjected to three different watering regimes (control, moderate drought, or severe drought) in a field with acidic silty loam soil (pH 5.2) (Naylor et al., 2017). At the time of sample collection (164 days post-germination), gravimetric soil moisture content was found to be significantly different (p = 1.56E-17, one-way ANOVA) between all three treatments:16.1% for control (n = 12, SD = 2.89%), 5.5% for moderate drought (n = 12, SD = 1.27%), and 3.7% for severe drought (n = 12, SD = 0.67%). Aboveground phenotypes measured at root collection demonstrate that despite millet's drought tolerance, drought treatment had a significantly negative impact on plant growth (**Supplementary Figures S4–S6**). Plant height was negatively impacted by drought stress across three millet species (phenotypic data for one species was not collected; Wilcoxon rank-sum test, $p < 0.001$), with the greatest impact observed under severe drought stress. Additionally, one variety (*E. esculenta*) displayed a significant reduction in grain ear length (Wilcoxon rank-sum test, $p < 0.01$) during severe drought, and median values of ear length decreased with increasing drought severity across all three species. Together these results suggest that drought treatment negatively impacted millet fitness, and that the degree of impact was correlated with drought severity.

To investigate how bacterial communities shifted during increasing levels of drought stress in millet, we profiled the soil, rhizosphere, and root endophyte communities by barcoded amplicon sequencing. We observed that while there is a significant difference between the alpha diversity in bulk soil, rhizosphere, and endosphere samples ($p < 0.05$, Tukey's test), there is not a significant difference between the drought treatments within the same sample type (**Figure 1A**). It is also noteworthy that while the root endosphere communities are less diverse than their corresponding rhizospheres in the control and moderate drought conditions, this is not the case for severe drought (**Figure 1A**). Additionally, drought provoked a relative increase in *Actinobacteria* within root endophyte, rhizosphere, and unexpectedly, bulk soil communities (**Figure 1B**). Moderate drought, which was initiated later in plant development, failed to provoke a strong enrichment in *Actinobacteria* within roots or rhizosphere, a result that is consistent with recent research that demonstrated that drought occurring earlier in development provokes a more substantial shift in *Actinobacteria* (Xu et al., 2018).

To explore how bacterial community composition varied across both host species and treatment, PERMANOVA and ordination analyses were performed on Bray Curtis distances. These analyses revealed significant differences in composition across the dataset are driven by primarily by sample type (F-statistic = 17.864, $p < 0.001$), with weaker effects contributed by host species (F-statistic = 4.952, $p < 0.001$), and watering treatment (F-statistic = 3.989, $p < 0.001$); the strong clustering by sample type is confirmed by Principle Coordinate Analysis (**Figure 1C**). When considering root endophyte communities alone, the percent of variance attributable to water treatment is 9.6% ($p < 0.001$), and the percent of variance attributable to host species is 21.2% ($p < 0.001$), and Constrained Analysis of Principle Coordinates reveals clustering by both species and treatment (**Figure 1D**). Taken together, these results demonstrate that the millet root microbiome responds to drought treatment in a manner similar to other previously reported plant systems, making them suitable systems for the experiments described below.

Actinobacteria Enrichment Pattern Occurs Along the Length of the Root

We hypothesized that enrichment of *Actinobacteria* would be observable throughout the root system rather than in specific root zones or types. After profiling the bacterial communities at sub-root system spatial resolution (**Supplementary Figure S1**), we found that an enrichment of *Actinobacteria* under drought treatment was observed within single roots and across all three subsections of an individual root, with concomitant

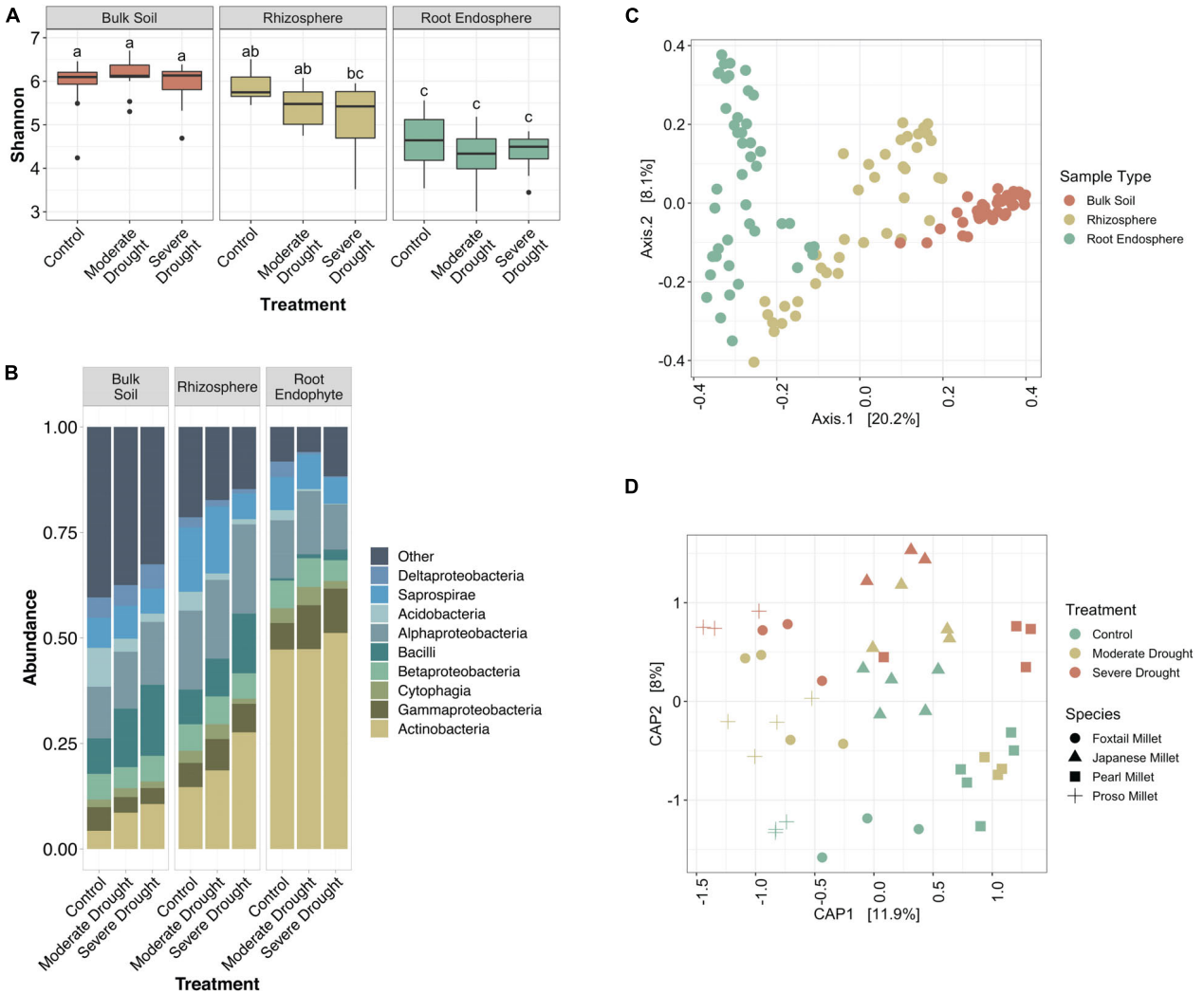

FIGURE 1 | Millet root microbiome profiles vary by severity of drought. **(A)** Box-and-whiskers plot of Shannon's diversity of bulk soil, rhizosphere, and root endophyte communities subjected to a gradient of water conditions (control, moderate drought, and severe drought). Letters indicate significantly different groups ($p < 0.05$, Tukey's test) From left to right sample size: n = 13, 13, 13, 12, 12, 15, 16, 15, 13. **(B)** Relative abundance of the top 9 most abundant bacterial classes in each compartment of the root microbiome. **(C)** Ordination plot (PCoA) of all samples based on Bray-Curtis dissimilarity, colored by the source material. **(D)** Constrained ordination plot (CAP) of root endophyte samples based on Bray-Curtis dissimilarity. Colors indicate treatment type and shape indicates host species.

decreases in most *Proteobacterial* classes (**Figure 2**). Additionally, *Actinobacteria* are the predominant indicator taxa of drought within each subsection according to Dufrene-Legendre indicator species analysis (**Figure 3**; Dufrêne and Legendre, 1997). This demonstrates that *Actinobacterial* enrichment is not unique to the actively growing root tip where most new microbial recruitment to the root endosphere is thought to occur (Shyam et al., 2017). Notably, however, both *Firmicutes* and *Chloroflexi* appeared more often as indicators of the watered condition, in contrast to what has been observed in several other studies.

Additionally, as part of this experiment, a comparison of intrareplicate and intraplant variation within root sample types was conducted. We hypothesized that due to the stochastic nature of root colonization events and founder effects at smaller physical scales, variation between replicates would be greater in subsections rather than whole root systems. As expected, we observed that as the spatial resolution increases from whole root systems toward individual root subsections, variation between sample replicates increases (**Supplementary Figure S7**). Additionally, we observed that root communities of replicates from the same plant are more similar to each other than replicates from different plants (F-statistic = 507.4, $p < 0.0001$, **Supplementary Figure S8**) and replicates from the same root are again more similar compared to replicates from different roots of the same plant (F-statistic = 7.453, $p < 0.007$, **Supplementary Figure S8**). Interestingly, root tips account for greater dissimilarity when comparing subsections of roots both within and between plants, likely indicating that root tips are sites of stochastic colonization while older middle and basal

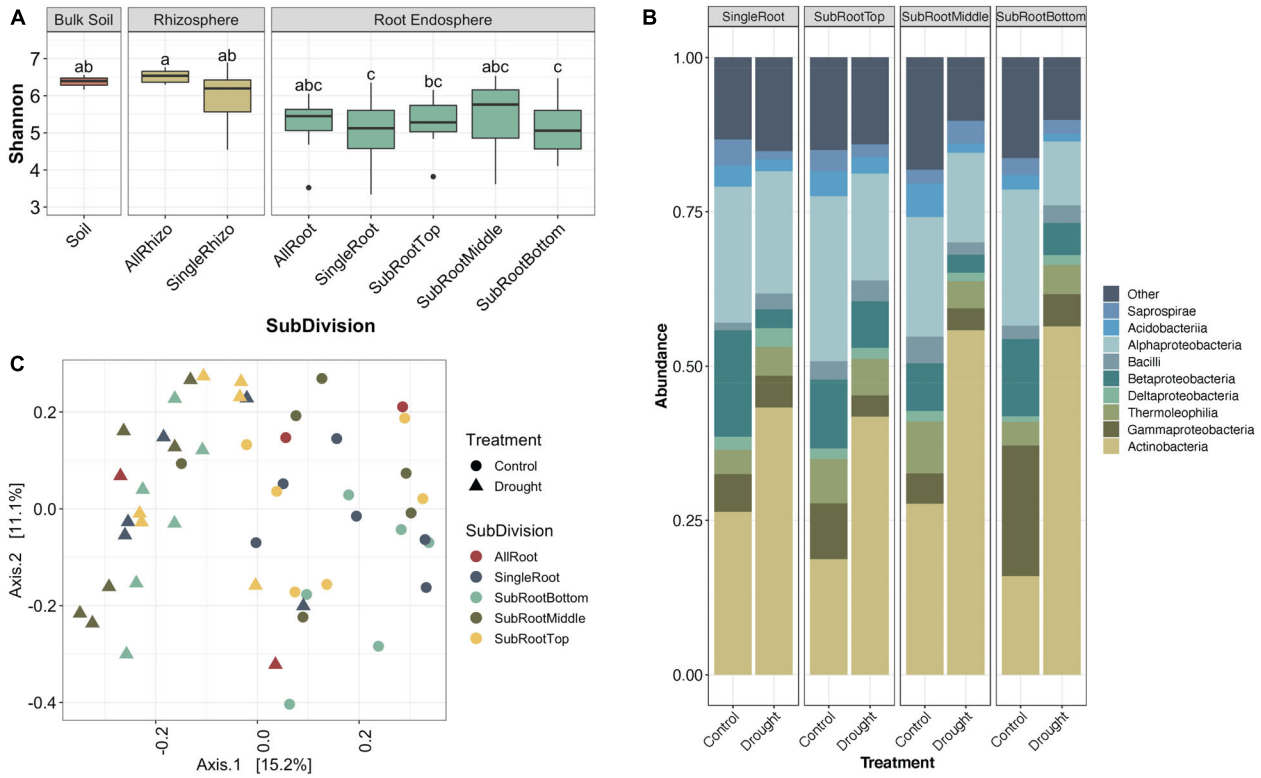

FIGURE 2 | Variation in sorghum root microbiome communities by root age. **(A)** Box-and-whiskers plot of Shannon's diversity of bulk soil, rhizosphere, and root endophyte communities separated by root age. SubDivision (x-axis) indicates whether samples came from whole root systems (AllRoot; the bulk of roots remaining after six individual roots were collected), individual roots (SingleRoot), or subsectioned roots (SubRootTop is closest to the plant and SubRootBottom is the root tip). Letters indicate significantly different groups ($p < 0.05$, Tukey's test). **(B)** Relative abundance of the top 9 most abundant bacterial classes in the root endosphere separated by water treatment. **(C)** PCoA plot of root samples based on Bray-Curtis dissimilarity, colored by root age where open circles are well-watered control roots and triangles are drought-stressed roots.

sections of roots have communities stabilized through selection and competition (**Supplementary Figure S8**).

Localized Drought Causes Enrichment of Actinobacteria

While the enrichment of *Actinobacteria* bacteria during drought does not appear to depend on the developmental stage of root tissue, it remains unclear whether this enrichment is driven by localized processes at the site of drought, or by systemic responses affecting the entire root system. Using Japanese millet grown in a split-irrigation design (**Supplementary Figure S2**), Constrained Analysis of Principal Components (CAP) of amplicon-based bacterial community profiling of the roots and rhizosphere revealed that root endophyte communities from the watered side of the were more similar to the communities of fully watered plants, while the drought-treated side of the split-irrigation plants were more similar to communities found in fully drought-treated plants (**Figures 4A,B**). Comparisons of the root endophyte community relative abundance patterns between the two sides of split-irrigation plants and between their fully watered and drought treated counterparts demonstrated that there is an increase in the abundance of *Actinobacteria* in drought-treated roots in both full drought and split-drought treatments (**Figure 4C**). Collectively, these results suggest that *Actinobacterial* enrichment occurs locally at the site of drought induction rather than systemically.

Root Death Does Not Drive Enrichment of Actinobacteria

A subset of *Actinobacteria* lineages can exist as saprophytes (Barka et al., 2016), deriving their carbon from dead and decaying plant material. As localized root tissue death can accompany severe drought stress (Liu et al., 2009), we surmised that the observed local enrichment in *Actinobacteria* could be driven by root death. To test this hypothesis, we induced localized root death through mechanical severing and compared levels of *Actinobacteria* recruitment across the root system under drought stress and induced root death treatments (**Supplementary Figure S3**). To confirm root death, we used a live-dead stain to test for cell viability. A subset of cells remained viable for 3 days following root separation, but by 9 days cells within separated roots were no longer viable (**Supplementary Figure S9**). After community profiling of the root (**Figure 5**) and rhizosphere (**Supplementary Figure S10**)

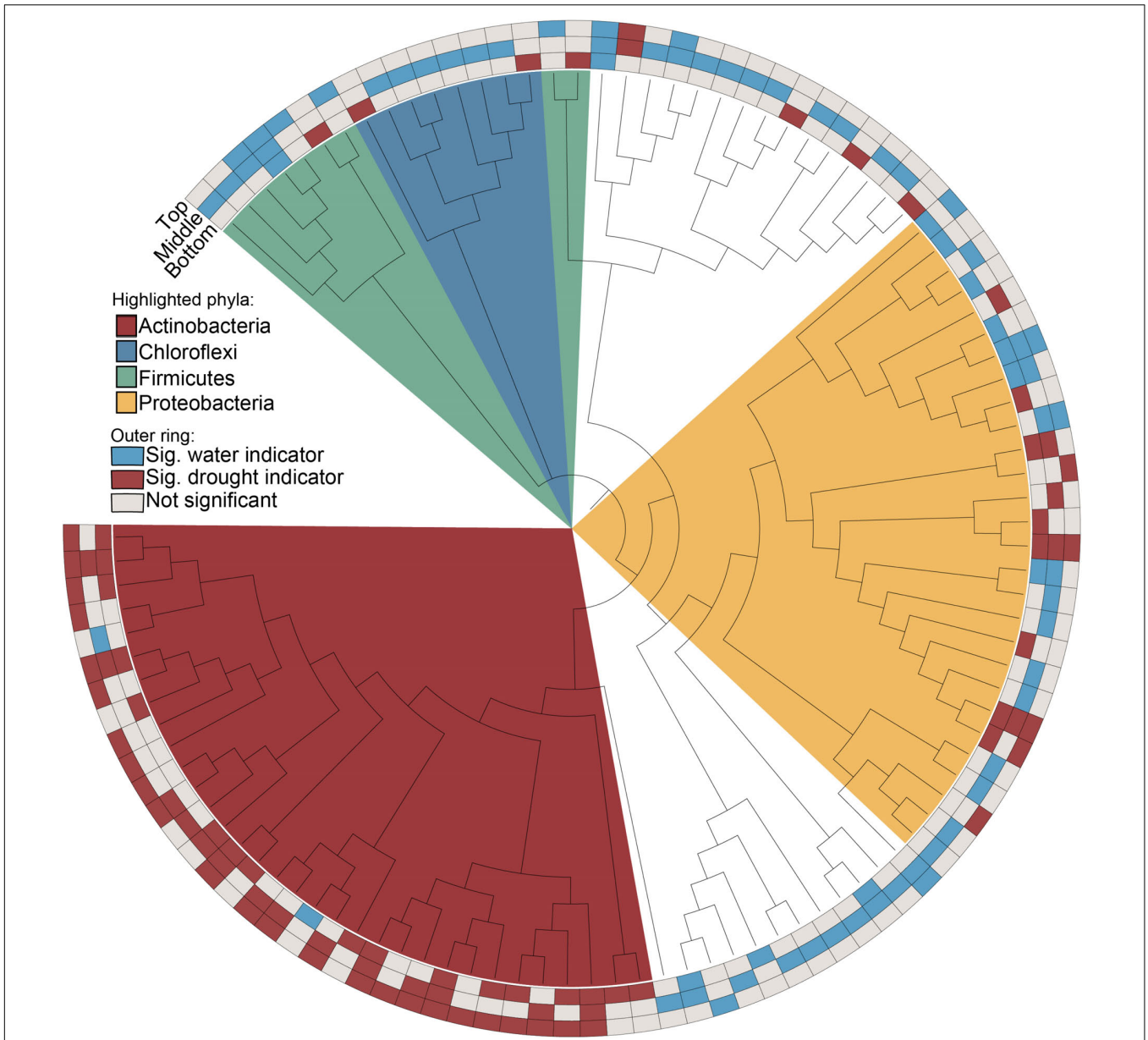

FIGURE 3 | Indicators of drought and watered conditions by root subsection (root tip, middle, or base). Nodes represent genera where taxonomic information was available to group ASVs by this rank. Red and blue boxes indicate nodes that are significant indicators of drought and water conditions after Dufrene-Legendre analysis, respectively ($p < 0.05$, indcls >0.5). Nodes are highlighted by phyla [*Actinobacteria* (red), *Chloroflexi* (blue), *Firmicutes* (green), *Proteobacteria* (yellow)].

fractions, we observed that in addition to the expected differences in bacterial community composition between drought-treated and watered samples, communities in living or dead tissue showed significant differences. Performing PERMANOVA on the root endophyte samples showed that water treatment explains 23.2% of variance in beta-diversity ($p < 0.001$), and tissue death explained 11.6% ($p = 0.003$).

Contrary to our hypothesis, an enrichment of *Actinobacteria* was not observed in dead roots compared to living roots under either watering condition (**Figure 5**). Additionally, performing Dufrene-Legendre indicator species analysis showed that there were no *Actinobacteria* indicators for dead root communities in either watered or drought-stressed tissues. Collectively, these results suggest that their drought-driven shift is unlikely to be attributable to saprophytic activity stimulated through root death. Interestingly, in addition to the expected increase in *Actinobacteria* from watered to drought-stress observed within living roots, a small increase is also observable within the dead roots (**Figure 5B**). A cell viability assay (**Supplementary Figure S9**) demonstrated that a portion of cells within detached roots are still viable after 3 days, suggesting that overall detached roots might be continuing to function metabolically

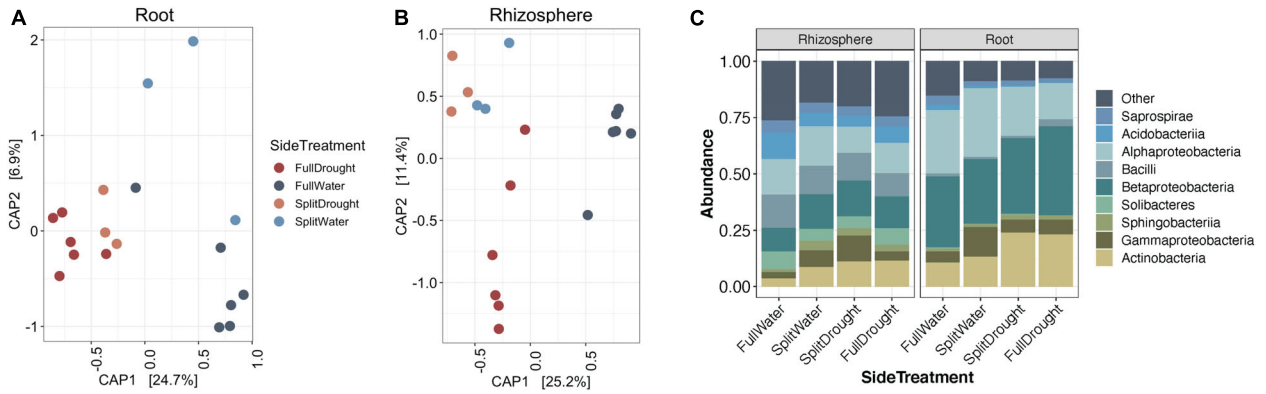

FIGURE 4 | Effect of a split-pot watering system on the root microbiome. **(A)** CAP plot of root endosphere samples colored by water treatment in Japanese millet. **(B)** CAP plot of rhizosphere samples colored by water treatment in Japanese millet. **(C)** Relative abundance of the top 9 most abundant bacterial classes in either the rhizosphere or endosphere of the different watering treatments of Japanese millet.

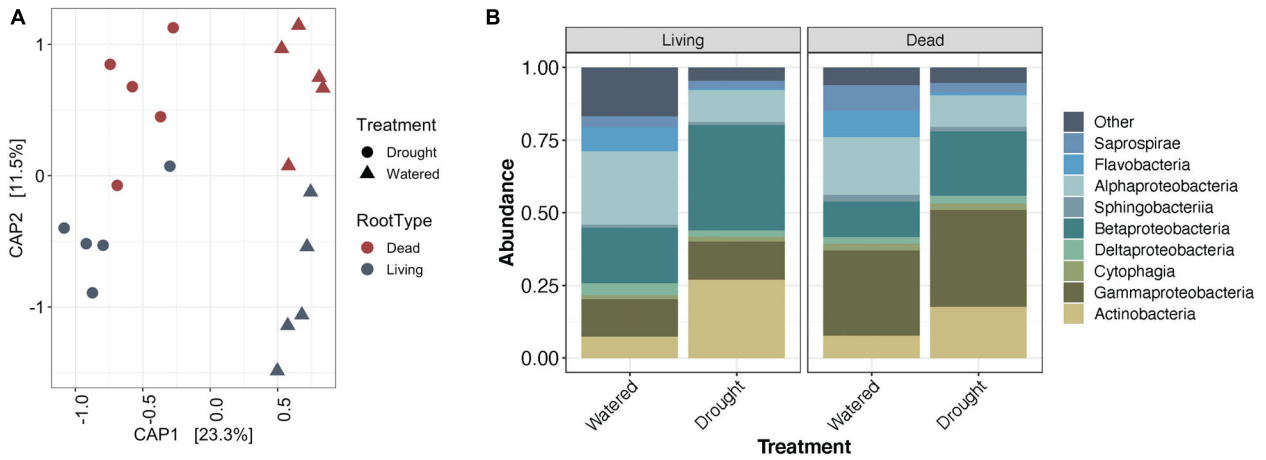

FIGURE 5 | Impact of root death on Japanese millet root endophyte communities. **(A)** CAP plot of root endosphere samples colored by root type and shaped by water treatment. **(B)** Relative abundance of the top 9 most abundant bacterial classes in the root endosphere separated by root type and water treatment.

for a period of time, which could explain the observed slight *Actinobacterial* enrichment if plant metabolism is a primary driver of this phenomenon.

Drought Enrichment of Actinobacteria Is Consistent Across Hosts and Drought Treatments

We consistently observed enrichment of *Actinobacteria* across multiple experiments including both field and greenhouse studies, multiple millet species, and varying degrees and localizations of drought stress (**Figure 6**). While *Actinobacteria* as a phylum appears to become generally enriched under drought, other phyla such as the *Proteobacteria* are less consistent in their drought enrichment patterns, with taxa capable of being a significant indicator of both water and drought conditions across different experiments (**Figure 6** and **Supplementary Table S1**). Interestingly, other phyla known to be composed of predominantly monoderm taxa such as the *Chloroflexi* and *Firmicutes* are not enriched under drought and in fact show more significant indicators of watered conditions (**Figure 6**).

DISCUSSION

Actinobacterial Enrichment Under Drought Occurs Irrespective of Root Tissue Age

Our study provides an increased-resolution spatial dissection of the effect of drought stress on the development of the root microbiome and addresses several hypotheses regarding the underlying causes of recently reported increases in *Actinobacteria* that accompany drought stress. Through an exploration of the microbial communities in whole root systems, single roots, and sub-sectioned roots, we found an enrichment of *Actinobacteria* is a common phenomenon along the apical

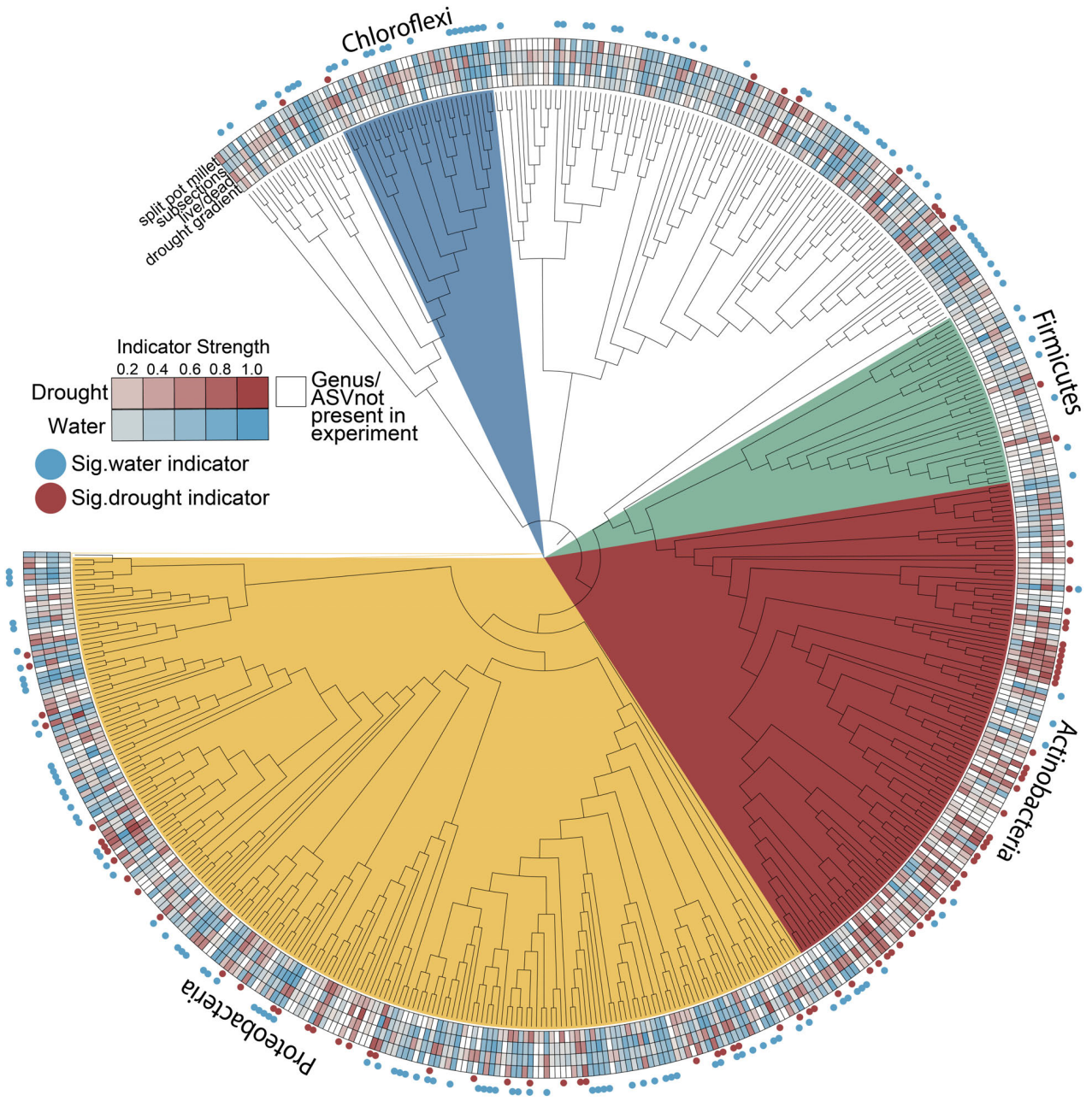

FIGURE 6 | Root endophyte indicator values for drought and water conditions across all experiments. Nodes represent genera where sufficient taxonomic information was available to group ASVs by this rank; ASVs without genus-level annotations were included but ungrouped. Heatmaps connote indicator strength for drought and watered conditions (red and blue, respectively; white indicates taxa not present in a given experiment) and filled circles connote taxa that were a significant indicator of drought (red) or watered (blue) conditions in at least one experiment ($p < 0.05$, indcls >0.5).

axis of a root (**Figure 3**). Since the majority of endophytic colonization of the root is thought to occur at the root tip and at positions where lateral roots are emerging (Shyam et al., 2017), this suggests that the underlying cause of enrichment is not simply increased rates of colonization by *Actinobacteria*, but perhaps also increased proliferation of established *Actinobacterial* endophytes within older root tissue, in comparison to other bacterial phyla. If correct, this implies that any plant-derived molecular signal that contributes to this phenomenon should be present not only within rhizosphere exudates, but also within the endosphere compartment as well. Several proposed molecular mechanisms for the observed *Actinobacterial* enrichment, including shifts in amino acids and carbohydrate biosynthesis and ROS production (Xu and Coleman-Derr, 2019), would likely affect both rhizosphere and endosphere compartments.

Other studies have explored how root associated microbial communities change across the apical axis of the root under non-drought conditions (Liljeroth et al., 1991; Yang and Crowley, 2000; Baudoin et al., 2002; Kawasaki et al., 2016). In a comparative analysis of microbiome composition between the root tip and root base of nodal roots in *Brachypodium*, Kawasaki et al. (2016) identified a relative increase in relative abundance of both *Betaproteobacteria* and *Gammaproteobacteria* lineages within the younger, growing root tip as compared to the root base. Interestingly, our data do not display a similar pattern of enrichment for these lineages, which suggests bacterial taxa may have preferential colonization rates at the root tip that differ across hosts or environments.

Actinobacterial Enrichment Under Drought Is Localized to Sites of Drought Application

While it remains unclear what host mechanisms underlie the cause of the increase in *Actinobacteria* within the root system under drought, our data demonstrate that this enrichment is observed only within roots that are experiencing drought, and not found across the entire root system. For this reason, we propose that host-mediated causes would lie in localized host responses to drought, rather than systemic responses. This would, for instance, potentially exclude shifts in plant metabolites synthesized in the leaves and transported into the root system, that likely result from altered rates of photosynthesis during drought (Pinheiro and Chaves, 2011).

Shifts in plant metabolism during drought that are localized to portions of roots subjected to drought have been identified. For example, it was recently shown that in soils with heterogeneous moisture levels, there is an increased accumulation of abscisic acid (ABA), the phytohormone regulator of drought stress response, within roots found in drier regions of soil as compared to those found in regions of higher moisture (Puértolas et al., 2015). The effect of plant-produced ABA on the root microbiome has yet to be determined, though ABA is known to turn on genes for ROS production in the apoplast (Miller et al., 2010; Brito et al., 2019), which could have an impact on the bacterial community (Xu and Coleman-Derr, 2019). Perhaps more importantly, ABA acts antagonistically to systemic levels and activity of salicylic acid (SA) (de Torres Zabala et al., 2009) and in turn SA has been shown to influence root microbiome composition (Lebeis et al., 2015; Liu et al., 2018). Additionally, it is interesting to note that *Actinobacteria*, such as *Streptomyces*, are known to trigger systemic acquired resistance (SAR), traditionally associated with pathogens (Newitt et al., 2019). Taken together, this suggests that the enrichment of *Actinobacteria* may be driven by a localized hormone mediated response to drought, and that this enrichment itself may drive additional systemic changes in plant immunity.

Actinobacterial Enrichment Under Drought Is Not Driven by Root Death

Many soil *Actinobacteria* function as saprophytes, consuming dead organic material (Barka et al., 2016). We had hypothesized that *Actinobacteria* may perceive root death within the drought-stressed root system and that this triggers their increased activity and abundance. However, we demonstrate that microbial communities of severed roots had fewer *Actinobacteria* than intact roots under both watered and drought treatments; in fact, *Actinobacteria* are the predominant indicators of living roots tissue. It is possible saprophytic colonization and activity does contribute to long term *Actinobacterial* increases under drought, and that such shifts take longer to develop than the time frame used in this study.

While historically categorized as free-living saprophytes, recent work on the root microbiome suggests that many *Actinobacteria* may have a less well understood phase of development or lifestyle associated with the endosphere, which leads to alternate functions and potentially even changes in cellular morphology (Ramijan et al., 2018; van der Meij et al., 2018). It is known that some bacteria occupy different niches (i.e., play different functional roles) depending on the presence of certain environmental triggers, such as carbon sources (Duffy and Défago, 1999; Sánchez et al., 2010). Indeed, some *Actinobacterial* lineages long considered saprophytic have been shown to, under certain environmental conditions, enhance plant growth through competition with plant pathogens (Millard and Taylor, 1927; Newitt et al., 2019). Since it is unknown what triggers the switch to a saprophytic lifestyle, and *Actinobacteria* are abundant in both living and dead roots, we could hypothesize that the bacteria are attracted to inert components of plant cell walls that are present under both conditions, and the endophytes do not express saprophytic functions within the living root environment.

Variation in Enriched Genera Within Actinobacteria

Drought-induced enrichment of *Actinobacteria* has been observed in this study across multiple experiments with different host plants, which supports a growing body of evidence that this is a widespread pattern during drought (Naylor et al., 2017; Santos-Medellín et al., 2017; Edwards et al., 2018; Fitzpatrick et al., 2018; Xu et al., 2018). Additionally, our work supports previous studies that show differences in enrichment at finer taxonomic resolution (Naylor et al., 2017; Fitzpatrick et al., 2018). That is, though *Actinobacteria* show consistent enrichment as a phylum, the families and genera that are enriched may vary between host plants or experiments (**Figure 6**). *Streptomyces* is perhaps the most notable *Actinobacteria* genus that has been described to have plant-growth promoting abilities, particularly during abiotic or pathogen stress (Yandigeri et al., 2012; Qin et al., 2015; Singh et al., 2016; Xu et al., 2018; Newitt et al., 2019). While *Streptomyces* are known to produce spores, previous studies have ruled out spore-production as the sole explanation for *Actinobacterial* enrichment under drought as there are other enriched *Actinobacterial* genera that do not contain the genetic prerequisites for spore formation (Naylor et al., 2017). Additional dissection of the host and microbial molecular response to drought stress using a combination of genetic and omic tools may help to narrow down the underlying cause of this phenomenon.

CONCLUSION

It has been well established that the composition of the root microbiome varies based on host genetics (Naylor et al., 2017; Fitzpatrick et al., 2018), host age (Edwards et al., 2018; Xu et al., 2018), environment (Bulgarelli et al., 2012; Lundberg et al., 2012; Edwards et al., 2015), and proximity to the root (Naylor and Coleman-Derr, 2018). Recent studies have demonstrated that during drought stress, there is an enrichment of *Actinobacteria* in the root endosphere, and this occurs across taxonomically diverse plant hosts (Naylor et al., 2017; Santos-Medellín et al., 2017; Edwards et al., 2018; Fitzpatrick et al., 2018; Xu et al., 2018). In this study, we used drought-tolerant millets to investigate where in the root system this enrichment occurs, in order to better understand the driving force behind it. We first show that location along the root apical axis does not affect this enrichment, suggesting that the signal is not specific to one root-zone. Subsequently, we demonstrate that the enrichment occurs only in roots that are directly perceiving drought, therefore it is not likely due to a signal that moves throughout the root system. Finally, we show that a specific localized response–root death–is not the primary cause of *Actinobacteria* enrichment. Future efforts to identify the underlying molecular causes of this phenomena are clearly necessary, and the results presented here may help inform such efforts.

DATA AVAILABILITY STATEMENT

The datasets generated for this study can be found in the NCBI Short Read Archive at accession PRJNA607579, https://github.com/colemanderr-lab/Simmons-2020.

AUTHOR CONTRIBUTIONS

PB and AH designed the multi-species field experiment. TS and DC-D designed the greenhouse, lab, and sorghum field experiments. AG and RP performed sample collection and phenotypic measurements for the multi-species experiment. TS performed the sample collection for the remaining experiments, sample preparation, and library preparation. GP performed the microscopy. TS, AS, and DC-D performed the statistical analyses and manuscript preparation.

FUNDING

This research was funded in part through grants from the Department of Energy DE-SC0014081, and the United States Department of Agriculture, CRIS 2030-21430-008-00D.

ACKNOWLEDGMENTS

We thank Daniel Caddell, Dhruv Patel, and Heidi Wipf for critical reading of the manuscript and Hannah Spinner for sample collection and preparation.

SUPPLEMENTARY MATERIAL

The Supplementary Material for this article can be found online at: https://www.frontiersin.org/articles/10.3389/fpls.2020.00599/full#supplementary-material

REFERENCES

Barka, E. A., Vatsa, P., Sanchez, L., Gaveau-Vaillant, N., Jacquard, C., Meier-Kolthoff, J. P., et al. (2016). Taxonomy, physiology, and natural products of actinobacteria. *Microbiol. Mol. Biol. Rev.* 80, 1–43. doi: 10.1128/MMBR.00044-16

Baudoin, E., Benizri, E., and Guckert, A. (2002). Impact of growth stage on the bacterial community structure along maize roots, as determined by metabolic and genetic fingerprinting. *Appl. Soil Ecol.* 19, 135–145.

Bolyen, E., Rideout, J. R., Dillon, M. R., Bokulich, N. A., Abnet, C., Al-Ghalith, G. A., et al. (2018). QIIME 2: reproducible, interactive, scalable, and extensible microbiome data science. *PeerJ Preprints* 37, 852–857. doi: 10.7287/peerj.preprints.27295v2

Brito, C., Dinis, L.-T., Ferreira, H., Coutinho, J., Moutinho-Pereira, J., and Correia, C. M. (2019). Salicylic acid increases drought adaptability of young olive trees by changes on redox status and ionome. *Plant Physiol. Biochem.* 141, 315–324. doi: 10.1016/j.plaphy.2019.06.011

Bulgarelli, D., Rott, M., Schlaeppi, K., Ver Loren, van Themaat, E., Ahmadinejad, N., et al. (2012). Revealing structure and assembly cues for *Arabidopsis* root-inhabiting bacterial microbiota. *Nature* 488, 91–95. doi: 10.1038/nature11336

Callahan, B. J., McMurdie, P. J., Rosen, M. J., Han, A. W., Johnson, A. J. A., and Holmes, S. P. (2016). DADA2: high-resolution sample inference from Illumina amplicon data. *Nat. Methods* 13, 581–583. doi: 10.1038/nmeth.3869

Canarini, A., Kaiser, C., Merchant, A., Richter, A., and Wanek, W. (2019). Root exudation of primary metabolites: mechanisms and their roles in plant responses to environmental stimuli. *Front. Plant Sci.* 10:157. doi: 10.3389/fpls.2019.00157

Coleman-Derr, D., and Tringe, S. G. (2014). Building the crops of tomorrow: advantages of symbiont-based approaches to improving abiotic stress tolerance. *Front. Microbiol.* 5:283. doi: 10.3389/fmicb.2014.00283

de Torres Zabala, M., Bennett, M. H., Truman, W. H., and Grant, M. R. (2009). Antagonism between salicylic and abscisic acid reflects early host-pathogen conflict and moulds plant defence responses. *Plant J.* 59, 375–386. doi: 10.1111/j.1365-313X.2009.03875.x

D'odorico, P., and Porporato, A. (2006). ""SOIL moisture dynamics in water-limited ecosystemS," in *Dryland Ecohydrology*, eds P. D'Odorico and A. Porporato (Dordrecht: Springer), 31–46.

Duffy, B. K., and Défago, G. (1999). Environmental factors modulating antibiotic and siderophore biosynthesis by *Pseudomonas fluorescens* biocontrol strains. *Appl. Environ. Microbiol.* 65, 2429–2438.

Dufrêne, M., and Legendre, P. (1997). Species assemblages and indicator species:the need for a flexible asymmetrical approach. *Ecol. Monogr.* 67, 345–366.

Edwards, J., Cameron, J., Santos-Medellín, C., Lurie, E., Natraj, K., Podishetty, N. K., et al. (2015). Structure, variation, and assembly of the root-associated microbiomes of rice. *Proc. Natl. Acad. Sci. U.S.A.* 112, E911–E920. doi: 10.1073/pnas.1414592112

Edwards, J. A., Santos-Medellín, C. M., Liechty, Z. S., Nguyen, B., Eugene, L., Shane, E., et al. (2018). Compositional shifts in root-associated bacterial and archaeal microbiota track the plant life cycle in field-grown rice. *PLoS Biol.* 16:e2003862. doi: 10.1371/journal.pbio.2003862

Fitzpatrick, C. R., Julia, C., Wang, P. W., Guttman, D. S., Kotanen, P. M., and Johnson, M. T. J. (2018). Assembly and ecological function of the root microbiome across angiosperm plant species. *Proc. Natl. Acad. Sci. U.S.A.* 115, E1157–E1165. doi: 10.1073/pnas.1717617115

Kang, Y., Shahbaz, K., and Xiaoyi, M. (2009). Climate change impacts on crop yield, crop water productivity and food security – A review. *Prog. Nat. Sci. Commun. State Key Labor. China* 19, 1665–1674.

Kawasaki, A., Suzanne, D., Ryan, P. R., Mathesius, U., Devilla, R., Jones, A., et al. (2016). Microbiome and exudates of the root and rhizosphere of brachypodium distachyon, a model for wheat. *PLoS ONE* 11:e0164533. doi: 10.1371/journal.pone.0164533

Köberl, M., Henry, M., Ramadan, E. M., and Gabriele, B. (2011). Desert farming benefits from microbial potential in arid soils and promotes diversity and plant health. *PLoS ONE* 6:e24452. doi: 10.1371/journal.pone.0024452

Kogan, F., Wei, G., and Wenze, Y. (2019). Drought and food security prediction from NOAA new generation of operational satellites, geomatics, *Nat. Hazards Risk* 10, 651–666.

Kumar, A., Vidisha, T., Amarjeet, K., Vikas, K., and Kritika, G. (2018). Millets: a solution to agrarian and nutritional challenges. *Agric. Food Secur.* 7, 1–15.

Lebeis, S. L., Paredes, S. H., Lundberg, D. S., Natalie, B., Jase, G., Meredith, M., et al. (2015). PLANT MICROBIOME. salicylic acid modulates colonization of the root microbiome by specific bacterial taxa. *Science* 349, 860–864. doi: 10.1126/science.aaa8764

Lesk, C., Pedram, R., and Navin, R. (2016). Influence of extreme weather disasters on global crop production. *Nature* 529, 84–87. doi: 10.1038/nature16467

Letunic, I., and Bork, P. (2019). Interactive tree of life (iTOL) v4: recent updates and new developments. *Nucleic Acids Res.* 47, W256–W259. doi: 10.1093/nar/gkz239

Liljeroth, E., Burgers, S. L. G. E., and Van Veen, J. A. (1991). Changes in bacterial populations along roots of wheat (*Triticum aestivum* L.) seedlings. *Biol. Fertil. Soils* 10, 276–280.

Liu, H., Lilia, C. C., Peer, M. S., and Paul, G. D. (2018). Activation of the salicylic acid signalling pathway in wheat had no significant short-term impact on the diversity of root-associated microbiomes. *Pedobiologia* 70, 6–11.

Liu, Y., Yan, X., and Bassham, D. C. (2009). Autophagy is required for tolerance of drought and salt stress in plants. *Autophagy* 5, 954–963. doi: 10.4161/auto.5.7.9290

Lundberg, D. S., Sarah, L. L., Paredes, S. H., Yourstone, S., Gehring, J., Malfatti, S., et al. (2012). Defining the core *Arabidopsis thaliana* root microbiome. *Nature* 488, 86–90. doi: 10.1038/nature11237

Marasco, R., Eleonora, R., Besma, E., Gianpiero, V., Francesca, M., Sara, B., et al. (2012). A drought resistance-promoting microbiome is selected by root system under desert farming. *PLoS ONE* 7:e48479. doi: 10.1371/journal.pone.0048479

Marasco, R., María, J. M., Marco, F., Jean-Baptiste, R., Giuseppe, M., Jenny, M. B., et al. (2018). Rhizosheath microbial community assembly of sympatric desert speargrasses is independent of the plant host. *Microbiome* 6:215. doi: 10.1186/s40168-018-0597-y

Millard, W. A., and Taylor, C. W. (1927). Antagonism of micro-organisms as the controlling factor in the: inhibition of scab by green-manuring. *Ann. Appl. Biol.* 14, 202–216.

Miller, G., Nobuhiro, S., Ciftci-Yilmaz, S., and Mittler, R. (2010). Reactive oxygen species homeostasis and signalling during drought and salinity stresses. *Plant Cell Environ.* 33, 453–467. doi: 10.1111/j.1365-3040.2009.02041.x

Naylor, D., and Coleman-Derr, D. (2018). Drought stress and root-associated bacterial communities. *Front. Plant Sci.* 8:2223. doi: 10.3389/fpls.2017.02223

Naylor, D., Stephanie, D., Elizabeth, P., and Coleman-Derr, D. (2017). Drought and host selection influence bacterial community dynamics in the grass root microbiome. *ISME J.* 11, 2691–2704. doi: 10.1038/ismej.2017.118

Newitt, J. T., Prudence, S. M. M., Hutchings, M. I., and Worsley, S. F. (2019). Biocontrol of cereal crop diseases using streptomycetes. *Pathogens* 8:E78. doi: 10.3390/pathogens8020078

Patil, J. V. (2017). *Millets and Sorghum*. Chichester: John Wiley & Sons, Ltd.

Petricka, J. J., Winter, C. M., and Benfey, P. N. (2012). Control of *Arabidopsis* root development. *Annu. Rev. Plant Biol.* 63, 563–590.

Pinheiro, C., and Chaves, M. M. (2011). Photosynthesis and drought: can we make metabolic connections from available data? *J. Exp. Bot.* 62, 869–882. doi: 10.1093/jxb/erq340

Puértolas, J., Conesa, M. R., Ballester, C., and Dodd, I. C. (2015). Local root abscisic acid (ABA) accumulation depends on the spatial distribution of soil moisture in potato: implications for ABA signalling under heterogeneous soil drying. *J. Exp. Bot.* 66, 2325–2334. doi: 10.1093/jxb/eru501

Qin, S., Qian, M., Wei-Wei, F., Yu, W., Xiao, Z., Xing, K., et al. (2015). Biodiversity and plant growth promoting traits of culturable endophytic actinobacteria associated with jatropha curcas l. Growing in panxi dry-hot valley soil. Applied soil ecology: a section of agriculture. *Ecosyst. Environ.* 93, 47–55.

Ramijan, K., Eveline, U., Joost, W., Zheren, Z., Wondergem, J. A. J., van der Meij, A., et al. (2018). Stress-induced formation of cell wall-deficient cells in filamentous actinomycetes. *Nat. Commun.* 9:5164. doi: 10.1038/s41467-018-07560-9

Ray, D. K., Mueller, N. D., West, P. C., and Foley, J. A. (2013). Yield trends are insufficient to double global crop production by 2050. *PLoS ONE* 8:e66428. doi: 10.1371/journal.pone.0066428

Rubin, R. L., Jan, van Groenigen, K., and Hungate, B. A. (2017). Plant growth promoting rhizobacteria are more effective under drought: a meta-analysis. *Plant Soil* 416, 309–323.

Sánchez, S., Adán, C., Angela, F., Yolanda, G., Alba, R., Mauricio, S., et al. (2010). Carbon source regulation of antibiotic production. *J. Antibiot.* 63, 442–459. doi: 10.1038/ja.2010.78

Santos-Medellín, C., Joseph, E., Zachary, L., Bao, N., and Venkatesan, S. (2017). Drought stress results in a compartment-specific restructuring of the rice root-associated microbiomes. *mBio* 8:e00764-17. doi: 10.1128/mBio.00764-17

Sathya, A., Rajendran, V., and Subramaniam, G. (2017). Plant growth-promoting actinobacteria: a new strategy for enhancing sustainable production and protection of grain legumes. *3 Biotech*. 7:102. doi: 10.1007/s13205-017-0736-3

Shyam, L. K., Joubert, P. M., and Doty, S. L. (2017). Bacterial endophyte colonization and distribution within plants. *Microorganisms* 5:E77. doi: 10.3390/microorganisms5040077

Simmons, T., Caddell, D. F., Siwen, D., and Coleman-Derr, D. (2018). Exploring the root microbiome: extracting bacterial community data from the soil, rhizosphere, and root endosphere. *J. Visualized Exp.* e57561. doi: 10.3791/57561

Singh, S. P., Gupta, R., Gaur, R., and Srivastava, A. K. (2016). *Streptomyces* Spp. alleviate rhizoctonia solani -mediated oxidative stress in solanum lycopersicon: streptomyces induced changes in oxidative stress markers in tomato. *Ann. Appl. Biol.* 168, 232–242.

Spinoni, J., Vogt, J. V., Naumann, G., Barbosa, P., and Dosio, A. (2018). Will drought events become more frequent and severe in europe? Future drought events in europe. *Int. J. Climatol. Adv. Nat. Technol. Hazards Res.* 38, 1718–1736.

Suárez-Moreno, Z. R., Vinchira-Villarraga, D. M., Vergara-Morales, D. I., Leonardo, C., Ramos, F. A., Corrado, G., et al. (2019). Plant-growth promotion and biocontrol properties of three *Streptomyces* Spp. isolates to control bacterial rice pathogens. *Front. Microbiol.* 10:290. doi: 10.3389/fmicb.2019.00290

van der Meij, A., Willemse, J., Schneijderberg, M. A., René, G., Raaijmakers, J. M., and van Wezel, G. P. (2018). Inter- and intracellular colonization of arabidopsis roots by endophytic actinobacteria and the impact of plant hormones on their antimicrobial activity. *Antonie Van Leeuwenhoek* 111, 679–690. doi: 10.1007/s10482-018-1014-z

Vicente-Serrano, S. M., and Lopez-Moreno, J. I. (2014). Evidence of increasing drought severity caused by temperature rise in southern Europe. *Environ. Res. Lett.* 9:044001. doi: 10.1088/1748-9326/9/4/044001

Xu, L., and Coleman-Derr, D. (2019). Causes and consequences of a conserved bacterial root microbiome response to drought stress. *Curr. Opin. Microbiol.* 49, 1–6. doi: 10.1016/j.mib.2019.07.003

Xu, L., Dan, N., Zhaobin, D., Tuesday, S., Grady, P., Hixson, K. K., et al. (2018). Drought delays development of the sorghum root microbiome and enriches for monoderm bacteria. *Proc. Natl. Acad. Sci. U.S.A.* 115, E4284–E4293. doi: 10.1073/pnas.1807275115

Yandigeri, M. S., Kamlesh, K. M., Divya, S., Nityanand, M., Singh, D. P., Manoj, K. S., et al. (2012). Drought-tolerant endophytic actinobacteria promote growth of wheat (triticum aestivum) under water stress conditions. *Plant Growth Regul.* 68, 411–420.

Yang, C. H., and Crowley, D. E. (2000). Rhizosphere microbial community structure in relation to root location and plant iron nutritional status. *Appl. Environ. Microbiol.* 66, 345–351. doi: 10.1128/aem.66.1.345-351.2000

Conflict of Interest: The authors declare that the research was conducted in the absence of any commercial or financial relationships that could be construed as a potential conflict of interest.

Advantages of publishing in Frontiers

OPEN ACCESS
Articles are free to read for greatest visibility and readership

FAST PUBLICATION
Around 90 days from submission to decision

HIGH QUALITY PEER-REVIEW
Rigorous, collaborative, and constructive peer-review

TRANSPARENT PEER-REVIEW
Editors and reviewers acknowledged by name on published articles

Frontiers
Avenue du Tribunal-Fédéral 34
1005 Lausanne | Switzerland

Visit us: www.frontiersin.org
Contact us: frontiersin.org/about/contact

REPRODUCIBILITY OF RESEARCH
Support open data and methods to enhance research reproducibility

DIGITAL PUBLISHING
Articles designed for optimal readership across devices

FOLLOW US
@frontiersin

IMPACT METRICS
Advanced article metrics track visibility across digital media

EXTENSIVE PROMOTION
Marketing and promotion of impactful research

LOOP RESEARCH NETWORK
Our network increases your article's readership